

AD_____

AWARD NUMBER: DAMD17-02-1-0457

TITLE: Evaluation of Novel Agents Which Target Neovasculature of Breast Tumors

PRINCIPAL INVESTIGATOR: Michael G. Rosenblum, Ph.D.

CONTRACTING ORGANIZATION: The University of Texas M.D. Anderson Cancer Center
Houston, Texas 77030

REPORT DATE: April 2006

TYPE OF REPORT: Final

PREPARED FOR: U.S. Army Medical Research and Materiel Command
Fort Detrick, Maryland 21702-5012

DISTRIBUTION STATEMENT: Approved for Public Release;
Distribution Unlimited

The views, opinions and/or findings contained in this report are those of the author(s) and should not be construed as an official Department of the Army position, policy or decision unless so designated by other documentation.

REPORT DOCUMENTATION PAGE				Form Approved OMB No. 0704-0188	
Public reporting burden for this collection of information is estimated to average 1 hour per response, including the time for reviewing instructions, searching existing data sources, gathering and maintaining the data needed, and completing and reviewing this collection of information. Send comments regarding this burden estimate or any other aspect of this collection of information, including suggestions for reducing this burden to Department of Defense, Washington Headquarters Services, Directorate for Information Operations and Reports (0704-0188), 1215 Jefferson Davis Highway, Suite 1204, Arlington, VA 22202-4302. Respondents should be aware that notwithstanding any other provision of law, no person shall be subject to any penalty for failing to comply with a collection of information if it does not display a currently valid OMB control number. PLEASE DO NOT RETURN YOUR FORM TO THE ABOVE ADDRESS.					
1. REPORT DATE (DD-MM-YYYY) 01-04-2006		2. REPORT TYPE Final		3. DATES COVERED (From - To) 1 Apr 2002 – 31 Mar 2006	
4. TITLE AND SUBTITLE Evaluation of Novel Agents Which Target Neovasculature of Breast Tumors				5a. CONTRACT NUMBER	
				5b. GRANT NUMBER DAMD17-02-1-0457	
				5c. PROGRAM ELEMENT NUMBER	
6. AUTHOR(S) Michael G. Rosenblum, Ph.D. E-Mail: mrosenbl@mdanderson.org				5d. PROJECT NUMBER	
				5e. TASK NUMBER	
				5f. WORK UNIT NUMBER	
7. PERFORMING ORGANIZATION NAME(S) AND ADDRESS(ES) The University of Texas M.D. Anderson Cancer Center Houston, Texas 77030				8. PERFORMING ORGANIZATION REPORT NUMBER	
9. SPONSORING / MONITORING AGENCY NAME(S) AND ADDRESS(ES) U.S. Army Medical Research and Materiel Command Fort Detrick, Maryland 21702-5012				10. SPONSOR/MONITOR'S ACRONYM(S)	
				11. SPONSOR/MONITOR'S REPORT NUMBER(S)	
12. DISTRIBUTION / AVAILABILITY STATEMENT Approved for Public Release; Distribution Unlimited					
13. SUPPLEMENTARY NOTES					
14. ABSTRACT The unique fusion toxin VEGF121/rGel specifically kills both log-phase and confluent vascular endothelial cells expressing the KDR receptor for VEGF (PNAS 99:7866, 2002). We have discovered 22 unique genes consistently up-regulated in endothelial cells treated with VEGF121/rGel (confirmed by Western and RT-PCR). VEGF121/rGel (i.v.) treatment against an orthotopic breast model resulted in significant delay of tumor growth, by ~50%. In addition, tumors completely regressed in 3/6 (50%) of treated mice. In the metastatic breast model, treatment with VEGF121/rGel reduced both the number and area of lung foci by 58% and 50% respectively. Immunohistochemical analysis demonstrated that VEGF121/rGel targeted lung tumor vasculature but not normal vasculature. In addition, the number of blood vessels per mm2 in metastatic foci was 198 + 37 versus 388 + 21 for treated and control respectively. Approximately 62% of metastatic colonies from the VEGF/rGel treated group had <10 vessels/colony compared to 23% in the control group. Metastatic foci had a 3 fold lower Ki-67 labeling index compared to control tumors. This suggests that VEGF121/rGel has impressive anti-tumor activity in breast cancer. In addition, VEGF121/rGel prevented osteolytic lesions in a prostate cancer bone tumor model, and inhibited new bone formation in an ex vivo model with murine calvaria. Thus, VEGF121/rGel may be useful in inhibiting breast cancer skeletal metastases.					
15. SUBJECT TERMS Fusion Toxins, Co-Culture Studies, Hypoxia, MDA-MB-231, Gene Array, Analysis, Vascular Targeting, Pharmacology					
16. SECURITY CLASSIFICATION OF:			17. LIMITATION OF ABSTRACT	18. NUMBER OF PAGES	19a. NAME OF RESPONSIBLE PERSON
a. REPORT	b. ABSTRACT	c. THIS PAGE			USAMRMC
U	U	U	UU	217	19b. TELEPHONE NUMBER (include area code)

Table of Contents

Cover.....	01
SF 298.....	02
Introduction.....	04
Body.....	04
Key Research Accomplishments.....	28
Reportable Outcomes.....	29
Conclusions.....	30
References.....	31
Key Personnel.....	35
Appendices.....	36

Evaluation of Novel Agents Which Target Neovasculature of Breast Tumors

Introduction

Biological studies examining the development of the vascular tree in normal development and in disease states have identified numerous cytokines and their receptors responsible for triggering and maintaining this process (*1-7*). Tumor neovascularization is central not only to the growth and development of the primary lesion but appears to be a critical factor in the development and maintenance of metastases (*8-12*). For example, clinical studies in bladder cancer (*9*) have demonstrated a correlation between micro-vessel density and metastases. In addition, studies of breast cancer metastases by Fox et al. and Aranda et al (*11-12*) have demonstrated that microvessel count in primary tumors appears to be related to the presence of metastases in lymph nodes and micrometastases in bone marrow.

The cytokine vascular endothelial growth factor-A (VEGF-A) and its receptors Flt-1 (Receptor 1, R1) and KDR (Receptor 2, R2) have been implicated as one of the central mediators of normal angiogenesis and tumor neovascularization (*13-20*). Up-regulation or over-expression of KDR or VEGF-A have been implicated as poor prognostic markers in various clinical studies of colon, breast and pituitary cancers (*21-23*). Recently, Padro et al (*24*) have suggested that both VEGF-A and KDR may play a role in the neovascularization observed in bone marrow during AML tumor progression and may provide evidence that the VEGF/KDR pathway is important in leukemic growth particularly in the bone marrow.

For these reasons, there have been several groups interested in developing therapeutic agents and approaches targeting the VEGF-A pathway. Agents which prevent VEGF-A binding to its receptor, antibodies which directly block the KDR receptor itself and small molecules which block the kinase activity of the KDR and thereby block growth factor signaling are all under development (*25-37*). Recently, our laboratory reported the development of a growth factor fusion construct of VEGF₁₂₁ and the recombinant toxin gelonin (*38*). Our studies demonstrated that this agent was specifically cytotoxic only to cells expressing the KDR receptor and was not cytotoxic to cells over-expressing the Flt-1 receptor. In addition, this agent was shown to localize within tumor vasculature and caused a significant damage to vascular endothelium in both PC-3 prostate and MDA-MB-231 orthotopic xenograft tumor models.

The current study seeks to extend our original observations describing the in vitro biological effects of this novel fusion construct and we examined the effects of this agent in both orthotopic and metastatic tumor models.

Progress Report Body:

Original SOW:

1. Establish In Vivo Activity of the VEGF₁₂₁/rGel Fusion Toxin in the MDA-MB231 Tumor Models

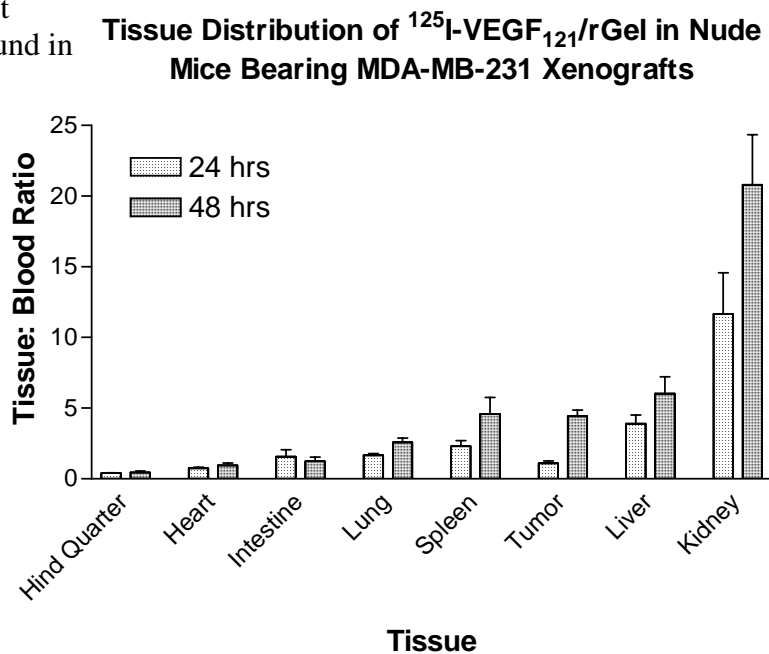
Task 1: Radiolabeling

Numerous methods were employed initially to label the target protein. We settled on using Bolton-Hunter reagent which generated the highest yield of material capable of specific binding to purified, immobilized KDR receptor. Highly purified VEGF₁₂₁/rGel was radiolabeled using ¹²⁵I with this reagent and the material was adjusted to a specific activity of 602 Ci/mMol.

Task 2: Tissue Distribution

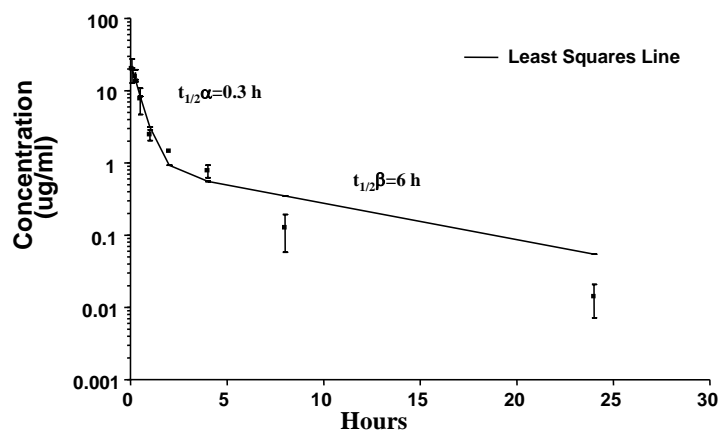
Mice bearing orthotopically-placed MDA-MB231 tumors were administered 4 μCi of VEGF₁₂₁/rGel (i.v., tail vein). At 24 and 48 hrs after administration, groups of 6 mice were sacrificed and various organs were excised, weighed and counted to determine ¹²⁵I activity.

As shown in this figure, the highest concentration of radiolabel was found in kidney > liver > tumor > spleen. At 48 hrs, the tissue: blood ratio in these organs increased particularly for kidney and tumor. The high levels found in kidney may be related to high levels of the flt-1 receptor found in this organ.



The pharmacokinetics of VEGF₁₂₁/rGel were additionally described using this radiolabeled material. Balb/c mice were injected with 1 μCi of labeled material and at various times after administration, groups of 3 mice were sacrificed and blood samples were removed and centrifuged. Aliquots of plasma were counted to determine radioactivity and the results were analyzed for conventional pharmacokinetic analyses using conventional mathematical modeling (pK Analyst from MicroMath, Inc). As shown in the figure below, the VEGF₁₂₁/rGel cleared from plasma with initial and terminal half-lives of 0.3 and 6h respectively. Therefore this agent has a relatively long half-life despite the significant uptake in kidney.

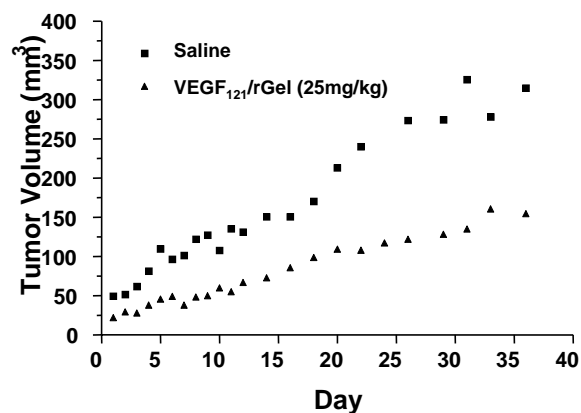
Clearance of VEGF₁₂₁/rGel From Plasma

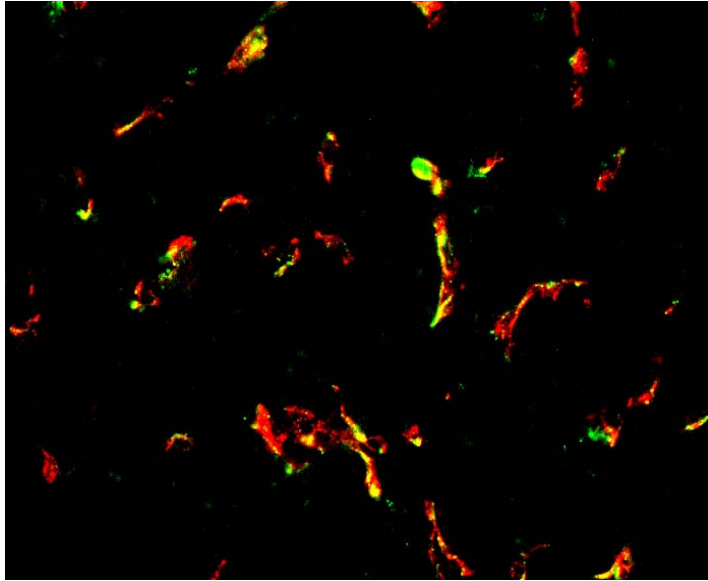


Task 3: Antitumor Effects-Orthotopic Model

Given the pharmacokinetic and tissue distribution data described above, we designed a treatment schedule comprised of 5 injections spaced 48 hrs apart (10 day course). Using this schedule, we delineated the Maximum Tolerated Dose as this schedule to be ~40 mg/kg. The effect of VEGF₁₂₁/rGel administration on orthotopically-placed MDA-MB-231 tumor bearing mice (6 per group) is shown in the Figure below. As shown, treatment significantly retarded tumor growth. In addition, 3/6 mice in the treated group demonstrated complete disappearance of the tumor compared to 0/6 in the saline-treated group.

Effect of VEGF₁₂₁/rGel on Orthotopically Placed MDA-MB-231 Tumor Cells in Nude Mice



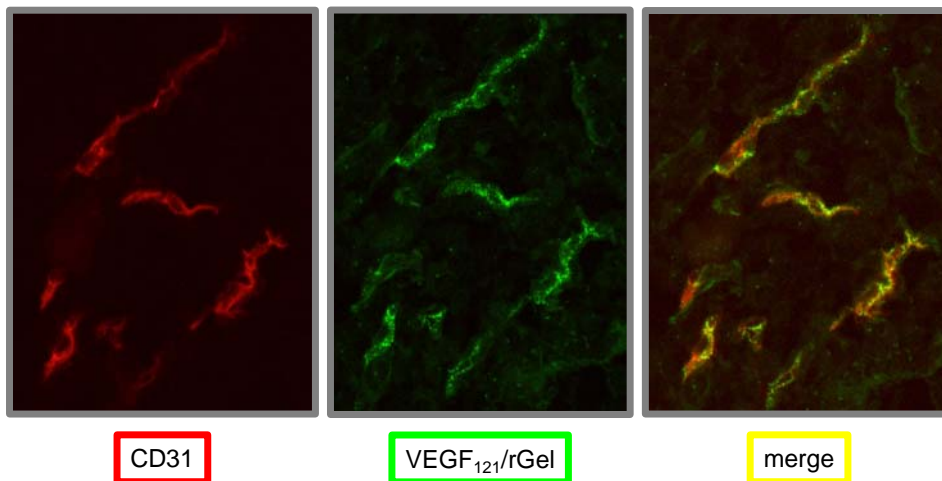


VEGF₁₂₁/rGel was primarily detected on endothelium of the orthotopically placed breast tumor. In average, sixty percent of vessels positive for MECA 32 were also positive for gelonin in the group of VEGF₁₂₁/rGel – injected mice. In the tumor regions of increased vascularity (hot spots), up to 90% of tumor vessels were labeled by anti-gelonin IgG. Vessels with bound VEGF₁₂₁/rGel were homogeneously distributed within the tumor vasculature. Vessels in normal organs were unstained with the exception of the kidney where weak and diffuse staining was detected in the glomeruli. Free gelonin did not localize to tumor or normal vessels in any of the mice, indicating that only targeted gelonin was able to bind to the tumor endothelium. These results indicate that VEGF₁₂₁/rGel specifically localizes to tumor vessels, which demonstrate high density and favorable distribution of the VEGF₁₂₁/rGel – binding sites.

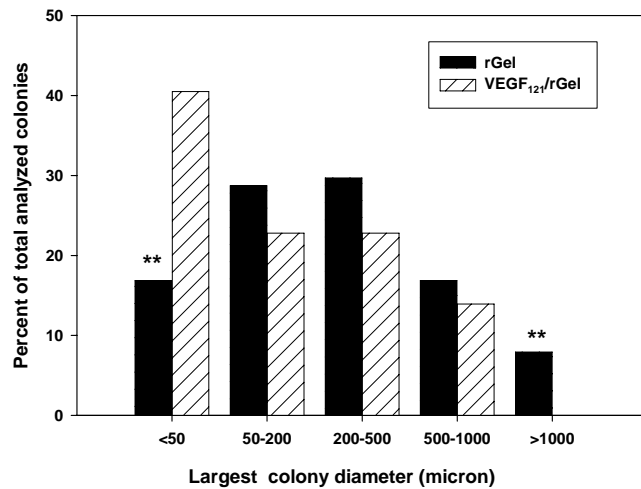
Task 4: Antitumor Effects-Metastatic Model

We evaluated the effect of VEGF₁₂₁/rGel fusion toxin treatment on the growth of metastatic MDA-MB-231 tumor cells in nude mice. Tumor cells (0.5×10^6 per mouse) were injected i.v. and 8 days after inoculation, mice (6 per group) were treated 6 times either with VEGF₁₂₁/rGel (100 µg/dose) or free gelonin. Three weeks after treatment, mice were sacrificed and the lungs were harvested and examined. The surface lung foci in the VEGF₁₂₁/rGel – treated mice were reduced by 58 % as compared to gelonin control animals (means were 22.4 and 53.3 for VEGF₁₂₁/rGel and control, respectively; $p < 0.05$). The mean area of lung colonies from VEGF₁₂₁/rGel-treated mice was also 50% smaller than control mice (210 ± 37 µm versus 415 ± 10 µm for VEGF₁₂₁/rGel and control, respectively; $p < 0.01$). In addition, the vascularity of metastatic foci as assessed by the mean number of blood vessels per mm² in metastatic foci was significantly reduced (198 ± 37 versus 388 ± 21 for treated and control, respectively). Approximately 62% of metastatic colonies from the VEGF₁₂₁/rGel-treated group had fewer than 10 vessels per colony as compared to 23% in the control group. The VEGF receptor (Flk-1) was intensely detected on the metastatic vessels in the control but not on the vessels in the VEGF₁₂₁/rGel-treated group.

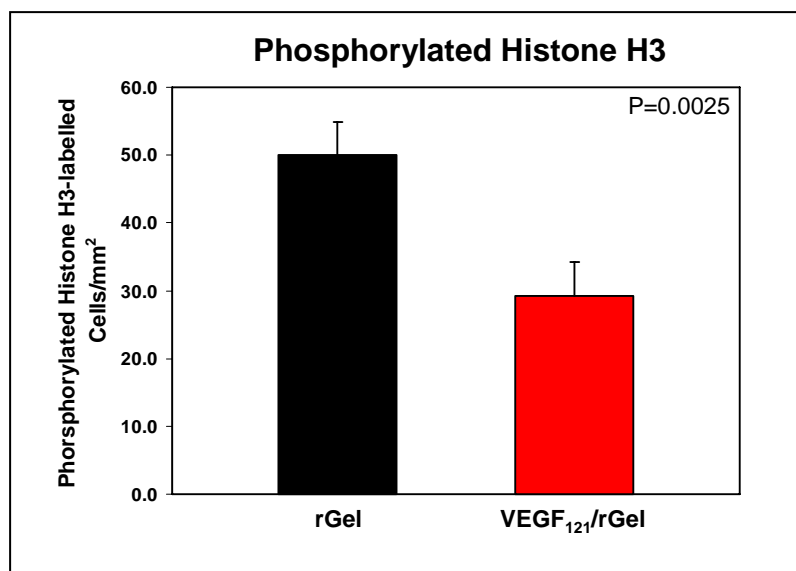
VEGF₁₂₁/rGel Localizes to Vasculature of Breast Tumor Foci in the Lungs of Mice



Mice bearing MDA-MB-435s lung tumor foci were injected i.v. with 50 µg of VEGF₁₂₁/rGel or 20 µg of free rGel (only tissues from VEGF₁₂₁/rGel injected mice are shown). One hour later, mice were sacrificed and tissues excised. Lung sections were double-stained using an anti-CD31 antibody and an anti-gelonin antibody to detect blood vessels (red) and localized VEGF₁₂₁/rGel (green), respectively. Co-localization of the stains is indicated by a yellow color. Free rGel did not localize to the vasculature of lung tumor foci (not shown). No VEGF₁₂₁/rGel staining was detected in any of the normal tissues examined (lung, liver, kidney, heart, spleen, pancreas, brain).



VEGF₁₂₁/rGel reduces number of large colonies in the metastatic lungs. Female SCID mice, aged 4-5 weeks, were injected in a tail vein with 0.1 ml of MDA-MB-231 cell suspension (5×10^5 cells). The mice were randomly separated into two groups (6 mice per group) and were treated with either VEGF₁₂₁/rGel or rGel starting the 8th day after the injection of cells. VEGF₁₂₁/rGel was delivered at 100 μ g per dose intraperitoneally, 6 times total with the interval of 3 days, for a total dose of 31.5 mg/kg. The molar equivalent of rGel (40 μ g) was delivered at the same schedule. Intraperitoneal rather than intravenous injection was chosen solely to prevent necrosis of the tail vein due to repeated injections. Three weeks after termination of the treatment, the animals were sacrificed and their lungs were removed. One lobe was fixed in Bouin's fixative and the other lobe was snap-frozen. After fixation in Bouin's fixative, the tumor colonies on the lung surface appear white, whereas the normal lung tissue appears brown. The number of tumor colonies on the surface of each lung was counted and the weight of each lung was measured. The values obtained from individual mice in the VEGF₁₂₁/rGel and rGel groups were averaged per group. Treatment with VEGF₁₂₁/rGel but not with free rGel significantly reduced by between 42-58% both the number of colonies per lung and the size of the metastatic foci present in lung. The greatest impact on vascularization was observed on mid-size and extremely small tumors (62 and 69% inhibition respectively) while large tumors demonstrated the least effect (10% inhibition). The majority of lesions in the VEGF₁₂₁/rGel-treated mice (~70%) were avascular whereas only 40% of lesions from the control group did not have vessels within the metastatic lung foci.



Frozen sections of lungs derived from VEGF₁₂₁/rGel- and rGel-treated mice bearing MDA-MB-231 lung tumor foci were stained with a phosphorylated histone H3 antibody. The number of tumor cells with phosphorylated histone H3 positive nuclei (mitotic cells) was counted in five high power fields of tumor sections from five mice per treatment group. The mean number per group \pm SEM is presented and statistical significance was determined using the student's *t*-test.

Metastatic foci present in lung had a 3-fold lower Ki-67 labeling number compared to control tumors. These data strongly suggest that the anti-tumor vascular-ablative effect of VEGF₁₂₁/rGel could be utilized not only for treating primary tumors but also for inhibiting metastatic spread.

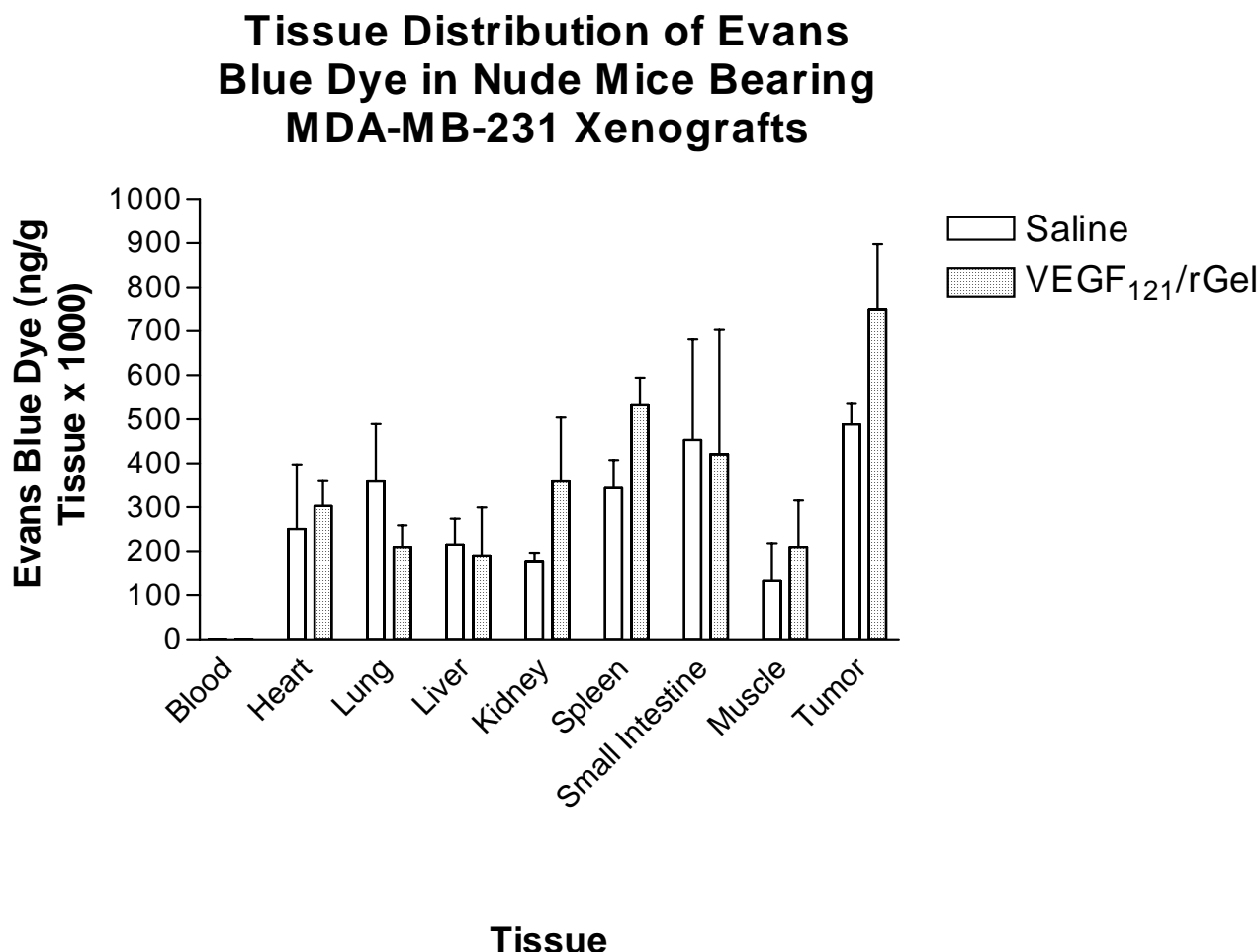
Task 5: Effects on Tissue Necrosis and Thrombosis:

Please note that a complete manuscript detailing the impressive anti-metastatic effects of VEGF₁₂₁/rGel in this breast tumor model is attached in the Appendix #3 (The Vascular-Ablative Agent, VEGF₁₂₁/rGel, Inhibits Pulmonary Metastases of MDA-MB-231 Breast Tumors, by Ran et al (<http://www.neoplasia.com/pdf/manuscript/neo04631.pdf>)).

Task 6: Effects of VEGF/rGel on Tumor and normal tissue Vascular Permeability

Several studies have been performed to examine the effects of the VEGF₁₂₁/rGel fusion construct on vascular permeability. We performed the initial assessment on vascular permeability using ¹²⁵I labeled albumin exactly as described in the initial SOW. However, after several studies, we were unable to demonstrate an effect on tumor vasculature despite several other lines of histological evidence to the contrary. We therefore changed methodologies to assess in vivo vascular integrity to utilize the Evans Blue dye. In this method, MDA-MB-231 tumor cells (2×10^6) are placed in the mammary fat pad and allowed to develop into palpable tumors. The mice are treated with either VEGF₁₂₁/rGel (40 mg/kg, QOD X 5) or saline and 24 hrs after the final treatment; the mice are injected (i.v.) with 200 μ l of dye (20 mg/ml). After 0.5 hr, the mice are sacrificed, blood is collected and the mice are perfused with 5 ml of PBS/heparin. The various

tissues (including tumor) are harvested and weighed into glass test tubes. A sample (0.5 ml) or N-N-DMF is added to each tube and allowed to incubate at room temp for 48 h. The concentration of Evans Blue dye is assessed spectrophotometrically (A_{630}) against a standard curve for the dye. The results are then expressed as either % of control or as ng dye/mg tissue.



As shown in the figure above, we found a small (25%) but statistically-significant increase in the vascular permeability in tumor tissue, normal spleen and kidney with a concomitant small decrease (not statistically significant) in the vascular permeability of normal lung tissue. Histology and pathology studies are currently ongoing to evaluate the effects of VEGF₁₂₁/rGel on normal tissues as a part of the pre-IND evaluation package on this agent and these studies on vascular permeability may be evaluated in concert with observed effects on histology. In addition, in this next (unfunded) year, we plan to extend these observations on vascular permeability to evaluate the magnitude and timeline for these effects. We believe these observations may be of critical importance in developing the timing of imaging studies for the Phase I/II trial of this agent.

Task 7: Effects on Tumor Hypoxia

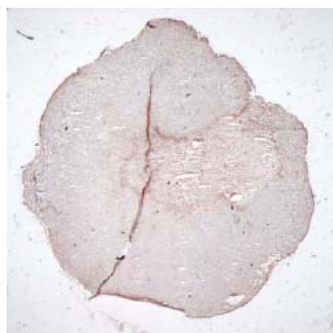
MDA-MB-231 tumor cells (2.5×10^6) were orthotopically placed in 6 week Balb/c mice (3 mice per group). After the tumors had become established ($15-45 \text{ mm}^3$), the mice were injected intraperitoneally with VEGF₁₂₁/rGel, rGel or Saline through a tail vein four times over a 7 day period. The total dose of VEGF₁₂₁/rGel was 40 mg/kg. Eighteen hours after administration of the final dose, mice were injected i.p. with hypoxyprobe (1.4 mg; Chemicon International, Inc.) One hour later the mice were sacrificed and tissues harvested. Frozen tumor sections were stained for hypoxia using an anti-hypoxyprobe antibody provided in the hypoxyprobe kit (HP1-100; Chemicon International, Inc.). Necrotic regions were identified using hematoxylin staining. The pixel area of the entire section and the sum of the pixel area of hypoxic/necrotic tumor regions was determined using Metaview software (Universal Imaging Corporation). The data indicate that 10% of the cross-sectional area of VEGF₁₂₁/rGel-treated tumors were hypoxic/necrotic, while only 3% for PBS, and 0% for rGel. The mechanism of antitumor action of VEGF₁₂₁/rGel primarily entails tumor hypoxia secondary to vascular damage.

MDA-MB-231 Tumors Treated with VEGF₁₂₁/rGel and Stained for Hypoxyprobe

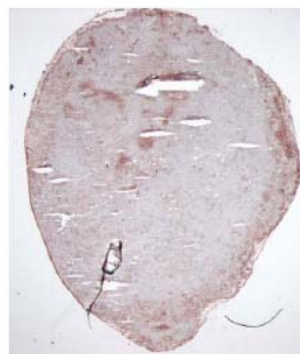
Mouse 51



Mouse 55

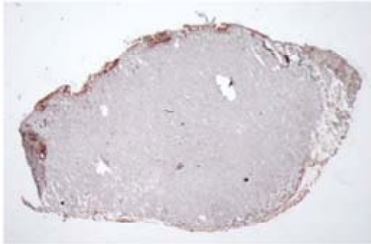


Mouse 60

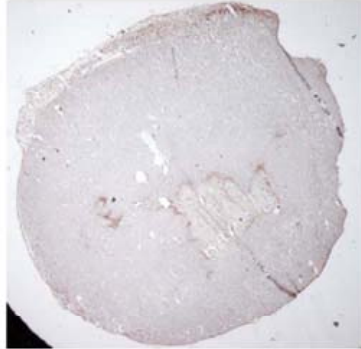


MDA-MB-231 Tumors Treated with PBS and Stained for Hypoxyprobe

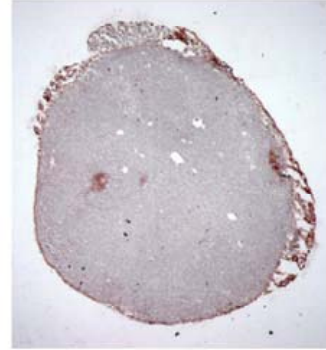
Mouse 36



Mouse 37

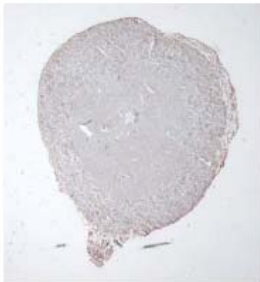


Mouse 58



MDA-MB-231 Tumors Treated with rGel and Stained for Hypoxyprobe

Mouse 39



Mouse 45



Mouse 59



Task 8: Co-Culture of Endothelial Cells and MDA-MB231 Tumor Cells

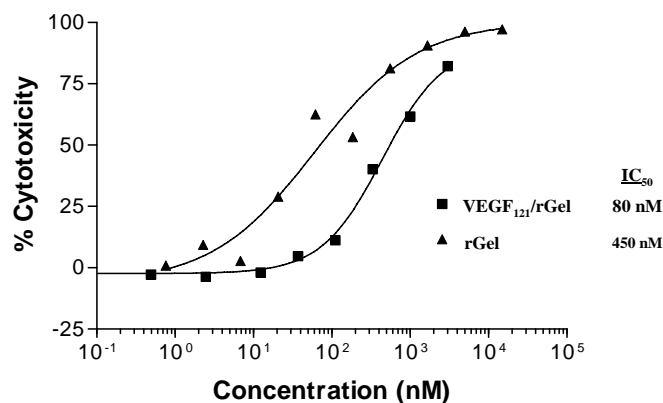
We utilized the Falcon multi-well culture plates to culture the MDA-MB-231 tumor cells. Suspended above these cells, we placed an insert containing log-phase PAE/KDR cells. The 2 cell lines are cultured in the same DMEM/F-12 growth media, so no adaptation was required. We then proceeded to Task 9 (below).

Task 9: Studies of VEGF₁₂₁/rGel Effects on Endothelial and Breast Tumor Cells

In the co-culture chambers, the 2 cell lines were treated with various doses of the VEGF₁₂₁/rGel fusion construct targeting the KDR receptor on endothelial cells. The MDA-MB-231 cells lack this receptor and were not affected by the doses utilized. At various times after drug administration, both cell lines were harvested, the RNA extracted and analyzed using the Gene Chip as described to assess the impact of treatment on over 7,000 genes including proteins involved in signal transduction, stress response, cell cycle control and metastasis. As shown

below, we demonstrate the cytotoxic effects of the fusion construct on endothelial cells. Initial studies demonstrated that the initially-proposed PAE/KDR endothelial cells would be utilized, however, Gene Chip analysis showed no hybridization to isolated RNA samples. Troubleshooting demonstrated that there is insufficient homology of the porcine cell RNA to that of the human probes on the Gene Chip; therefore, HUVEC cells were substituted for this phase of study. As shown below, HUVECs showed specific cytotoxicity of the fusion construct compared to rGel itself although the magnitude of the differential is lower than that of the PAE/KDR cells.

Cytotoxicity of VEGF₁₂₁/rGel on HUVECs



As shown below, extensive micro-array analyses were performed on breast tumor cells as well as on endothelial cells as described in the original SOW. We identified a total of 22 unique genes upregulated (>2-fold in at least 3 out of 4 arrays) by treatment with VEGF₁₂₁/rGel. These include genes involved in the control of cell adhesion, apoptosis, transcription regulation, chemotaxis and inflammatory response. These micro-array data were confirmed using Western analysis and RT-PCR and are further detailed in the attached manuscript (see appendices #5) submitted to the Journal of Biological Chemistry.

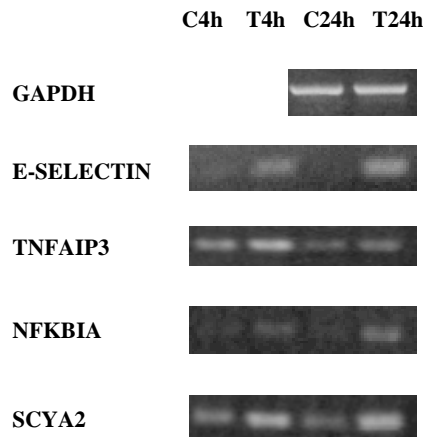
Genes overexpressed in HUVECs by 24 hr treatment with VEGF₁₂₁/rGel:

- E Selectin (endothelial adhesion molecule 1)**
- Small inducible cytokine A2 (monocyte chemotactic protein 1)**
- Tumor necrosis factor, alpha-induced protein 3**
- Nuclear factor of kappa light polypeptide gene enhancer in B-cells inhibitor, alpha**
- Kinesin-like 5 (mitotic kinesin-like protein 1)**
- Small inducible cytokine A4**
- Jun B proto-oncogene**
- Nidogen 2**
- Prostaglandin-endoperoxide synthase 2**
- Dual specificity phosphatase 5**
- Small inducible cytokine subfamily A (Cys-Cys), member 11 (eotaxin)**

Plasminogen activator, urokinase
Vascular cell adhesion molecule 1
H2A histone family, member L
Small inducible cytokine A7 (monocyte chemotactic protein 3)
Spermidine/spermine N1-acetyltransferase
Syndecan 4 (amphiglycan, ryudocan)
Chemokine (C-X-C motif), receptor 4 (fusin)
Nuclear factor of kappa light polypeptide gene enhancer in B-cells 1 (p105)
Baculoviral IAP repeat-containing 3
Kruppel-like factor 4
Early growth response 1

All of the genes described above are known in the literature, however their association with cytotoxic events related to toxins such as rGel and activity on endothelial cells was previously unsuspected. To confirm these observations, these studies were repeated and RT-PCR was also employed (figure below) to more closely assess the timelines for gene modulation. As shown below, our RT-PCR essentially confirmed the upregulation of E-selectin, TNF AIP3, NFkB and SCYA2 genes in control(C) versus treated(T) samples at 4 and 24 hrs after exposure which confirms the results of the Gene Chip analysis of the 5 most highly upregulated genes.

Up-regulation of mRNA in HUVECs treated with VEGF₁₂₁/rGel



C: No Treatment Controls

Task 10: Effects of VEGF₁₂₁/rGel Exposure on Endothelial Cells Followed by Hypoxia

This past year, we performed extensive studies of the cellular response and concomitant gene regulation of endothelial and tumor (MDA-MD-231) cells exposed to VEGF₁₂₁/rGel. Modulation of gene expression was assessed using an mRNA micro-array analysis as described in the Original SOW. We also looked at various times at the genes modified in tumor cells treated with the construct in the presence of endothelial cells and under both hypoxic and normoxic conditions as an approximation of intratumoral conditions in vivo. Tables 1-3 describe the various genes upregulated and downregulated in both tumor cells alone and in co-culture with endothelial cells exposed to VEGF₁₂₁/rGel or VEGF₁₂₁ under both normoxic and hypoxic conditions.

TABLE 1**Change in Gene Regulation of MDA-MB-231 cells (> 3-fold)**
Hypoxic Conditions**24h treatment with VEGF₁₂₁**

Gene Designation	Name	Fold over Control
------------------	------	-------------------

Upregulated

NM_006993	Nucleoplosmin/Nucleoplasmin 3	4.1
NM_003341	Ubiquitin-conjugating enzyme E2E 1 (UBE2E1)	4.0
NM_021939	FK506 binding protein 10	3.6

Downregulated

AK055846	Similar to Actin interacting protein 2	17.0
NM_000587	Complement component 7	5.3

24h treatment with VEGF₁₂₁/rGel**Upregulated**

NM_003528	Histone 2, H2be	4.0
NM_000584	Interleukin 8 (IL-8)	3.7
NM_006993	Nucleoplosmin/Nucleoplasmin 3	3.7
NM_001875	Carbamoyl-phosphate synthetase 1	3.2
NM_021939	FK506 binding protein 10	3.1
NM_025195	Tribbles homolog 1	3.1

Downregulated

AK055846	Similar to Actin interacting protein 2	25.2
NM_000587	Complement component 7	4.6

24h treatment with VEGF₁₂₁/rGel vs. VEGF₁₂₁**Upregulated**

AL137326	Genomic DNA; cDNA DKFZp434B0650	5.8
NM_003528	Histone 2, H2be	4.8
NM_000584	Interleukin 8 (IL-8)	4.7
NM_002260	Killer cell lectin-like receptor subfamily C, member 2	3.9
NM_025195	Tribbles homolog 1	3.9

Downregulated

None observed

TABLE 2**Change in Gene Regulation of MDA-MB-231 cells (> 3-fold) in Co-culture with PAE/KDR cells under Normoxic Conditions****72h treatment with VEGF₁₂₁****Upregulated**

D86978	KIAA0225	8.4
AB001915	NG,NG-dimethylarginine dimethylaminohydrolase	5.7
NM_018191	Regulator of chromosome condensation (RCC1) and BTB (POZ) domain containing protein 1 (RCBTB1)	4.0
NM_004517	Integrin-linked kinase (ILK)	3.5

Downregulated

NM_032799	Zinc finger, DHHC domain containing 12 (ZDHHC12)	16.0
NM_005798	Ret finger protein 2 (RFP2), transcript variant 1	15.9
D87446	KIAA0257	13.5
AF038440	phospholipase D2 (PLD2)	6.5
AJ251973	Steerin-1	5.2
AL050041	Genomic DNA; cDNA DKFZp566L0424	4.4
NM_004391	Cytochrome P450 (CYP8B1)	4.0
NM_014736	KIAA0101	3.9
NM_002309	leukemia inhibitory factor (LIF)	3.6
NM_007150	zinc finger protein 185 (LIM domain) (ZNF185)	3.6
Y17456	LSFR2	3.5
NM_005597	nuclear factor I/C (NFIC)	3.5
AK025003	FLJ21350 fis	3.3
AF178669	p34	3.2
AK057059	Similar to K ⁺ channel protein, beta subunit	3.0
NM_007076	Huntingtin interacting protein E (HYPE)	3.0

72h treatment with VEGF₁₂₁/rGel**Upregulated**

D86978	KIAA0225	8.8
AK024586	FLJ20933 fis	5.0
AB001915	NG,NG-dimethylarginine dimethylaminohydrolase	4.9
NM_018191	Regulator of chromosome condensation (RCC1) and BTB (POZ) domain containing protein 1 (RCBTB1)	4.1
NM_024680	Likely ortholog of mouse E2F transcription factor 8 (E2F8)	3.3
NM_033084	Fanconi anemia, complementation group D2 (FANCD2)	3.0
NM_003937	Kynureninase (L-kynurenine hydrolase) (KYNU)	3.0

Downregulated

NM_032799	Zinc finger, DHHC domain containing 12 (ZDHHC12)	10.4
NM_003486	Solute carrier family 7, member 5 (SLC7A5)	5.4
NM_017801	Chemokine-like factor super family 6 (CKLFSF6)	4.8

NM_002621	Properdin P factor, complement (PFC)	4.8
AL122088	cDNA DKFZp564C0671 (from clone DKFZp564C0671)	4.8
NM_004207	Solute carrier family 16, member 3 (SLC16A3)	4.7
NM_015700	HIRA interacting protein 5 (HIRIP5)	4.5
AJ251973	Steerin-1	4.2
NM_012155	Echinoderm microtubule associated protein like 2 (EML2)	4.1
NM_004295	TNF receptor-associated factor 4 (TRAF4)	4.0
NM_024111	MGC4504	4.0
AK025003	FLJ21350 fis	3.9
NM_007324	Zinc finger, FYVE domain containing 9 (ZFYVE9)	3.9
NM_144726	FLJ31951	3.8
NM_021158	Tribbles homolog 3 (TRIB3)	3.8
NM_002928	Regulator of G-protein signaling 16 (RGS16)	3.8
NM_005717	Actin related protein 2/3 complex, subunit 5 (ARPC5)	3.7
NM_024567	FLJ21616	3.6
NM_003341	Ubiquitin-conjugating enzyme E2E 1 (UBE2E1)	3.6
NM_133436	Asparagine synthetase (ASNS)	3.6
NM_001348	Death-associated protein kinase 3 (DAPK3)	3.5
BC010350	TAF9-like RNA polymerase II, TATA box binding protein (TBP)-associated factor	3.5
NM_130469	Jun dimerization protein 2 (JDP2)	3.4
NM_001517	General transcription factor IIH, polypeptide 4 (GTF2H4)	3.4
NM_003275	Tropomodulin 1 (TMOD1)	3.4
NM_033332	CDC14 cell division cycle 14 homolog B (CDC14B)	3.3
NM_007076	Huntingtin interacting protein E (HYPE)	3.1
NM_017816	FLJ20425 (LYAR)	3.1
NM_000050	Argininosuccinate synthetase (ASS)	3.1
AB010067	RBP56/hTAFII68	3.1
X02160	Insulin receptor precursor	3.0

72h treatment with VEGF₁₂₁/rGel vs. VEGF₁₂₁

Upregulated

NM_005798	Ret finger protein 2 (RFP2), transcript variant 1	10.7
D87446	KIAA0257	5.4
NM_001336	Cathepsin Z (CTSZ)	3.5
AK024586	FLJ20933 fis	3.2
NM_003548	Histone 2, H4 (HIST2H4)	3.1
NM_006290	Tumor necrosis factor, alpha-induced protein 3 (TNFAIP3)	3.1
NM_004454	Ets variant gene 5 (ets-related molecule) (ETV5)	3.1
NM_013282	Ubiquitin-like 1 (UHRF1)	3.1
NM_002260	Killer cell lectin-like receptor (KLRC2)	3.1
NM_0147736	KIAA0101	3.1

Downregulated

NM_004207	Solute carrier family 16 (SLC16A3)	5.7
NM_001282	Adaptor-related protein (AP2B1)	5.1

NM_144726	FLJ31951	4.5
NM_007324	Zinc finger, FYVE domain containing 9 (ZFYVE9)	4.3
NM_004295	TNF receptor-associated factor 4 (TRAF4)	4.0
M80899	AHNAK	3.7
NM_012155	Echinoderm microtubule associated protein like 2 (EML2)	3.3
NM_001517	General transcription factor IIH, polypeptide 4 (GTF2H4)	3.3
NM_024111	MGC4504	3.2
NM_016333	Serine/arginine repetitive matrix 2 (SRRM2)	3.1
NM_014437	Solute carrier family 39 (SLC39A1)	3.1
NM_001348	Death-associated protein kinase 3 (DAPK3)	3.1
NM_003341	Ubiquitin-conjugating enzyme E2E 1 (UBE2E1)	3.1
NM_018113	Lipocalin-interacting membrane receptor (LIMR)	3.0

TABLE 3

Change in Gene Regulation of MDA-MB-231 cells (> 3-fold) in Co-culture with PAE/KDR cells under Hypoxic Conditions

72h treatment with VEGF₁₂₁

Upregulated

NM_032023	Ras association (RalGDS/AF-6) domain family 4 (RASSF4)	96.1
NM_024531	G protein-coupled receptor 172A (GPR172A)	8.0
AK001020	FLJ10158 fis	3.9

Downregulated

AF083386	Putative WHSC1 protein (WHSC1)	31.4
NM_015271	Tripartite motif-containing 2 (TRIM2)	4.1

72h treatment with VEGF₁₂₁/rGel

Upregulated

NM_016073	Hepatoma-derived growth factor, related protein 3 (HDGFRP3)	8.4
BC010926	Histone 1, H4h	7.6
NM_003543	Histone 1, H4h (HIST1H4H)	4.3
L40326	Hepatitis B virus X-associated protein 1	4.0
AL049965	cDNA DKFZp564A232 (from clone DKFZp564A232)	4.0
R85474	Soares adult brain N2b4HB55Y	4.0
NM_005658	TNF receptor-associated factor 1 (TRAF1)	3.8
AP000557	genomic DNA, chromosome 22q11.2, BCRL2 region	3.8
NM_016113	Transient receptor potential cation channel (TRPV2)	3.7
BI462740	603202190F1 NIH_MGC_97 cDNA clone IMAGE:5268046	3.5
NM_004521	Kinesin family member 5B (KIF5B)	3.5
NM_014890	Downregulated in ovarian cancer 1 (DOC1)	3.2
NM_003452	Zinc finger protein 189 (ZNF189)	3.0
AB037770	KIAA1349	3.0

Downregulated

NM_144726	FLJ31951	4.8
NM_006874	E74-like factor 2 (ets domain transcription factor) (ELF2)	4.6
AK026965	FLJ23312 fis	3.7
NM_015271	Tripartite motif-containing 2 (TRIM2)	3.4
NM_001282	Adaptor-related protein complex 2, beta 1 subunit (AP2B1)	3.1

72h treatment with VEGF₁₂₁/rGel vs. VEGF₁₂₁

Upregulated

NM_016073	Hepatoma-derived growth factor, related protein 3 (HDGFRP3)	9.4
BC010926	Histone 1, H4h	8.0
NM_005658	TNF receptor-associated factor 1 (TRAF1)	5.1
NM_004521	Kinesin family member 5B (KIF5B)	4.7
NM_014890	Downregulated in ovarian cancer 1 (DOC1)	4.4

BC015134	Clone IMAGE:3934391	3.7
L40326	Hepatitis B virus X-associated protein 1	3.6
AB037770	KIAA1349	3.2
NM_030965	ST6 (alpha-N-acetyl-neuraminyl-2,3-beta-galactosyl-1,3)-N-acetylglactosaminide alpha-2,6-sialyltransferase 5 (ST6GALNAC5)	3.1
NM_003452	Zinc finger protein 189 (ZNF189)	3.1
NM_006807	Chromobox homolog 1(CBX1)	3.0
X07289	HF.10	3.0
NM_018137	HMT1 hnRNP methyltransferase-like 6 (HRMT1L6)	3.0

Downregulated

NM_032023	Ras association (RalGDS/AF-6) domain family 4 (RASSF4)	88.6
NM_024531	G protein-coupled receptor 172A (GPR172A)	8.9
NM_144726	FLJ31951	5.2
NM_006874	E74-like factor 2 (ets domain transcription factor) (ELF2)	4.3
U57645	Helix-loop-helix proteins Id-1 (ID-1) and Id-1' (ID-1)	4.2
NM_003341	Ubiquitin-conjugating enzyme E2E 1 (UBE2E1)	3.5
AK001020	FLJ10158 fis	3.3
NM_020353	Phospholipid scramblase 4 (PLSCR4),	3.2
NM_016518	Pipecolic acid oxidase (PIPOX),	3.2
NM_000484	Amyloid beta (A4) precursor protein (protease nexin-II, Alzheimer disease) (APP)	3.1
NM_001282	Adaptor-related protein complex 2, beta 1 subunit (AP2B1)	3.0
AL163284	Chromosome 21 segment HS21C084	3.0

As shown in the tables above, both VEGF₁₂₁ and VEGF₁₂₁/rGel induce and suppress a different subset of genes on breast tumor cells, as expected. Treatment of breast tumor cells in co-culture with endothelial cells with VEGF₁₂₁/rGel for 72 hrs in hypoxic conditions appeared to significantly downregulate (89 fold) Ras family protein and the G-coupled receptor 172A. In contrast, histone 1 and hepatoma-derived growth factor-related protein 3 (HDGFRP3) were both highly upregulated. The effects of VEGF/rGel on MDA-MB-231 tumor cells appears to be significantly different under normoxic conditions was significantly different as shown in Table 2. Both Ret finger protein 2 and KIA were upregulated while SLC16A3 and AP2B1 were downregulated in response to VEGF/rGel.

Original SOW Tasks still to be accomplished in the requested (no-cost) extension year 2005-2006:

Task 11: Confirmation of In Vitro Gene Chip Findings with PCR Analysis of Tumor Samples

This information is critical to confirm our co-culture studies with actual data from xenograft MDA-MB-231 models. We now have RT-PCR confirmation of the findings using the Gene Chip analysis. This narrows the gene search and we can focus on the specific genes using conventional RT-PCR in tumor xenograft specimens. In addition, we plan an extensive analysis to determine the temporal nature of these potential changes. This data will be critical for our

planned clinical trials of this agent in breast cancer patients and may allow a more complete understanding of the molecular profile for cellular changes induced by this agent.

Task 12: Use of VEGF₁₂₁/rGel in combination with chemotherapeutic agents against MDA-MB231

We believe that combination of various modalities is critical to successful therapeutic approaches. Recent impressive data presented at ASCO (2005) demonstrate the power of combination of Herceptin antibody with conventional chemotherapy in an adjuvant setting in breast cancer patients. Much of the design for the adjuvant study with Herceptin was derived from combination therapy studies in xenograft models. Our original proposal SOW also included a final task to perform combination studies of VEGF₁₂₁/rGel with conventional agents. For the original reasons outlined we plan to continue combination studies in this next year. We believe this data may be eventually useful to identify potential synergistic/additive combinations for eventual clinical trials.

Unanticipated, Novel Findings of related to VEGF₁₂₁/rGel and This Proposal

Breast cancer metastases to bone are associated with significant morbidity and mortality. Patients with advanced breast cancer experience frequent bone metastasis. However, the pathophysiological processes leading to the development of breast skeletal metastases remains poorly understood. Since breast skeletal metastases are essentially untreatable, improvements in our understanding of the biological mechanisms behind breast cancer metastases to bone could enhance the development of regimens to treat this disease. Therefore, we have initiated studies to improve our understanding of the development of breast skeletal metastases by examining how breast tumors remodel bone, which result in both osteoblastic and osteolytic lesions. Osteoclastogenesis plays a central role in the development and maintenance of normal bone tissue, which requires osteoblastic matrix deposition and osteoclastic resorption to be closely coordinated. Interference with the process of osteoclastogenesis alters the kinetics of bone remodeling resulting in abnormal bone development. There is general consensus that the hematopoietically derived osteoclast is the pivotal cell in the degradation of the bone matrix. Osteoclast pre-cursor cells have been shown to be recruited to the future site of resorption by VEGF-A and RANKL, two cytokines that are expressed in the immediate vicinity of the bone surface. In addition, both of the major receptors of VEGF-A have been observed in osteoclasts, although some reports cite only the presence of Flt-1. The VEGF-Flt-1 interaction has been implicated in the recruitment process of osteoclast pre-cursor cells from hematopoietic tissue to the site of bone resorption. However, the role of each receptor, and its regulation, has yet to be established.

It has been hypothesized that osteoclasts play a critical role in the establishment of osteoblastic bone metastases by inducing bone resorption, which allows breast tumor cells to invade the bone and therefore promote tumor growth. VEGF plays an important role in the vascularization of bone tissues, as a mitogen for endothelial cells and as a chemo-attractant for both osteoblasts and osteoclasts. Therefore, establishing the precise role that each VEGF receptor plays in the maturation of osteoclast pre-cursor cells to osteoclasts is a critical step towards understanding the interaction that occurs between breast tumor cells and the bone microenvironment.

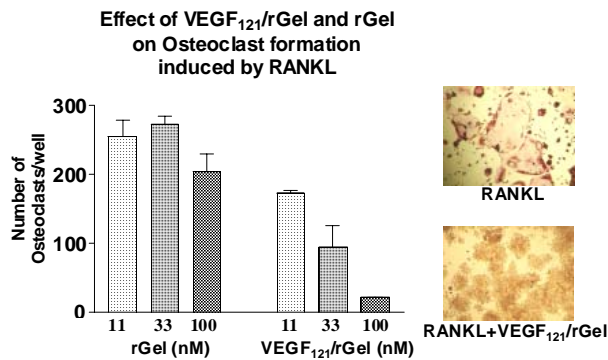


Figure 1. Effect of VEGF₁₂₁/rGel and rGel on RANKL-mediated osteoclast formation. Raw 264.7 cells were cultured overnight in 24-well plates. Osteoclast formation was induced by addition of 100 ng/ml RANKL with increasing concentrations of VEGF₁₂₁/rGel or rGel. Cells were allowed to differentiate for 96 hours followed by determination of the number of osteoclasts per well. Each experiment was performed in triplicate. The data shown is representative of three separate experiments. RANKL or RANKL + rGel-treated Raw 264.7 cells differentiate into large multi-nucleated TRAP-positive osteoclasts. In contrast, RANKL + VEGF₁₂₁/rGel-treated cells do not differentiate and do not stain for TRAP.

We have begun preliminary experiments examining the effect of VEGF₁₂₁/rGel on osteoclast formation in two model systems: (1) RAW 264.7 cells, cultured mouse osteoclast precursor cells that differentiate into mature osteoclasts upon stimulation with RANKL and (2) Bone marrow-derived macrophages (BMM), mouse primary cells that require stimulation with macrophage colony stimulating factor (MCSF) followed by RANKL for differentiation into osteoclasts. VEGF₁₂₁/rGel dramatically reduces osteoclastogenesis of both RAW 264.7 (Figure 1) and bone marrow-derived macrophages (Figure 2). Interestingly, a significantly lower concentration of VEGF₁₂₁/rGel is required to inhibit osteoclastogenesis in the primary bone marrow-derived cells than in RAW264.7 cells.

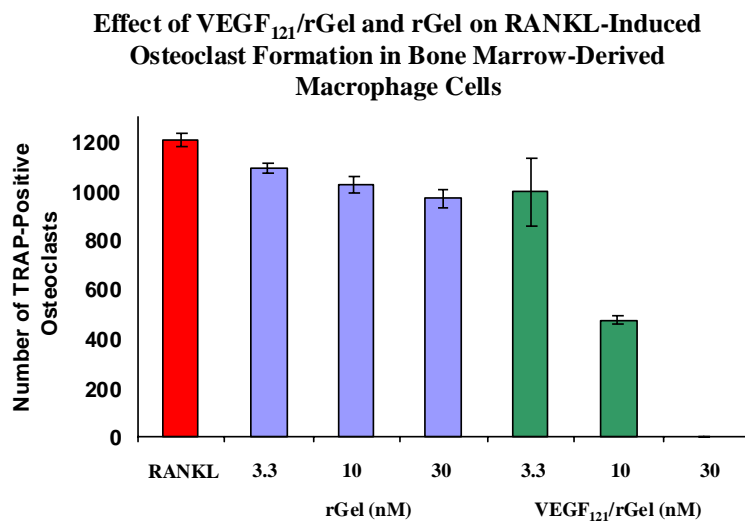


Figure 2. Effect of VEGF₁₂₁/rGel and rGel on RANKL-mediated osteoclast formation in bone marrow-derived macrophages (BMM). BMM cells were cultured overnight in 24-well plates with MCSF. Osteoclast formation was induced by addition of 100 ng/ml RANKL with increasing concentrations of VEGF₁₂₁/rGel or rGel. Cells were allowed to differentiate for 96 hours followed

by determination of the number of osteoclasts per well. Each experiment was performed in duplicate. RANKL or RANKL + rGel-treated BMM cells differentiate into large multinucleated TRAP-positive osteoclasts. In contrast, RANKL + VEGF₁₂₁/rGel-treated cells do not differentiate and do not stain for TRAP.

Treatment of Raw 264.7 cells with VEGF₁₂₁/rGel and rGel for 24 hours

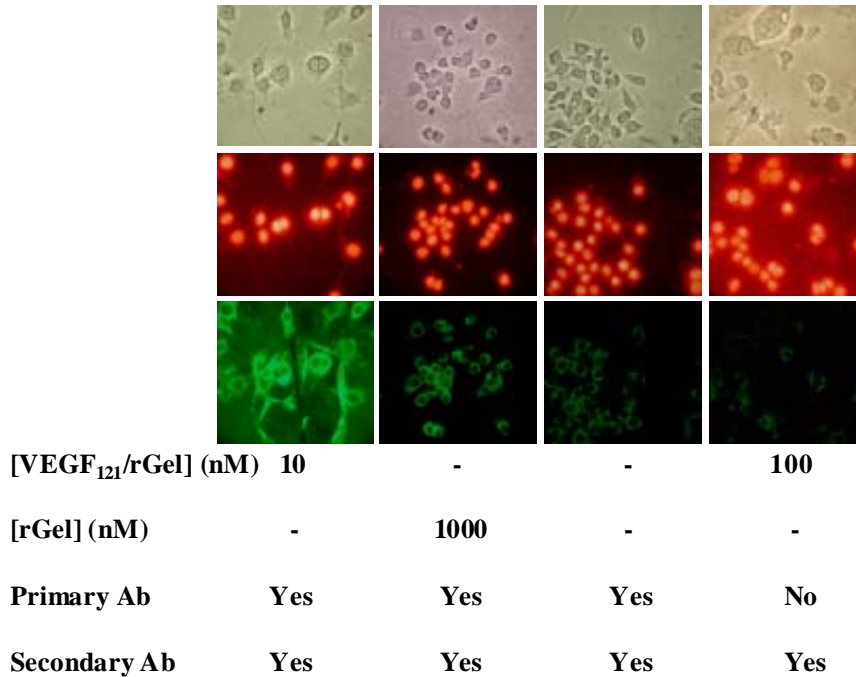


Figure 3. VEGF₁₂₁/rGel is internalized into RAW 264.7 cells. One thousand RAW 264.7 cells were plated into chamber slides and cultured overnight. Cells were then treated with VEGF₁₂₁/rGel and rGel for 24 hours. After the cell surface was stripped of membrane-bound VEGF₁₂₁/rGel or rGel, non-specific binding sites were blocked with 5% BSA and cells were permeabilized. Cells were treated with rabbit anti-gelonin (1:100) overnight followed by FITC-conjugated secondary antibody (1:80). Nuclei were stained with Propidium Iodide (middle row). VEGF₁₂₁/rGel is specifically internalized into RAW 264.7 cells (Column 1) as a 100-fold increase in rGel results in significantly lower internalization. Columns 3 and 4 serve as negative controls without antigen or primary antibody respectively.

We next examined whether the inhibition of osteoclastogenesis by VEGF₁₂₁/rGel is mediated by entry of the molecule into the cell or solely by disruption via cell signaling, we performed immunohistochemistry experiments on RAW 264.7 cells. Our results, shown in Figure 3, indicate that VEGF₁₂₁/rGel is internalized into the osteoclast pre-cursor cells within 24 hours, and that the internalization is due to the presence of VEGF₁₂₁, not gelonin. Thus, it is likely that inhibition of osteoclastogenesis is mediated (at least in part) by one of the receptors for VEGF₁₂₁, Flt-1 (VEGFR-1) or Flk-1/KDR (VEGFR-2).

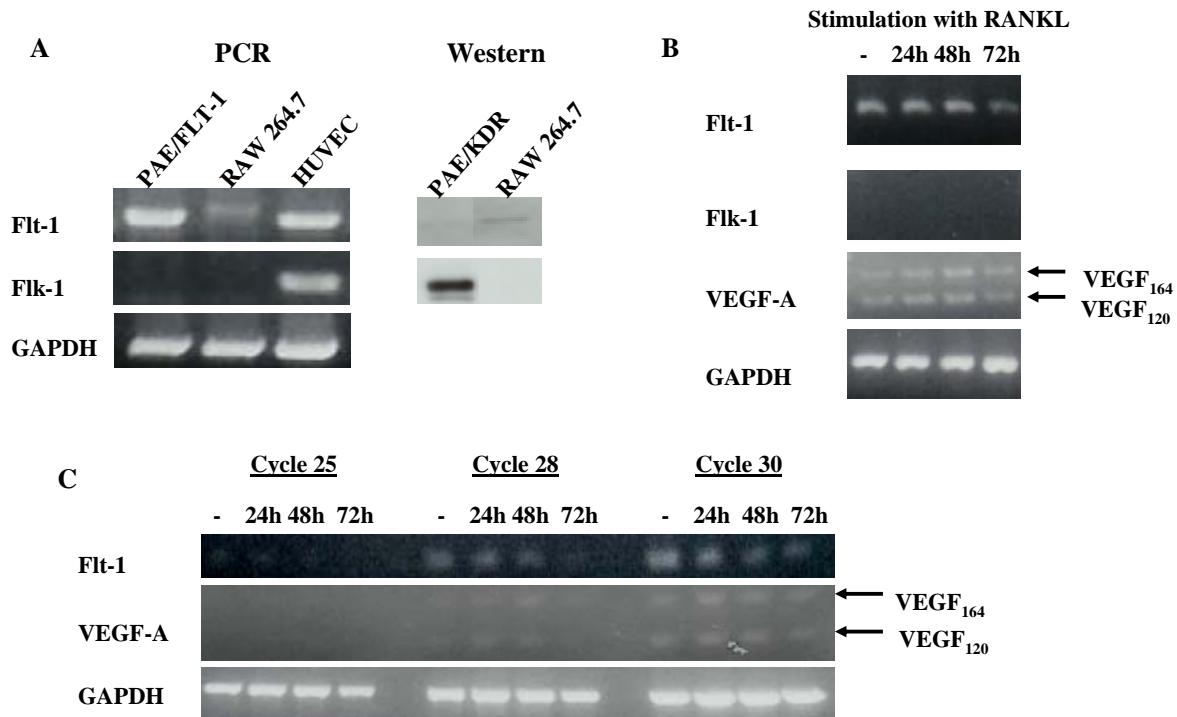


Figure 4

Figure 4. Flt-1 levels are down-regulated during osteoclastogenesis. The osteoclast precursor cell line RAW 264.7 cell line was cultured for 72 hours with MCSF with or without stimulation with RANKL for 24, 48 and 72 hours. Total RNA was harvested and subjected to PCR analysis using primers specific for Flk-1, Flt-1 and two isoforms of VEGF-A(164 and 120). RAW cells do not express Flk-1 but do express levels of Flt-1 receptor at levels lower than that of HUVEC. PCR analysis also suggests that Flt-1 is expressed by RAW cells, and that these levels decline during RANKL-stimulated osteoclastogenesis. RAW cells also express VEGF₁₂₀ and VEGF₁₆₄ isoforms, but not the VEGF₁₈₉ and VEGF₁₄₄ isoforms (not shown), (similar to MDA-MB-231 cells).

In order to understand whether the effect of VEGF₁₂₁/rGel is receptor-mediated, we initiated experiments to identify the presence of VEGF₁₂₁ receptors, and their role during osteoclastogenesis. This information is critical because the receptor target through which VEGF₁₂₁/rGel effects are mediated on osteoclasts is not known. This is significant because VEGF₁₂₁/rGel may inhibit breast cancer osteoblastic and osteolytic lesions in bone as a result of osteoclastogenesis inhibition. We have identified the presence of Flt-1, but not Flk-1, in BMM cells by PCR analysis (Figure 4). Interestingly, the levels of Flt-1 appear to decrease during osteoclast formation.

To determine the role of VEGF₁₂₁ receptors in VEGF₁₂₁/rGel-mediated cytotoxicity of osteoclast precursor cells, we pre-incubated RAW264.7 and BMM cells with neutralizing

antibodies to Flt-1 and Flk-1 for one hour prior to addition of VEGF₁₂₁/rGel, and monitored internalization of VEGF₁₂₁/rGel. Pretreatment of RAW264.7 cells and BMM cells with neutralizing antibodies to Flt-1, but not Flk-1, inhibited the localization of VEGF₁₂₁/rGel into these cells (Figure 3). In addition, PlGF was able to inhibit the VEGF₁₂₁/rGel-mediated cytotoxicity in both RAW264.7 and BMM cells. Taken together, this indicates that the Flt-1 receptor, but not the Flk-1 receptor, is responsible for mediating VEGF₁₂₁/rGel- induced cytotoxicity in osteoclast progenitor cells. FACS analysis indicated that 99% of the RAW264.7 cells expressed Flt-1 and 8% expressed Flk-1 and that 41.9% of the CD11b positive BMM cells expressed Flt-1 and 5.4% expressed Flk-1.

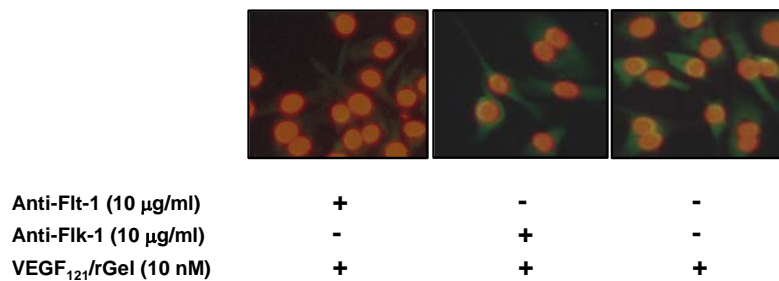


Figure 5. Flt-1, but not Flk-1, mediates the endocytosis and cytotoxic effect of VEGF₁₂₁/rGel. A, cells were pre-treated for one hour with 10 µg/ml of neutralizing antibodies to either Flt-1 or Flk-1 prior to the addition of 10 nM VEGF₁₂₁/rGel. The cells were fixed, acid-washed to remove surface-bound material, permeabilized, and immunostained for the presence of rGel (green). The cells were counterstained with propidium iodide (red) to identify nuclei.

In order to determine the role of VEGF and its receptors on bone formation *ex vivo*, we measured new bone formation by isolating calvariae from 4 day old mouse pups and cultured in media containing conditioned media from MDA PCa 2b cells. These cells were derived from a bone metastasis of prostate cancer and induce a specific increase in osteoblast growth and differentiation. VEGF₁₂₁/rGel-treatment showed complete inhibition of prostate cancer conditioned media-mediated bone formation. We have now begun to assess the role of VEGF and its receptors in this process.

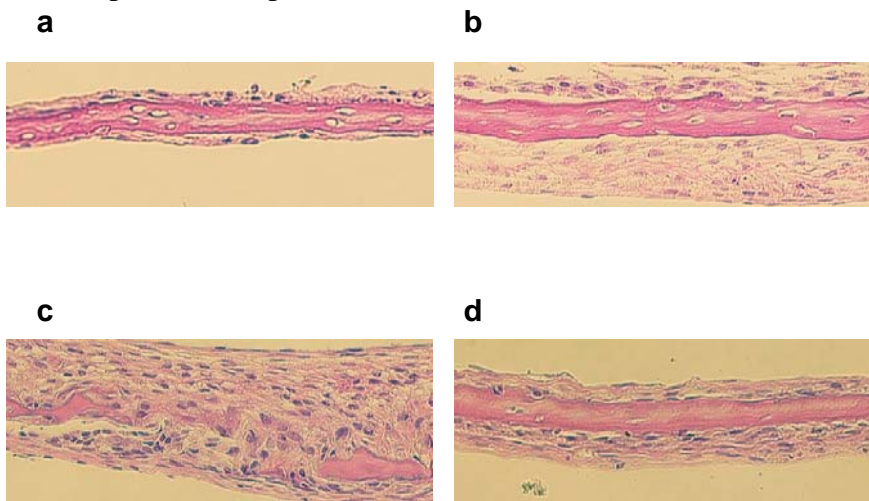


Figure 4. VEGF₁₂₁/rGel inhibits PCa 2b CM-mediated bone formation. Each calvaria was dissected into two. Effect of treatment was assessed in comparison to the internal negative or positive control. All experiments were done in triplicate. Concentrated conditioned media from PCa 2b cells was used to stimulate new bone formation in mouse calvariae isolated from 4-day old pups (final concentration of CM = 1x). To assess the effect of VEGF₁₂₁/rGel on PCa 2b-mediated bone formation, calvaria were either treated with CM alone or CM + 100 nM VEGF₁₂₁/rGel. Media was replaced after three days. Seven days after the start of the experiment, calvariae were fixed in 10% formalin, decalcified, and processed for H&E staining. a and b. Calvaria treated with media alone did not show any new bone formation (a) whereas, PCa 2b conditioned media stimulated new bone formation (b). c and d. PCa 2b CM-mediated bone formation (c) was inhibited by addition of 100 nM VEGF₁₂₁/rGel (d).

We have begun a very preliminary assessment of the effect of VEGF₁₂₁/rGel on the growth of MDA-MB-231 breast cancer cells in the tibia of nude mice. Approximately one million cells were injected, and treatment with VEGF₁₂₁/rGel and Saline began the following day. Unfortunately, many of the animals could not complete the study due to drug-related toxicity. A histomorphometric assessment of the very few animals remaining show bone tumor area/total bone area to be 0.896 in control mice (n=2) and 0.676 in VEGF₁₂₁/rGel-treated mice (n=3). The data is not significant because of the final number of animals, but suggests that VEGF₁₂₁/rGel-treatment can result in significant inhibition of bone loss. We plan to repeat this experiment at a lower dose of VEGF₁₂₁/rGel, and to reduce the total number of cells injected.

Key Research Accomplishments

- **Described the Pharmacokinetics and Tissue Distribution of VEGF₁₂₁/rGel to allow rational development of an optimal therapeutic schedule on which to base both murine and eventual clinical studies.**
- **Described significant in vivo antitumor effects of VEGF₁₂₁/rGel against orthotopically-placed breast tumor xenografts. Demonstrated complete regression of primary orthotopic breast tumors in 50% of treated mice (3/6).**
- **Identified significant vascular-ablative effects of VEGF₁₂₁/rGel on breast metastatic foci present in lung. Identified the impact this agent appears to have in suppressing the development of tumor metastases by destruction of tumor vascular endothelium and drug-induced downregulation of flk-1 receptors in tumor endothelium.**
- **Identified a unique aspect of therapy using VEGF₁₂₁/rGel in that lung metastases of treated mice have virtually no vasculature and appear to grow to the approximate limit of oxygen diffusion for avascular tissues.**
- **Identified 22 unique genes associated with the development cytotoxic effects of the rGel toxin component on vascular endothelial cells.**
- **Confirmed the Gene Chip results via RT-PCR and Western analysis. Provided a unique gene “fingerprint” for intoxication of cells by VEGF₁₂₁/rGel which provides information as to the exact molecular mechanism of action of this agent and may provide a molecular rationale for combinations with other therapeutic agents.**
- **Identified a unique set of genes upregulated and downregulated in MDA-MB-231 breast tumor cells co-cultured with endothelial cells in response to treatment with VEGF₁₂₁/rGel and under both normoxic and hypoxic conditions.**

- **Provided significant rationale for continued pre-clinical development of VEGF₁₂₁/rGel as a vascular-ablative agent in breast cancer.**
- **Described the unique ability of this fusion construct to inhibit skeletal tumor metastases in vivo. The mechanism of action appears to be through direct inhibition of normal osteoclast function which appears to be essential for bone remodeling in the development of skeletal metastases.**
- **Identified an unanticipated mechanism of action of this fusion construct which indicates a role for VEGF in development of skeletal metastases.**

Reportable Outcomes:

Abstracts:

1. **In Vitro and Animal Model Studies of VEGF₁₂₁/rGel Fusion Toxin Effects on Breast Cancer Cells.** *Khalid A. Mohamedali, Lawrence Cheung, Sophia Ran, Philip Thorpe and Michael G. Rosenblum.* MD Anderson Cancer Center, Houston, TX and U.T. Southwestern, Dallas, TX. AACR Meeting in April 2002, San Francisco, CA.
2. **VEGF121-gelonin fusion toxin specifically localizes to tumor blood vessels and induces robust vascular damage in human tumor xenograft models.** *Sophia Ran, Khalid Mohamedali, Lawrence Cheung, Philip E. Thorpe, and Michael G. Rosenblum.* Southwestern Medical Center, UT at Dallas, Dallas, TX, and M.D. Anderson Cancer Center, Houston, TX. AACR Meeting in April 2002, San Francisco, CA.
3. **VEGF121-gelonin fusion protein inhibits breast cancer metastasis in nude mice.** *Sophia Ran, Khalid Mohamedali, Philip E. Thorpe, and Michael G. Rosenblum.* University of Texas at Dallas, Dallas, TX; M.D. Anderson Cancer Center, Houston, TX. AACR Meeting in July 2003, Washington, DC.
4. **Vascular Targeting with VEGF₁₂₁/rGel Inhibits Angiogenesis: Specific Effects Assessed Using Micro-Array Analysis.** *Mohamedali KA, Gomez-Manzano C, Ramdas L, Xu J, Cheung L, Luster T, Thorpe P, Rosenblum MG.* 04-AB-5397-AACR, March 2004, Orlando, FL.
5. **Targeting Skeletal Metastases in Prostate Cancer with a Novel VEGF₁₂₁ Fusion Toxin.** *Poblenz AT, Mohamedali KA, Rosenblum MG, Darnay BG.* SA-099. ASBMR, October 2004, Seattle, WA.
6. **The Vascular Targeting Agent VEGF₁₂₁/rGel Inhibits Bone Remodeling and Skeletal Metastases through a Unique Mechanism.** *Mohamedali K, Poblenz A, Sikes C, Luster T, Navone N, Thorpe P, Darnay B, Rosenblum MG.* AACR Meeting in April 2005, Anaheim, CA.
7. **Identification of the Role of VEGF Receptors in Bone Remodeling by the Vascular Targeting Agent VEGF₁₂₁/rGel.** *Mohamedali K, Poblenz A, Kim S, Yang J, Navone N, Thorpe P, Darnay B., Rosenblum MG.* AACR Meeting in April 2006, Washington, DC.

Manuscripts:

1. Mohamedali KA, Poblenz AT, Sikes C, Novone N, Thorpe P, Darnay B and Rosenblum M. Inhibition of Prostate Tumor Growth and Bone Remodeling by the Vascular Targeting Agent VEGF₁₂₁/rGel. Manuscript accepted for publication pending revisions, Cancer Research (See Appendices #2).

2. Ran S, Mohamedali K, Thorpe P, Rosenblum M. The vascular-ablative agent VEGF₁₂₁/rGel inhibits pulmonary metastases of MDA-MB-231 breast tumors. *Neoplasia* 7(5):486-496, 2005 (See Appendices #3).
3. Lyu M-A, Kurzrock R, Rosenblum M. The immunocytokine scFv23/TNF targeting HER-2/neu induces synergistic cytotoxic effects with 5-fluorouracil in TNF-resistant pancreatic cancer cells. *Neoplasia*, submitted. (See Appendices #4).
4. Mohamedali K, Gomez-Manzano C, Ramdas L, Xu J, Cheung L, Zhang W, Thorpe P, Rosenblum M. VEGF₁₂₁/rGel fusion toxin targets the KDR receptor to inhibit vascular endothelial growth *in vitro* and *in vivo*: specific effects assessed using microarray analysis. *Journal of Biological Chemistry*, submitted (See Appendices #5).
5. Mohamedali KA, Ran S, Cheung L, Marks JW, Hittelman WN, Waltenberger J, Thorpe P, Rosenblum MG. Mechanistic and Internalization Studies of VEGF₁₂₁/rGel: Cytotoxicity on Endothelial Cells Mediated by VEGFR2 but not by VEGFR1. *International Journal of Cancer*, accepted for publication pending revisions (See Appendices#).

Conclusions:

Vascular targeting as an approach to tumor therapy holds significant promise for the treatment of solid tumors. However, many current approaches attempting to inhibit the neovascularization process through small molecule inhibitors of VEGFR signaling, antibodies to VEGF itself or to the VEGFR2 have not met with success. This is due in part to the multiply-redundant and robust process which tumor vascularization represents. On the other hand, lethal damage to tumor endothelium using the VEGF₁₂₁/rGel fusion toxin is a comparatively unique approach. This construct has remarkable and long-term antitumor effects in xenograft models as opposed to other agents that have limited activity in their own right. Dr. Louise Gorchow, Head of CTEP has indicated in a public presentation that the VEGF₁₂₁/rGel fusion toxin is one of a very few agents with these properties. The data presented above and in the attached Appendix demonstrates that this agent can reduce the growth of both orthotopic breast tumors and can significantly limit the metastatic spread of a breast metastatic model. In addition, the lung metastases that do survive appear to have a much lower vascular supply and a limited tumor cell turnover rate suggesting a reduced growth and metastatic potential. No other vascular targeting agents have thus far demonstrated such unique effects in an *in vivo* model. Of interest will be to examine the impact this fusion toxin will have on survival in this metastatic model. In addition, our findings examining the mechanism of direct action of the fusion construct on endothelial cells has significance in more exactly understanding how toxins work at the molecular level and may be an important first step in understanding how to more effectively employ these agents for therapeutic advantage. Furthermore, the importance of understanding how vascular targeting agents affect tumor cells indirectly may also have therapeutic significance in understanding the rationale for combinations of these vascular targeting agents with conventional chemotherapeutic agents, or with radiotherapeutic or biological agents. Finally, we have identified that development of breast tumor skeletal metastases apparently require VEGF and the VEGF-receptor pathway. Our studies have demonstrated that the VEGF₁₂₁/rGel fusion construct can significantly inhibit skeletal metastases through a unique inhibition of osteoclast maturation and function *in vitro* and probably *in vivo*. This suggests that the VEGF₁₂₁/rGel fusion construct may therefore be useful for the prevention and treatment of skeletal metastases in breast cancer and perhaps for skeletal metastases in other types of cancers as well.

References

1. Birnbaum, D. VEGF-FLT1 receptor system: a new ligand-receptor system involved in normal and tumor angiogenesis. *Jpn.J.Cancer Res.*, 86: 1, 1995.
2. Kerbel, R. S. Tumor angiogenesis: past, present and the near future. *Carcinogenesis*, 21: 505-515, 2000.
3. Bando, H. and Toi, M. Tumor angiogenesis, macrophages, and cytokines. *Adv.Exp.Med.Biol.*, 476: 267-284, 2000.
4. Falterman, K. W., Ausprunk, H., and Klein, M. D. Role of tumor angiogenesis factor in maintenance of tumor-induced vessels. *Surg.Forum*, 27: 157-159, 1976.
5. Patt, L. M. and Houck, J. C. Role of polypeptide growth factors in normal and abnormal growth. *Kidney Int.*, 23: 603-610, 1983.
6. Ravi, R., Mookerjee, B., Bhujwalla, Z. M., Sutter, C. H., Artemov, D., Zeng, Q., Dillehay, L. E., Madan, A., Semenza, G. L., and Bedi, A. Regulation of tumor angiogenesis by p53-induced degradation of hypoxia-inducible factor 1alpha. *Genes Dev.*, 14: 34-44, 2000.
7. Folkman, J. Proceedings: Tumor angiogenesis factor. *Cancer Res.*, 34: 2109-2113, 1974.
8. Strugar, J., Rothbart, D., Harrington, W., and Criscuolo, G. R. Vascular permeability factor in brain metastases: correlation with vasogenic brain edema and tumor angiogenesis. *J.Neurosurg.*, 81: 560-566, 1994.
9. Jaeger, T. M., Weidner, N., Chew, K., Moore, D. H., Kerschmann, R. L., Waldman, F. M., and Carroll, P. R. Tumor angiogenesis correlates with lymph node metastases in invasive bladder cancer. *J.Urol.*, 154: 69-71, 1995.
10. Melnyk, O., Zimmerman, M., Kim, K. J., and Shuman, M. Neutralizing anti-vascular endothelial growth factor antibody inhibits further growth of established prostate cancer and metastases in a pre-clinical model. *J.Urol.*, 161: 960-963, 1999.
11. Aranda, F. I. and Laforga, J. B. Microvessel quantitation in breast ductal invasive carcinoma. Correlation with proliferative activity, hormonal receptors and lymph node metastases. *Pathol.Res.Pract.*, 192: 124-129, 1996.
12. Fox, S. B., Leek, R. D., Bliss, J., Mansi, J. L., Gusterson, B., Gatter, K. C., and Harris, A. L. Association of tumor angiogenesis with bone marrow micrometastases in breast cancer patients. *J.Natl.Cancer Inst.*, 89: 1044-1049, 1997.
13. Senger, D. R., Van de, W. L., Brown, L. F., Nagy, J. A., Yeo, K. T., Yeo, T. K., Berse, B., Jackman, R. W., Dvorak, A. M., and Dvorak, H. F. Vascular permeability factor (VPF, VEGF) in tumor biology. *Cancer Metastasis Rev.*, 12: 303-324, 1993.
14. McMahon, G. VEGF receptor signaling in tumor angiogenesis. *Oncologist.*, 5 Suppl 1: 3-10, 2000.

15. Obermair, A., Kucera, E., Mayerhofer, K., Speiser, P., Seifert, M., Czerwenka, K., Kaider, A., Leodolter, S., Kainz, C., and Zeillinger, R. Vascular endothelial growth factor (VEGF) in human breast cancer: correlation with disease-free survival. *Int.J.Cancer*, 74: 455-458, 1997.
16. Miyoshi, C. and Ohshima, N. Vascular endothelial growth factor (VEGF) expression regulates angiogenesis accompanying tumor growth in a peritoneal disseminated tumor model. *In Vivo*, 15: 233-238, 2001.
17. Neufeld, G., Cohen, T., Gengrinovitch, S., and Poltorak, Z. Vascular endothelial growth factor (VEGF) and its receptors. *FASEB J.*, 13: 9-22, 1999.
18. Shibuya, M. Role of VEGF-flt receptor system in normal and tumor angiogenesis. *Adv.Cancer Res.*, 67: 281-316, 1995.
19. Detmar, M. The role of VEGF and thrombospondins in skin angiogenesis. *J.Dermatol.Sci.*, 24 Suppl 1: S78-S84, 2000.
20. Verheul, H. M. and Pinedo, H. M. The Role of Vascular Endothelial Growth Factor (VEGF) in Tumor Angiogenesis and Early Clinical Development of VEGF-Receptor Kinase Inhibitors. *Clin.Breast Cancer*, 1 Suppl 1: S80-S84, 2000.
21. McCabe, C. J., Boelaert, K., Tannahill, L. A., Heaney, A. P., Stratford, A. L., Khaira, J. S., Hussain, S., Sheppard, M. C., Franklyn, J. A., and Gittoes, N. J. Vascular endothelial growth factor, its receptor KDR/Flk-1, and pituitary tumor transforming gene in pituitary tumors. *J.Clin.Endocrinol.Metab*, 87: 4238-4244, 2002.
22. Kranz, A., Mattfeldt, T., and Waltenberger, J. Molecular mediators of tumor angiogenesis: enhanced expression and activation of vascular endothelial growth factor receptor KDR in primary breast cancer. *Int.J.Cancer*, 84: 293-298, 1999.
23. Harada, Y., Ogata, Y., and Shirouzu, K. Expression of vascular endothelial growth factor and its receptor KDR (kinase domain-containing receptor)/Flk-1 (fetal liver kinase-1) as prognostic factors in human colorectal cancer. *Int.J.Clin.Oncol.*, 6: 221-228, 2001.
24. Padro, T., Bieker, R., Ruiz, S., Steins, M., Retzlaff, S., Burger, H., Buchner, T., Kessler, T., Herrera, F., Kienast, J., Muller-Tidow, C., Serve, H., Berdel, W. E., and Mesters, R. M. Overexpression of vascular endothelial growth factor (VEGF) and its cellular receptor KDR (VEGFR-2) in the bone marrow of patients with acute myeloid leukemia. *Leukemia*, 16: 1302-1310, 2002.
25. Wedge, S. R., Ogilvie, D. J., Dukes, M., Kendrew, J., Curwen, J. O., Hennequin, L. F., Thomas, A. P., Stokes, E. S., Curry, B., Richmond, G. H., and Wadsworth, P. F. ZD4190: an orally active inhibitor of vascular endothelial growth factor signaling with broad-spectrum antitumor efficacy. *Cancer Res.*, 60: 970-975, 2000.
26. Laird, A. D., Vajkoczy, P., Shawver, L. K., Thurnher, A., Liang, C., Mohammadi, M., Schlessinger, J., Ullrich, A., Hubbard, S. R., Blake, R. A., Fong, T. A., Strawn, L. M., Sun,

- L., Tang, C., Hawtin, R., Tang, F., Shenoy, N., Hirth, K. P., McMahon, G., and Cherrington SU6668 is a potent antiangiogenic and antitumor agent that induces regression of established tumors. *Cancer Res.*, 60: 4152-4160, 2000.
27. Haluska, P. and Adjei, A. A. Receptor tyrosine kinase inhibitors. *Curr.Opin.Investig.Drugs*, 2: 280-286, 2001.
 28. Fabbro, D., Ruetz, S., Bodis, S., Pruschy, M., Csermak, K., Man, A., Campochiaro, P., Wood, J., O'Reilly, T., and Meyer, T. PKC412--a protein kinase inhibitor with a broad therapeutic potential. *Anticancer Drug Des*, 15: 17-28, 2000.
 29. Fabbro, D., Buchdunger, E., Wood, J., Mestan, J., Hofmann, F., Ferrari, S., Mett, H., O'Reilly, T., and Meyer, T. Inhibitors of protein kinases: CGP 41251, a protein kinase inhibitor with potential as an anticancer agent. *Pharmacol.Ther.*, 82: 293-301, 1999.
 30. Sun, L. and McMahon, G. Inhibition of tumor angiogenesis by synthetic receptor tyrosine kinase inhibitors. *Drug Discov.Today*, 5: 344-353, 2000.
 31. Solorzano, C. C., Baker, C. H., Bruns, C. J., Killion, J. J., Ellis, L. M., Wood, J., and Fidler, I. J. Inhibition of growth and metastasis of human pancreatic cancer growing in nude mice by PTK 787/ZK222584, an inhibitor of the vascular endothelial growth factor receptor tyrosine kinases. *Cancer Biother.Radiopharm.*, 16: 359-370, 2001.
 32. Drevs, J., Hofmann, I., Hugenschmidt, H., Wittig, C., Madjar, H., Muller, M., Wood, J., Martiny-Baron, G., Unger, C., and Marme, D. Effects of PTK787/ZK 222584, a specific inhibitor of vascular endothelial growth factor receptor tyrosine kinases, on primary tumor, metastasis, vessel density, and blood flow in a murine renal cell carcinoma model. *Cancer Res.*, 60: 4819-4824, 2000.
 33. Dimitroff, C. J., Klohs, W., Sharma, A., Pera, P., Driscoll, D., Veith, J., Steinkampf, R., Schroeder, M., Klutchko, S., Sumlin, A., Henderson, B., Dougherty, T. J., and Bernacki, R. J. Anti-angiogenic activity of selected receptor tyrosine kinase inhibitors, PD166285 and PD173074: implications for combination treatment with photodynamic therapy. *Invest New Drugs*, 17: 121-135, 1999.
 34. Mendel, D. B., Schreck, R. E., West, D. C., Li, G., Strawn, L. M., Tanciongco, S. S., Vasile, S., Shawver, L. K., and Cherrington, J. M. The angiogenesis inhibitor SU5416 has long-lasting effects on vascular endothelial growth factor receptor phosphorylation and function. *Clin.Cancer Res.*, 6: 4848-4858, 2000.
 35. Prewett, M., Huber, J., Li, Y., Santiago, A., O'Connor, W., King, K., Overholser, J., Hooper, A., Pytowski, B., Witte, L., Bohlen, P., and Hicklin, D. J. Antivascular endothelial growth factor receptor (fetal liver kinase 1) monoclonal antibody inhibits tumor angiogenesis and growth of several mouse and human tumors. *Cancer Res.*, 59: 5209-5218, 1999.
 36. Chen, Y., Wiesmann, C., Fuh, G., Li, B., Christinger, H. W., McKay, P., de Vos, A. M., and Lowman, H. B. Selection and analysis of an optimized anti-VEGF antibody: crystal

structure of an affinity-matured Fab in complex with antigen. *J.Mol.Biol.*, 293: 865-881, 1999.

37. Ryan, A. M., Eppler, D. B., Hagler, K. E., Bruner, R. H., Thomford, P. J., Hall, R. L., Shopp, G. M., and O'Neill, C. A. Preclinical safety evaluation of rhuMAbVEGF, an antiangiogenic humanized monoclonal antibody. *Toxicol.Pathol.*, 27: 78-86, 1999.
38. Veenendaal, L. M., Jin, H., Ran, S., Cheung, L., Navone, N., Marks, J. W., Waltenberger, J., Thorpe, P., and Rosenblum, M. G. In vitro and in vivo studies of a VEGF121/rGelolin chimeric fusion toxin targeting the neovasculature of solid tumors. *Proc.Natl.Acad.Sci.U.S.A*, 99: 7866-7871, 2002.

Key Personnel

Michael G. Rosenblum, Ph.D.	9/1/2003-1/01/2006
Mi-Ae Lyu	7/1/2002-3/31/2005
Sophia Ran	7/1/2002-3/31/2005
Maria Sambade	7/1/2002-3/31/3005
Julia Merchant	7/1/2002-8/28/2003
Michelle McCall	11/1/2003-1/1/2004

Appendices

Manuscripts:

1. Veenendaal, L. M., Jin, H., Ran, S., Cheung, L., Navone, N., Marks, J. W., Waltenberger, J., Thorpe, P., and Rosenblum, M.G. In vitro and in vivo studies of a VEGF₁₂₁/rGelonin chimeric fusion toxin targeting the neovasculature of solid tumors. *Proc. Natl. Acad. Sci. U.S.A.*, 99: 7866-7871, 2002.
2. Mohamedali KA, Poblentz AT, Sikes C, Novone N, Thorpe P, Darnay B and Rosenblum M. Inhibition of Bone Remodeling and Prostate Skeletal Metastases by the Vascular Targeting Agent VEGF₁₂₁/rGel. *Nature Medicine*, submitted.
3. Ran S, Mohamedali K, Thorpe P, Rosenblum M. The vascular-ablative agent VEGF₁₂₁/rGel inhibits pulmonary metastases of MDA-MB-231 breast tumors. *Neoplasia* 7(5):486-496, 2005.
4. Lyu M-A, Kurzrock R, Rosenblum M. The immunocytokine scFv23/TNF targeting HER-2/neu induces synergistic cytotoxic effects with 5-fluorouracil in TNF-resistant pancreatic cancer cells. *Neoplasia*, submitted.
5. Mohamedali K, Gomez-Manzano C, Ramdas L, Xu J, Cheung L, Zhang W, Thorpe P, Rosenblum M. VEGF₁₂₁/rGel fusion toxin targets the KDR receptor to inhibit vascular endothelial growth *in vitro* and *in vivo*: specific effects assessed using microarray analysis. *Journal of Biological Chemistry*, submitted.
6. Mohamedali KA, Ran S, Cheung L, Marks JW, Hittelman WN, Waltenberger J, Thorpe P, Rosenblum MG. Mechanistic and Internalization Studies of VEGF₁₂₁/rGel: Cytotoxicity on Endothelial Cells Mediated by VEGFR2 but not by VEGFR1. *International Journal of Cancer*, accepted for publication pending revisions.

Abstracts:

7. **In Vitro and Animal Model Studies of VEGF₁₂₁/rGel Fusion Toxin Effects on Breast Cancer Cells.** *Khalid A. Mohamedali, Lawrence Cheung, Sophia Ran, Philip Thorpe and Michael G. Rosenblum.* MD Anderson Cancer Center, Houston, TX and U.T. Southwestern, Dallas, TX. AACR Meeting in April 2002, San Francisco, CA.
8. **VEGF₁₂₁-gelonin fusion toxin specifically localizes to tumor blood vessels and induces robust vascular damage in human tumor xenograft models.** *Sophia Ran, Khalid Mohamedali, Lawrence Cheung, Philip E. Thorpe, and Michael G. Rosenblum.* Southwestern Medical Center, UT at Dallas, Dallas, TX, and M.D. Anderson Cancer Center, Houston, TX. AACR Meeting in April 2002, San Francisco, CA.
9. **VEGF₁₂₁-gelonin fusion protein inhibits breast cancer metastasis in nude mice.** *Sophia Ran, Khalid Mohamedali, Philip E. Thorpe, and Michael G. Rosenblum.* University of Texas at Dallas, Dallas, TX; M.D. Anderson Cancer Center, Houston, TX. AACR Meeting in July 2003, Washington, DC.
10. **Vascular Targeting with VEGF₁₂₁/rGel Inhibits Angiogenesis: Specific Effects Assessed Using Micro-Array Analysis.** *Mohamedali KA, Gomez-Manzano C, Ramdas L, Xu J, Cheung L, Luster T, Thorpe P, Rosenblum MG.* 04-AB-5397-AACR, March 2004, Orlando, FL.
11. **Targeting Skeletal Metastases in Prostate Cancer with a Novel VEGF₁₂₁ Fusion Toxin.** *Poblentz AT, Mohamedali KA, Rosenblum MG, Darnay BG.* SA-099. ASBMR, October 2004, Seattle, WA.

12. **The Vascular Targeting Agent VEGF₁₂₁/rGel Inhibits Bone Remodeling and Skeletal Metastases through a Unique Mechanism.** *Mohamedali K, Poblentz A, Sikes C, Luster T, Navone N, Thorpe P, Darnay B, Rosenblum MG.* AACR Meeting in April 2005, Anaheim, CA.
13. **Identification of the Role of VEGF Receptors in Bone Remodeling by the Vascular Targeting Agent VEGF₁₂₁/rGel.** *Mohamedali K, Poblentz A, Kim S, Yang J, Navone N, Thorpe P, Darnay B, Rosenblum MG.* AACR Meeting in April 2006, Washington, DC.

In vitro and *in vivo* studies of a VEGF₁₂₁/rGelonin chimeric fusion toxin targeting the neovasculature of solid tumors

Liesbeth M. Veenendaal^{*†}, Hangqing Jin^{*}, Sophia Ran[‡], Lawrence Cheung^{*}, Nora Navone^{§¶}, John W. Marks^{*}, Johannes Waltenberger[¶], Philip Thorpe[‡], and Michael G. Rosenblum^{*,**}

^{*}Immunopharmacology and Targeted Therapy Section, Department of Bioimmunotherapy, and [§]Genitourinary Medical Oncology Research, M. D. Anderson Cancer Center, 1515 Holcombe Boulevard, Houston, TX 77030-4009; [†]Hamon Center for Therapeutic Oncology Research, Southwestern Medical Center, University of Texas, 2201 Inwood Road, Dallas, TX 75390-8594; and [¶]Med Klinik und Poliklinik der Universität Ulm, Abteilung Innere Medizin II, Robert-Koch-Strasse 8, 89081 Ulm, Germany

Communicated by Richard E. Smalley, Rice University, Houston, TX, March 18, 2002 (received for review November 13, 2001)

Vascular endothelial growth factor (VEGF) plays a key role in the growth and metastasis of solid tumors. We generated a fusion protein containing VEGF₁₂₁ linked by a flexible G₄S tether to the toxin gelonin (rGel) and expressed this as a soluble protein in bacteria. Purified VEGF₁₂₁/rGel migrated as an 84-kDa homodimer under non-reducing conditions. VEGF₁₂₁/rGel bound to purified, immobilized Flk-1, and the binding was competed by VEGF₁₂₁. Both VEGF₁₂₁/rGel and VEGF₁₂₁ stimulated cellular kinase insert domain receptor (KDR) phosphorylation. The VEGF₁₂₁/rGel fusion construct was highly cytotoxic to endothelial cells overexpressing the KDR/Flk-1 receptor. The IC₅₀ of the construct on dividing endothelial cells expressing 10⁵ or more KDR/Flk-1 receptors per cell was 0.5–1 nM, as compared with 300 nM for rGel itself. Dividing endothelial cells overexpressing KDR were approximately 60-fold more sensitive to VEGF₁₂₁/rGel than were nondividing cells. Endothelial cells overexpressing FLT-1 were not sensitive to the fusion protein. Human melanoma (A-375) or human prostate (PC-3) xenografts treated with the fusion construct demonstrated a reduction in tumor volume to 16% of untreated controls. The fusion construct localized selectively to PC-3 tumor vessels and caused thrombotic damage to tumor vessels with extravasation of red blood cells into the tumor bed. These studies demonstrate the successful use of VEGF₁₂₁/rGel fusion construct for the targeted destruction of tumor vasculature *in vivo*.

Vascular endothelial growth factor (VEGF)-A plays a central role in the growth and metastasis of solid tumors (1–10). Through alternative splicing of RNA, human VEGF exists as at least four isoforms of 121, 165, 189, or 206 aa (11–14). The lowest molecular weight isoform, designated VEGF₁₂₁, is a non-heparan sulfate-binding isoform that exists in solution as a disulfide-linked homodimer.

The angiogenic actions of VEGF are mediated through two related receptor tyrosine kinases, kinase domain receptor (KDR) and FLT-1 in the human, and Flk-1 and Flt-1 in the mouse. Both are largely restricted to vascular endothelial cells (15–18). KDR/Flk-1 and FLT-1 receptors are overexpressed on the endothelium of tumor vasculature (15–24). In contrast, these receptors are almost undetectable in the vascular endothelium of adjacent normal tissues (18). The receptors for VEGF thus seem to be excellent targets for the development of therapeutic agents that inhibit tumor growth and metastatic spread through inhibition of tumor neovascularization. To this end, VEGF₁₂₁ would be an appropriate carrier to deliver a toxic agent selectively to tumor vascular endothelium.

The recombinant toxin gelonin (rGel) is a single chain N-glycosidase similar in its action to ricin A chain (25–28). Immunotoxins and fusion constructs containing rGel specifically kill tumor cells *in vitro* and *in vivo* (ref. 29 and M.G.R., L.C., C. R. Parach, and J.W.M., unpublished work) and have antitumor activity in mice. Gelonin does not seem to generate capillary leak syndrome (31), which limits use of other toxins.

Molecular engineering enabled the synthesis of novel chimeric molecules having therapeutic potential (32, 33). Chimeric fusion constructs targeting the IL-2 receptor, the EGF receptor, and other growth factor/cytokine receptors have been described (34, 35). Studies by Ramakrishnan *et al.* (36) showed that a chemical conjugate of VEGF and truncated diphtheria toxin has impressive cytotoxic activity on cell lines expressing receptors for VEGF. Further studies with VEGF/DT fusion constructs demonstrated selective toxicity to Caprice's sarcoma cells and dividing endothelial cells *in vitro* and *in vivo* (37).

Materials and Methods

The PCR reagents were obtained from Fisher Scientific, and the molecular biology enzymes were purchased from Roche Molecular Biochemicals or New England Biolabs. Bacterial strains, pET bacterial expression plasmids, and recombinant enterokinase were obtained from Novagen. All other chemicals were obtained from Sigma or Fisher Scientific.

Metal affinity resin (Talon) was obtained from CLONTECH. Other chromatography resin and materials were purchased from Amersham Pharmacia. Endothelial cell growth supplement from bovine neural tissue was obtained from Sigma. Murine brain endothelioma bEnd.3 cells were provided by Werner Risau (Max Plank Institute, Munich, Germany). Porcine aortic endothelial cells transfected with either the human FLT-1 receptor (PAE/FLT-1) or the KDR receptor (PAE/KDR) were developed as described (38). Soluble mouse Flk-1 was expressed in Sf9 cells as described by Warren *et al.* (24). The human melanoma A-375 M cell line was obtained from American Type Culture Collection. Tissue culture reagents were from GIBCO/BRL or Mediatech Cellgro (Herndon, VA). Rabbit anti-gelonin antisera was obtained from the Veterinary Medicine Core Facility at M. D. Anderson Cancer Center. BALB/c nude mice were purchased from The Jackson Laboratory and maintained under sterile pathogen-free conditions according to American Association of Laboratory Animal Care standards.

Construction of VEGF₁₂₁/rGel. The cDNA encoding human VEGF₁₂₁ and recombinant gelonin were fused together by using the splice overlap extension PCR method with VEGF and gelonin DNA as templates. Primers used were: VEGF Nterm, (5'-TGGTCCCAGGCTCATATGGCACCCATGGCAGAA-3'); VEGF Cterm, (5'-TCTAGACCGGAGCCACCGCCAC-

Abbreviations: VEGF, vascular endothelial growth factor; rGel, recombinant toxin gelonin.

[†]Present address: Krukenstraat 69, 3512 NE, Utrecht, The Netherlands.

[¶]Present address: M. D. Anderson Cancer Center, Genitourinary Medical Oncology Research, 1515 Holcombe Boulevard, Box 427, Houston, TX 77030-4009.

^{**}To whom reprint requests should be addressed at: Immunopharmacology and Targeted Therapy Section, Department of Bioimmunotherapy, M. D. Anderson Cancer Center, 1515 Holcombe Boulevard, Box 44, Houston, TX 77030-4009. E-mail: mrosenbl@notes.mdacc.tmc.edu.

CCCGCCTCGGCTTGTC-3'); Gel Nterm, (5'-GGTGGCG-GTGGCTCCGGTCTAGACACCGTGAGC-3'); Gel Cterm, (5'-AAGGCTCGTGTCGACCTCGAGTCATTAAGCTT-TAGGATCTTTATC-3'). A G₄S linker was incorporated between the VEGF₁₂₁ and the rGel sequences. Purified PCR products were digested with the restriction enzymes *Bsp*HI and *Xho*I and ligated into the pET-32a. The constructs were transformed into *Escherichia coli* strain AD494 (DE3) pLys S for expression of the fusion protein.

Protein Expression in *E. coli*. Bacterial colonies transformed with the plasmid carrying the VEGF₁₂₁/rGel insert were cultured in LB growth medium (Sigma) containing 200 µg/ml ampicillin, 70 µg/ml chloramphenicol, and 15 µg/ml kanamycin at 37°C overnight in a shaker bath at 240 rpm. The cultures then were diluted 1:20 with fresh LB medium with antibiotics and grown to early log phase ($A_{600} = 0.6$) at 37°C. Thereafter, the cultures were diluted 1:1 with fresh LB medium plus antibiotics; protein synthesis was induced at 23°C by the addition of 0.1 mM isopropyl β-D-thiogalactoside (IPTG) overnight. The cells were collected by centrifugation, resuspended in 10 mM Tris-HCl (pH 8.0), and frozen.

Protein Purification. Frozen bacterial cells were thawed, sonicated (5× for 10 sec each), and then lysed further by the addition of 1 mg/ml lysozyme in 10 mM Tris-HCl (pH 8.0) for 30 min at 4°C. The bacterial lysates were ultracentrifuged at 60,000 × *g* for 45 min at 4°C, adjusted to 40 mM Tris-HCl (pH 8.0), filtered (0.22 µm filter), and then loaded at room temperature onto a Talon-containing column. The column was washed with 40 mM Tris-HCl (pH 8.0) and 500 mM NaCl containing 5 mM imidazole and eluted with 100 mM imidazole. Protein-containing fractions were dialyzed into 20 mM Tris-HCl (pH 7.4) and 50 mM NaCl. The fusion protein was digested for 4 h at room temperature with recombinant enterokinase (20 units/mg of fusion protein) in the presence of 2 mM CaCl₂ to remove the hexa-histidine tag and then dialyzed into 20 mM Tris-HCl (pH 8.0)/50 mM NaCl. The samples were filter-sterilized before further use and stored at 4°C.

Anti-VEGF and Anti-rGel Western Blot Analysis. Protein samples were analyzed by SDS/15% PAGE under reducing conditions. The gel was electrophoretically transferred to nitrocellulose overnight at 4°C in transfer buffer (25 mM Tris-HCl, pH 7.6/190 mM glycine/20% HPLC-grade methanol). The membranes were blocked by the addition of 5% BSA in Western blocking buffer [Tris-buffered saline (0.05 M Tris, 0.15 M NaCl) (TBS)/0.5% Tween-20] and then incubated for 1 h with rabbit anti-gelonin polyclonal antibody (2 µg/ml in TBS/Tween) or mouse anti-VEGF monoclonal antibody 2C3 (2 µg/ml in TBS/Tween). The membrane then was incubated with goat-anti-rabbit IgG horseradish peroxidase (HRP) or goat-anti-mouse IgG-HRP (1: 5,000 dilution in TBS/Tween). Then, the membrane was developed with the Amersham Pharmacia enhanced chemiluminescence (ECL) detection system and exposed to x-ray film.

Rabbit Reticulocyte Lysate Assay. The functional activity of rGel and VEGF₁₂₁/rGel were assayed by using a cell-free protein translation inhibition assay kit from Amersham Pharmacia as described by the manufacturer.

Binding of VEGF₁₂₁/rGel to Flk-1. Binding to Flk-1 was tested on microtiter plates coated with soluble mouse Flk-1. Plates were treated with 2 µg/ml of NeutrAvidin (Pierce) for 6 h. Purified, biotinylated Flk-1 (24) was incubated with NeutrAvidin-coated wells for 2 h. VEGF₁₂₁ or VEGF₁₂₁/rGel was added to the wells at various concentrations in the presence of PBS containing 2% (vol/vol) BSA. After 2 h of incubation, plates were washed and incubated with nonblocking mouse monoclonal anti-VEGF an-

tibody, 2C3 (39), or rabbit polyclonal anti-gelonin IgG. For competition studies of VEGF₁₂₁/rGel and VEGF₁₂₁, binding of the VEGF₁₂₁/rGel fusion protein was detected by using a rabbit anti-gelonin antibody. Mouse and rabbit IgG were detected by HRP-labeled goat anti-mouse and anti-rabbit antibodies, respectively (Dako). Peroxidase activity was measured by adding O-phenylenediamine (0.5 mg/ml) and hydrogen peroxide (0.03% vol/vol) in citrate-phosphate buffer (pH 5.5). The reaction was stopped by the addition of 100 µl of 0.18 M of H₂SO₄. The absorbance was read at 490 nM. In competition experiments, a 10-fold molar excess of VEGF₁₂₁ was premixed with VEGF₁₂₁/rGel before addition to the plate.

Cytotoxicity of VEGF₁₂₁/rGel to Adult Bovine Aortic Arch-Derived Endothelial (ABAE) Cells. Log-phase ABAE cells in DMEM [10% (vol/vol) FBS] were diluted to 4,000 cells per 200 µl. Aliquots (200 µl) were added to 96-well flat-bottomed tissue culture plates and incubated at 37°C for 1–72 h in 5% CO₂. Purified VEGF₁₂₁/rGel or rGel were diluted in culture medium to various concentrations, added to the plate, and the cultures were incubated for 72 h. Remaining adherent cells were stained by the addition of 100 µl of crystal violet [0.5% in 20% (vol/vol) methanol]. Dye-stained cells were solubilized by the addition of 100 µl of Sorenson's buffer [0.1 M sodium citrate, pH 4.2 in 50% (vol/vol) ethanol]. The absorbance was measured at 595 nM.

Cytotoxicity of VEGF₁₂₁/rGel to Mouse Brain-Derived Endothelial Cells bEnd.3. Cells were seeded at a density of 50,000 per well in 24-well plates. Twenty-four hours later, VEGF₁₂₁/rGel or rGel alone were added at various concentrations. After 5 days of treatment at 37°C, remaining attached cells were trypsinized and counted. The results are presented as total cell number per well. Two identical experiments were performed in duplicate. Standard error in all experiments was less than 5% of the mean.

Cytotoxicity of VEGF₁₂₁/rGel to PAE/KDR Cells and PAE/FLT-1 Cells. Log-phase PAE/KDR cells and PAE/FLT-1 cells in F-12 medium [10% (vol/vol) FBS] were diluted to 3,000 cells per 200 µl. Aliquots (200 µl) were added to 96-well flat-bottomed tissue culture plates and incubated at 37°C for 24 h in 5% CO₂. Purified VEGF₁₂₁/rGel or rGel were diluted in culture medium, added to the plate, and incubated for 72 h. Adherent cells were quantified by using the crystal violet staining method described above.

Kinase Activity of KDR in PAE/KDR Cells Exposed to VEGF₁₂₁/rGel or VEGF₁₂₁. PAE/KDR cells were incubated overnight in F-12 culture medium and then incubated at 37°C for 5 min with 100 µM Na₃VO₄. VEGF or VEGF₁₂₁/rGel then were added and, at various times, cells were lysed by the addition of a lysis buffer [50 mM Hepes, pH 7.4/150 mM NaCl/1 mM EGTA/10 mM sodium pyrophosphate/1.5 mM MgCl₂/100 mM NaF/10% (vol/vol) glycerol/1% Triton X-100]. Cell lysates were centrifuged (16,000 × *g*), the supernatants were removed, and their protein concentrations were determined. Lysate supernatants were incubated with 9 µg anti-phosphotyrosine monoclonal antibody (Santa Cruz Biotechnology) for 2 h at 4°C and then precipitated by the addition of Protein A Sepharose beads for 2 h at 4°C. Beads were washed and mixed with SDS sample buffer, heated for 5 min at 100°C, centrifuged, analyzed by SDS/10% PAGE, and then transferred to nitrocellulose filters. The membranes were blocked with 5% nonfat dry milk and incubated with rabbit polyclonal anti-KDR antibody (1:250; Santa Cruz Biotechnology) for 1 h at room temperature. The membranes then were washed, incubated with a peroxidase-linked goat anti-rabbit antibody (1:2,000) for 1 h at room temperature, and then enhanced chemiluminescence reagent (Amersham Pharmacia) was used to visualize the immunoreactive bands.

Immunohistochemical Analysis of VEGF₁₂₁/rGel in Tumor Xenografts.

Mice (three mice per group) bearing PC-3 tumors were injected intravenously with 50 μ g of the fusion protein gelonin. The mean tumor volume per group was 260 mm³. Thirty minutes later, mice were killed, exsanguinated, and all major tissues were snap-frozen. Frozen sections were cut and double stained with pan-endothelial marker MECA-32 (5 μ g/ml) followed by detection of the localized fusion protein by using rabbit anti-gelonin antibody (10 μ g/ml). MECA-32 rat IgG was visualized with goat anti-rat IgG conjugated to FITC (red fluorescence). Anti-gelonin antibody was detected with goat anti-rabbit IgG conjugated to Cy-3 (green fluorescence). Colocalization of both markers was indicated by a yellow color. Anti-gelonin antibody had no reactivity with tissue sections from mice injected with saline or VEGF₁₂₁. To determine the percentage of vessels with localized fusion protein, the number of vessels stained with MECA-32 (red), gelonin (green), or both (yellow) were counted at a magnification of $\times 200$ in at least 10 fields per section. Two slides from each mouse were analyzed, and the average percentage of positive vessels was calculated.

In Vivo Therapy in Xenograft Models. Human melanoma. Female nu/nu mice were divided into groups of five mice each. Log-phase A-375M human melanoma cells were injected s.c. (5×10^6 cells per mouse) into the right flank. After the tumors had become established (≈ 50 mm³), the mice were injected with VEGF₁₂₁/rGel through a tail vein five times over an 11 day period. The total dose of VEGF/rGel was 17 or 25 mg/kg. Other mice received rGel alone at a dose totaling 10 mg/kg. Mice were killed by cervical dislocation after the 40th day of tumor measurement.

Human prostate cancer. Male nude mice weighing ≈ 20 g were divided into groups of five mice each. Log-phase PC-3 human prostate tumor cells were injected s.c. (5×10^6 cells per mouse) in the right flank. The mice were injected with VEGF₁₂₁/rGel through a tail vein every 2–3 days for 11 days. The total dose of VEGF₁₂₁/rGel was 20 mg/kg. Other mice received rGel alone at a dose totaling 10 mg/kg. Tumor volume was calculated according to the formula: volume = $L \times W \times H$, where L = length, W = width, H = height.

A histological study was performed in which groups of three mice bearing PC-3 tumors were given i.v. injections of either saline or VEGF₁₂₁/rGel (2.5 mg/kg). Forty-eight hours later, the mice were killed, and organs and tumors were removed and fixed in formalin. Paraffin sections were prepared, stained with hematoxylin and eosin, and examined by light microscopy.

Results

Plasmid Construction, Bacterial Expression, and Purification of Fusion Protein. The cDNA encoding human VEGF₁₂₁, a G4S flexible tether, and rGel were joined with a PCR-based method (see Fig. 6, which is published as supporting information on the PNAS web site, www.pnas.org). The construct was ligated into the pET-32a vector, transformed into *E. coli* strain AD494(DE3) plys S, and the fusion protein was expressed and purified from bacterial supernatant. Fig. 7, which is published as supporting information on the PNAS web site, shows the SDS/PAGE analysis of protein expression after induction with IPTG. The lane containing the induced culture shows a new protein at 62 kDa, which is the expected molecular weight for the fusion protein plus the 21 kDa purification tag. This material was purified by binding and elution from immobilized metal affinity (IMAC) resin. Cleavage with recombinant enterokinase removed the tag resulting in a 42-kDa protein under reducing conditions (Fig. 7). The construct migrated as a homodimer at 84 kDa under nonreducing conditions. The fusion construct was immunoreactive with antibodies to both VEGF and rGel (Fig. 7). One liter of induced bacterial culture initially contained $\approx 2,000$ μ g of soluble fusion construct. Initial IMAC purification re-

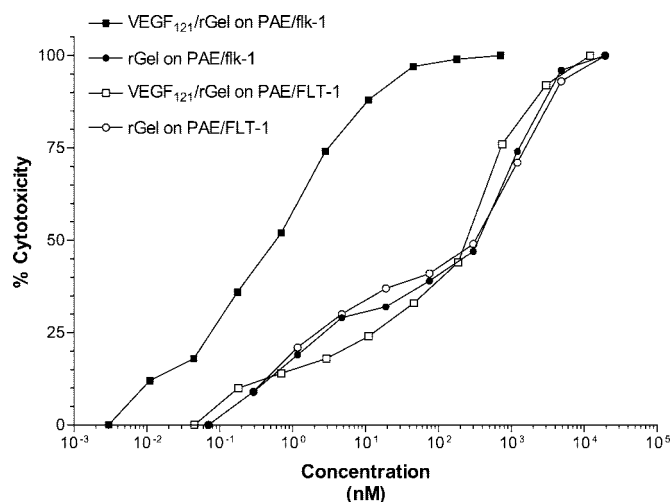


Fig. 1. Cytotoxicity of VEGF₁₂₁/rGel to KDR-expressing PAE-transfected cells. Cells transfected with either the FLT-1 or KDR receptor were treated with various doses of VEGF₁₂₁/rGel or rGel for 72 h. Cells expressing the FLT-1 receptor were equally insensitive to VEGF₁₂₁/rGel and rGel (IC₅₀ \approx 300 nM). In contrast, cells expressing KDR were about 200-fold more sensitive to the fusion construct (IC₅₀ of 0.5 nM) than they were to rGel.

sulted in 750 μ g of VEGF₁₂₁/rGel product (yield 37.5%), and digestion with recombinant enterokinase generated 400 μ g of target protein (yield 20%). Subsequent purification yielded 230 μ g of VEGF₁₂₁/rGel final product (11.5% overall yield).

Biological Activity of the rGel Component. The ability of VEGF₁₂₁/rGel and rGel to inhibit translation in a cell-free system was determined by using a rabbit reticulocyte translation assay. The purified VEGF₁₂₁/rGel and rGel had IC₅₀ values of ≈ 47 and 185 pM, respectively, showing that fusion of rGel and VEGF₁₂₁ did not reduce the activity of the toxin component.

Binding of VEGF₁₂₁/rGel to Soluble Flk-1 Receptor. The fusion protein was tested for its ability to bind to the Flk-1 receptor by ELISA. Fig. 8, which is published as supporting information on the PNAS web site, shows that VEGF₁₂₁/rGel and native human VEGF₁₂₁ bind equally well to Flk-1 at all concentrations, indicating that the VEGF component of the fusion protein is fully capable of binding to Flk-1. The specificity of binding of VEGF₁₂₁/rGel to Flk-1 was confirmed by using a 10-fold molar excess of free VEGF₁₂₁.

VEGF₁₂₁/rGel and VEGF₁₂₁-Induced Phosphorylation of KDR. PAE/KDR cells overexpressing the KDR were incubated with VEGF₁₂₁/rGel fusion construct or VEGF₁₂₁ itself, and Western analysis of phospho-tyrosine content of the receptors was measured at various later time points. As shown in Fig. 9, which is published as supporting information on the PNAS web site, addition of VEGF₁₂₁/rGel or VEGF₁₂₁ increased phosphotyrosine content. There were two phases of phosphorylation; an early phase (1–10 min) and a later phase (4–8 h). The time course of induction of KDR phosphorylation was the same for VEGF₁₂₁/rGel and VEGF₁₂₁. Phosphorylation of FLT-1 in PAE/FLT-1 cells treated with either VEGF₁₂₁/rGel or VEGF₁₂₁ was not observed, as expected from the weaker signaling of FLT-1 compared with KDR observed by others (40).

Cytotoxicity of VEGF₁₂₁/rGel to Endothelial Cells in Vitro. VEGF₁₂₁/rGel was specifically toxic to KDR/Flk-1 expressing endothelial cells *in vitro* (Fig. 1 and Table 1). The IC₅₀ values for VEGF₁₂₁/rGel on log-phase PAE/KDR, ABAE, and bEnd.3 cells, which express $1\text{--}3 \times 10^5$ KDR/Flk-1 receptors per cell, was 0.06 to 1 nM. Cells

Table 1. Correlation between number of VEGF receptors per cell and sensitivity to VEGF₁₂₁/rGel

Cell type	Number of FLT-1 sites per cell	Number of KDR sites per cell	IC ₅₀ for VEGF ₁₂₁ /rGel, nM	IC ₅₀ for rGel, nM	Targeting index*
PAE/KDR (log phase)	0	2–3 × 10 ⁵ (ref. 41)	0.5	300	600
PAE/KDR (confluent)	0	2–3 × 10 ⁵ (ref. 38)	30	5,000	167
bEnd3 (log phase)	N.D.	2 × 10 ⁵ †	1	100	100
ABAE (log phase)	0	0.4 × 10 ⁵ (ref. 56)	0.059	0.524	8.9
HUVEC (hypoxia)	N.D.	0.023 × 10 ⁵ (ref. 30)	700	>1,000	≈1
HUVEC (normoxia)	N.D.	0.017 × 10 ⁵ (ref. 30)	800	>1,000	≈1
PAE/FLT-1 (log phase)	0.5 × 10 ⁵ (ref. 38)	N.D.	300	300	1
PAE/FLT-1 (confluent)	0.5 × 10 ⁵ (ref. 38)	N.D.	>5,000	10,000	<2
A-375 (log phase)	N.D.	N.D.	330	109	0.3
PC-3 (log phase)	N.D.	N.D.	225	100	0.4

Numbers in parentheses indicate text reference. N.D., not done.

*Targeting index is defined as: (IC₅₀/IC₅₀)(rGel/VEGF₁₂₁/rGel).

†S. Ran, unpublished data.

expressing FLT-1 and having low endogenous expression of KDR (PAE/FLT-1, HUVEC) were several hundred-fold more resistant to VEGF₁₂₁/rGel than were the KDR/Flk-1 expressing cells. Thus, FLT-1 appears not to mediate cytotoxicity of VEGF₁₂₁/rGel, in agreement with earlier reports (41). The ratio of IC₅₀ values of rGel to VEGF₁₂₁/rGel was calculated for each cell type. This ratio (the targeting index) represents the ability of the VEGF component of the fusion construct to mediate the delivery of the toxin to the endothelial cell surface and into the intracellular ribosomal compartment. As summarized in Table 1, bEnd.3 and ABAE cells were, respectively, 100-fold and 9-fold more sensitive to the fusion construct than they were to free rGel.

Selective Cytotoxicity of VEGF₁₂₁/rGel for Dividing PAE/KDR Cells.

VEGF₁₂₁/rGel was 60-fold more toxic to PAE/KDR cells in log-phase growth than it was to PAE/KDR cells that had been grown to confluence and rested (Table 1). This effect was not caused by differences in KDR expression, because the cells expressed the same number of KDR receptors per cell in both phases of growth. The log-phase PAE/KDR cells also were more sensitive to rGel itself than were the confluent cells, suggesting that the quiescence of confluent cells impacts their sensitivity to both targeted and nontargeted rGel. It is possible that the rate or route of entry of both VEGF₁₂₁/rGel and rGel is different for dividing and nondividing cells.

Inhibition of Tumor Growth *in Vivo* by VEGF₁₂₁/rGel. Saline-treated human melanoma (A-375M) tumors showed an increase in tumor volume 24-fold (from 50 mm³ to 1200 mm³) over the 30-day observation period (Fig. 2). Treatment of the mice with VEGF₁₂₁/rGel strongly retarded tumor growth. At high doses of VEGF₁₂₁/rGel totaling 25 mg/kg, tumor growth was completely prevented, but all mice died from drug toxicity on day 19. At lower doses totaling 17 mg/kg, all mice survived. Tumor growth was completely prevented throughout the 14-day course of treatment, but thereafter, tumor regrowth slowly recurred. Compared with controls, mice treated with VEGF₁₂₁/rGel at doses totaling 17 mg/kg showed a 6-fold decrease in tumor volume (1,200 mm³ vs. 200 mm³).

Human prostatic carcinoma (PC-3) tumors increased 12-fold in volume during the 26-day observation period (Fig. 3). Treatment of the mice with five doses of VEGF₁₂₁/rGel totaling 20 mg/kg virtually abolished tumor growth, even after cessation of treatment. Tumor volume in the treated group only increased from 100 to 200 mm³ over the course of the experiment. Compared with controls, treatment with VEGF₁₂₁/rGel resulted in a 7-fold decrease in tumor volume (1,400 mm³ vs. 200 mm³).

Localization of VEGF₁₂₁/rGel to Vascular Endothelium in PC-3 Tumor Xenografts.

Mice bearing s.c. PC-3 tumors were given one i.v. dose of VEGF₁₂₁/rGel (2.5 mg/kg) or free gelonin (1 mg/kg) and, 30 min later, the mice were exsanguinated. Frozen sections of tumor and normal organs were examined immunohistochemically. VEGF₁₂₁/rGel was detected primarily on vascular endothelium of PC-3 tumors (Fig. 4). On average, 62% of vessels positive for MECA 32 also were positive for VEGF₁₂₁/rGel, as detected by using anti-gelonin antibody. In tumor regions of increased vascularity (“hot spots”), approximately 90% of tumor vessels had bound VEGF₁₂₁/rGel. Vessels in normal organs were unstained, with the exception of the kidney, where weak and diffuse staining was detected in the glomeruli. Free gelonin did not localize to tumor or normal vessels in any of the mice. These results indicate that VEGF₁₂₁/rGel localized specifically to tumor vessels after i.v. injection.

Destruction and Thrombosis of Tumor Vessels by VEGF₁₂₁/rGel.

Mice bearing s.c. PC-3 tumors were given one i.v. dose of VEGF₁₂₁/rGel (2.5 mg/kg) or saline. The mice were killed 48 h later, and the tumors and various organs were removed. Paraffin sections were prepared and stained with hematoxylin and eosin. The tumors from VEGF₁₂₁/rGel recipients (Fig. 5) displayed damaged vascular endothelium, thrombosis of vessels, and extravasation of RBC components into the tumor interstitium. Normal tissues had un-

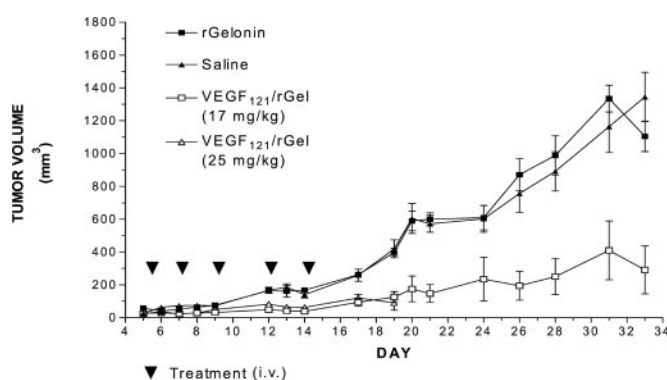


Fig. 2. Inhibition of human melanoma growth in mice by VEGF/rGel. Groups of nude mice bearing A-375M tumors were treated intravenously with saline, rGel, or fusion construct every 2–3 days for 11 days. Administration of rGel did not affect tumor growth. Treatment with VEGF₁₂₁/rGel at a total dose of either 17 mg/kg or 25 mg/kg significantly suppressed tumor growth. However, treatment at the 25 mg/kg dose level resulted in mortality by day 19. None of the animals dosed at 17 mg/kg showed gross evidence of toxicity.

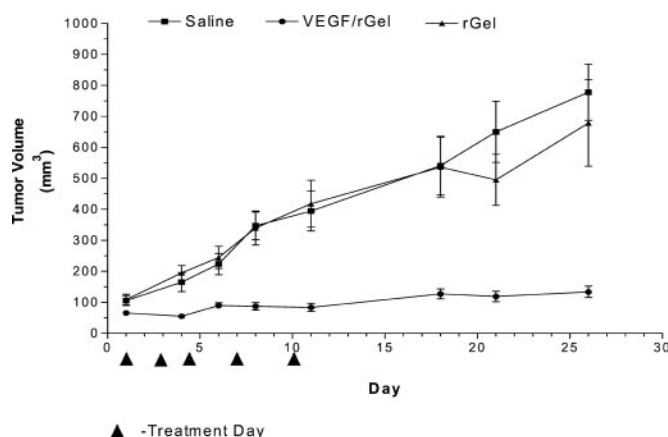


Fig. 3. Inhibition of human prostate carcinoma growth in mice by VEGF/rGel. Groups of nude mice bearing PC-3 tumors were treated intravenously with saline, rGel, or the VEGF₁₂₁/rGel fusion construct (20 mg/kg total dose) every 2–3 days for 11 days. Administration of rGel (10 mg/kg) had no effect on tumor growth. In contrast, treatment with the fusion construct completely inhibited tumor growth for 26 days and resulted in a 7-fold reduction in tumor volume compared with saline-treated or rGel-treated controls.

damaged vasculature. Treatment of mice with saline had no effect on tumor or normal tissues. As assessed by image analysis, necrotic areas of the tumor increased from $\approx 4\%$ in saline-treated mice to $>12\%$ after treatment with the fusion construct.

Discussion

The expression of VEGF and its receptors has been closely linked to tumor vascularity, metastasis, and progression (42–45). Several groups have developed antiangiogenic drugs that block kinase activity of the VEGF receptors (46) or monoclonal antibodies that block VEGF–receptor interactions (47, 48).

The current study demonstrates a chimeric fusion construct containing VEGF and the plant toxin gelonin. VEGF₁₂₁/rGel was found to be selectively toxic to dividing endothelial cells overexpressing the KDR/Flk-1 receptor. Nondividing (confluent) endothelial cells were almost 60-fold more resistant than were dividing cells to the fusion construct and also were more resistant to free rGel (Table 1). These findings accord with those of previous studies by Wild *et al.* (32), who showed that conjugates of VEGF and DT

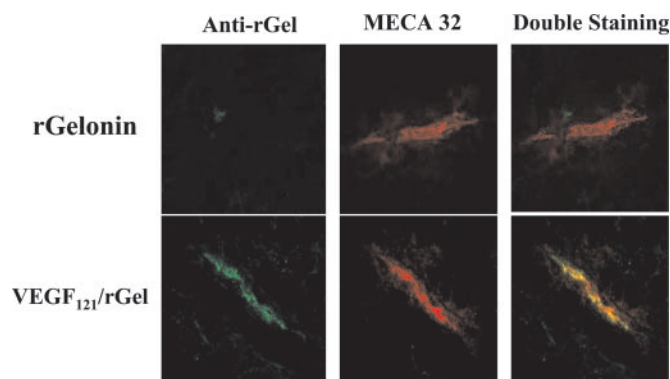


Fig. 4. Specific localization of VEGF/rGel to tumor vasculature in PC3 tumors. Nude mice bearing human prostate PC-3 tumors were injected i.v. with VEGF₁₂₁/rGel or rGel (2.5 mg/kg). Thirty minutes after administration, tissues were removed and snap frozen. Sections were stained with immunofluorescent reagents to detect murine blood vessels (MECA-32, red) and with anti-rGel (green). Vessels stained with both reagents appear yellow. VEGF/rGel localized to tumor vessels, whereas rGel did not. Vessels in all normal organs other than the kidney (glomerulus) were unstained by VEGF/rGel.

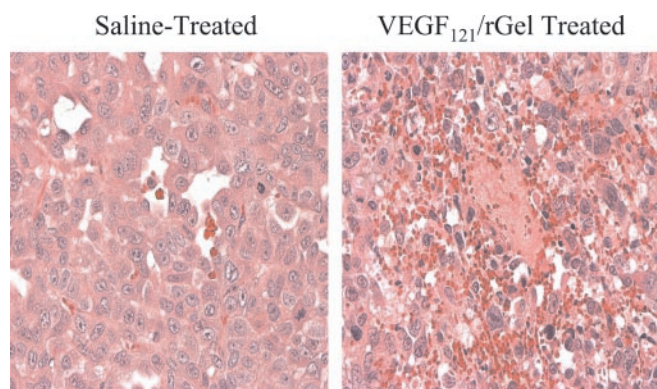


Fig. 5. Destruction and thrombosis of tumor blood vessels by VEGF/rGel. Nude mice bearing human prostate PC-3 tumors were treated i.v. with one dose of VEGF₁₂₁/rGel (2.5 mg/kg). Forty-eight hours after administration, tissues were snap-frozen, sectioned, and stained with hematoxylin and eosin. As shown in this representative image, tumors from mice treated with the fusion construct had damaged vascular endothelium. Clots were visible in the larger vessels of the tumors, and erythrocytes were visible in the tumor interstitium, indicating a loss of vascular integrity. In contrast, histological damage was not visible in any normal organs, including the kidneys, of treated mice.

were highly toxic to log-phase cells but were not toxic to confluent endothelial cells. The greater sensitivity of dividing endothelial cells to VEGF-toxin constructs may be because of differences in intracellular routing or catabolism of the construct as observed with other targeted therapeutic agents (49).

Cytotoxicity studies demonstrated that expression of the KDR/Flk-1 receptor is needed for VEGF₁₂₁/rGel to be cytotoxic. Cells overexpressing KDR/Flk-1 ($>1 \times 10^5$ sites per cell) were highly sensitive to the VEGF₁₂₁/rGel fusion construct, whereas cells expressing fewer than 0.4×10^5 sites per cell were no more sensitive to the fusion toxin than they were to free rGel. Again, the requirement to surpass a threshold level of KDR/Flk-1 for cytotoxicity may contribute to the safety of VEGF₁₂₁/rGel. In normal organs, including the kidney glomerulus and pulmonary vascular endothelium (19), the level of KDR/Flk-1 may be below that needed to cause toxicity. The number of receptors for VEGF on endothelial cells in the vasculature of normal organs has been reported by Brown *et al.* (19, 50) to be significantly lower than on tumor vasculature. Indeed, we could not detect binding of VEGF₁₂₁/rGel to normal vascular endothelium in organs other than the kidney, where weak binding was observed. Furthermore, no damage to vascular endothelium was observed in normal organs, including the kidney.

Other gelonin-based-targeted therapeutics also have been observed to become toxic to cells only when a certain threshold level of binding is surpassed. In a recent study of immunotoxins directed against the c-erb-2/HER2/neu oncogene product, immunotoxins were not cytotoxic to tumor cells expressing less than about 1×10^6 HER2/neu sites per cell (29). The lack of sensitivity of cells having low levels of receptors is presumably because the cells internalize too little of the toxin or traffic it to compartments that do not permit translocation of the toxin to the ribosomal compartment.

Our study also demonstrates that the presence of FLT-1, even at high levels, does not seem to mediate cellular toxicity of the VEGF₁₂₁/rGel fusion toxin. Although VEGF binds to the FLT-1 receptor (51), the current study (40, 52) has been unable to demonstrate receptor phosphorylation as a result of ligand binding. Dougher and Terman (53) suggested that receptor phosphorylation may be required for KDR signaling and internalization. If so, the receptor–fusion–toxin complex may not internalize efficiently enough after binding to FLT-1 for the fusion protein to be routed to an intracellular compartment from

which the toxin can escape to the cytosol. The relative contributions of the FLT-1 and KDR receptors to the biological effects of VEGF examined by using a monoclonal antibody that blocks the interaction of VEGF with KDR/Flk-1 but not FLT-1 demonstrate that KDR/Flk-1 is the major receptor determining the vascular permeability-inducing and angiogenic effects of VEGF in tumors (48).

Although VEGF₁₂₁/rGel induces phosphorylation of KDR receptor, we observed no growth-stimulatory effects of the fusion toxin on VEGF receptor-expressing cells. These findings are in keeping with studies of other fusion toxins such as IL-2/DT that initially stimulate target cells in a manner similar to that of IL-2 itself, but ultimately kill the target cells through the actions of the internalized toxin (54).

The antitumor effects of the VEGF₁₂₁/rGel fusion construct against both melanoma and human prostate carcinoma xenografts was impressive in magnitude and prolonged. A-375M and PC-3 cells in culture were resistant to the fusion construct *in vitro*, despite the reported presence of KDR on the melanoma (but not on PC-3) cells (55). Therefore, the antitumor effects observed *in vivo* appear not to be caused by direct cytotoxic

effects of VEGF₁₂₁/rGel on the tumor cells themselves. The antitumor effect seems to be exerted indirectly on the tumor cells through specific damage to tumor vasculature. The VEGF₁₂₁ fusion toxin localized to tumor blood vessels after i.v. administration. Vascular damage and thrombosis of tumor blood vessels were observed within 48 h of administration of VEGF₁₂₁/rGel to PC-3 mice, consistent with the primary action of the construct being exerted on tumor vascular endothelium.

In summary, our results indicate that selective destruction of tumor vasculature can be achieved with VEGF₁₂₁/rGel in mice, giving impressive antitumor effects. Gross morphological toxicity to the normal organs was not visible in animals treated with a therapeutic dose. These studies suggest that VEGF₁₂₁/rGel has potential as an antitumor agent for treating cancer patients.

We thank Ms. J. Merchant for her excellent assistance in the preparation of this report. This study was supported by grants from the University of Utrecht and the Dutch Cancer Foundation, Koningin Wilhelmina Fonds, Cancer Center Support Grant 5P30CA16672-26 from the National Cancer Institute, National Institutes of Health Grant ROI CA 7495, and Arcus Therapeutics LLC, Boston. This research was conducted, in part, by The Clayton Foundation for Research.

- Klagsbrun, M. & D'Amore, P. A. (1991) *Annu. Rev. Physiol.* **53**, 217–239.
- Folkman, J. & Shing, Y. (1992) *J. Biol. Chem.* **267**, 10931–10934.
- Folkman, J. (1991) *J. Natl. Cancer Inst.* **82**, 4–6.
- Weidner, N., Semple, J. P., Welch, W. R. & Folkman, J. (1991) *N. Engl. J. Med.* **324**, 1–8.
- Leung, D. W., Cachianes, G., Kuang, W. J., Goeddel, D. V. & Ferrara, N. (1989) *Science* **246**, 1306–1309.
- Senger, D. R., Galli, S. J., Dvorak, A. M., Perruzzi, C. A., Harvey, V. S. & Dvorak, H. F. (1983) *Science* **219**, 983–985.
- Ferrara, N. & Henzel, W. J. (1989) *Biochem. Biophys. Res. Commun.* **161**, 851–858.
- Plouet, J., Schilling, J. & Gospodarowicz, D. (1989) *EMBO J.* **8**, 3801–3806.
- Poon, R. T., Fan, S. T. & Wong, J. (2001) *J. Clin. Oncol.* **19**, 1207–1215.
- Price, D. J., Miralem, T., Jiang, S., Steinberg, R. & Avraham, H. (2001) *Cell Growth Differ.* **12**, 129–135.
- Cvetkovic, D., Movsas, B., Dicker, A. P., Hanlon, A. L., Greenberg, R. E., Chapman, J. D., Hanks, G. E. & Tricoli, J. V. (2001) *Urology* **57**, 821–825.
- Conn, G., Bayne, M. L., Soderman, D. D., Kwok, P. W., Sullivan, K. A., Palisi, T. M., Hope, D. A. & Thomas, K. A. (1990) *Proc. Natl. Acad. Sci. USA* **87**, 2628–2632.
- Leenders, W., van Altena, M., Lubsen, N., Ruiter, D. & De Waal, R. (2001) *Int. J. Cancer* **91**, 327–333.
- Houck, K. A., Ferrara, N., Winer, J., Cachianes, G., Li, B. & Leung, D. W. (1991) *Mol. Endocrinol.* **5**, 1806–1814.
- Neufeld, G., Cohen, T., Gengrinovitch, S. & Poltorak, Z. (1999) *FASEB J.* **13**, 9–22.
- Shibuya, M., Yamaguchi, S., Yamane, A., Ikeda, T., Tojo, A., Matushime, H. & Sato, M. (1990) *Oncogene* **5**, 519–524.
- De Vries, C., Escobedo, J. A., Ueno, H., Houck, K., Ferrara, N. & Williams, L. T. (1992) *Science* **225**, 989–991.
- Peters, K. G., De Vries, C. & Williams, L. T. (1993) *Proc. Natl. Acad. Sci. USA* **90**, 8915–8919.
- Brown, L. F., Berse, B., Jackman, R. W., Tognazzi, K., Guidi, A. J., Dvorak, H. F., Senger, D. R., Connolly, J. L. & Schnitt, S. J. (1995) *Hum. Pathol.* **26**, 86–91.
- Plate, K. H., Breier, G., Millauer, B., Ullrich, A. & Risau, W. (1993) *Cancer Res.* **53**, 5822–5827.
- Easty, D. J., Herlyn, M. & Bennett, D. C. (1995) *Int. J. Cancer* **60**, 129–136.
- Hatva, E., Kaipainen, A., Mentula, P., Jaaskelainen, J., Paetau, A., Haltia, M. & Alitalo, K. (1995) *Am. J. Pathol.* **146**, 368–378.
- Takahashi, A., Sasaki, H., Kim, S. J., Tobisu, K., Kakizoe, T., Tsukamoto, T., Kumamoto, Y., Sugimura, T. & Terada, M. (1994) *Cancer Res.* **54**, 4233–4237.
- Warren, R. S., Yuan, H., Matli, M. R., Gillett, N. A. & Ferrara, N. (1995) *J. Clin. Invest.* **95**, 1789–1797.
- Stirpe, F., Olsnes, S. & Pihl, A. (1980) *J. Biol. Chem.* **255**, 6947–6953.
- Sivam, G., Pearson, J. W., Bohn, W., Oldham, R. K., Sadoff, J. C. & Morgan, A. C., Jr. (1987) *Cancer Res.* **47**, 3169–3173.
- Sperti, S., Brigotti, M., Zamboni, M., Carnicelli, D. & Montanaro, L. (1991) *Biochem. J.* **277**, 281–284.
- Rosenblum, M. G., Kohr, W. A., Beattie, K. L., Beattie, W. G., Marks, W., Toman, P. D. & Cheung, L. (1995) *J. Interferon Cytokine Res.* **15**, 547–555.
- Rosenblum, M. G., Shawver, L. K., Marks, J. W., Brink, J., Cheung, L. & Langton-Webster, B. (1999) *Clin. Cancer Res.* **5**, 865–874.
- Brogi, E., Schattelman, G., Wu, T., Kim, E. A., Varticovski, L. & Keyt, B. (1996) *J. Clin. Invest.* **97**, 469–476.
- Gawlak, S. L., Neubauer, M., Klei, H. E., Chang, C. Y., Einspahr, H. M. & Siegall, C. B. (1997) *Biochemistry* **36**, 3095–3103.
- Wild, R., Dhanabal, M., Olson, T. A. & Ramakrishnan, S. (2000) *Br. J. Cancer* **83**, 1077–1083.
- Ueda, M., Psarras, K., Jinno, H., Ikeda, T., Enomoto, K., Kitajima, M., Futami, J., Yamada, H. & Seno, M. (1997) *Breast Cancer* **4**, 253–255.
- Dore, J. M., Gras, E. & Wijdenes, J. (1997) *FEBS Lett.* **402**, 50–52.
- Sweeney, E. B. & Murphy, J. R. (1995) *Essays Biochem.* **30**, 119–131.
- Ramakrishnan, S., Olson, T. A., Bautch, V. L. & Mohanraj, D. (1996) *Cancer Res.* **56**, 1324–1330.
- Arora, N., Masood, R., Zheng, T., Cai, J., Smith, D. L. & Gill, P. S. (1999) *Cancer Res.* **59**, 183–188.
- Waltenberger, J., Claesson-Welsh, L., Siegbahn, A., Shibuya, M. & Heldin, C. H. (1994) *J. Biol. Chem.* **269**, 26988–26995.
- Brekken, R. A., Huang, X., King, S. W. & Thorpe, P. E. (1998) *Cancer Res.* **58**, 1952–1959.
- Esser, S., Lampugnani, M. G., Corada, M., Dejana, E. & Risau, W. (1998) *J. Cell Sci.* **111**, 1853–1865.
- Backer, M. V., Budker, V. G. & Backer, J. M. (2001) *J. Controlled Release* **74**, 349–355.
- Kim, K. J., Li, B., Winer, J., Armanini, M., Gillett, N., Phillips, H. S. & Ferrara, N. (1993) *Nature (London)* **362**, 841–844.
- Millauer, B., Longhi, M. P., Plate, K. H., Shawver, L. K., Risau, W., Ullrich, A. & Strawn, L. M. (1996) *Cancer Res.* **56**, 1615–1620.
- Takahashi, Y., Kitadai, Y., Bucana, C. D., Cleary, K. R. & Ellis, L. M. (1995) *Cancer Res.* **55**, 3964–3968.
- Baker, E. A., Bergin, F. G. & Leaper, D. J. (2000) *Mol. Pathol.* **53**, 307–312.
- Mendel, D. B., Schreck, R. E., West, D. C., Li, G., Strawn, L. M., Tanciongco, S. S., Vasile, S., Shawver, L. K. & Cherrington, J. M. (2000) *Clin. Cancer Res.* **6**, 4848–4858.
- Kozin, S. V., Boucher, Y., Hicklin, D. J., Bohlen, P., Jain, R. K. & Suit, H. D. (2001) *Cancer Res.* **61**, 39–44.
- Brekken, R. A., Overholser, J. P., Stastny, V. A., Waltenberger, J., Minna, J. D. & Thorpe, P. E. (2000) *Cancer Res.* **60**, 5117–5124.
- Walz, G., Zanker, B., Brand, K., Waters, C., Genbauffe, F. & Zeldis, J. B. (1989) *Proc. Natl. Acad. Sci. USA* **86**, 9485–9488.
- Brown, L. F., Berse, B., Jackman, R. W., Tognazzi, K., Guidi, A. J. & Dvorak, H. F. (1995) *Hum. Pathol.* **26**, 86–91.
- Shibuya, M. (2001) *Int. J. Biochem. Cell Biol.* **33**, 409–420.
- Kanno, S., Oda, N., Abe, M., Terai, Y., Ito, M., Shitara, K., Tabayashi, K., Shibuya, M. & Sato, Y. (2000) *Oncogene* **19**, 2138–2146.
- Dougher, M. & Terman, B. I. (1999) *Oncogene* **18**, 1619–1627.
- St. Croix, B., Rago, C., Velculescu, V., Traverso, G., Romans, K. E. & Montgomery, E. (2000) *Science* **289**, 1197–1202.
- Liu, B., Earl, H. M., Baban, D., Shoaibi, M., Fabra, A., Kerr, D. J. & Seymour, L. W. (1995) *Biochem. Biophys. Res. Commun.* **217**, 721–727.
- Vaisman, N., Gospodarowicz, D. & Neufeld, G. (1990) *J. Biol. Chem.* **266**, 19461–19466.

Inhibition of Bone Remodeling and Prostate Skeletal Metastases by the Vascular Targeting Agent VEGF₁₂₁/rGel

Khalid A. Mohamedali¹, Ann T. Poblenz¹, Chuck Sikes², Nora Navone², Philip Thorpe³,
Bryant Darnay¹ and Michael G. Rosenblum¹

¹Department of Experimental Therapeutics, The University of Texas M. D. Anderson Cancer Center, Houston, Texas 77030, USA. ²Department of Genitourinary Medical Oncology, The University of Texas M. D. Anderson Cancer Center, Houston, TX 77030, USA. ³Department of Pharmacology, Simmons Comprehensive Cancer Center, The University of Texas Southwestern Medical Center, Dallas, Texas 75390, USA.

Correspondence to: Michael G. Rosenblum, Ph. D., The University of Texas M. D. Anderson Cancer Center, Department of Experimental Therapeutics, Unit 44, 1515 Holcombe Blvd., Houston, Texas 77030. Tel: 713-792-3554; Fax: 713-794-4261 or 713-745-3916; E-mail: mrosenbl@mdanderson.org.

Research supported in part by the Clayton Foundation for Research and The Department of Defense (DAMD-17-02-1-0457).

Abstract

The pathophysiological processes underlying the development of skeletal metastases remain incompletely understood and these lesions respond poorly to therapeutic intervention. Vascular endothelial growth factor A (VEGF-A) and its receptors are known to play a role in both osteoclastogenesis and in tumor growth. We previously described a fusion toxin composed of VEGF₁₂₁ and the toxin gelonin and its ability to target cells overexpressing VEGF receptors. Systemic treatment of nude mice bearing skeletal prostate (PC-3) tumors with VEGF₁₂₁/rGel dramatically inhibited the growth of prostate bone metastases and 50% percent of treated mice demonstrated complete regression of bone tumors with no development of lytic bone lesions. Immunohistochemical analysis additionally demonstrated that VEGF₁₂₁/rGel treatment suppressed tumor-mediated osteoclastogenesis in vivo. In vitro treatment of murine osteoclast precursors obtained from either bone marrow or cell lines (RAW264.7) revealed that VEGF₁₂₁/rGel was selectively cytotoxic to osteoclast precursor cells rather than mature osteoclasts. Maturation of precursor cells by treatment with RANKL resulted in down-regulation of Flt-1 receptors and resistance to the cytotoxic effects of VEGF₁₂₁/rGel. Analysis by flow cytometry and RT-PCR showed that both bone marrow-derived monocytes (BMM) and RAW264.7 cells both display high levels of Flt-1 but low levels of Flk-1 receptors for VEGF. Internalization of VEGF₁₂₁/rGel into osteoclast precursor cells was suppressed by pre-treatment with an Flt-1 neutralizing antibody or by PlGF, but not with an Flk-1 neutralizing antibody. VEGF₁₂₁/rGel not only inhibits neovascularization of tumor bone lesions, but also inhibits osteoclast maturation/recruitment in vivo and it appears that both processes are important in the

resulting suppression of skeletal osteolytic lesions. This is a novel and unique mechanism of action for this class of agents and suggests a potentially new approach to treatment or prevention of skeletal metastases. In addition, these data demonstrate that VEGF₁₂₁/rGel is a useful probe to investigate the role of VEGF and its cognate receptors in the development of skeletal metastases.

Introduction

Osteoclastogenesis differentiation and activation plays a central role in the development and maintenance of normal bone tissue, which requires osteoblastic matrix deposition and osteoclastic resorption to be closely coordinated (for review, see ¹). Interference with the process of osteoclastogenesis alters the kinetics of bone remodeling resulting in abnormal bone development²⁻⁵. There is general consensus that the hematopoietically-derived osteoclast is the pivotal cell in the degradation of the bone matrix⁶ and stimulation of osteoclastic bone resorption is the primary mechanism responsible for bone destruction in metastatic cancer⁷⁻⁹.

The progression of osteolytic metastases requires the establishment of close functional interactions between tumor cells and bone cells¹⁰⁻¹². Osteoclast precursor cells may be stimulated to differentiate or activated directly by tumor-secreted soluble factors such as GM-CSF, M-CSF, interleukins, TGF- β and VEGF among others^{7,9,13-15}. The secretion of some of these factors by cancer cells regulates expression of RANKL on the surface of stromal osteoblasts, thereby increasing osteoclast-mediated bone resorption^{16,17}.

While there is now little doubt that the VEGF-A cytokine family has an essential role in the regulation of embryonic and postnatal physiologic angiogenic processes, their role in skeletal growth, endochondral bone formation and differentiation of osteoclast pre-cursor cells is substantially less well-understood. Osteoclast pre-cursor cells have been shown to be recruited to the future site of resorption by VEGF-A and RANKL, two cytokines that are expressed in the immediate vicinity of the bone surface^{18,19}. VEGF mRNA is expressed by hypertrophic chondrocytes in the epiphyseal growth plate, suggesting that a VEGF gradient is needed for directional growth and cartilage invasion

by metaphyseal blood vessels²⁰. Treatment with a soluble VEGFR-1 antibody to block VEGF results in almost complete suppression of blood vessel invasion and impaired trabecular bone formation²⁰, a development that is reversed by cessation of the anti-VEGF treatment. A similar phenotype is observed when *Vegf* is deleted in the cartilage of developing mice by means of Cre-*loxP*-mediated, tissue-specific gene ablation²¹. In addition, examination of VEGF^{120/120} mice shows delayed recruitment of blood vessels into the perichondrium as well as delayed invasion of vessels into the primary ossification center, indicating a significant role of VEGF at both early and late stages of cartilage vascularization²².

VEGF plays an important role in the vascularization of bone tissues^{23,24}; increases osteoclast-mediated bone resorption^{25,26}; induces osteoclast chemotaxis and recruits osteoclasts to the site of bone remodeling^{19,27}; and can partially rescue M-CSF deficiency in *op/op* mice²⁶.

While VEGF receptors have been the increasing focus of attention as therapeutic targets, both by us^{28,29} and others³⁰⁻³², the context has usually been in terms of vascular targeting and anti-angiogenic therapy. The VEGF receptors Flt-1/FLT-1 (VEGFR-1) and Flk-1/KDR (VEGFR-2) are over-expressed on the endothelium of tumor vasculature³³⁻³⁹ including lung, brain, breast, colon, prostate, skin and ovarian cancers. In contrast, these receptors are almost undetectable in the vascular endothelium of adjacent normal tissues⁴⁰ and, therefore, appear to be excellent targets for the development of therapeutic agents that inhibit tumor growth and metastatic spread through inhibition of tumor neovascularization.

Both of the major receptors of VEGF-A have been observed in osteoclasts^{20,26,41}, although some reports cite only the presence of Flt-1^{41,42}. The VEGF-Flt-1 interaction has been implicated in the recruitment process of osteoclast pre-cursor cells from hematopoietic tissue to the site of bone resorption^{41,43,44}. However, the role of each receptor, and its regulation, has yet to be established. Osteoclasts play a critical role in the establishment of osteoblastic bone metastases by inducing bone resorption, which allows cancer cells to invade the bone and therefore promote tumor growth. Therefore, establishing the precise role that each VEGF receptor plays in the maturation of osteoclast pre-cursor cells to osteoclasts is a critical step towards understanding the interaction that occurs between tumor cells and the bone microenvironment.

We previously developed and characterized a novel growth factor fusion construct composed of VEGF₁₂₁ and the highly cytotoxic plant toxin gelonin (rGel)²⁹. Our previous studies have demonstrated an impressive vascular targeting and vascular ablative activity of VEGF₁₂₁/rGel against tumor neovasculature in a variety of soft-tissue tumor xenograft models. In the current study, we used the VEGF₁₂₁/rGel fusion toxin to inhibit growth of tumor cells in a prostate cancer skeletal metastasis model and as a probe to investigate the role of VEGF and its cognate receptors in the development of skeletal metastases.

Results

VEGF₁₂₁/rGel inhibits growth of intrafemoral PC-3 tumors and reduces the number of tumor-induced osteoclasts.

The anti-tumor effect of the fusion protein VEGF₁₂₁/rGel was evaluated in a prostate cancer bone model by injecting PC-3 tumor cells into the distal epiphysis of the right femur of athymic nude mice. The mice were treated every other day (five total treatments) with a total dose of 45 mg/kg of VEGF₁₂₁/rGel or saline. Tumor growth was monitored by X-ray analysis and animals with large osteolytic lesions or bone lysis were sacrificed. One hundred percent (100%) of tumor-innoculated mice treated with saline developed osteolytic lesions (Fig. 1a, left panels) and 50% survival occurred 40 days after tumor placement (Fig. 1b). In contrast, treatment with VEGF₁₂₁/rGel resulted in suppression of intrafemoral growth of tumor osteolytic lesions as assessed radiologically (Fig. 1a, right panels) and 50% of the VEGF₁₂₁/rGel-treated mice survived past 140 days without sign of osteolysis (Fig. 1b). H&E staining showed nests of PC-3 cells in bone marrow of mice treated with saline (Fig. 1c, top panel) and isolated pockets of PC-3 cells in some bone marrow sections from VEGF₁₂₁/rGel-treated mice (Fig. 1c, arrows, middle panel), as well as bone sections without any visible tumor cells from mice treated with VEGF₁₂₁/rGel (Fig. 1c, bottom panel).

We next examined PC-3 tumor cells to identify whether the observed VEGF₁₂₁/rGel-mediated inhibition of PC-3- induced osteolysis was a direct effect on the tumor cells. As shown in Fig 2a, the VEGF₁₂₁/rGel fusion construct was not specifically cytotoxic to tumor cells compared to the rGel toxin alone suggesting that these cells

express an insufficient number of VEGF receptors to mediate specific VEGF₁₂₁/rGel cytotoxicity. This was confirmed by RT-PCR analysis (Fig. 2a, inset).

Immunohistochemical analysis of tissue sections for osteoclasts (TRAP staining) revealed a dramatic increase in the number of osteoclasts in the tumor-bearing leg of mice treated with saline (Fig. 2b). In contrast, bone sections of VEGF₁₂₁/rGel-treated mice showed the same number of osteoclasts as those present in the contralateral (control) leg, suggesting that VEGF₁₂₁/rGel may play a role in inhibiting tumor-mediated osteoclast proliferation and/or differentiation.

VEGF₁₂₁/rGel affects osteoclast pre-cursor cells but not terminally differentiated osteoclasts

To understand the effect of VEGF₁₂₁/rGel in the bone microenvironment and test if VEGF₁₂₁/rGel may be directly targeting osteoclast pre-cursor cells *in vivo*, we next evaluated the effect of VEGF₁₂₁/rGel on RANKL-induced osteoclast differentiation of RAW264.7 cells and bone marrow-derived monocytes (BMM) *in vitro*. Treatment with increasing concentrations of VEGF₁₂₁/rGel, but not rGel, showed a dramatic decrease of TRAP⁺ multi-nucleated osteoclasts in both RAW264.7 (Fig. 3a and 3b) and BMM (Fig. 3d and 3e) cells. The observed effect was not mediated by either VEGF₁₂₁ or gelonin alone but is a characteristic unique to the combined fusion protein. The IC₅₀ of VEGF₁₂₁/rGel on undifferentiated RAW264.7 cells was 40 nM compared to 900 nM for rGel, indicating that the cytotoxicity of VEGF₁₂₁/rGel was mediated through VEGF₁₂₁ and suggested the presence of a receptor recognizing VEGF₁₂₁ (Fig. 3c). Similar to the RAW264.7 cells, the IC₅₀ of VEGF₁₂₁/rGel (8 nM) on undifferentiated BMM cells was

substantially lower than that of rGel (Fig. 4f, exact IC_{50} not determined). VEGF₁₂₁/rGel demonstrated a greater cytotoxic effect on BMM compared to undifferentiated RAW264.7 cells. In addition, we observed that VEGF₁₂₁/rGel, but not rGel, inhibited the M-CSF-dependent survival of monocytes (data not shown). Thus, VEGF₁₂₁/rGel not only inhibited RANKL-mediated differentiation of osteoclast precursors, but also exhibited cytotoxicity towards undifferentiated cells in a targeted manner.

The observed inhibitory effect of VEGF₁₂₁/rGel on osteoclastogenesis could be due to a reduced density of osteoclast progenitor cells. Insufficient number of osteoclast progenitor cells may lead to impaired contact between committed progenitors, leading to inability to form multi-nucleated osteoclasts. We next investigated the susceptibility of primary mouse monocytes and their terminally differentiated counterparts to VEGF₁₂₁/rGel cytotoxicity. BMM cells were treated with VEGF/rGel or rGel at various times after RANKL stimulation. Cells treated with VEGF₁₂₁/rGel simultaneously with RANKL stimulation showed a dose-dependent inhibition of osteoclastogenesis (Fig. 4a, b and d) as described above. However, osteoclastogenesis proceeded normally if BMM cells were allowed to differentiate for 60 h prior to the addition of VEGF₁₂₁/rGel (Fig. 4c and d). The apparent cytotoxicity of VEGF₁₂₁/rGel to osteoclast pre-cursor cells but not to mature osteoclasts was further investigated by adding VEGF₁₂₁/rGel at different time points after RANKL stimulation of both RAW264.7 and BMM cells (Table 1). The increase in the IC_{50} of VEGF₁₂₁/rGel corresponded to the length of time following RANKL stimulation of both RAW264.7 (Table 1a) and BMM (Table 1b) cells. In RAW264.7 cells, the IC_{50} of VEGF₁₂₁/rGel increased from 30 nM when added simultaneously with RANKL to 300 nM when added 96 h after RANKL stimulation,

whereas the IC_{50} of rGel did not change significantly. The change in IC_{50} of VEGF₁₂₁/rGel on BMM cells was more dramatic, increasing from 8 nM to 100 nM if VEGF₁₂₁/rGel was added 24 h post RANKL stimulation. Addition of VEGF₁₂₁/rGel 48 h post RANKL stimulation increased the IC_{50} to > 400 nM.

VEGF₁₂₁/rGel but not rGel is internalized into RAW264.7 cells and BMM cells through a specific mechanism

Based on our previous studies, specific VEGF-driven cytotoxicity is receptor-dependant and we next examined by immunostaining whether VEGF₁₂₁/rGel was delivered into the cytoplasm of the osteoclast pre-cursor cells. VEGF₁₂₁/rGel, but not rGel, localized in the cytoplasm of RAW264.7 cells and this internalization data is consistent with our studies on the cytotoxic effect of this agent (Fig. 5a). We assessed if internalization of VEGF₁₂₁/rGel was mediated by a VEGF receptor by examining by Western blot analysis if VEGF₁₂₁/rGel activated pp44/42, a known down-stream target of VEGF receptor activation. Treatment with VEGF₁₂₁/rGel resulted in similar activation of pp44/42, as did treatment with equimolar amounts of VEGF₁₂₁ alone (Fig. 5b). rGel did not induce stimulation of pp44/42, indicating that the effect of VEGF₁₂₁/rGel is mediated by a VEGF₁₂₁ receptor, rather than a non-specific mechanism (Fig.5b). Treatment with PlGF, an Flt-1-specific ligand, resulted in pp44/42 activation underscoring the presence of this receptor on the surface of osteoclast pre-cursor cells.

RAW264.7 and BMM cells express Flt-1

Because VEGF₁₂₁/rGel cytotoxicity on both RAW264.7 and BMM cells appears to be mediated by receptors for VEGF₁₂₁, we determined the levels of Flk-1 and Flt-1 in these cells. RT-PCR analysis indicated low levels of Flt-1, but no Flk-1 transcript, in RAW264.7 cells (Fig. 6a, lanes 1-3). Western blot analysis of RAW264.7 cells confirmed this observation (Fig. 6b). FACS analysis indicated that 99% of the RAW264.7 cells expressed Flt-1 (Fig. 6c) and 8% expressed Flk-1 (Fig. 6d). RT-PCR analysis of BMM cells showed an amplification of both Flt-1 and Flk-1 (Fig. 6a, lanes 4-6) and FACS analysis showed that 41.9% of the CD11b positive BMM cells expressed Flt-1 and 5.4% expressed Flk-1 (Fig. 6e-g). RT-PCR analysis of BMM cells following stimulation of RANKL-mediated osteoclastogenesis showed no change in the levels of Flk-1, but treatment appeared to downregulate the Flt-1 transcript (Fig. 6h). RT-PCR analysis of mVEGF isoforms detected low levels of VEGF₁₆₄ and VEGF₁₂₀ transcript but no VEGF₁₈₈ (data not shown). The downregulation of Flt-1 mRNA in BMM cells following stimulation of osteoclastogenesis by RANKL was confirmed by testing samples at different cycles of the RT-PCR analysis (data not shown) and further validated by densitometric analysis as described in Methods. All bands were individually compared to its internal GAPDH standard loaded in the same fashion in order to normalize the data. Flk-1 did not show a significant change in expression 96 h post RANKL stimulation whereas Flt-1 did exhibit a down-regulation of 3.4 fold 96 h post RANKL stimulation compared to untreated BMM (Fig. 6i).

Localization of VEGF₁₂₁/rGel into RAW264.7 and BMM cells may be mediated by Flt-1

To determine the role of VEGF₁₂₁ receptors in VEGF₁₂₁/rGel-mediated cytotoxicity of osteoclast precursor cells, we pre-incubated RAW264.7 and BMM cells with neutralizing antibodies to Flt-1 and Flk-1 for one hour prior to addition of VEGF₁₂₁/rGel, and monitored internalization of VEGF₁₂₁/rGel. Pretreatment of RAW264.7 cells and BMM cells with neutralizing antibodies to Flt-1, but not Flk-1 inhibited the localization of VEGF₁₂₁/rGel into these cells (Fig 7a). We assessed the role of each receptor in VEGF₁₂₁/rGel –mediated cytotoxicity by pre-incubating RAW264.7 and BMM cells with Flt-1 or Flk-1 neutralizing antibodies or with PIGF for 1h prior to the addition of VEGF₁₂₁/rGel. PIGF was able to inhibit the VEGF₁₂₁/rGel-mediated cytotoxicity in both RAW264.7 and BMM cells (Fig. 7b). Taken together, this indicates that the Flt-1 receptor, but not the Flk-1 receptor, is responsible for mediating VEGF₁₂₁/rGel- induced cytotoxicity in osteoclast progenitor cells.

Discussion

Prostate cancer is highly metastatic and the primary site of prostate cancer metastases is bone. The survival rate of patients with prostate cancer metastases is about 31%, compared to a nearly 100% 5-year survival rate if the cancer is locally confined. Several reports⁴⁵⁻⁵⁰ have implicated VEGF in prostate carcinogenesis and metastatic spread in addition to its well-established role in angiogenesis. VEGF is also produced by tumor cells to facilitate nesting of metastatic cells in bone and to promote neovascularization²⁰ which are two critical events necessary to the successful formation of skeletal metastases.

Receptor kinase inhibitors, antibodies targeting the receptors for VEGF and other strategies are all under development as strategies to disrupt tumor angiogenesis⁵¹⁻⁵⁶. Growth factor fusion constructs such as VEGF₁₂₁/rGel have a tremendous potential to interfere with tumor angiogenesis by targeted destruction of tumor endothelium. However, our observation that the anti-angiogenic VEGF₁₂₁/rGel construct can significantly impact skeletal prostate metastases is a novel finding for agents in this class although studies by Dai et al⁵⁷ and Shariat et al⁵⁸ have suggested a link between VEGF expression and metastatic spread (including skeletal metastases) in prostate tumors. Another unanticipated finding is that this agent can disrupt osteoclast activity and a third finding is that the cytotoxic effect of the VEGF₁₂₁/rGel construct on osteoclasts can be mediated through interaction with the Flt-1 receptor. These observations provide a potentially new series of pathways, which may be exploited not only for prostate metastases to bone but theoretically for treatment of other osteolytic tumors as well.

Previous studies in our laboratory have clearly demonstrated that the cytotoxicity and cellular internalization of VEGF₁₂₁/rGel on vascular endothelial cells is mediated through binding to the Flk-1/KDR receptor and not the Flt-1 receptor. However, the current study demonstrates that Flt-1 and not Flk-1 on osteoclast precursor cells appears to be primarily responsible for mediating the cytotoxic effects of VEGF₁₂₁/rGel. Using competition assays with specific blocking antibodies against either Flt-1 or Flk-1, as well as using the Flt-1-specific ligand PlGF, our data suggests that Flt-1 may be the receptor utilized for internalization by VEGF₁₂₁/rGel in this system. PlGF may recruit Flt-1 positive cells from the bone-marrow microenvironment⁵⁹. This indicates that VEGF₁₂₁/rGel may also intervene with monocyte migration/activation as this event is mediated by Flt-1⁴³. Taken together, our studies suggest that the biological role and character of the two receptors for VEGF is different on osteoclasts compared to vascular endothelial cells⁶⁰⁻⁶². Our results imply a more complex biology for these receptors than has been previously appreciated. VEGF₁₂₁/rGel appears to be an excellent probe to investigate the biology of Flt-1 and Flk-1/KDR receptors and their interaction in complex systems.

Of the VEGF receptors, Flt-1 was the first to be discovered⁶³, and yet its function is not understood as well as other VEGF receptors. It was originally suggested that Flt-1 merely functions as a decoy receptor, tempering the activation of Flk-1/KDR⁶⁴. Conflicting data at the present suggests that the function and signaling of Flt-1 is complex and appears to be dependent on developmental stage and on cell type⁶⁰⁻⁶². Importantly Flt-1, but not Flk-1/KDR, is associated with inhibition of hematopoietic stem cell cycling, differentiation, and hematopoietic recovery in adults⁶⁵, and hematopoietic cell

motility^{43,59} and since VEGF₁₂₁/rGel targets osteoclast precursor cells specifically expressing Flt-1, this may suggest that the Flt-1 receptor may be an overlooked therapeutic target to specifically modulate osteolytic bone diseases.

The dual ability of VEGF₁₂₁/rGel to target neovasculature as well as osteoclast precursor cells, represents a novel application of this fusion protein with significant clinical potential. Because VEGF is involved in both angiogenesis and osteolysis (Fig. 8), VEGF₁₂₁/rGel may disrupt tumor growth both by preventing angiogenesis and by inhibiting the process of bone remodeling. This, in turn, prevents further tumor invasion and osteolytic penetration of tumor into bone. Since osteolysis is an integral component of osteoblastic lesions as well, it remains to be seen if VEGF₁₂₁/rGel is as efficacious in these models and xenograft model studies are currently under way to address this issue. Based on our data, the “trojan horse” approach employed by VEGF₁₂₁/rGel might be useful for the treatment of bone-related malignancies such as bone metastases, and may also be useful in treating other bone-related malignancies such as the osteoclast component of Pagets disease and hematopoietic diseases such as multiple myeloma. Our study clearly shows that the Flt-1 receptor may be of equal if not greater importance in bone biology and warrants further study regarding its importance in the normal bone remodeling process and in various pathological states.

Methods

Materials

Bacterial strains, pET bacterial expression plasmids and recombinant enterokinase were obtained from Novagen (Madison, WI). All other chemicals were from Sigma Chemical Company (St. Louis, MO) or Fisher Scientific (Pittsburgh, PA). TALON metal affinity resin was obtained from Clontech laboratories (Palo Alto, CA). Other chromatography resin and materials were from Pharmacia Biotech (Piscataway, NJ). Tissue culture reagents were from Gibco BRL (Gaithersburg, MD) or Mediatech Cellgro (Herndon, VA). Rabbit anti-gelonin antisera were obtained from the Veterinary Medicine Core Facility at MDACC. Anti-Flt-1 (sc-9029), and anti-Flk-1 (sc-315,sc-19530) polyclonal antibodies were purchased from Santa Cruz Biotechnology, Inc. (Santa Cruz, CA). R-Phycoerythrin (R-PE)-conjugated Flk-1 monoclonal antibody and Alexa Fluor 488-conjugated CD11b (Mac-1) monoclonal antibody were purchased from BD Pharmingen (San Diego, CA). R-Phycoerythrin-conjugated secondary antibodies were purchased from Jackson ImmunoResearch Laboratories Inc. (West Grove, PA). Neutralizing antibodies to Flt-1 (AF471) and Flk-1 (AF644), recombinant mM-CSF and rPIGF were purchased from R&D Systems (Minneapolis, MN).

Cell lines

All media were supplemented with 100 units/ml penicillin, 100 units/ml streptomycin, and 10% fetal bovine serum (FBS). Porcine aortic endothelial cells transfected with the human KDR (PAE/KDR) or FLT-1 (PAE/FLT-1) receptors were a

generous gift from Dr. J. Waltenberger. Cells were maintained as a monolayer in F12 nutrient medium (HAM). Mouse brain endothelial (bEnd3) cells and the prostate cancer cell line PC-3 were maintained as monolayer cultures in DMEM with 10% non-essential amino acids. The cultured mouse osteoclast precursor cells RAW264.7 was maintained in DMEM-F12 medium. BMM cells were maintained in α -MEM medium with M-CSF (R&D Systems Inc., Minneapolis MN). Cells were harvested by treatment with Versene (0.02% EDTA/PBS) or Trypsin/EDTA (0.025%/0.01%).

Primary Bone Marrow Cell Culture

Bone marrow cells from the tibiae and femora were aseptically dissected from mice 8-12 weeks of age. Bone ends were cut off, and marrow was forced out in α -MEM supplemented with 10% FBS and 100 units/ml penicillin (α -MEM). The marrow suspension was filtered through a fine meshed sieve to remove bone particles and gentle pipetting was used to obtain a single cell suspension. The bone marrow cells were washed and plated at $1.5-2 \times 10^7$ cells/10 cm dish with 10 ml of α -MEM and cultured for 24h in the presence of M-CSF (10ng/ml). Non-adherent cells were then washed and re-suspended in α -MEM, plated at 2.5×10^4 cells per well in a 96 well dish for cytotoxicity assays or 5×10^3 pre well in a 96 well plate for osteoclast assays, RNA extraction and Western blot analysis. Cells were then cultured for 3 days in the presence of 10 ng/ml M-CSF before they were used for further experiments.

Animals

Male athymic BALB/c nude mice were obtained from the Animal Production Area of the National Cancer Institute, Frederick Cancer Research Facility (Frederick, MD). Black 6 mice (C57BL/6J) were obtained from Charles River (Wilmington, MA). Mice were maintained in a laminar air-flow cabinet under specific pathogen-free conditions and used at 8-12 weeks of age. All facilities were approved by the American Association for Accreditation of Laboratory Animal Care (AAALAC) in accordance with the current regulations and standards of the United States Department of Agriculture, the Department of Health and Human Services, and the NIH. Mice were fed Purina rodent chow and tap water ad libitum.

Expression and purification of VEGF₁₂₁/rGel

The construction, expression and purification of VEGF₁₂₁/rGel has been previously described²⁹. The fusion toxin was stored in sterile PBS at -20°C.

Cytotoxicity of VEGF₁₂₁/rGel and rGel

Cytotoxicity of VEGF₁₂₁/rGel and rGel against log phase PC-3, RAW264.7 and BMM cells was performed as described²⁹. Log phase cells (3×10^3 PC-3, 5×10^3 RAW264.7 or 2.5×10^4 BMM) were plated in 96-well flat-bottom tissue culture plates and allowed to attach overnight. Purified VEGF₁₂₁/rGel and rGel were diluted in culture media and added to the wells in 5-fold serial dilutions. Cells were incubated for 72 h. The remaining adherent cells were stained with crystal violet (0.5% in 20% methanol) and

solubilized with Sorenson's buffer (0.1 M sodium citrate, pH 4.2, in 50% ethanol).

Absorbance was measured at 630 nm.

In Vitro Osteoclast Differentiation

BMM and RAW 264.7 cells were cultured in 96-well dishes at a density of 5×10^3 cells per well and 3×10^3 cells per well, respectively. Cell cultures were initially treated with 100 ng/ml RANKL and 10ng/ml M-CSF (for BMM) and also subject to a medium change on day 3. We assessed osteoclast differentiation by counting the total number of multinucleated (>3 nuclei), TRAP-positive cells per well 96 h post-treatment using the Leucocyte Acid phosphatase kit (Sigma-Aldrich , St. Louis, MO, USA).

Time-dependent cytotoxicity

Non-adherent, primary monocytes (50×10^3 /well) were cultured overnight in 24-well plates. Cells were then treated with RANKL (100 ng/ml) in the absence or presence of increasing concentrations of VEGF₁₂₁/rGel or rGel added either with RANKL stimulation and TRAP stained at 96h post-treatment, added with RANKL stimulation and TRAP stained at 60h post treatment, or added at 60h post RANKL stimulation and TRAP stained at 96h. Cells were fixed, stained for TRAP and TRAP+ multinucleated cells were counted in each condition.

RNA extraction

BMM and RAW cells were treated with their respective IC₅₀ VEGF₁₂₁/rGel doses in the presence and absence of RANKL (and M-CSF for BMM cells) for 24 to 96 h.

Control cells, including bEnd3, PAE/KDR and PAE/FLT-1 cells, were treated with PBS. Total RNA was extracted using the RNeasy mini-kit (Qiagen, Valencia, CA) and its integrity verified by electrophoresis on a denaturing formaldehyde-agarose gel and on a 2100 Bioanalyzer (Agilent, Foster City, CA).

RT-PCR analysis

Levels of Flt-1/FLT-1, Flk-1/KDR and VEGF-A were assessed by RT-PCR analysis. GAPDH primers were used as controls. The primers were as follows: Flk-1/KDR forward – 5' ATTACTTGCAGGGGACAG; Flk-1/KDR reverse – 5' GGAACAAATCTCTTTTCTGG; Flk-1 forward – 5' CATGCACAGTCTACGCCAACC; Flk-1 reverse – 5' CGCAACATGTTTACACTTCGGT; Flt-1/FLT-1 forward – 5' CAAATGCAACGTACAAAGA; Flt-1/FLT-1 reverse – 5' AGAGTGGCAGTGAGGTTTTTT; Flt-1 forward – 5' ACTGAAACTAGGCAAATCGCTCG; Flt-1 reverse – 3' GCGGATCTGTACAGTCGTCG; VEGF-A forward – 5' TGAAGTGATCAAGTTCATGGACGT; VEGF-A reverse – 5' TCACCGCCTTGGCTTGTC; GAPDH forward - 5' GTCTTCACCACCATGGAG; and GAPDH reverse - 5' CCACCCTGTTGCTGTAGC. Isolated RNA was subjected to first-strand cDNA synthesis as described by the manufacturer of the Superscript First Strand synthesis system (Invitrogen, Carlsbad, CA). RT-PCR was performed using a Robocycler Gradient 96 machine (Stratagene, La Jolla, CA). Negative controls (samples without Taq polymerase or with water instead of RNA) were included. Amplified RT-PCR products were analyzed on 2% agarose gels containing ethidium bromide and

subjected to densitometric analysis using Alpha Innotech FluorChem8900 (San Leandro, CA).

Western blot analysis

Total cell extracts of PAE/KDR and PAE/FLT-1 cells were obtained by lysing cells in Cell Lysis buffer (50 mM Tris, pH 8.0, 0.1 mM EDTA, 1 mM DTT, 12.5 mM MgCl_2 , 0.1 M KCl, 20% glycerol) supplemented with protease inhibitors (leupeptin (0.5%), aprotinin (0.5%) and PMSF (0.1%). Protein samples were separated by SDS-PAGE under reducing conditions and electrophoretically transferred to a PVDF memberane overnight at 4 °C in transfer buffer (25 mM Tris-HCl, pH 7.6, 190 mM glycine, 20% HPLC-grade methanol). The membranes were incubated overnight with appropriate antibodies (1:200 in 5% milk) followed by incubation with goat-anti-rabbit IgG horseradish peroxidase, developed using the Amersham ECL detection system and exposed to X-ray film.

FACS Analysis

RAW246.7 and BMM cells were harvested and washed with PBS, resuspended in staining buffer (PBS + 2% FBS) at a concentration of 10×10^6 cells/ml. One hundred microliter aliquots of RAW246.7 and BMM cells were incubated with 2 μg and 0.5 μg anti-Flt-1 or R-PE conjugated anti-Flk-1 antibody respectively. Cells were incubated with primary antibodies for 1 h at 4°C. In addition, BMM cells were incubated for 1 h (4°C) with 0.2 μg Alexa Fluor 488-conjugated CD11b antibody for detection of the monocyte/macrophage population. 0.5 μg R-PE conjugated secondary antibody (Jackson

Immunoresearch, West Grove, PA) was employed to detect anti Flt-1. Samples were analyzed on a BD FACS Calibur flow cytometer (BD, San Jose, CA), using CellQuest Pro acquisition software (BD, San Jose, CA). Instrumentation set-up and electronic compensation for spectral overlap was performed using cell samples single-stained with FITC or R-PE. At least 10,000 events were collected for each sample.

Internalization of VEGF₁₂₁/rGel into RAW264.7 and BMM cells

Cells were incubated with various concentrations of VEGF₁₂₁/rGel or rGel at the timepoints indicated. To demonstrate receptor specificity, Cells were pre-treated with Flt-1 or Flk-1 neutralizing antibodies for one hour prior to treatment with VEGF₁₂₁/rGel or rGel. Glycine buffer (500 mM NaCl, 0.1 glycine, pH 2.5) was used to strip the cell surface of non-internalized VEGF₁₂₁/rGel. Cells were fixed with 3.7% formaldehyde and permeabilized with 0.2% Triton X-100. Non-specific binding sites were blocked with 5% BSA in PBS. Cells were then incubated with a rabbit anti-gelonin polyclonal antibody (1:200) followed by a TRITC-conjugated anti-rabbit secondary antibody (1:80). Nuclei were stained with propidium iodide (1µg/ml) in PBS. The slides were fixed with DABCO media, mounted and visualized under fluorescence (Nikon Eclipse TS1000) and confocal (Zeiss LSM 510) microscopes. Competition assays were performed by plating RAW264.7 (5×10^3) and BMM (2.5×10^4) cells in 96 well plates and pre-incubating the cells for 1 h with increasing doses of PlGF (prior to addition of 20 nM VEGF₁₂₁/rGel. Results were analyzed by staining the remaining adherent cells with crystal violet as described above.

Intrabone injections

The PC-3 cells were harvested by a 1 min treatment with Trypsin/EDTA. The culture flask was tapped to detach the cells. The cells were washed in PBS and resuspended in PBS in preparation for implantation into the mice. Animals were anesthetized with intramuscular injections of ketamine (100 mg/kg) plus acepromazine (2.5 mg/kg). Aliquots of 5×10^4 of PC-3 cells were diluted in 5 μ l of growth medium and then injected into the distal epiphysis of the right femur of each mouse using a 28-gauge Hamilton needle. The contralateral femur was used as an internal control. Twenty mice were randomized into two treatment groups. Treatment began one week after tumor placement. The animals were treated (i.v.) with the following protocol: Group 1 - 200 μ l saline every other day for nine days (5 treatments); Group 2 - 180 μ g VEGF₁₂₁/rGel in 200 μ l saline every other day for nine days (5 treatments). Mice were monitored weekly for tumor bulk and bone loss. Mice were killed in case of excessive bone loss as per AAALAC guidelines and pathologic examination of the subject bones was performed.

Processing of bone tissue samples

Formalin-fixed, paraffin-embedded tissue samples from the tumors were prepared by the Department of Veterinary Medicine at M. D. Anderson Cancer Center. The subject bones were dissected free of muscle, fixed in 10% buffered formalin, decalcified in 5% formic acid, and then embedded in paraffin. Longitudinal 3- μ m thick sections were obtained from each sample and stained with H&E. TRAP staining was performed as described by the manufacturer of the kit (Sigma Aldrich, St. Louis, MO).

Figure Legends

Figure 1 VEGF₁₂₁/rGel inhibits tumor growth and osteolysis in the PC-3 xenograft model and increases the survival of mice. **(a)** Effect of VEGF₁₂₁/rGel in nude mice with PC-3 tumors in bone. Mice were injected with 5×10^4 PC-3 cells into the distal epiphysis of the right femur, using the contralateral femur as an internal control. Mice received 5 treatments with either saline or 180µg VEGF₁₂₁/rGel 2 days apart, starting 2 days post PC-3 tumor placement. Animals were analyzed by X-ray, and radiograms shown are representative of 20 mice. Arrows indicate location of osteolytic lesion, which were only found in the saline-treated animals (left panels), but not in the majority of VEGF₁₂₁/rGel treated animals (right panels). **(b)** A survival curve of the mice in this study. All control mice were sacrificed by day 67. Asterisk one mouse (without tumor) that did not recover from anesthesia. Sections of femurs two weeks after injection of PC-3 tumor cells were stained for H&E to analyze the presence of PC-3 cell burden (c). Mice treated with saline show proliferation of PC-3 tumor cells (upper panel). In contrast, mice treated with VEGF₁₂₁/rGel show isolated pockets of PC-3 tumor cells (middle panel). Shown in the lower panel is a representative bone section in which PC-3 tumor cells had been placed from a mouse treated with VEGF₁₂₁/rGel, showing absence of tumor.

Figure 2 PC-3 cells are not specifically targeted by VEGF₁₂₁/rGel. **(a)** Cytotoxicity of VEGF₁₂₁/rGel and rGel on PC-3 cells. PC-3 cells (5×10^3) were plated in 96- well plates and the cytotoxicity of increasing concentrations of VEGF₁₂₁/rGel and rGel were evaluated by crystal violet staining following incubation for 72 h. Values represent the mean of three separate experiments. **(a, inset)** Expression of KDR and FLT-1 RNA was

evaluated by RT-PCR. Total RNA was isolated as described in “Methods” and 500ng RNA of each sample was subject to RT-PCR prior to separation on a 2% agarose gel containing ethidium bromide for visualization of RNA. **(b)** Effect of VEGF₁₂₁/rGel on the number of osteoclasts in bone sections of nude mice with PC-3 tumor cells.

VEGF₁₂₁/rGel reduces the number of osteoclasts and inhibits tumor growth *in vivo*.

Figure 3 VEGF₁₂₁/rGel inhibits RANKL-mediated osteoclastogenesis in RAW264.7

cells and mouse primary monocytes. Each experiment was performed in triplicate. The data shown is representative of three separate experiments. **(a)** RAW264.7 cells (1×10^4 /well) were cultured overnight in 24-well plates. Cells were treated with RANKL (100 ng/ml) in the absence or presence of increasing concentrations of VEGF₁₂₁/rGel or rGel.

After 4 days, cells were fixed, TRAP stained, and the total number of multinucleated (>3 nuclei) TRAP⁺ osteoclasts was counted. **(b)** Appearance of TRAP stained RAW264.7 cells following incubation with RANKL without or with VEGF₁₂₁/rGel or rGel. **(c)**

Cytotoxicity of VEGF₁₂₁/rGel and rGel was assessed in 96-well plates. 5×10^3

RAW264.7 cells were plated in 96-well plates and incubated over night. Cells were then subjected to increasing concentrations of VEGF₁₂₁/rGel and rGel for 72 h, followed by

staining with crystal violet. **(d)** Non-adherent mouse bone marrow-derived monocytes were isolated from the tibia and femur of mice and plated in 24-well plates (5×10^4 /well)

and incubated with M-CSF (10 ng/ml). After 3 days, the cells were washed and

stimulated with M-CSF (10 ng/ml) in the absence or presence of increasing concentrations of VEGF₁₂₁/rGel or rGel and RANKL (100 ng/ml). Medium was changed on day 3. On day 5 the cells were fixed, stained for TRAP, and the total number of

TRAP⁺ osteoclasts was counted. **(e)** Appearance of TRAP stained BMM cells following incubation with RANKL and M-CSF without or with VEGF₁₂₁/rGel or rGel. **(f)**

Cytotoxicity of VEGF₁₂₁/rGel and rGel was assessed in 96-well plates. Non-adherent mouse bone marrow-derived monocytes isolated from the tibia and femur of mice were plated (25×10^4 /well) and incubated with M-CSF (10 ng/ml) for three days. Cells were then washed and subjected to increasing concentrations of VEGF₁₂₁/rGel and rGel for 72 h, followed by staining with crystal violet.

Figure 4 VEGF₁₂₁/rGel is cytotoxic to mouse primary monocytes, but not mature osteoclasts. The effect of VEGF₁₂₁/rGel and rGel on primary monocytes was investigated at various time-points after RANKL stimulation. The data shown is representative of three separate experiments. Non-adherent, primary monocytes (50×10^3 /well) were cultured overnight in 24-well plates. Cells were then treated with RANKL (100 ng/ml) in the absence or presence of increasing concentrations of VEGF₁₂₁/rGel or rGel added either with RANKL stimulation and TRAP stained at 96 h post-treatment **(a)**, added with RANKL stimulation and TRAP stained at 60 h post treatment **(b)**, or added at 60 h post RANKL stimulation and TRAP stained at 96 h **(c)**. **(d)** Cells were fixed, stained for TRAP and multinucleated (>3 nuclei), TRAP⁺ cells were counted in each condition. The data shown is representative of three separate experiments and error bars represent mean \pm s.e.m. for each sample done in triplicate. RL: RANKL

Figure 5 VEGF₁₂₁/rGel is internalized into RAW264.7 cells and stimulates ERK activation. **(a)** Intracellular delivery of VEGF₁₂₁/rGel in RAW264.7 cells. RAW264.7 cells were treated with either VEGF₁₂₁/rGel or rGel for 24 hrs. The cells were fixed, acid-washed to remove surface-bound material, permeabilized, and immunostained for the presence of rGel (green). The cells were counterstained with propidium iodide (red) to identify nuclei. **(b)** 0.6 x 10⁶ RAW264.7 cells were plated in 6 well plates and incubated for 24 hours. Cells were then serum starved over night prior to incubation of 7nM VEGF₁₂₁, 7 nM VEGF₁₂₁/rGel, 1 nM PlGF or 100nM rGel for the indicated time points. 5nM RANKL was used as a control. Cells were then harvested and 50ug of the whole cell lysate was subjected to SDS-PAGE Western blot analysis with the indicated antibodies. Data show is representative of 3 separate experiments.

Figure 6 Expression of Flt-1 and Flk-1 in RAW264.7 and BMM cells. **(a)** RT-PCR analysis. Total RNA was extracted from RAW264.7, BMM, and bEnd3 cells were subject to RT-PCR analysis using 500ng RNA and primers for Flt-1, Flk-1/KDR and GAPDH. bEnd3 cells (lanes 7-9) express both Flt-1 and Flk-1 and were used as a control. RAW264.7 cells (lanes 1-3) express Flt-1 but not Flk-1. BMM cells (lanes 4-6) express Flt-1 and low levels of Flk-1. **(b)** Western blot analysis of RAW264.7 cells. Expression of Flt-1, but not Flk-1, is confirmed. **(c-g)** FACS analysis of RAW264.7 and BMM cells for Flt-1 and Flk-1 receptors. 1 x 10⁶ cells were used per sample. RAW264.7 cells incubated with antibodies recognizing the extracellular portion of Flt-1 **(c)** or Flk-1 **(d)** revealed that 99% of the cells expressed Flt-1 but only 8% of the cells expressed Flk-1. **(e)** BMM cells were identified with an antibody recognizing CD11b and double stained

with antibodies to Flt-1 (f) or Flk-1 (g). Approximately 42% of the positively identified BMM cells expressed Flt-1 but only 5.4% of the cells expressed Flk-1. Data shown is representative of four separate experiments. **(h)** BMM cells stimulated to differentiate by RANKL (100 ng/ml) were harvested at the time points indicated and analyzed by RT-PCR. Flt-1 mRNA is down-regulated during RANKL-mediated differentiation of bone marrow-derived cells of monocyte/macrophage lineage to osteoclasts. GAPDH was utilized as a loading control. **(i)** Densitometric analysis of Flt-1 and Flk-1 expression in BMM cells during osteoclastogenesis. After RT-PCR, 5, 10, and 20 μ l of each sample was loaded on a 2% agarose gel and evaluated densitometrically. Each sample was normalized with its individual GAPDH control within its own group and then compared to each other. The Flt-1 transcript was downregulated by 3.4-fold during differentiation of osteoclast pre-cursor cells whereas Flk-1 transcript levels did not change. Data shown represent three separate RNA preparations and is representative of 3 separate experiments.

Figure 7 Flt-1, but not Flk-1, mediates the cytotoxic effect of VEGF₁₂₁/rGel. **(a)** Cells were pre-treated for one hour with 10 μ g/ml of neutralizing antibodies to either Flt-1 or Flk-1 prior to the addition of 10 nM VEGF₁₂₁/rGel. The cells were fixed, acid-washed to remove surface-bound material, permeabilized, and immunostained for the presence of rGel (green). The cells were counterstained with propidium iodide (red) to identify nuclei. **(b)** 5×10^3 RAW264.7 cells were plated in 96-well plates and incubated overnight. Cells were then incubated with increasing concentrations of recombinant mouse PlGF for 1 hour prior to the addition of 30nM VEGF₁₂₁/rGel 72 h. **(c)** Non-adherent mouse bone marrow-derived monocytes were isolated from the tibia and femur of mice

and plated in 96-well plates (25×10^4 /well) and incubated with M-CSF (10 ng/ml). After 3 days, the cells were washed subjected to increasing concentrations of recombinant mouse PlGF for 1 hour prior to the addition of 8nM VEGF₁₂₁/rGel for 72 h. After 3 days, the remaining RAW264.7 and BMM cells were stained with crystal violet to evaluate cytotoxicity of VEGF₁₂₁/rGel and rGel. Data show is representative of two separate experiments and error bars represent mean \pm s.e.m. for each concentration done in quadruplets.

Figure 8 Proposed dual role for VEGF₁₂₁/rGel in invasion and osteolytic penetration in bone. Tumor growth following skeletal metastases requires the proliferation of new blood vessels as well as resorption of bone. VEGF and its receptors play a critical role in both pathways and in the development of skeletal metastases in breast cancer. The fusion protein VEGF₁₂₁/rGel is a useful molecule to probe the roles of VEGF and its receptors, as it can prevent both angiogenesis and bone resorption by competing with VEGF as well as exerting cytotoxic effects.

Table 1

a) Cytotoxicity of VEGF₁₂₁/rGel and rGel over 72 hours on RAW264.7 cells after treatment with RANKL

Agent	Treatment with RANKL (h)	IC ₅₀ (nM)
VEGF ₁₂₁ /rGel	0	30
	24	30
	72	200
	96	300
rGel	0	450
	24	500
	72	500
	96	500

b) Cytotoxicity of VEGF₁₂₁/rGel and rGel over 72 hours on BMM cells after treatment with RANKL and M-CSF

Agent	Treatment with RANKL (h)	IC ₅₀ (nM)
VEGF ₁₂₁ /rGel	0	8
	24	100
	48	>400
	72	>400

Reference List

1. Boyle,W.J., Simonet,W.S. & Lacey,D.L. Osteoclast differentiation and activation. *Nature* 423, 337-342 (2003).
2. Dai,J. *et al.* Chronic alcohol ingestion induces osteoclastogenesis and bone loss through IL-6 in mice. *J. Clin. Invest* 106, 887-895 (2000).
3. Kim,S. *et al.* Stat1 functions as a cytoplasmic attenuator of Runx2 in the transcriptional program of osteoblast differentiation. *Genes Dev.* 17, 1979-1991 (2003).
4. Naruse,M. *et al.* Inhibition of osteoclast formation by 3-methylcholanthrene, a ligand for arylhydrocarbon receptor: suppression of osteoclast differentiation factor in osteogenic cells. *Biochem. Pharmacol.* 67, 119-127 (2004).
5. Odgren,P.R. *et al.* The role of RANKL (TRANCE/TNFSF11), a tumor necrosis factor family member, in skeletal development: effects of gene knockout and transgenic rescue. *Connect. Tissue Res.* 44 Suppl 1, 264-271 (2003).
6. Karsenty,G. The genetic transformation of bone biology. *Genes Dev.* 13, 3037-3051 (1999).
7. Francini,G. *et al.* Production of parathyroid hormone and parathyroid-hormone-related protein by breast cancer cells in culture. *J. Cancer Res. Clin. Oncol.* 119, 421-425 (1993).
8. Roodman,G.D. Biology of osteoclast activation in cancer. *J. Clin. Oncol.* 19, 3562-3571 (2001).
9. Taube,T., Elomaa,I., Blomqvist,C., Beneton,M.N. & Kanis,J.A. Histomorphometric evidence for osteoclast-mediated bone resorption in metastatic breast cancer. *Bone* 15, 161-166 (1994).
10. Boyce,B.F., Yoneda,T. & Guise,T.A. Factors regulating the growth of metastatic cancer in bone. *Endocr. Relat Cancer* 6, 333-347 (1999).
11. Mbalaviele,G. *et al.* Cadherin-6 mediates the heterotypic interactions between the hemopoietic osteoclast cell lineage and stromal cells in a murine model of osteoclast differentiation. *J. Cell Biol.* 141, 1467-1476 (1998).
12. Mundy,G.R. & Yoneda,T. Facilitation and suppression of bone metastasis. *Clin. Orthop. Relat Res.* 34-44 (1995).
13. Guise,T.A. & Chirgwin,J.M. Transforming growth factor-beta in osteolytic breast cancer bone metastases. *Clin. Orthop. Relat Res.* S32-S38 (2003).

14. Kumta,S.M. *et al.* Expression of VEGF and MMP-9 in giant cell tumor of bone and other osteolytic lesions. *Life Sci.* 73, 1427-1436 (2003).
15. Nakata,A. *et al.* Inhibition by interleukin 18 of osteolytic bone metastasis by human breast cancer cells. *Anticancer Res.* 19, 4131-4138 (1999).
16. Bendre,M.S. *et al.* Expression of interleukin 8 and not parathyroid hormone-related protein by human breast cancer cells correlates with bone metastasis in vivo. *Cancer Res.* 62, 5571-5579 (2002).
17. Thomas,R.J. *et al.* Breast cancer cells interact with osteoblasts to support osteoclast formation. *Endocrinology* 140, 4451-4458 (1999).
18. Engsig,M.T. *et al.* Matrix metalloproteinase 9 and vascular endothelial growth factor are essential for osteoclast recruitment into developing long bones. *J. Cell Biol.* 151, 879-889 (2000).
19. Henriksen,K., Karsdal,M., Delaisse,J.M. & Engsig,M.T. RANKL and vascular endothelial growth factor (VEGF) induce osteoclast chemotaxis through an ERK1/2-dependent mechanism. *J. Biol. Chem.* 278, 48745-48753 (2003).
20. Gerber,H.P. *et al.* VEGF couples hypertrophic cartilage remodeling, ossification and angiogenesis during endochondral bone formation. *Nat. Med.* 5, 623-628 (1999).
21. Haigh,J.J., Gerber,H.P., Ferrara,N. & Wagner,E.F. Conditional inactivation of VEGF-A in areas of collagen2a1 expression results in embryonic lethality in the heterozygous state. *Development* 127, 1445-1453 (2000).
22. Zelzer,E. *et al.* Skeletal defects in VEGF(120/120) mice reveal multiple roles for VEGF in skeletogenesis. *Development* 129, 1893-1904 (2002).
23. Carlevaro,M.F., Cermelli,S., Cancedda,R. & Descalzi,C.F. Vascular endothelial growth factor (VEGF) in cartilage neovascularization and chondrocyte differentiation: auto-paracrine role during endochondral bone formation. *J. Cell Sci.* 113 (Pt 1), 59-69 (2000).
24. Horner,A. *et al.* Immunolocalisation of vascular endothelial growth factor (VEGF) in human neonatal growth plate cartilage. *J. Anat.* 194 (Pt 4), 519-524 (1999).
25. Nakagawa,M. *et al.* Vascular endothelial growth factor (VEGF) directly enhances osteoclastic bone resorption and survival of mature osteoclasts. *FEBS Lett.* 473, 161-164 (2000).
26. Niida,S. *et al.* Vascular endothelial growth factor can substitute for macrophage colony-stimulating factor in the support of osteoclastic bone resorption. *J. Exp. Med.* 190, 293-298 (1999).

27. Min,J.K. *et al.* Vascular endothelial growth factor up-regulates expression of receptor activator of NF-kappa B (RANK) in endothelial cells. Concomitant increase of angiogenic responses to RANK ligand. *J. Biol. Chem.* 278, 39548-39557 (2003).
28. Liu,Y., Cheung,L.H., Thorpe,P. & Rosenblum,M.G. Mechanistic studies of a novel human fusion toxin composed of vascular endothelial growth factor (VEGF)₁₂₁ and the serine protease granzyme B: directed apoptotic events in vascular endothelial cells. *Mol. Cancer Ther.* 2, 949-959 (2003).
29. Veenendaal,L.M. *et al.* In vitro and in vivo studies of a VEGF₁₂₁/rGelolin chimeric fusion toxin targeting the neovasculature of solid tumors. *Proc. Natl. Acad. Sci. U. S. A* 99, 7866-7871 (2002).
30. Arora,N. *et al.* Vascular endothelial growth factor chimeric toxin is highly active against endothelial cells. *Cancer Res.* 59, 183-188 (1999).
31. Olson,T.A., Mohanraj,D., Roy,S. & Ramakrishnan,S. Targeting the tumor vasculature: inhibition of tumor growth by a vascular endothelial growth factor-toxin conjugate. *Int. J. Cancer* 73, 865-870 (1997).
32. Ramakrishnan,S., Olson,T.A., Bautch,V.L. & Mohanraj,D. Vascular endothelial growth factor-toxin conjugate specifically inhibits KDR/flk-1-positive endothelial cell proliferation in vitro and angiogenesis in vivo. *Cancer Res.* 56, 1324-1330 (1996).
33. Fine,B.A., Valente,P.T., Feinstein,G.I. & Dey,T. VEGF, flt-1, and KDR/flk-1 as prognostic indicators in endometrial carcinoma. *Gynecol. Oncol.* 76, 33-39 (2000).
34. Gille,H. *et al.* Analysis of biological effects and signaling properties of Flt-1 (VEGFR-1) and KDR (VEGFR-2). A reassessment using novel receptor-specific vascular endothelial growth factor mutants. *J. Biol. Chem.* 276, 3222-3230 (2001).
35. McMahon,G. VEGF receptor signaling in tumor angiogenesis. *Oncologist.* 5 Suppl 1, 3-10 (2000).
36. Neufeld,G., Tessler,S., Gitay-Goren,H., Cohen,T. & Levi,B.Z. Vascular endothelial growth factor and its receptors. *Prog. Growth Factor Res.* 5, 89-97 (1994).
37. Senger,D.R. *et al.* Vascular permeability factor (VPF, VEGF) in tumor biology. *Cancer Metastasis Rev.* 12, 303-324 (1993).
38. Shibuya,M. Role of VEGF-flt receptor system in normal and tumor angiogenesis. *Adv. Cancer Res.* 67, 281-316 (1995).

39. Takahashi,A. *et al.* Markedly increased amounts of messenger RNAs for vascular endothelial growth factor and placenta growth factor in renal cell carcinoma associated with angiogenesis. *Cancer Res.* 54, 4233-4237 (1994).
40. Peters,K.G., De Vries,C. & Williams,L.T. Vascular endothelial growth factor receptor expression during embryogenesis and tissue repair suggests a role in endothelial differentiation and blood vessel growth. *Proc. Natl. Acad. Sci. U. S. A* 90, 8915-8919 (1993).
41. Matsumoto,Y. *et al.* Possible involvement of the vascular endothelial growth factor-Flt-1-focal adhesion kinase pathway in chemotaxis and the cell proliferation of osteoclast precursor cells in arthritic joints. *J. Immunol.* 168, 5824-5831 (2002).
42. Sawano,A. *et al.* Flt-1, vascular endothelial growth factor receptor 1, is a novel cell surface marker for the lineage of monocyte-macrophages in humans. *Blood* 97, 785-791 (2001).
43. Barleon,B. *et al.* Migration of human monocytes in response to vascular endothelial growth factor (VEGF) is mediated via the VEGF receptor flt-1. *Blood* 87, 3336-3343 (1996).
44. Clauss,M. *et al.* The vascular endothelial growth factor receptor Flt-1 mediates biological activities. Implications for a functional role of placenta growth factor in monocyte activation and chemotaxis. *J. Biol. Chem.* 271, 17629-17634 (1996).
45. Casanova,M.L. *et al.* A critical role for ras-mediated, epidermal growth factor receptor-dependent angiogenesis in mouse skin carcinogenesis. *Cancer Res.* 62, 3402-3407 (2002).
46. Kelavkar,U.P. *et al.* Overexpression of 15-lipoxygenase-1 in PC-3 human prostate cancer cells increases tumorigenesis. *Carcinogenesis* 22, 1765-1773 (2001).
47. Wong,Y.C., Wang,Y.Z. & Tam,N.N. The prostate gland and prostate carcinogenesis. *Ital. J. Anat. Embryol.* 103, 237-252 (1998).
48. Chen,J., De,S., Brainard,J. & Byzova,T.V. Metastatic properties of prostate cancer cells are controlled by VEGF. *Cell Commun. Adhes.* 11, 1-11 (2004).
49. Zeng,Y. *et al.* Expression of vascular endothelial growth factor receptor-3 by lymphatic endothelial cells is associated with lymph node metastasis in prostate cancer. *Clin. Cancer Res.* 10, 5137-5144 (2004).
50. Ismail,A.H., Altaweel,W., Chevalier,S., Kassouf,W. & Aprikian,A.G. Expression of vascular endothelial growth factor-A in human lymph node metastases of prostate cancer. *Can. J. Urol.* 11, 2146-2150 (2004).

51. Paz,K. & Zhu,Z. Development of angiogenesis inhibitors to vascular endothelial growth factor receptor 2. current status and future perspective. *Front Biosci.* 10, 1415-1439 (2005).
52. Ueda,Y. *et al.* VEGFR1, a novel binding antagonist of VEGF, inhibits angiogenesis in vitro and in vivo. *Anticancer Res.* 24, 3009-3017 (2004).
53. Ruan,G.R. *et al.* Effect of antisense VEGF cDNA transfection on the growth of chronic myeloid leukemia K562 cells in vitro and in nude mice. *Leuk. Res.* 28, 763-769 (2004).
54. O'Farrell,A.M. *et al.* Effects of SU5416, a small molecule tyrosine kinase receptor inhibitor, on FLT3 expression and phosphorylation in patients with refractory acute myeloid leukemia. *Leuk. Res.* 28, 679-689 (2004).
55. Verheul,H.M. & Pinedo,H.M. Vascular endothelial growth factor and its inhibitors. *Drugs Today (Barc.)* 39 Suppl C, 81-93 (2003).
56. Ferrara,N., Hillan,K.J., Gerber,H.P. & Novotny,W. Discovery and development of bevacizumab, an anti-VEGF antibody for treating cancer. *Nat. Rev. Drug Discov.* 3, 391-400 (2004).
57. Dai,J. *et al.* Vascular endothelial growth factor contributes to the prostate cancer-induced osteoblast differentiation mediated by bone morphogenetic protein. *Cancer Res.* 64, 994-999 (2004).
58. Shariat,S.F. *et al.* Association of preoperative plasma levels of vascular endothelial growth factor and soluble vascular cell adhesion molecule-1 with lymph node status and biochemical progression after radical prostatectomy. *J. Clin. Oncol.* 22, 1655-1663 (2004).
59. Hattori,K. *et al.* Placental growth factor reconstitutes hematopoiesis by recruiting VEGFR1(+) stem cells from bone-marrow microenvironment. *Nat. Med.* 8, 841-849 (2002).
60. Fong,G.H., Zhang,L., Bryce,D.M. & Peng,J. Increased hemangioblast commitment, not vascular disorganization, is the primary defect in flt-1 knock-out mice. *Development* 126, 3015-3025 (1999).
61. Hiratsuka,S., Minowa,O., Kuno,J., Noda,T. & Shibuya,M. Flt-1 lacking the tyrosine kinase domain is sufficient for normal development and angiogenesis in mice. *Proc. Natl. Acad. Sci. U. S. A* 95, 9349-9354 (1998).
62. Matsumoto,T. & Claesson-Welsh,L. VEGF receptor signal transduction. *Sci. STKE.* 2001, RE21 (2001).
63. De Vries,C. *et al.* The fms-like tyrosine kinase, a receptor for vascular endothelial growth factor. *Science* 255, 989-991 (1992).

64. Park,J.E., Chen,H.H., Winer,J., Houck,K.A. & Ferrara,N. Placenta growth factor. Potentiation of vascular endothelial growth factor bioactivity, in vitro and in vivo, and high affinity binding to Flt-1 but not to Flk-1/KDR. *J. Biol. Chem.* 269, 25646-25654 (1994).
65. Gerber,H.P. *et al.* VEGF regulates haematopoietic stem cell survival by an internal autocrine loop mechanism. *Nature* 417, 954-958 (2002).

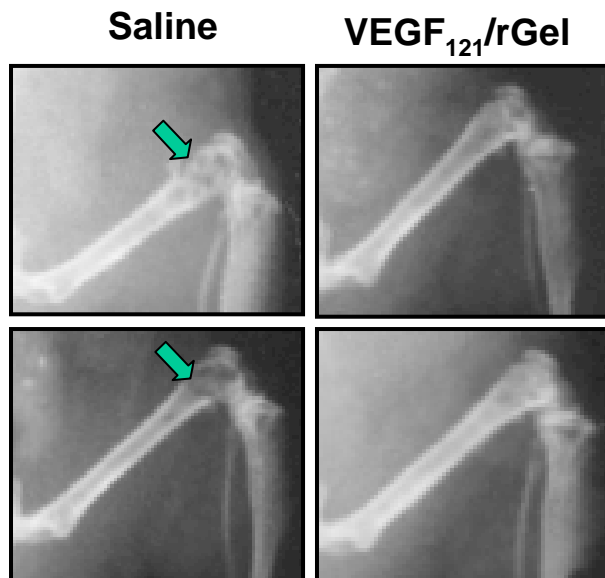
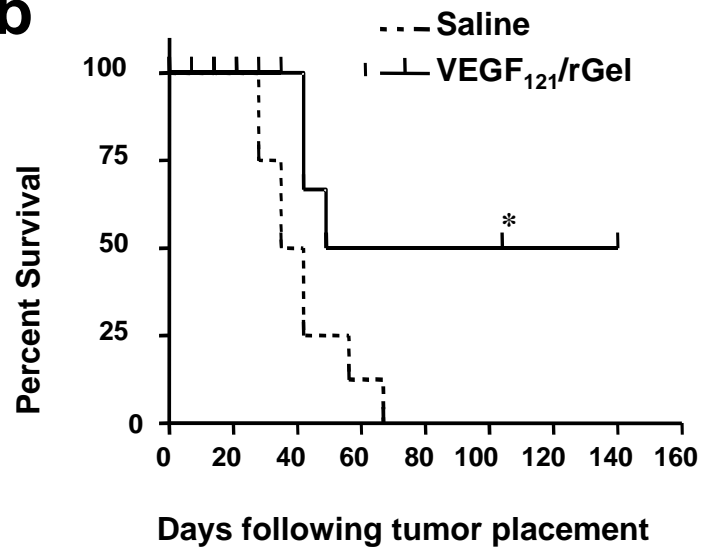
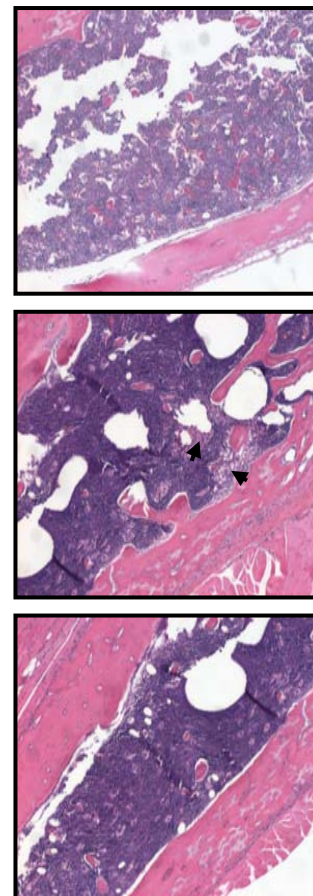
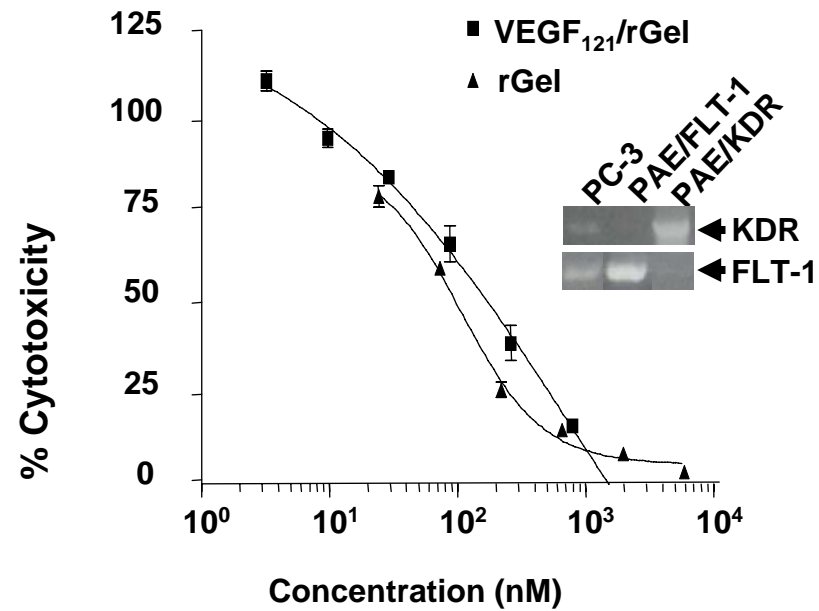
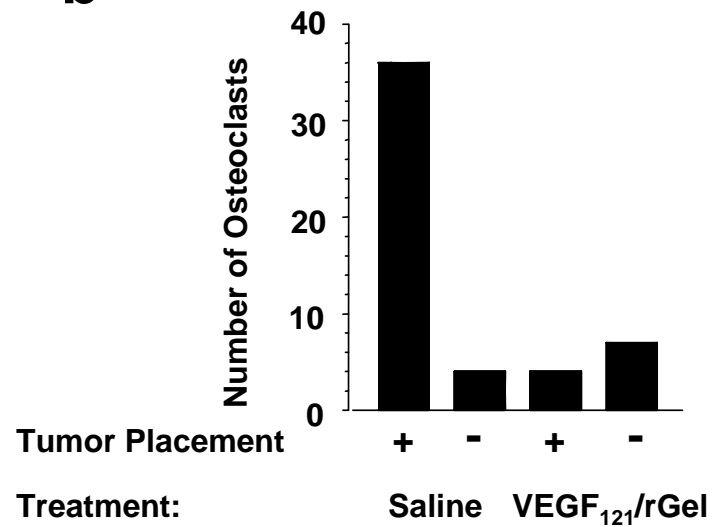
a**b****c**

Figure 1

a**b****Figure 2**

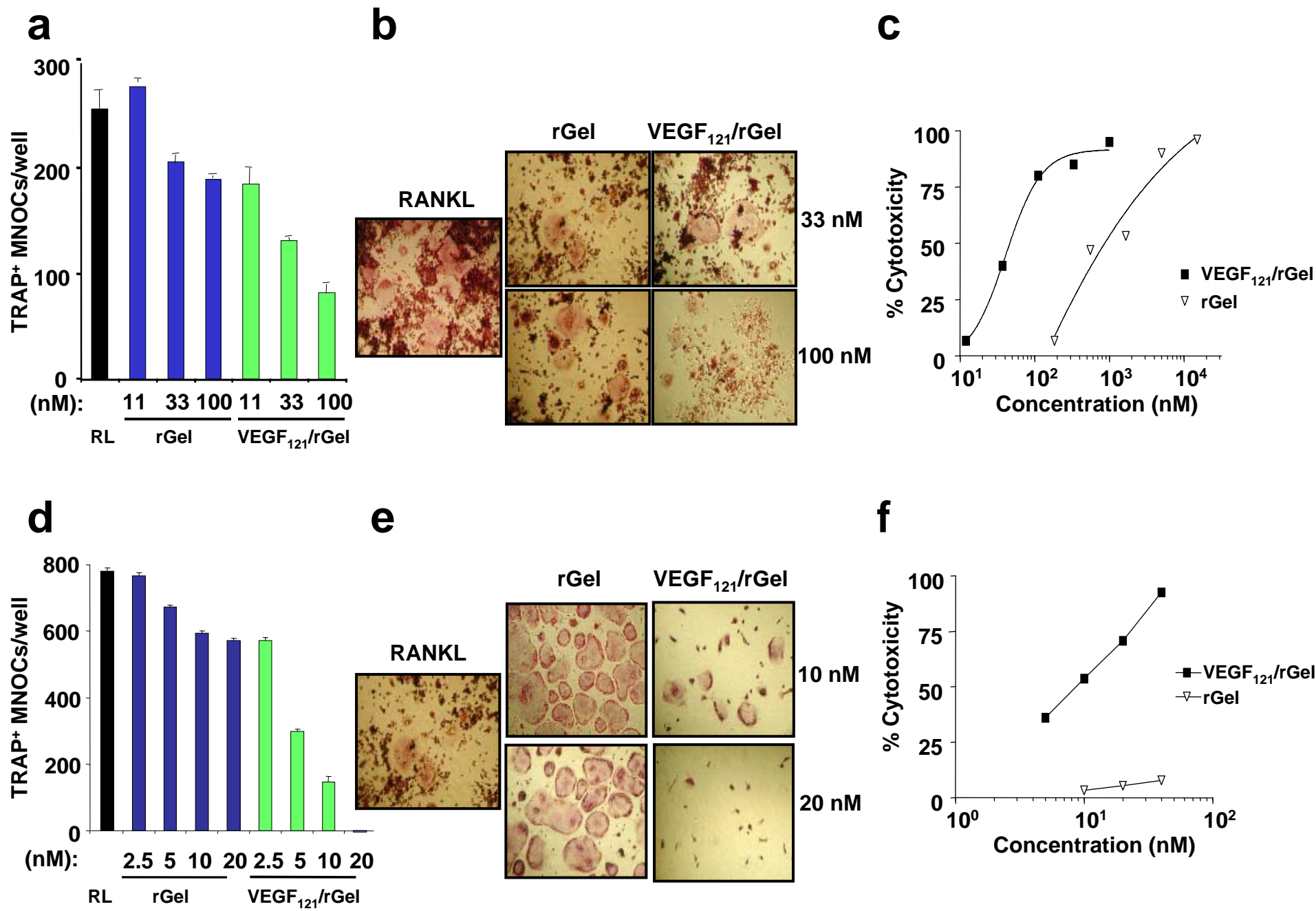


Figure 3

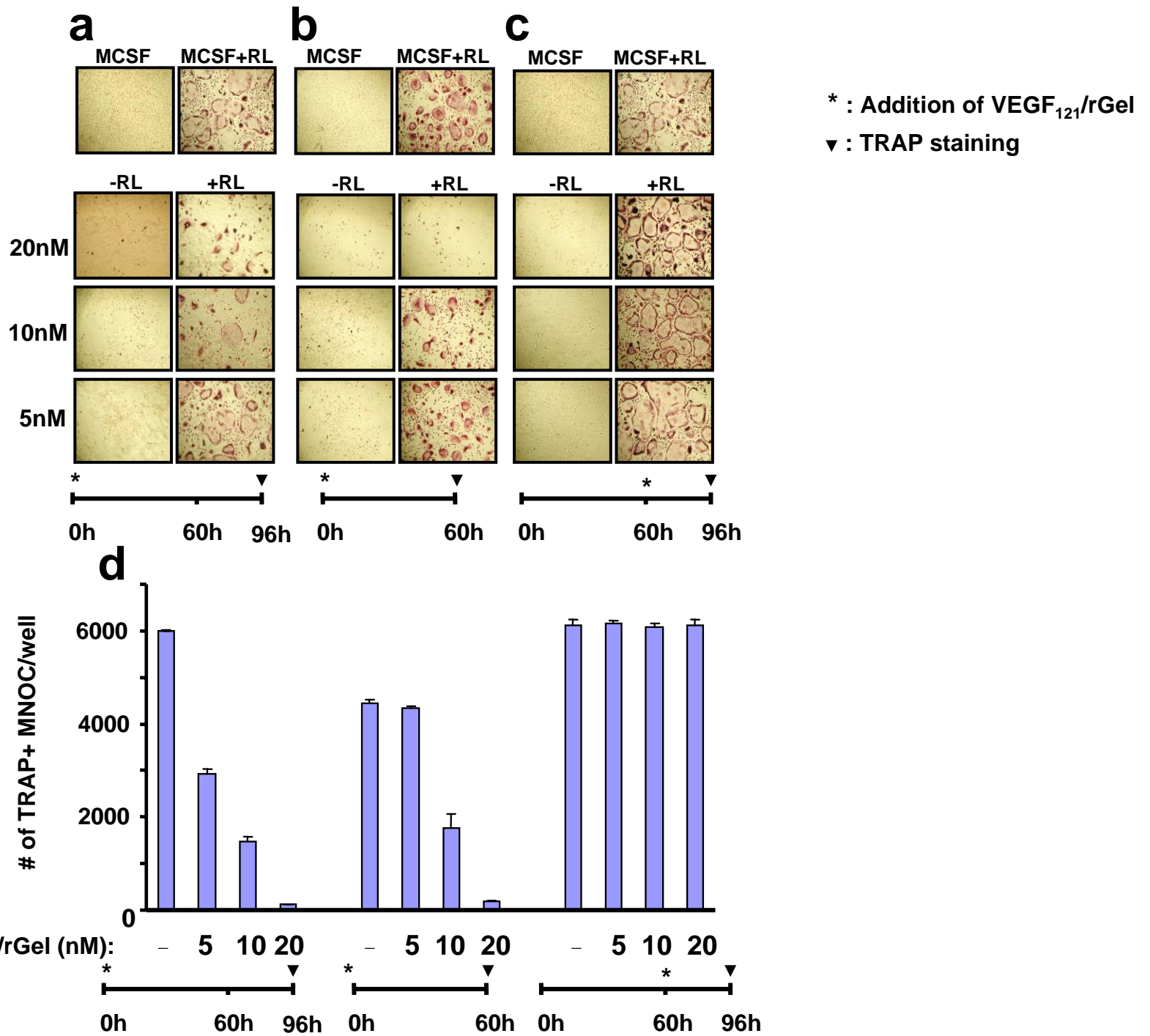
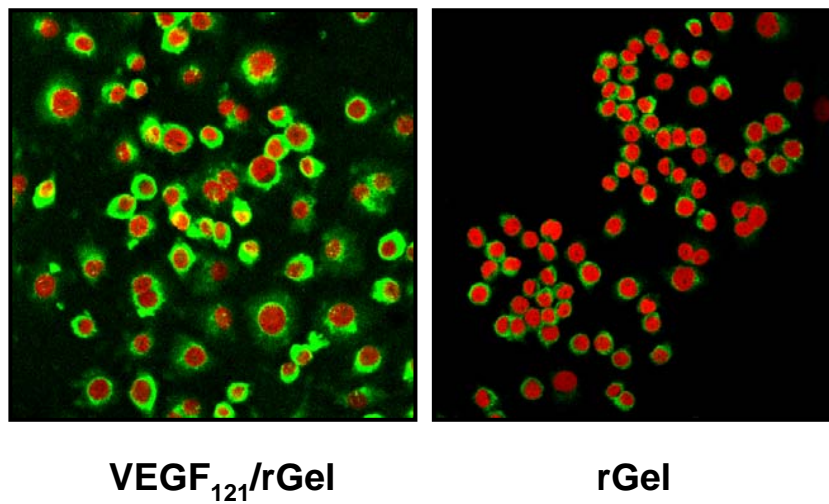


Figure 4

a



b

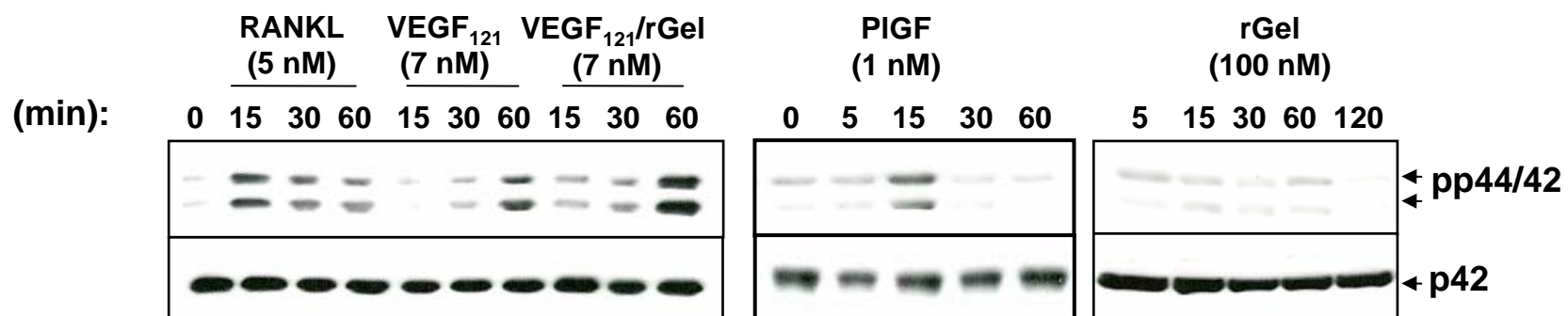


Figure 5

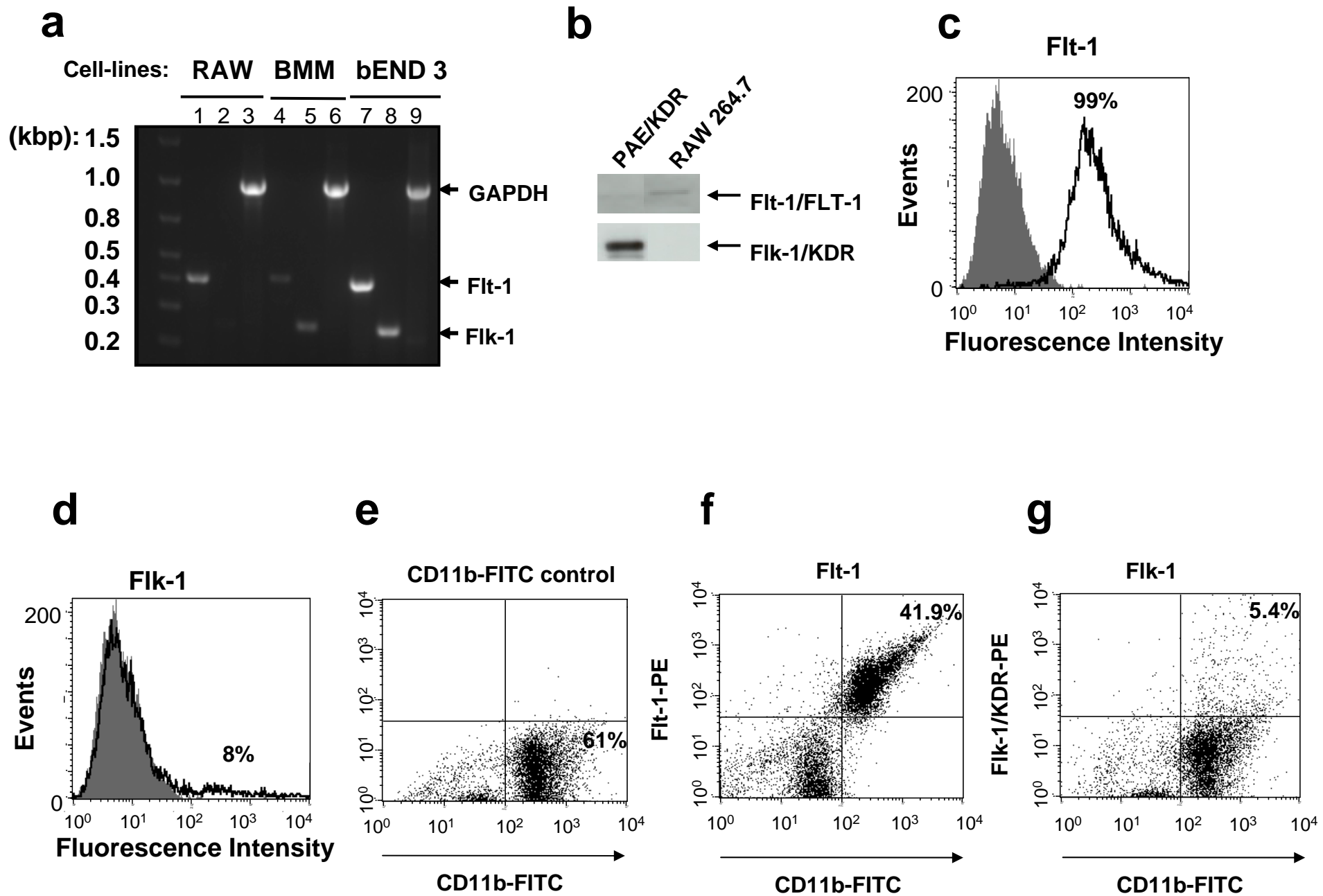
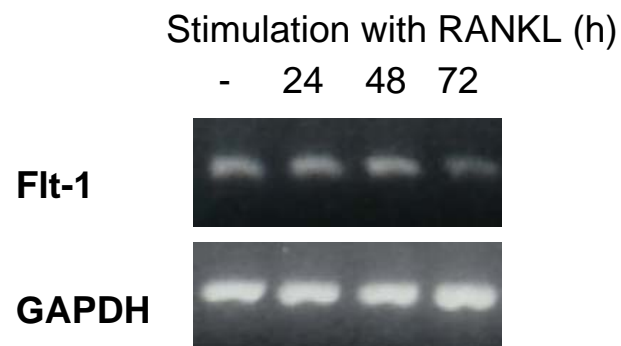


Figure 6

h



i

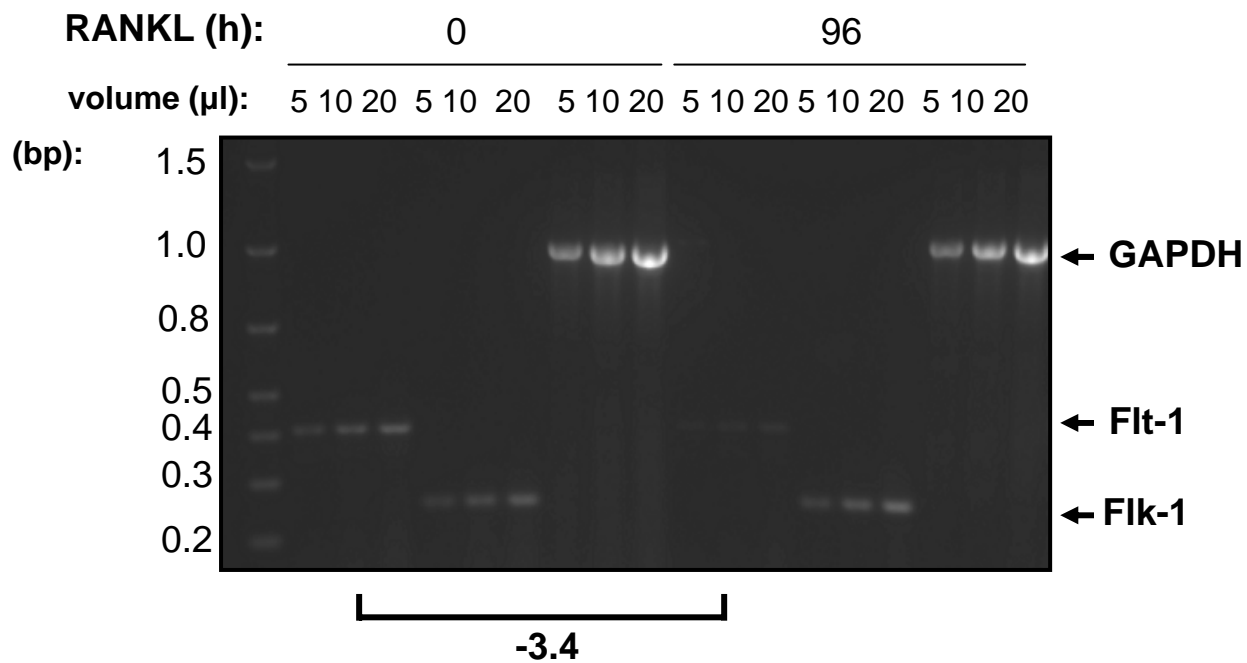
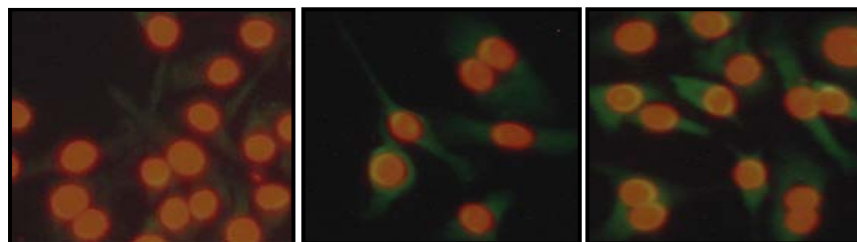
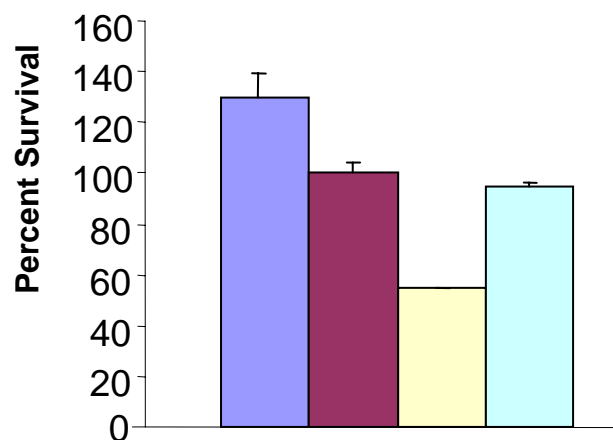


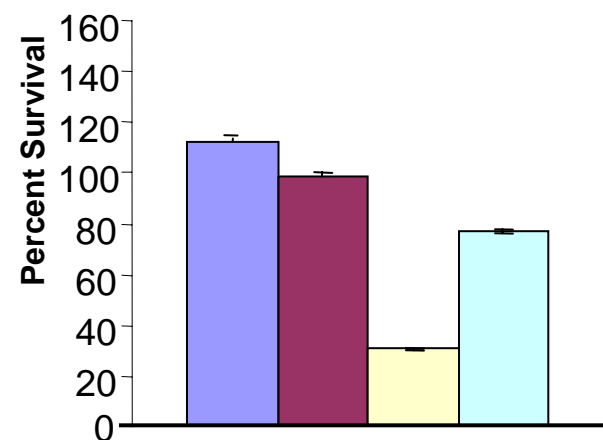
Figure 6

a

Anti-Flt-1 (10 μ g/ml)	+	-	-
Anti-Flk-1 (10 μ g/ml)	-	+	-
VEGF ₁₂₁ /rGel (10 nM)	+	+	+

b

PIGF (25 nM)	+	-	-	+
VEGF ₁₂₁ /rGel (40 nM)	-	-	+	+
MCSF (10 ng/ml)	-	-	-	-

c

PIGF (25 nM)	+	-	-	+
VEGF ₁₂₁ /rGel (40 nM)	-	-	+	+
MCSF (10 ng/ml)	-	-	-	-

Figure 7

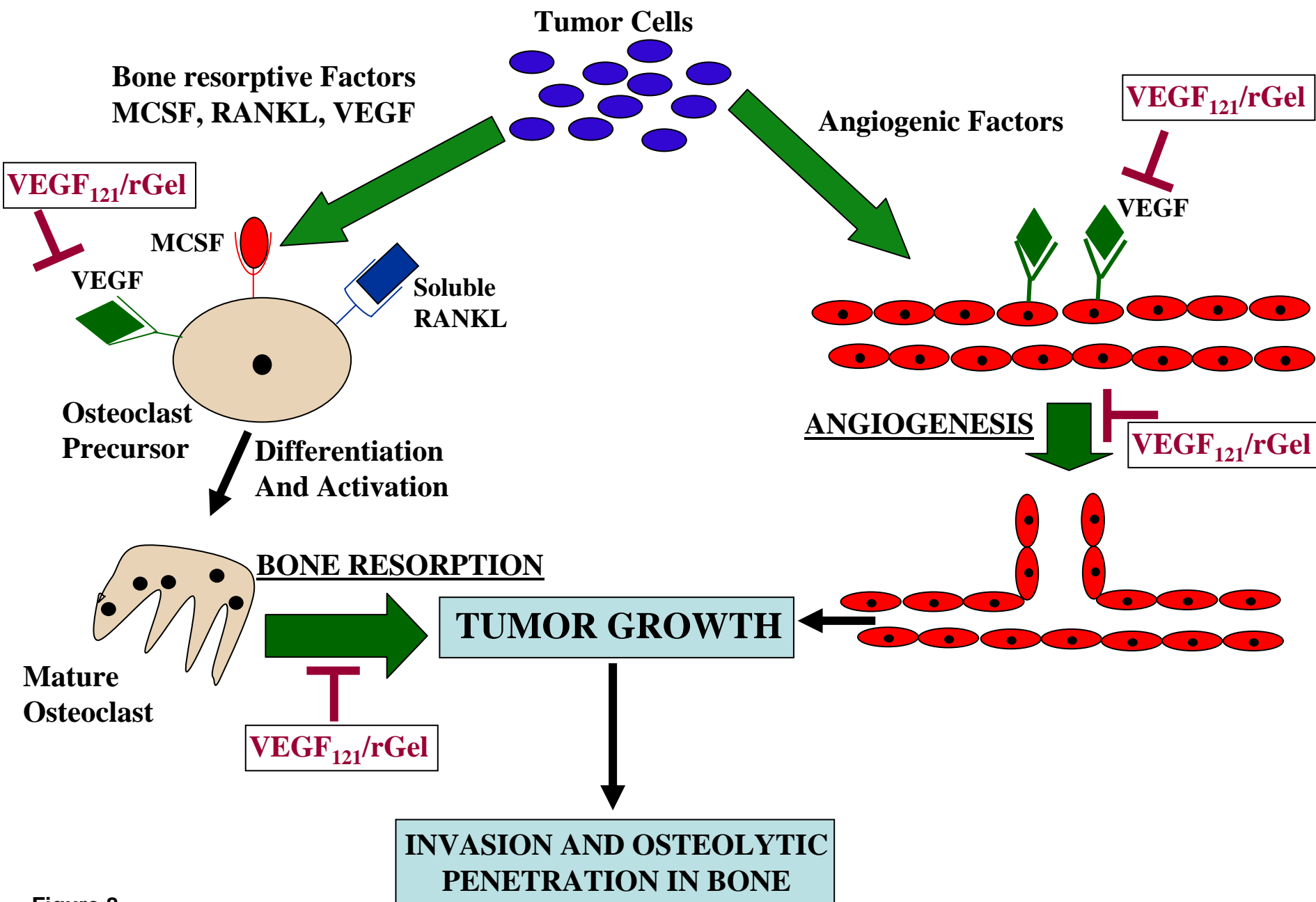


Figure 8

The Vascular-Ablative Agent VEGF₁₂₁/rGel Inhibits Pulmonary Metastases of MDA-MB-231 Breast Tumors¹

Sophia Ran^{*,†}, Khalid A. Mohamedali[†], Troy A. Luster^{*}, Philip E. Thorpe^{*} and Michael G. Rosenblum[†]

^{*}Simmons Comprehensive Cancer Center and Department of Pharmacology, University of Texas Southwestern Medical Center, Dallas, TX, USA; [†]Department of Experimental Therapeutics, The University of Texas M. D. Anderson Cancer Center, Houston, TX; [‡]Present Address: Department of Medical Microbiology, Immunology and Cell Biology, School of Medicine, Southern Illinois University, Springfield, IL 62794-9626

Abstract

VEGF₁₂₁/rGel, a fusion protein composed of the growth factor VEGF₁₂₁ and the recombinant toxin gelonin (rGel), targets the tumor neovasculature and exerts impressive cytotoxic effects by inhibiting protein synthesis. We evaluated the effect of VEGF₁₂₁/rGel on the growth of metastatic MDA-MB-231 tumor cells in SCID mice. VEGF₁₂₁/rGel treatment reduced surface lung tumor foci by 58% compared to controls (means were 22.4 and 53.3, respectively; $P < .05$) and the mean area of lung colonies by 50% ($210 \pm 37 \text{ m}^2$ vs $415 \pm 10 \text{ m}^2$ for VEGF₁₂₁/rGel and control, respectively; $P < .01$). In addition, the vascularity of metastatic foci was significantly reduced (198 ± 37 vs 388 ± 21 vessels/mm² for treated and control, respectively). Approximately 62% of metastatic colonies from the VEGF₁₂₁/rGel-treated group had fewer than 10 vessels per colony compared to 23% in the control group. The VEGF receptor Flk-1 was intensely detected on the metastatic vessels in the control but not in the VEGF₁₂₁/rGel-treated group. Metastatic foci present in lungs had a three-fold lower Ki-67 labeling index compared to control tumors. Thus, the antitumor vascular-ablative effect of VEGF₁₂₁/rGel may be utilized not only for treating primary tumors but also for inhibiting metastatic spread and vascularization of metastases.

Neoplasia (2005) 7, 486–496

Keywords: VEGF, gelonin, fusion toxin, vascular targeting, metastatic breast tumors.

Introduction

Biologic studies examining the development of vascular tree in normal development and in disease states have identified numerous cytokines and their receptors that are responsible for triggering and maintaining this process [1–7]. Tumor neovascularization is not only central to the growth and development of the primary lesion, but appears to be a critical factor in the development and maintenance of metastases [8–12]. Clinical studies in bladder cancer [9] have demonstrated a correlation between microvessel den-

sity (MVD) and metastases. In addition, studies of breast cancer metastases by Aranda and Laforga [11] and Fox et al. [12] have demonstrated that microvessel count in primary tumors appears to be related to the presence of metastases in lymph nodes and micrometastases in bone marrow.

The cytokine vascular endothelial growth factor-A (VEGF-A) and its receptors Flt-1/FLT-1 (VEGFR-1) and Flk-1/KDR (VEGFR-2) have been implicated as one of the central mediators of normal angiogenesis and tumor neovascularization [13–20]. Upregulation or overexpression of the KDR receptor or the VEGF-A ligand itself has been implicated as poor prognostic markers in various clinical studies of colon, breast, and pituitary cancers [21–23]. Recently, Padro et al. [24] have suggested that both VEGF-A and Flk-1/KDR may play a role in the neovascularization observed in bone marrow during acute myeloid leukemia tumor progression and may provide evidence that the VEGF/VEGFR-2 pathway is important in leukemic growth.

For these reasons, there have been several groups interested in developing therapeutic agents and approaches targeting the VEGF-A pathway. Agents that prevent VEGF-A binding to its receptors, antibodies that directly block the Flk-1/KDR receptor, and small molecules that block the kinase activity of Flk-1/KDR, and thereby block growth factor signaling, are all under development [25–37]. Recently, our laboratory reported the development of a growth factor fusion construct of VEGF₁₂₁ and the recombinant toxin gelonin (rGel) [38]. The rGel toxin is a single-chain *N*-glycosidase that is similar in its action to ricin-A chain [39]. Immunotoxins and fusion toxins containing rGel have been shown to

Abbreviations: SCID, severe combined immunodeficient; VEGF, VEGF-A, vascular endothelial growth factor-A; Flt-1, FLT-1, VEGFR-1, vascular endothelial growth factor receptor-1; Flk-1, KDR, VEGFR-2, vascular endothelial growth factor receptor-2; rGel, gelonin; i.v., intravenous. Address all correspondence to: Michael G. Rosenblum, PhD, Department of Experimental Therapeutics, The University of Texas M. D. Anderson Cancer Center, Unit 44, 1515 Holcombe Boulevard, Houston, TX 77030. E-mail: mrosenbl@mdanderson.org

¹This research was supported, in part, by the following: Clayton Foundation for Research, Department of Defense (DAMD-17-02-1-0457), and the Gillson-Longenbaugh Foundation.

Received 27 September 2004; Revised 3 December 2004; Accepted 7 December 2004.

Copyright © 2005 Neoplasia Press, Inc. All rights reserved 1522-8002/05/\$25.00
DOI 10.1593/neo.04631

specifically kill tumor cells *in vitro* and *in vivo* [40–43]. In currently ongoing clinical studies, gelonin does not appear to generate vascular leak syndrome (VLS) that limits the use of other toxins [44]. In addition, the development of hepatotoxicity commonly observed with toxin molecules has thus far not been observed for rGel-based agents. Our studies demonstrated that this agent was specifically cytotoxic only to cells expressing the KDR receptor and was not cytotoxic to cells overexpressing the FLT-1 receptor. In addition, this agent was shown to localize within the tumor vasculature and caused a significant damage to the vascular endothelium in both PC-3 prostate and A375 orthotopic xenograft tumor models.

There is now a significant body of evidence suggesting that breast tumor development, differentiation, and metastatic spread appear to be critically dependent on tumor neovascularization. Current studies suggest that the development of breast cancer primary tumors or metastatic sites > 2 mm are critically dependent on the growth of tumor neovasculature. We, therefore, evaluated the effect of VEGF₁₂₁/rGel fusion toxin treatment on the growth of metastatic MDA-MB-231 tumor cells in SCID mice. Our data strongly suggest that the vascular-ablative effect of VEGF₁₂₁/rGel may be used for inhibiting metastatic spread and the vascularization of metastases.

Materials and Methods

Materials

Bacterial strains, pET bacterial expression plasmids, and recombinant enterokinase were obtained from Novagen (Madison, WI). All other chemicals were from Sigma Chemical Co. (St. Louis, MO) or Fisher Scientific (Pittsburgh, PA). TALON metal affinity resin was obtained from Clontech Laboratories (Palo Alto, CA). Other chromatography resins and materials were from Amersham Pharmacia Biotech (Piscataway, NJ). Endothelial cell growth supplement (ECGS) from bovine neural tissue was obtained from Sigma. Murine brain endothelioma (bEnd.3) cells were provided by Professor Werner Risau (Max Plank Institute, Munich, Germany). Tissue culture reagents were from Gibco BRL (Gaithersburg, MD) or Mediatech Cellgro (Herndon, VA).

Antibodies

Rat antimouse CD31 antibody was from PharMingen (San Diego, CA). Rabbit antigelonin antibody was produced in the Veterinary Medicine Core Facility at MDACC. The hybridoma producing the mouse monoclonal w6/32 antibody directed against human HLA antigen was purchased from ATCC. The w6/32 antibody was purified from hybridoma supernatant using protein A resin. MECA 32, a pan mouse endothelial cell antibody, was kindly provided by Dr. E. Butcher (Stanford University, Stanford, CA) and served as a positive control for immunohistochemical studies. The Ki-67 antibody was from Abcam, Inc. (Cambridge, UK). Antibodies to KDR and FLT-1 were from Santa Cruz Biotechnology (Santa Cruz, CA). Goat antirat, antimouse, and

antirabbit secondary antibodies conjugated to HRP were purchased from Dako (Carpinteria, CA). Protein A/G agarose resin was purchased from Pierce (Rockford, IL).

Cell Culture

Porcine aortic endothelial cells transfected with the KDR receptor (PAE/KDR) or the FLT-1 receptor (PAE/FLT-1) were a generous gift from Dr. J. Waltenberger. MDA-MB-231 cells were a generous gift from Dr. Janet Price. MDA-MB-231, MDA-MB-435, PAE/KDR, and PAE/FLT-1 cells were maintained as a monolayer in F12 Nutrient Media (HAM) supplemented with 100 U/ml penicillin, 100 U/ml streptomycin, and 10% fetal bovine serum. SK-BR3 cells were maintained in RPMI 1640 media supplemented with 100 U/ml penicillin, 100 U/ml streptomycin, and 10% fetal bovine serum. BT474 cells were maintained in SK-BR3 media supplemented with 5 µg/ml insulin. Cells were harvested by treatment with Versene (0.02% EDTA) or trypsin–EDTA. Tumor cells intended for injection into mice were washed once and resuspended in serum-free medium without supplements. Cell number and viability were determined by staining with 0.2% trypan blue dye diluted in saline. Only single-cell suspensions of greater than 90% viability were used for *in vivo* studies.

Expression and Purification of VEGF₁₂₁/rGel

The construction, expression, and purification of VEGF₁₂₁/rGel have been previously described [38]. The fusion toxin was stored in sterile PBS at –20°C.

Cytotoxicity of VEGF₁₂₁/rGel and rGel

The cytotoxicity of VEGF₁₂₁/rGel and rGel against log phase PAE/KDR and PAE/FLT-1 cells has been previously described [38]. Here, we assessed the cytotoxicity of VEGF₁₂₁/rGel and rGel against log phase human breast cancer cells and compared their cytotoxicity to PAE/KDR cells. Cells were grown in 96-well flat-bottom tissue culture plates. Purified VEGF₁₂₁/rGel and rGel were diluted in culture media and added to the wells in five-fold serial dilutions. Cells were incubated for 72 hours. The remaining adherent cells were stained with crystal violet (0.5% in 20% methanol) and solubilized with Sorenson's buffer (0.1 M sodium citrate, pH 4.2 in 50% ethanol). Absorbance was measured at 630 nm.

Western Blot Analysis

Whole cell extracts were obtained by lysing cells in cell lysis buffer (50 mM Tris, pH 8.0, 0.1 mM EDTA, 1 mM DTT, 12.5 mM MgCl₂, 0.1 M KCl, and 20% glycerol) supplemented with protease inhibitors [leupeptin (0.5%), aprotinin (0.5%), and PMSF (0.1%)]. Protein samples were separated by SDS-PAGE under reducing conditions and electrophoretically transferred to a PVDF membrane overnight at 4°C in transfer buffer (25 mM Tris–HCl, pH 7.6, 190 mM glycine, and 20% HPLC-grade methanol). The samples were analyzed for KDR with rabbit anti-KDR polyclonal antibody and FLT-1 using an anti-FLT-1 polyclonal antibody. The membranes were then incubated with goat antirabbit IgG

horseradish peroxidase (HRP), developed using the ECL detection system (Amersham Pharmacia Biotech) and exposed to X-ray film.

Immunoprecipitation

Cells were lysed as described above. Five hundred micrograms of whole cell lysates of MDA-MB-231, MDA-MB-435, BT474, and SK-BR3 cells was mixed with 2 μ g of anti-KDR or anti-FLT-1 polyclonal antibodies in a final volume of 250 μ l and incubated for 2 hours at 4°C. One hundred micrograms of PAE/KDR and PAE/FLT-1 cell lysates was immunoprecipitated as controls. The mixtures were then incubated for 2 hours with Protein A/G agarose beads that had been blocked with 5% BSA. The beads were washed four times in lysis buffer and the samples, along with 30 μ g of PAE/KDR cell lysate, were run on a gel, transferred overnight onto a PVDF membrane, and probed using anti-KDR or anti-FLT-1 antibodies.

Isolation of RNA and Reverse Transcription Polymerase Chain Reaction (RT-PCR) Analysis

Total RNA was extracted using the RNeasy mini-kit (Qiagen, Valencia, CA) and its integrity was verified by electrophoresis on a denaturing formaldehyde agarose gel. RT-PCR analysis was performed using the following primers: KDR forward—5' ATTACTTGCAGGGGACAG; KDR reverse—5' GGAACAAATCTCTTTTCTGG; FLT-1 forward—5' CAAATGCAACGTACAAAGA; FLT-1 reverse—5' AGAGTGGCAGTGAGGTTTT; GAPDH forward—5' GTCGTCTTCAACCACCATGGAG; and GAPDH reverse—5' CCACCCTGTTGCTGTAGC. Isolated RNA was subjected to first-strand cDNA synthesis as described by the manufacturer of the Superscript First Strand synthesis system (Invitrogen, Carlsbad, CA). RT-PCR was performed using a Minicycler PCR machine (MJ Research, Inc., San Francisco, CA).

Localization of VEGF₁₂₁/rGel to Blood Vessels of MDA-MB-231 Lung Metastatic Foci

All animal experiments were carried out in accordance with institutional guidelines and protocols. Tumor cells (5×10^5 per mouse) were injected intravenously (i.v.) and, 4 to 5 weeks later, the mice began to show signs of respiratory distress. At this time, the mice were injected i.v. with VEGF₁₂₁/rGel (50 μ g/mouse) or free rGel (20 μ g/mouse, molar equivalent to VEGF₁₂₁/rGel). One hour later, the mice were sacrificed and exsanguinated. All major organs and tumor were harvested and snap-frozen for the preparation of cryosections. Frozen sections were double-stained with anti-CD-31 (5 μ g/ml) followed by detection of the localized fusion protein using rabbit antigelonin antibody (10 μ g/ml). CD-31 rat IgG was visualized by goat antirat IgG conjugated to Cy-3 (red fluorescence). Rabbit antigelonin antibody was detected by goat antirabbit IgG conjugated to FITC (green fluorescence). Colocalization of both markers was indicated by the yellow color. Anti-rGel antibody had no reactivity with tissues sections derived from mice injected with saline or with VEGF₁₂₁.

Metastatic Model of MDA-MB-231 Tumors

A maximum tolerated dose of 45 mg/kg for VEGF₁₂₁/rGel under the conditions described below was established. For treatment purposes, 70% of the MTD was used. We currently demonstrate a comparison with a diluent (saline) control as previous studies have demonstrated no impact of free rGel on the growth of tumor xenografts [38]. Female SCID mice, aged 4 to 5 weeks, were injected in a tail vein with 0.1 ml of MDA-MB-231 cell suspension (5×10^5 cells). The mice were randomly separated into two groups (six mice per group) and were treated with either VEGF₁₂₁/rGel or rGel starting on the eighth day after the injection of cells. VEGF₁₂₁/rGel was delivered at 100 μ g/dose intraperitoneally, for a total of six times, with the interval of 3 days. The molar equivalent of rGel (40 μ g) was delivered at the same schedule. Intraperitoneal, rather than intravenous, injection was chosen solely to prevent necrosis of the tail vein due to repeated injections. Animal weight was monitored. Three weeks after termination of the treatment, the animals were sacrificed and their lungs were removed. One lobe was fixed in Bouin's fixative and the other lobe was snap-frozen. After fixation in Bouin's fixative, the tumor colonies on the lung surface appeared white, whereas the normal lung tissue appeared brown. The number of tumor colonies on the surface of each lung was counted and the weight of each lung was measured. The values obtained from individual mice in the VEGF₁₂₁/rGel and rGel groups were averaged per group.

Determination of the Number, Size, and Vascular Density of Lung Metastatic Foci

Frozen samples of lung tissue were cut to produce sections of 6 μ m. Blood vessels were visualized by MECA 32 antibody and metastatic lesions were identified by morphology and w6/32 antibody, directed against human HLA antigens. Each section was also double-stained by MECA 32 and w6/32 antibodies to ensure that the analyzed blood vessels are located within a metastatic lesion. Slides were first viewed at low magnification ($\times 2$ objective) to determine the total number of foci per cross section. Six slides derived from individual mice in each group were analyzed and the number was averaged. Images of each colony were taken using a digital camera (CoolSnap) at magnifications of $\times 40$ and $\times 100$, and analyzed using Metaview software, which allows measurements of the smallest and largest diameter, perimeter (μ m), and area (mm^2). The vascular endothelial structures identified within a lesion were counted and the number of vessels per each lesion was determined and normalized per square millimeter. The mean number of vessels per square millimeter was calculated per slide and averaged per VEGF₁₂₁/rGel and rGel groups (six slides per group). The results are expressed as \pm SEM. The same method was applied to determine the mean number of vessels in nonmalignant tissues.

Immunohistochemical Analysis of Proliferation of Tumor Cells in Lung Colonies

Frozen sections of mouse normal organs and metastatic lungs were fixed with acetone for 5 minutes and rehydrated

with PBS-T for 10 minutes. All dilutions of antibodies were prepared in PBS-T containing 0.2% BSA. Primary antibodies were detected by appropriate antimouse, antirat, or antirabbit HRP conjugates. HRP activity was detected by developing with DAB substrate (Invitrogen, Carlsbad, CA). To determine number of cycling cells, sections were stained with the Ki-67 antibody followed by antimouse IgG HRP conjugate. Sections were analyzed at a magnification of $\times 100$. The number of cells positive for Ki-67 was normalized per square millimeter. The mean \pm SD per VEGF₁₂₁/rGel and control group is presented. The average numbers derived from analysis of each slide were combined per either VEGF₁₂₁/rGel or rGel group and analyzed for statistical differences.

Expression of Flk-1 in Metastatic Lung Tumors

The expression of Flk-1 on the vasculature of breast tumors metastatic to the lungs was also assessed using the RAFL-1 antibody as described by Ran et al. [45]. Frozen sections of lungs from mice treated with VEGF₁₂₁/rGel or free gelonin stained with monoclonal rat antimouse VEGFR-2 antibody RAFL-1 (10 μ g/ml). RAFL-1 antibody was detected by goat antirat IgG HRP.

Statistical Analysis

Results are expressed as mean \pm SEM, unless otherwise indicated. Statistical significance was determined by one-way analysis of variance followed by the Student's *t* test.

Results

Expression of KDR and FLT-1 RNA and Protein in Breast Cancer Cell Lines

Because VEGF₁₂₁ binds only to KDR and FLT-1, we first examined RNA and protein levels of these two receptors in several breast cancer cell lines: BT474, MDA-MB-231, MDA-MB-435, and SK-BR3. Total RNA was harvested from log phase cells, analyzed for integrity, and subjected to RT-PCR with primers KDR, FLT-1, and GAPDH (control). KDR and FLT-1 were immunoprecipitated from whole cell extracts and identified by Western blot analysis. PAE/KDR and PAE/FLT-1 cells were used as positive controls. None of the breast cancer cell lines expressed detectable levels of FLT-1 RNA or protein as determined by RT-PCR and Western blot analysis (data summarized in Table 1). RT-PCR analysis of MDA-MB-231 showed extremely low levels of KDR compared to PAE/

KDR. However, MDA-MB-231 cells did not express detectable amounts of KDR protein. The other breast cell lines did not express detectable amounts of KDR RNA or protein.

Cytotoxicity of VEGF₁₂₁/rGel on MDA-MB-231 Cells

We have previously demonstrated that VEGF₁₂₁/rGel is cytotoxic to endothelial cells expressing KDR but not FLT-1 [38]. As assessed by Western blot, none of the breast cancer cell lines examined appears to express FLT-1 or KDR—the receptors that bind VEGF₁₂₁. We additionally examined the cytotoxicity of VEGF₁₂₁/rGel and rGel on these breast cancer cell lines. BT474, MDA-MB-435, and SK-BR3 all show a slightly lower IC₅₀ for VEGF₁₂₁/rGel compared to rGel alone. In contrast, MDA-MB-231 cells in culture showed an IC₅₀ slightly higher than that observed for recombinant gelonin (Table 1 and Figure 1), indicating that VEGF₁₂₁/rGel does not have a specific target on MBA-MB-231 cells. The IC₅₀ of untargeted rGel toward MDA-MB-231 cells is similar to its IC₅₀ toward PAE/KDR cells (Figure 1). Compared to the IC₅₀ of VEGF₁₂₁/rGel toward PAE/KDR cells (1 nM), the IC₅₀ of VEGF₁₂₁/rGel toward the breast cancer cell lines examined was much higher, ranging from 30 to 300 nM. Indeed, the IC₅₀ of VEGF₁₂₁/rGel toward these breast cancer cell lines was in the IC₅₀ range of untargeted rGel toward the PAE/KDR cells. Taken together, these *in vitro* data suggest that MDA-MB-231 tumor cells are not specifically targeted by VEGF₁₂₁/rGel, and that any *in vivo* effect on the growth of tumors would be due to VEGF₁₂₁/rGel targeting the tumor vasculature rather than the tumor cells themselves.

Localization of VEGF₁₂₁/rGel to the Vasculature of MDA-MB-231 Lung Metastatic Foci

Mice bearing metastatic MDA-MB-231 tumors were injected intravenously with either VEGF₁₂₁/rGel or free rGel and, 1 hour later, the mice were exsanguinated. Frozen sections were prepared from the lung tumor foci and normal organs, and examined immunohistochemically to determine the location of the free rGel and the gelonin fusion construct. VEGF₁₂₁/rGel was primarily detected on the endothelium of tumor (Figure 2). Vessels with bound VEGF₁₂₁/rGel were homogeneously distributed within the tumor vasculature. No VEGF₁₂₁/rGel staining was detected in any of the normal tissues examined (lung, liver, kidney, heart, spleen, pancreas, and brain; data not shown). Free rGel did not localize to tumor or normal vessels in any of the mice, indicating that only targeted rGel was able to bind to the tumor

Table 1. Correlation between the Presence of VEGF₁₂₁ Receptors and Sensitivity to VEGF₁₂₁/rGel.

Cell Type	RT-PCR		Immunoprecipitation		IC ₅₀ (nM)		Targeting Index*
	KDR	FLT-1	KDR	FLT-1	VEGF ₁₂₁ /rGel	rGel	
BT474	—	—	—	—	300	2000	7
MDA-MB-231	+	—	—	—	150	40	0.3
MDA-MB-435	—	—	—	—	56	327	6
SK-BR3	—	—	—	—	200	500	2.5

*Targeting index is defined as (IC₅₀ rGel)/(IC₅₀ VEGF₁₂₁/rGel).

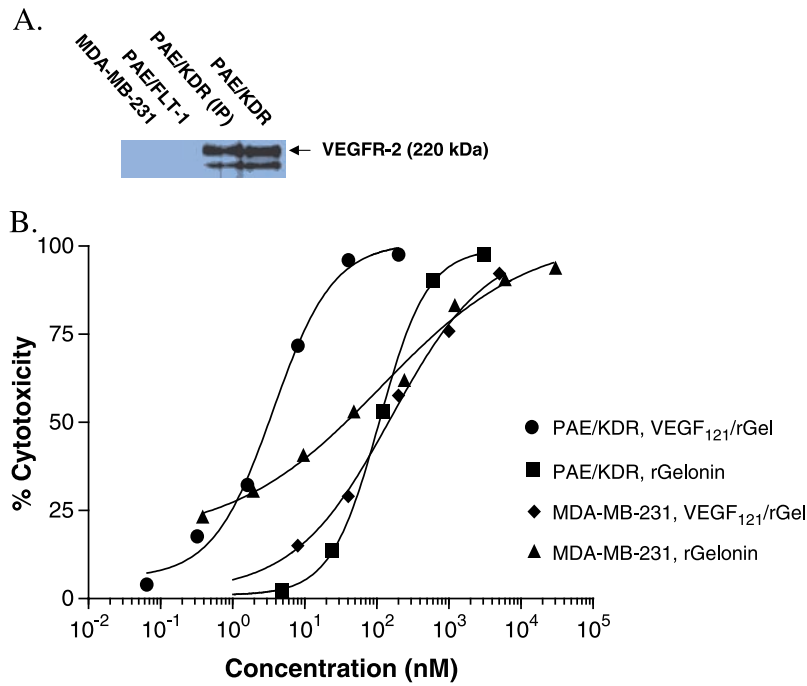


Figure 1. MDA-MB-231 cells are not targeted by VEGF₁₂₁/rGel due to the lack of expression of VEGFR-2/KDR. (A) Western analysis demonstrating the presence of KDR on endothelial cells transfected with the KDR receptor (PAE/KDR) but not on cells expressing the FLT-1 receptor (PAE/FLT-1, negative control). As shown, the MDA-MB-231 cells did not express detectable amounts of KDR. (B) Log phase MDA-MB-231 and PAE/KDR cells were treated with various doses of VEGF₁₂₁/rGel or rGel for 72 hours. VEGF₁₂₁/rGel was far more toxic than rGel toward PAE/KDR cells (IC_{50} of 1 vs 100 nM). In contrast, the cytotoxic effects of both agents were similar toward MDA-MB-231 cells (IC_{50} of 150 nM with VEGF₁₂₁/rGel vs 40 nM with rGel), demonstrating no specific cytotoxicity of the fusion construct compared to free toxin on these cells.

endothelium. These results indicate that VEGF₁₂₁/rGel specifically localizes to tumor vessels, which demonstrate a high density and a favorable distribution of the VEGF₁₂₁/rGel-binding sites.

MDA-MB-231 Model of Experimental Pulmonary Metastases and Rationale for Therapeutic Regimen
Human breast carcinoma MDA-MB-231 cells consistently lodge in lungs following intravenous injection into the tail vein

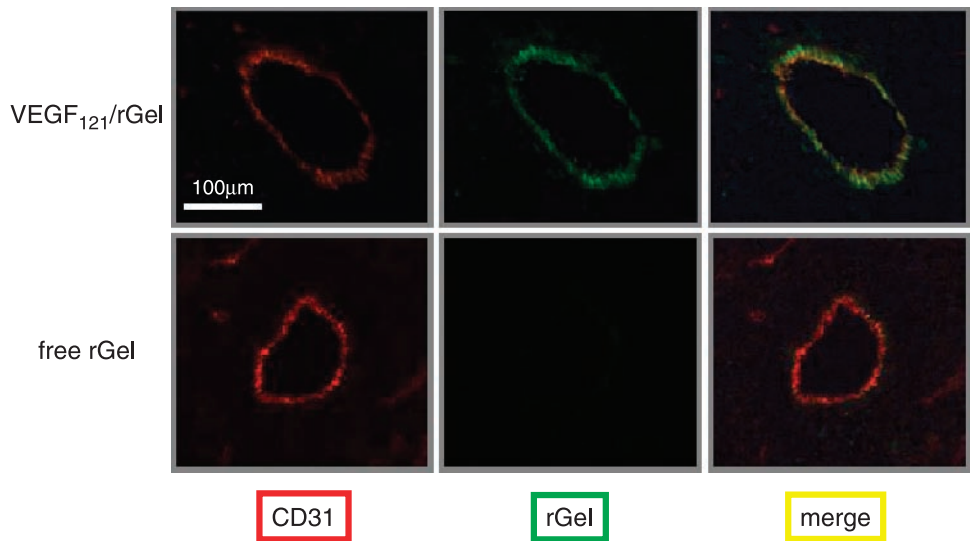


Figure 2. VEGF₁₂₁/rGel localizes to the vasculature of breast tumor foci in the lungs of mice. Female SCID mice were injected i.v. with 0.1 ml of MDA-MB-231 cell suspension (5×10^5 cells) as described in the Materials and Methods section. Six weeks later, mice were administered one dose (i.v., tail vein) of 100 μg of VEGF₁₂₁/rGel. Four hours later, the mice were sacrificed and the tumor-bearing lungs were fixed. Tissue sections were stained for blood vessels using the anti-CD-31 antibody (red) and the section was counterstained using an antigelonin antibody (green). Colocalization of the stains (yellow) demonstrates the presence of the VEGF₁₂₁/rGel fusion construct specifically in blood vessels and not on tumor cells.

of athymic or SCID mice. Micrometastases are first detected 3 to 7 days after injection of 5×10^5 cells, and macroscopic colonies develop in 100% of the injected mice within 4 to 7 weeks. Mortality occurs in all mice within 10 to 15 weeks. This model of experimental breast cancer metastasis examines the ability of tumor cells to survive in the blood circulation, extravasate through the pulmonary vasculature, and establish growing colonies in the lung parenchyma.

We evaluated the effect of VEGF₁₂₁/rGel on the growth and survival of the established micrometastases. We, therefore, started the treatment 8 days after injection of the tumor cells. By that time, based on our prior observations, tumor cells that were able to survive in the circulation and traverse the lung endothelial barrier are localized within the lung parenchyma and initiate tumor angiogenesis. Treatment with VEGF₁₂₁/rGel was given intraperitoneally for the following 3 weeks as described under the Materials and Methods section, with the mice receiving 70% of the maximum tolerated accumulative dose of the drug (900 μ g/mouse). Prior studies established that the VEGF₁₂₁/rGel given at such dose did not cause histopathologic changes in normal organs. The accumulative dose of total VEGF₁₂₁/rGel fusion protein did not induce significant toxicity as judged by animal behavior morphologic evaluation of normal organs. Transient loss of weight ($\sim 10\%$) was observed 24 hours after most of the treatments with complete weight recovery thereafter. Colonies were allowed to expand in the absence of treatment for the following 3 weeks to evaluate the long-term effect of VEGF₁₂₁/rGel on the size of the colonies, proliferation index of tumor cells, and their ability to induce new blood vessel formation.

Effect of VEGF₁₂₁/rGel on the Number and Size of MDA-MB-231 Tumor Lesions in Lungs

An antibody directed against human HLA was used to identify metastatic lesions of MDA-MB-231 cells on samples of lung tissue. Treatment with VEGF₁₂₁/rGel, but not with free rGel, significantly reduced by between 42% and 58% both the number of colonies per lung and the size of the metastatic foci present in the lung, as shown in Figure 3 and Table 2.

Effect of VEGF₁₂₁/rGel on the Vascularity of MDA-MB-231 Pulmonary Metastatic Foci

Blood vessels were visualized by MECA 32 antibody. The overall mean vascular density of lung colonies was reduced by 51% compared to the rGel-treated controls (Table 3 and Figure 4); however, the observed effect was nonuniformly distributed by tumor colony size. The greatest impact on vascularization was observed on mid-sized and extremely small tumors (62% and 69% inhibition, respectively), whereas large tumors demonstrated the least effect (10% inhibition). The majority of lesions in the VEGF₁₂₁/rGel-treated mice ($\sim 70\%$) was avascular, whereas only 40% of lesions from the control group did not have vessels within the metastatic lung foci.

Effect of VEGF₁₂₁/rGel on the Number of Cycling Cells in the Metastatic Foci

The growth rate of MDA-MB-231 cells was determined by staining cells with Ki-67 antibody, as described. The number of cycling tumor cells in lesions from the VEGF₁₂₁/rGel group was also reduced by $\sim 60\%$ compared to controls (Figure 5). This finding suggests that the vascularity of metastases directly affects tumor cell proliferation.

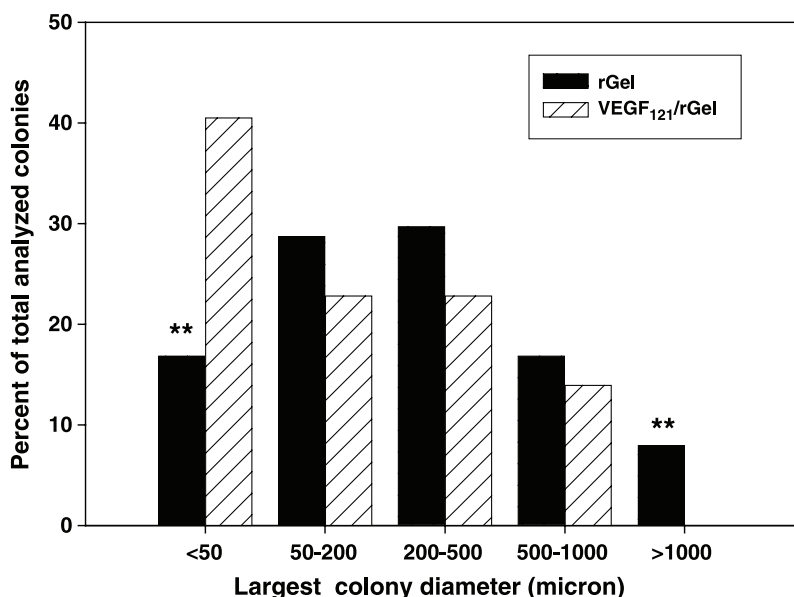


Figure 3. VEGF₁₂₁/rGel reduces number of large colonies in the metastatic lungs. The size of tumor colonies was analyzed on slides stained with w6/32 antibody, which specifically recognizes human HLA antigens. The antibody delineates colonies of human tumor cells and defines borders between metastatic lesions and mouse lung parenchyma. The largest size differences between VEGF₁₂₁/rGel and control groups were found in groups of colonies having diameters either less than 50 μ m or more than 1000 μ m. In the VEGF₁₂₁/rGel-treated mice, more than 40% of total foci was extremely small (<50 μ m) compared to 18% in the control group. The control mice had approximately 8% of the extremely large colonies (>1000 μ m), whereas VEGF₁₂₁/rGel-treated mice did not have colonies of this size.

Table 2. Effect of VEGF₁₂₁/rGel on the Number and Size of Pulmonary Metastases of MDA-MB-231 Human Breast Carcinoma Cells.

Parameter	Treatment*		% Inhibition versus rGel Treatment	P value†
	rGel	VEGF ₁₂₁ /rGel		
Number of surface colonies per lung (range)‡	53.3 ± 22 (33–80)	22.4 ± 9.2 (11–41)	58.0	0.03
Number of intraparenchymal colonies per cross section (range)§	22 ± 7.5 (18–28)	12.8 ± 5.5 (5–18)	42.0	0.02
Mean area of colonies (μm)¶	415 ± 10	201 ± 37	51.9	0.01
Mean % of colony-occupied area per lung section#	57.3 ± 19	25.6 ± 10.5	55.4	0.01

*Mice with MDA-MB-231 pulmonary micrometastases were treated intraperitoneally with VEGF₁₂₁/rGel or free gelonin as described under Materials and Methods and Results sections.

†P value was calculated using Student's *t* test.

‡Lungs were fixed with Bouin's fixative for 24 hours. The number of surface white colonies was determined for each sample and averaged among six mice from VEGF₁₂₁/rGel or rGel control group. Mean number per group ±SEM is shown. Numbers in parentheses represent the range of colonies in each group.

§Frozen sections were prepared from metastatic lungs. Sections were stained with 6w/32 antibody recognizing human tumor cells. The number of intraparenchymal colonies identified by brown color was determined for each cross section and averaged among six samples of individual mice from VEGF₁₂₁/rGel or rGel control group. The mean number per group ±SEM is shown. Numbers in parentheses represent the range of colonies in each group.

¶The area of foci identified by 6w/32 antibody was measured by using Metaview software. The total number of evaluated colonies was 101 and 79 for rGel and VEGF₁₂₁/rGel group, respectively. Six individual slides per group were analyzed. The mean area of colony in each group ±SEM is shown.

#The sum of all regions occupied by tumor cells and the total area of each lung cross section were determined and the percentage of metastatic regions from total was calculated. The values obtained from each slide were averaged among six samples from VEGF₁₂₁/rGel or rGel control group. The mean percent area occupied by metastases from the total area per group ±SEM is shown.

Effect of VEGF₁₂₁/rGel on Flk-1 Expression in Tumor Vessel Endothelium

The expression of Flk-1 on the remaining few vessels present in lung metastatic foci demonstrated a significant decline compared to that of lung foci present in control tumors

(Figure 6). This suggests that the VEGF₁₂₁/rGel agent is able to significantly downregulate the receptor or prevent the outgrowth of highly receptor-positive endothelial cells.

Discussion

Neovascularization is a particularly important hallmark of breast tumor growth and metastatic spread [46–50]. The growth factor VEGF-A and the receptor KDR have both been implicated in highly metastatic breast cancers [51–53]. We have previously demonstrated that the VEGF₁₂₁/rGel growth factor fusion toxin specifically targets Flk-1/KDR-expressing tumor vascular endothelial cells and inhibits the growth of subcutaneously implanted human tumor xenografts [38]. The current study was designed to evaluate its effect on the development of breast cancer metastases in lungs following intravenous injection of MDA-MB-231 cells.

The salient finding of our study of the VEGF₁₂₁/rGel construct is that: this fusion toxin is specifically cytotoxic to cells overexpressing the KDR receptor for VEGF. However, the human breast MDA-MB-231 cells employed for these studies do not express this receptor and, therefore, were not directly affected by this agent (Figure 1). Although the antitumor effects of VEGF₁₂₁/rGel observed from our *in vivo* studies appear to be solely the result of targeting the Flk-1-expressing tumor vasculature and not the tumor cells themselves, one cannot rule out a direct effect on tumor cells or a combination of targeting both the tumor and the vasculature. Administration of the VEGF₁₂₁/rGel construct to mice previously injected (i.v.) with tumor cells dramatically reduced the number of tumor colonies found in the lung, their size, and their vascularity. In addition, the number of cycling breast tumor cells within lung metastatic foci was found to be reduced by an average of 60%. This reduction compares favorably to the effect of DT-VEGF on the growth of pancreatic cancer [54] and to other vascular targeting agents such as Avastin, which had an overall clinical response rate of 9.3% in a Phase I/II dose escalation trial in previously treated metastatic breast cancers [55]. In addition to the reduced number of blood vessels present in lung metastases of treated mice, we also found that the few vessels present

Table 3. Effect of VEGF₁₂₁/rGel on the Vascularity of Pulmonary Metastases of MDA-MB-231 Human Breast Carcinoma Cells.

Size of Colonies		Largest Diameter Range (μm)	Number of Vascularized Colonies from Total Inhibition Analyzed (%)*		% Inhibition versus Radiation Treatment
Group†	Description		rGel	VEGF ₁₂₁ /rGel	
A	Extremely small	<50	7/24 (29%)	3/32 (9.3%)	69
B	Small	50–200	19/48 (39.5%)	6/24 (25%)	37
C	Mid-sized	200–500	25/30 (83.3%)	8/25 (32%)	62
D	Large	500–1000	17/17 (100%)	10/11 (90.0%)	10
E	Extremely large	>1000	8/8 (100%)	N/A	N/A
Number of vascular foci/total analyzed (%)‡			76/127 (59.8%)	27/92 (29.3%)	51

*Frozen lung sections from VEGF₁₂₁/rGel and rGel-treated mice were stained with MECA 32 antibody. A colony was defined as vascularized if at least one blood vessel branched out from the periphery and reached a center of the lesion. Six slides per group derived from individual mice were analyzed and data were combined.

†Colonies identified on each slide of a metastatic lung were subdivided into five groups (A–E) according to their largest diameter.

‡The total number of the analyzed colonies was 127 and 92 for rGel- and VEGF₁₂₁/rGel-treated groups, respectively. Seventy percent of foci in the VEGF₁₂₁/rGel-treated group was a vascular, whereas only 40% of lesions from the control group did not have vessels within the metastatic foci.

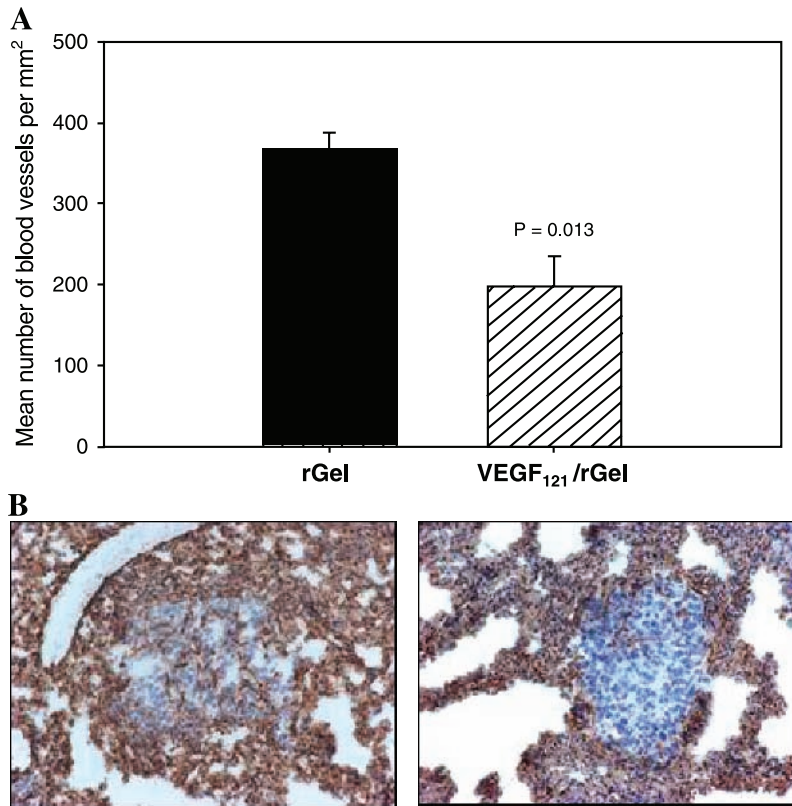


Figure 4. VEGF₁₂₁/rGel inhibits the vascularization of MDA-MB-231 pulmonary metastases. (A) Lungs derived from VEGF₁₂₁/rGel and rGel-treated mice were stained with MECA 32 antibody and the vascular density within the metastatic foci was determined. The mean number of vessels per square millimeter in lung metastases of VEGF₁₂₁/rGel-treated mice was reduced by approximately 50% compared to those in rGel-treated mice. (B) Representative images demonstrating reduction of vascular density in foci of comparable size in mice treated with rGel (left) and VEGF₁₂₁/rGel fusion protein (right).

had a greatly reduced expression of VEGFR-2. Therefore, this construct demonstrated an impressive long-term impact on the growth and development of breast tumor metastatic foci found in the lungs.

Targeting tumor vasculature with a variety of technologies has been shown to inhibit the growth and development of primary tumors as well as metastases. Recently, Shaheen et al. [56] demonstrated that small-molecule tyrosine kinase inhibitors active against the receptors for VEGF, fibroblast growth factor, and platelet-derived growth factors were also capable of inhibiting microvessel formation and metastases in tumor model systems. Previously, Seon et al. [57] demonstrated long-term antitumor effects of an antiendoglin antibody conjugated with ricin-A chain (RTA) in a human breast tumor xenograft model.

Surprisingly, one finding from our study was that administration of VEGF₁₂₁/rGel resulted in a three-fold decrease in the number of Ki-67-labeled (cycling) cells in the metastatic foci present in the lung (Figure 5). Clinical studies have suggested that tumor cell cycling may be an important prognostic marker for disease-free survival in metastatic breast cancer, but that Ki-67 labeling index, tumor MVD, and neovascularization appear to be independently regulated processes [58,59]. To our knowledge, this is the first report of a significant reduction in tumor labeling index produced by a vascular targeting agent.

Another critical finding from our studies is the observation that the vascular-ablative effects of the VEGF₁₂₁/rGel fusion construct alone were unable to completely eradicate lung metastases. Although the growth of larger pulmonary

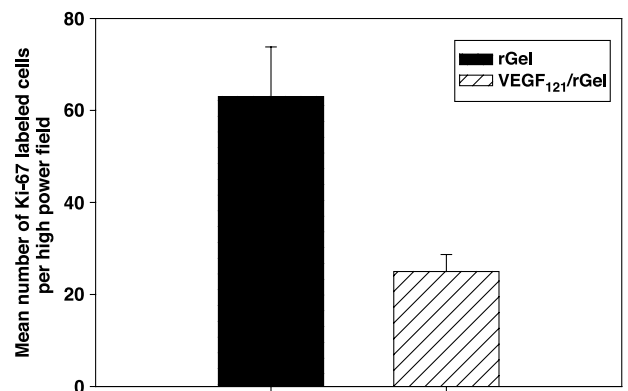


Figure 5. VEGF₁₂₁/rGel inhibits the proliferation of metastatic MDA-MB-231 cells in the lungs. Frozen sections of lungs derived from VEGF₁₂₁/rGel and rGel-treated mice were stained with Ki-67 antibody. Stained sections were examined under $\times 40$ objective to determine the number of tumor cells with positive nuclei (cycling cells). Positive cells were enumerated in 10 colonies per slide on six sections derived from individual mice per treatment group. The mean number per group \pm SEM is presented. VEGF₁₂₁/rGel treatment reduced the average number of cycling cells within the metastatic foci by approximately 60%.

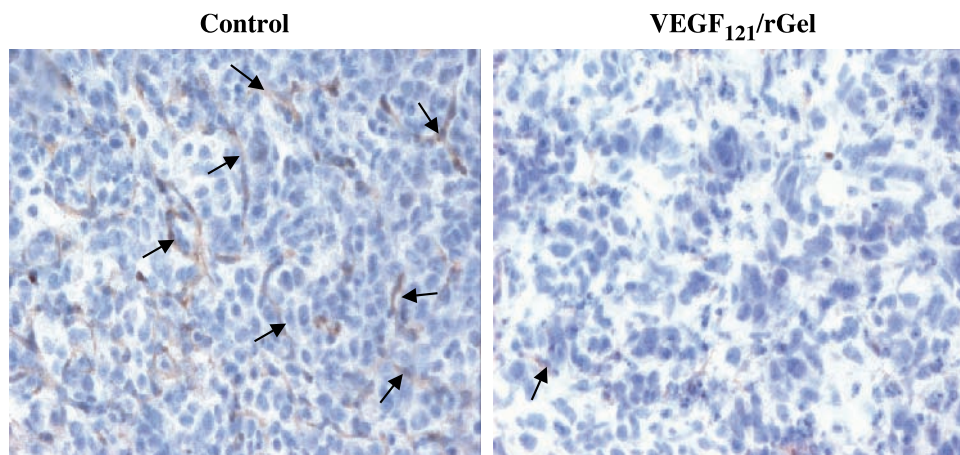


Figure 6. Detection of Flk-1/VEGFR-2 on the vasculature of metastatic lesions by the anti-VEGFR-2 antibody, RAFL-1. Frozen sections of lungs from mice treated with VEGF₁₂₁/rGel or free gelonin stained with monoclonal rat antimouse VEGFR-2 antibody RAFL-1 (10 μ g/ml). RAFL-1 antibody was detected by goat antirat IgG HRP, as described under the Materials and Methods section. Sections were developed with DAB and counterstained with hematoxylin. Representative images of lung metastases of comparable size (700–800 μ m in the largest diameter) from each treatment group are shown. Images were taken with an objective of $\times 20$. Note that the pulmonary metastases from the VEGF₁₂₁/rGel-treated group show both reduced vessel density and decreased intensity of anti-VEGFR-2 staining compared to control lesions.

metastases was completely inhibited by this therapeutic approach, the development of small, avascular, metastatic foci within lung tissues was observed. Our findings indicate that vasculature in the small and mid-sized metastatic lesions (diameter < 500 μ m) was much more susceptible to the action of VEGF₁₂₁/rGel than that in colonies with diameters larger than 500 μ m. Several explanations might account for this observation. First, the number of VEGF receptors on endothelial cells within the small, exponentially expanding colonies might be higher than that in the well-established lesions. This would lead to an increase in binding sites for VEGF₁₂₁/rGel and, hence, an increased toxicity toward vessels specifically in small colonies. Second, vascular endothelial cells in small colonies might have a reduced capacity to survive after drug assault compared to vessels in established lesions. This could be due to insufficient recruitment of supporting cells (pericytes/smooth muscle cells) to the newly formed vessels, and/or derangements in the production of and interaction with components of basement membrane. Currently, the precise mechanism of the differential anti-vascular toxicity on different size colonies is not completely understood. However, these data strongly suggest that the combination of vascular targeting agents with chemotherapeutic agents or with radiotherapeutic agents, which directly damage tumor cells themselves, may provide for greater therapeutic effect. Studies of several vascular targeting agents in combination with chemotherapeutic agents have already demonstrated a distinct *in vivo* antitumor advantage of this combination modality against experimental tumors in mice [60]. Studies by Pedley et al. [61] have also suggested that the combination of vascular targeting and radioimmunotherapy may also present a potent antitumor combination. Finally, studies combining hyperthermia and radiotherapy with vascular targeting agents have demonstrated an enhanced activity against mammary carcinoma tumors in mice [62]. Studies in our laboratory

combining VEGF₁₂₁/rGel and various chemotherapeutic agents, biologic agents, or therapeutic agents targeting tumor cells are currently ongoing.

The rGel toxin is a single-chain *N*-glycosidase that is similar in its action to ricin-A chain [39]. However, unlike ricin-A chain, the use of rGel does not appear to result in VLS [44]. Side effects have been observed with clinical administration of RTA-based, diphtheria toxin-based, and *Pseudomonas* exotoxin-based fusion proteins. These side effects include liver toxicity, development of neutralizing antibodies, and development of VLS. The development of neutralizing antibodies was found in 69% of patients treated with RTA immunotoxins [63], 37% of patients treated with PE-based constructs [64], and 92% of patients treated with DT constructs [65]. In contrast, our ongoing clinical trial with an rGel-based conjugate currently demonstrates a relatively low antigenicity of the rGel component, with only 2 of 22 patients developing antibodies to the rGel portion of the drug [44]. In addition, the development of hepatotoxicity and VLS is commonly observed, with toxin molecules thus far not having been observed for rGel-based agents. These findings support continuing development in a clinical setting of targeted therapy using rGel. In addition, our laboratory continues to develop designer toxins with reduced antigenicity and size [66].

The presented findings demonstrate that VEGF₁₂₁/rGel can clearly and specifically target Flk-1/KDR-expressing tumor vasculature both *in vitro* and *in vivo* and that this agent can have an impressive inhibitory effect on tumor metastases. Studies are continuing in our laboratory to examine the activity of this agent alone and in combination against a variety of orthotopic and metastatic tumor models.

References

- [1] Birnbaum D (1995). VEGF-FLT1 receptor system: a new ligand-receptor system involved in normal and tumor angiogenesis. *Jpn J Cancer Res* 86 (inside cover).

- [2] Kerbel RS (2000). Tumor angiogenesis: past, present and the near future. *Carcinogenesis* **21**, 505–515.
- [3] Bando H and Toi M (2000). Tumor angiogenesis, macrophages, and cytokines. *Adv Exp Med Biol* **476**, 267–284.
- [4] Falterman KW, Ausprunk H, and Klein MD (1976). Role of tumor angiogenesis factor in maintenance of tumor-induced vessels. *Surg Forum* **27**, 157–159.
- [5] Patt LM and Houck JC (1983). Role of polypeptide growth factors in normal and abnormal growth. *Kidney Int* **23**, 603–610.
- [6] Ravi R, Mookerjee B, Bhujwalla ZM, Sutter CH, Artemov D, Zeng Q, Dillehay LE, Madan A, Semenza GL, and Bedi L (2000). Regulation of tumor angiogenesis by p53-induced degradation of hypoxia-inducible factor 1 alpha. *Genes Dev* **14**, 34–44.
- [7] Folkman J (1974). Proceedings: tumor angiogenesis factor. *Cancer Res* **34**, 2109–2113.
- [8] Strugar J, Rothbart D, Harrington W, and Criscuolo GR (1994). Vascular permeability factor in brain metastases: correlation with vasogenic brain edema and tumor angiogenesis. *J Neurosurg* **81**, 560–566.
- [9] Jaeger TM, Weidner N, Chew K, Moore DH, Kerschmann RL, Waldman FM, and Carroll PR (1995). Tumor angiogenesis correlates with lymph node metastases in invasive bladder cancer. *J Urol* **154**, 69–71.
- [10] Melnyk O, Zimmerman M, Kim KJ, and Shuman M (1999). Neutralizing anti-vascular endothelial growth factor antibody inhibits further growth of established prostate cancer and metastases in a pre-clinical model. *J Urol* **161**, 960–963.
- [11] Aranda FI and Laforga JB (1996). Microvessel quantitation in breast ductal invasive carcinoma. Correlation with proliferative activity, hormonal receptors and lymph node metastases. *Pathol Res Pract* **192**, 124–129.
- [12] Fox SB, Leek RD, Bliss J, Mansi JL, Gusterson B, Gatter KC, and Harris AL (1997). Association of tumor angiogenesis with bone marrow micrometastases in breast cancer patients. *J Natl Cancer Inst* **89**, 1044–1049.
- [13] Senger DR, Van de Water L, Brown LF, Nagy JA, Yeo KT, Yeo TK, Berse B, Jackman RW, Dvorak AM, and Dvorak HF (1993). Vascular permeability factor (VPF, VEGF) in tumor biology. *Cancer Metastasis Rev* **12**, 303–324.
- [14] McMahon G (2000). VEGF receptor signaling in tumor angiogenesis. *Oncologist* **5** (Suppl 1), 3–10.
- [15] Öbermair A, Kucera E, Mayerhofer K, Speiser P, Seifert M, Czerwenka K, Kaider A, Leodolter S, Kainz C, and Zeillinger R (199). Vascular endothelial growth factor (VEGF) in human breast cancer: correlation with disease-free survival. *Int J Cancer* **74**, 455–458.
- [16] Miyoshi C and Ohshima N (2001). Vascular endothelial growth factor (VEGF) expression regulates angiogenesis accompanying tumor growth in a peritoneal disseminated tumor model. *In Vivo* **15**, 233–238.
- [17] Neufeld G, Cohen T, Gengrinovitch S, and Poltorak Z (1999). Vascular endothelial growth factor (VEGF) and its receptors. *FASEB J* **13**, 9–22.
- [18] Shibuya M (1995). Role of VEGF–flt receptor system in normal and tumor angiogenesis. *Adv Cancer Res* **67**, 281–316.
- [19] Detmar M (2000). The role of VEGF and thrombospondins in skin angiogenesis. *J Dermatol Sci* **24** (Suppl 1), S78–S84.
- [20] Verheul HM and Pinedo HM (2000). The role of vascular endothelial growth factor (VEGF) in tumor angiogenesis and early clinical development of VEGF-receptor kinase inhibitors. *Clin Breast Cancer* **1** (Suppl 1), S80–S84.
- [21] McCabe CJ, Boelaert K, Tannahill LA, Heaney AP, Stratford AL, Khaira JS, Hussain S, Sheppard MC, Franklyn JA, and Gittos NJ (2002). Vascular endothelial growth factor, its receptor KDR/Flk-1, and pituitary tumor transforming gene in pituitary tumors. *J Clin Endocrinol Metab* **87**, 4238–4244.
- [22] Kranz A, Mattfeldt T, and Waltenberger J (1999). Molecular mediators of tumor angiogenesis: enhanced expression and activation of vascular endothelial growth factor receptor KDR in primary breast cancer. *Int J Cancer* **84**, 293–298.
- [23] Harada Y, Ogata Y, and Shirouzu K (2001). Expression of vascular endothelial growth factor and its receptor KDR (kinase domain-containing receptor)/Flk-1 (fetal liver kinase-1) as prognostic factors in human colorectal cancer. *Int J Clin Oncol* **6**, 221–228.
- [24] Padro T, Bieker R, Ruiz S, Steins M, Retzlaff S, Burger H, Buchner T, Kessler T, Herrera F, Kienast J, et al. (2002). Overexpression of vascular endothelial growth factor (VEGF) and its cellular receptor KDR (VEGFR-2) in the bone marrow of patients with acute myeloid leukemia. *Leukemia* **16**, 1302–1310.
- [25] Wedge SR, Ogilvie DJ, Dukes M, Kendrew J, Curwen JO, Hennequin LF, Thomas AP, Stokes ES, Curry B, Richmond GH, et al. (2000). ZD4190: an orally active inhibitor of vascular endothelial growth factor signaling with broad-spectrum antitumor efficacy. *Cancer Res* **60**, 970–975.
- [26] Laird AD, Vajkoczy P, Shawver LK, Thurnher A, Liang C, Mohammadi M, Schlessinger M, Ullrich A, Hubbard SR, Blake RA, et al. (2000). SU6668 is a potent antiangiogenic and antitumor agent that induces regression of established tumors. *Cancer Res* **60**, 4152–4160.
- [27] Haluska P and Adjei AA (2001). Receptor tyrosine kinase inhibitors. *Curr Opin Invest Drugs* **2**, 280–286.
- [28] Fabbro D, Ruetz S, Bodis S, Pruschy M, Csermak K, Man A, Campochiaro P, Wood J, O'Reilly T, and Meyer T (2000). PKC412—a protein kinase inhibitor with a broad therapeutic potential. *Anticancer Drug Des* **15**, 17–28.
- [29] Fabbro D, Buchdunger E, Wood J, Mestan J, Hofmann F, Ferrari S, Mett H, O'Reilly T, and Meyer T (1999). Inhibitors of protein kinases: CGP 41251, a protein kinase inhibitor with potential as an anticancer agent. *Pharmacol Ther* **82**, 293–301.
- [30] Sun L and McMahon G (2000). Inhibition of tumor angiogenesis by synthetic receptor tyrosine kinase inhibitors. *Drug Discov Today* **5**, 344–353.
- [31] Solorzano CC, Baker CH, Bruns CJ, Killion JJ, Ellis LM, Wood J, and Fidler IJ (2001). Inhibition of growth and metastasis of human pancreatic cancer growing in nude mice by PTK 787/ZK222584, an inhibitor of the vascular endothelial growth factor receptor tyrosine kinases. *Cancer Biother Radiopharm* **16**, 359–370.
- [32] Drevs J, Hofmann I, Hugenschmidt H, Wittig C, Madjar H, Muller M, Wood J, Martiny-Baron G, Unger C, and Marne D (2000). Effects of PTK787/ZK 222584, a specific inhibitor of vascular endothelial growth factor receptor tyrosine kinases, on primary tumor, metastasis, vessel density, and blood flow in a murine renal cell carcinoma model. *Cancer Res* **60**, 4819–4824.
- [33] Dimitroff CJ, Klohs W, Sharma A, Pera P, Driscoll D, Veith J, Steinkampf R, Schroeder M, Klutcho S, Sumlin A, et al. (1999). Anti-angiogenic activity of selected receptor tyrosine kinase inhibitors, PD166285 and PD173074: implications for combination treatment with photodynamic therapy. *Invest New Drugs* **17**, 121–135.
- [34] Mendel DB, Schreck RE, West DC, Li G, Strawn LM, Tanciongco SS, Vasile S, Shawver LK, and Cherrington JM (2000). The angiogenesis inhibitor SU5416 has long-lasting effects on vascular endothelial growth factor receptor phosphorylation and function. *Clin Cancer Res* **6**, 4848–4858.
- [35] Prewett M, Huber J, Li Y, Santiago A, O'Connor W, King K, Overholser J, Hooper A, Pytowski B, Witte L, et al. (1999). Antivascular endothelial growth factor receptor (fetal liver kinase 1) monoclonal antibody inhibits tumor angiogenesis and growth of several mouse and human tumors. *Cancer Res* **59**, 5209–5218.
- [36] Chen Y, Wiesmann C, Fuh G, Li B, Christinger HW, McKay P, de Vos AM, and Lowman HB (1999). Selection and analysis of an optimized anti-VEGF antibody: crystal structure of an affinity-matured Fab in complex with antigen. *J Mol Biol* **293**, 865–881.
- [37] Ryan AM, Eppler DB, Hagler KE, Bruner RH, Thomford PJ, Hall RL, Shopp GM, and O'Neill CA (1999). Preclinical safety evaluation of rhu-MABVEGF, an antiangiogenic humanized monoclonal antibody. *Toxicol Pathol* **27**, 78–86.
- [38] Veenendaal LM, Jin H, Ran S, Cheung L, Navone N, Marks JW, Waltenberger J, Thorpe P, and Rosenblum MG (2002). *In vitro* and *in vivo* studies of a VEGF121/rGelolin chimeric fusion toxin targeting the neovasculature of solid tumors. *Proc Natl Acad Sci USA* **99**, 7866–7871.
- [39] Stirpe F, Olsnes S, and Pihl A (1980). Gelonin, a new inhibitor of protein synthesis, nontoxic to intact cells. Isolation, characterization, and preparation of cytotoxic complexes with concanavalin A. *J Biol Chem* **255**, 6947–6953.
- [40] Rosenblum MG, Cheung L, Kim SK, Mujoo K, Donato NJ, and Murray JL (1996). Cellular resistance to the antimitelanoma immunotoxin ZME-gelonin and strategies to target resistant cells. *Cancer Immunol Immunother* **42**, 115–121.
- [41] Rosenblum MG, Zuckerman JE, Marks JW, Rotbein J, and Allen WR (1992). A gelonin-containing immunotoxin directed against human breast carcinoma. *Mol Biother* **4**, 122–129.
- [42] Rosenblum MG, Murray JL, Cheung L, Rifkin R, Salmon S, and Bartholomew R (1991). A specific and potent immunotoxin composed of antibody ZME-018 and the plant toxin gelonin. *Mol Biother* **3**, 6–13.
- [43] Xu Y, Xu Q, Rosenblum MG, and Scheinberg DA (1996). Antileukemic activity of recombinant humanized M195-gelonin immunotoxin in nude mice. *Leukemia* **10**, 321–326.

- [44] Talpaz M, Kantarjian H, Freireich E, Lopez V, Zhang W, Cortes-Franco J, Scheinberg D, and Rosenblum MG (2003). Phase I clinical trial of the anti-CD-33 immunotoxin HuM195/rGel. *Abstract R5362, 94th Annual Meeting, American Association for Cancer Research* **44**, 1066.
- [45] Ran S, Huang X, Downes A, and Thorpe PE (2003). Evaluation of novel antimouse VEGFR2 antibodies as potential antiangiogenic or vascular targeting agents for tumor therapy. *Neoplasia* **5**, 297–307.
- [46] Axelsson K, Ljung BM, Moore DH II, Thor AD, Chew KL, Edgerton SM, Smith HS, and Mayall BH (1995). Tumor angiogenesis as a prognostic assay for invasive ductal breast carcinoma. *J Natl Cancer Inst* **87**, 997–1008.
- [47] Balsari A, Maier JA, Colnaghi MI, and Menard S (1999). Correlation between tumor vascularity, vascular endothelial growth factor production by tumor cells, serum vascular endothelial growth factor levels, and serum angiogenic activity in patients with breast carcinoma. *Lab Invest* **79**, 897–902.
- [48] Bosari S, Leek AK, DeLellis RA, Wiley BD, Heatley GJ, and Silverman ML (1992). Microvessel quantitation and prognosis in invasive breast carcinoma. *Hum Pathol* **23**, 755–761.
- [49] Bottini A, Berruti A, Bersiga A, Brizzi MP, Allevi G, Bolsi G, Aguggini S, Brunelli A, Betri E, Generali D, et al. (2002). Changes in microvessel density as assessed by CD34 antibodies after primary chemotherapy in human breast cancer. *Clin Cancer Res* **8**, 1816–1821.
- [50] Chu JS, Lee WJ, Chang TC, Chang KJ, and Hsu HC (1995). Correlation between tumor angiogenesis and metastasis in breast cancer. *J Formos Med Assoc* **94**, 373–378.
- [51] Nakopoulou L, Stefanaki K, Panayotopoulou E, Giannopoulou I, Athanassiadou P, Gakiopoulou-Givalou H, and Louvrou A (2002). Expression of the vascular endothelial growth factor receptor-2/Flk-1 in breast carcinomas: correlation with proliferation. *Hum Pathol* **33**, 863–870.
- [52] Brown LF, Guidi AJ, Schnitt SJ, Van De Water L, Iruela-Arispe ML, Yeo TK, Tognazzi K, and Dvorak HF (1999). Vascular stroma formation in carcinoma *in situ*, invasive carcinoma, and metastatic carcinoma of the breast. *Clin Cancer Res* **5**, 1041–1056.
- [53] Brown LF, Berse B, Jackman RW, Tognazzi K, Guidi AJ, Dvorak HF, Senger DR, Connolly JL, and Schnitt SJ (1995). Expression of vascular permeability factor (vascular endothelial growth factor) and its receptors in breast cancer. *Hum Pathol* **26**, 86–91.
- [54] Hotz HG, Gill PS, Masood R, Hotz B, Buhr HJ, Foitzik T, Hines OJ, and Reber HA (2002). Specific targeting of tumor vasculature by diphtheria toxin—vascular endothelial growth factor fusion protein reduces angiogenesis and growth of pancreatic cancer. *J Gastrointest Surg* **6**, 159–166.
- [55] Cobleigh MA, Langmuir VK, Sledge GW, Miller KD, Haney L, Novotny WF, Reimann JD, and Vassel D (2003). A phase I/II dose-escalation trial of bevacizumab in previously treated metastatic breast cancer. *Semin Oncol* **30** (5 Suppl 16), 117–124.
- [56] Shaheen RM, Davis DW, Liu W, Zebrowski BK, Wilson MR, Bucana CD, McConkey DJ, McMahon G, and Ellis LM (1999). Antiangiogenic therapy targeting the tyrosine kinase receptor for vascular endothelial growth factor receptor inhibits the growth of colon cancer liver metastasis and induces tumor and endothelial cell apoptosis. *Cancer Res* **59**, 5412–5416.
- [57] Seon BK, Matsuno F, Haruta Y, Kondo M, and Barcos M (1997). Long-lasting complete inhibition of human solid tumors in SCID mice by targeting endothelial cells of tumor vasculature with antihuman endoglin immunotoxin. *Clin Cancer Res* **3**, 1031–1044.
- [58] Honkoop AH, van Diest PJ, de Jong JS, Linn SC, Giaccone G, Hoekman K, Wagstaff J, and Pinedo HM (1998). Prognostic role of clinical, pathological and biological characteristics in patients with locally advanced breast cancer. *Br J Cancer* **77**, 621–626.
- [59] Vartanian RK and Weidner N (1994). Correlation of intratumoral endothelial cell proliferation with microvessel density (tumor angiogenesis) and tumor cell proliferation in breast carcinoma. *Am J Pathol* **144**, 1188–1194.
- [60] Siemann DW, Mercer E, Lepler S, and Rojiani AM (2002). Vascular targeting agents enhance chemotherapeutic agent activities in solid tumor therapy. *Int J Cancer* **99**, 1–6.
- [61] Pedley RB, El Emir E, Flynn AA, Boxer GM, Dearling J, Raleigh JA, Hill SA, Stuart S, Motha R, and Begent RH (2002). Synergy between vascular targeting agents and antibody-directed therapy. *Int J Radiat Oncol Biol Phys* **54**, 1524–1531.
- [62] Murata R, Overgaard J, and Horsman MR (2001). Combretastatin A-4 disodium phosphate: a vascular targeting agent that improves that improves the anti-tumor effects of hyperthermia, radiation, and mild thermoradiotherapy. *Int J Radiat Oncol Biol Phys* **51**, 1018–1024.
- [63] Schnell R, Vitetta E, Schindler J, Borchmann P, Barth S, Ghetie V, Hell K, Drillich S, Diehl V, and Engert A (2000). Treatment of refractory Hodgkin's lymphoma patients with an anti-CD25 ricin-A chain immunotoxin. *Leukemia* **14**, 129–135.
- [64] Kreitman RJ, Wilson WH, White JD, Stetler-Stevenson M, Jaffe ES, Giardina S, Waldmann TA, and Pastan I (2000). Phase I trial of recombinant immunotoxin anti-Tac(Fv)-PE38 (LMB-2) in patients with hematologic malignancies. *J Clin Oncol* **18**, 1622–1636.
- [65] LeMaistre CF, Saleh MN, Kuzel TM, Foss F, Platanias LC, Schwartz G, Ratain M, Rook A, Freytes CO, Craig F, et al. (1998). Phase I trial of a ligand fusion-protein (DAB389IL-2) in lymphomas expressing the receptor for interleukin-2. *Blood* **91**, 399–405.
- [66] Cheung LH, Marks JW, and Rosenblum MG (2004). Development of "designer toxins" with reduced antigenicity and size. *Abstract 3790, 95th Annual Meeting, American Association for Cancer Research* **45**, 874.

The Immunocytokine scFv23/TNF Targeting HER-2/neu Induces Synergistic Cytotoxic Effects with 5-Fluorouracil in TNF-Resistant Pancreatic Cancer Cells

*Mi-Ae Lyu, Razelle Kurzrock, and Michael G. Rosenblum**

Running Title: Synergistic effects of scFv23/TNF and 5-FU

Department of Experimental Therapeutics, The University of Texas M. D. Anderson Cancer Center, Houston, TX, USA

**Correspondence to:* Michael G. Rosenblum, Ph.D., Immunopharmacology and Targeted Therapy Laboratory, Department of Experimental Therapeutics, The University of Texas M. D. Anderson Cancer Center, 1515 Holcombe Blvd., Unit 0044, Houston, TX 77030, Tel: 713-792-3554; Fax: 713-794-4261; (e-mail: mrosenbl@mdanderson.org).

Research conducted, in part, by The Clayton Foundation for Research and supported, in part by DOD Grant DAMD17-02-1-10457-1.

Categories: Research Articles

Key Words: HER-2/neu, Pancreatic cancer, scFv23/TNF, 5-Fluorouracil, Combination therapy

Abstract

Human pancreatic cancer cells are highly resistant to TNF and HER-2/neu expression has been proposed as a negative prognostic marker in pancreatic intraepithelial neoplasia. Our approach was to utilize HER-2/neu expression on the surface of tumor cells as a therapeutic target employing the immunocytokine scFv23/TNF to deliver TNF directly to TNF-resistant tumor cells. Using a panel of human pancreatic cell lines (AsPc-1, Capan-1, Capan-2, and L3.6pl), we evaluated the in vitro response of cells to scFv23/TNF in combination with various chemotherapeutic agents. We found a correlation between the expression levels of HER-2/neu, TNF-R1 and cellular response to scFv23/TNF. L3.6pl cells expressing the highest levels of HER-2/neu and TNF-R1 were the most sensitive to scFv23/TNF. Simultaneous treatment with scFv23/TNF and 5-fluorouracil resulted in a synergistic cytotoxic effect whereas combinations of scFv23/TNF and doxorubicin or gemcitabine were antagonistic. Combining scFv23/TNF with 5-fluorouracil resulted in down-regulation of phospho-Akt and Bcl-2 as well as induction of apoptosis and this synergistic cytotoxic effect was dependent of caspases activation. Our studies clearly show that delivery of TNF to HER-2/neu expressing tumor cells, which are inherently resistant to TNF using scFv23/TNF may be an effective therapy for pancreatic cancer especially when utilized in combination with 5-fluorouracil.

Abbreviations List: scFv23/TNF, anti-HER-2/neu single chain antibody fused to TNF

Introduction

Pancreatic cancer remains one of the leading causes of cancer-related deaths in the United States and Europe [1-3]. This is a highly aggressive and metastatic tumor type virtually resistant to all chemotherapeutic and radiotherapeutic intervention [4,5]. Recent studies have demonstrated some clinical benefit to treatment with gemcitabine and gemcitabine-containing regimens [6-8].

There are numerous oncogenes such as HER-2/neu, HER-1 [9-13] which are over-expressed in pancreatic tumor biopsy specimens as well as mutations in various genes such as p53, Ki-ras, and p-21 [14-16]. Many of these genetic abnormalities play a major role in the development of the aggressive, metastatic and therapy-resistant phenotype presented clinically. Experimental therapeutic approaches using vaccines [17-20] or antibodies to target oncogene protein products [21-23] are underway or have been completed to provide more focused control of tumor growth.

Immunocytokines are a novel class of recombinant agents composed of cytokines fused to antibodies and these fusion constructs are capable of re-directing the biological effects of cytokines to target specific cells and to prevent non-target toxicity. We initially described a novel chemical conjugate of a tumor-targeting antibody and the cytokine tumor necrosis factor-alpha (TNF- α) [24,25]. Against antigen-positive cells, this chemical conjugate was more cytotoxic to target cells than TNF- α itself. More recently, we developed novel immunocytokine scFv23/TNF composed of a single-chain antibody targeting the HER-2/neu antigen fused to the gene for TNF- α [26]. This immunocytokine was also shown to be highly cytotoxic and specifically active against target cancer cells resistant to TNF- α itself [26, 27].

Because many human pancreatic tumor cell lines express HER-2/neu and tend to be generally resistant to TNF and chemotherapeutic agents, our approach was to utilize HER-2/neu

expression on the surface of tumor cells as a therapeutic target employing the HER-2/neu single chain antibody to deliver TNF directly to tumor cells. In this study, we described a novel immunocytokine scFv23/TNF targeting the HER-2/neu oncogene and which contains the cytokine TNF as the cytotoxic moiety. We found that this fusion construct to be highly cytotoxic to HER-2/neu-expressing pancreatic cancer cell lines at levels rivaling that of conventional chemotherapeutic agents. In addition, we tested scFv23/TNF in vitro with various chemotherapeutic agents and found synergistic cytotoxic effects only with 5-fluorouracil (5-FU) in TNF-resistant pancreatic cancer cell lines. Our data suggest that delivery of the cytokine TNF to HER-2/neu expressing pancreatic cancer cells using the immunocytokine scFv23/TNF may be an effective therapy for pancreatic cancer especially when utilized in combination with 5-FU.

Materials and Methods

Cell Culture

L3.6pl and Capan-1 human pancreatic cancer cell lines were kindly provided by Dr. Jerald Killian and Dr. Paul Chiao (M.D. Anderson Cancer Center, Houston). AsPc-1 and Capan-2 human pancreatic cancer cell lines were kindly provided by Dr. Dr. Keping Xie (M.D. Anderson Cancer Center, Houston). All four human pancreatic cancer cell lines were grown in Dulbecco's modified Eagle's medium (DMEM, Life Technologies Inc., Rockville, MD) supplemented with 10% heat-inactivated fetal bovine serum (FBS), 100 units/ml penicillin and 100 µg/ml streptomycin.

Chemotherapeutic agents and immunocytokine scFv23/TNF

5-fluorouracil (5-FU) was from Roche Laboratories (Nutley, NJ). Cisplatin and Etoposide (VP-16) were from Bristol Laboratories (Princeton, NJ). Doxorubicin was from Cetus Corporation (Emeryville, CA). Gemcitabine was from Eli Lilly Co. (Indianapolis, IN). The immunocytokine scFv23/TNF was produced in a bacterial expression host, purified to homogeneity and assessed for biological activity as previously described [26].

Antibodies and Chemicals

Monoclonal anti-HER-2/neu antibody (Ab), rabbit polyclonal anti-TNF-R1 Ab, rabbit polyclonal anti-TNF-R2 Ab, rabbit polyclonal anti-phospho Akt Ab, rabbit polyclonal anti-Akt Ab, mouse anti-Bcl-2 Ab, rabbit polyclonal anti-caspase-8 Ab, monoclonal anti-caspase-3 Ab, and monoclonal anti-PARP Ab were obtained from Santa Cruz Biotechnology, Santa Cruz, CA.

General caspase inhibitor (Z-VAD-FMK), caspase-8 inhibitor (Z-IETD-FMK), and caspase-3 inhibitor (Z-DEVD-FMK) were purchased from R&D Systems, Minneapolis, MN.

In Vitro Cytotoxicity Assays and Combination Studies

All human pancreatic cancer cells were seeded (1×10^4 /well) in flat-bottom 96-well microtiter plates (Becton Dickinson Labware, Franklin Lakes, NJ) and 24 hr later, scFv23/TNF, TNF or five chemotherapeutic agents (5-fluorouracil, cisplatin, etoposide, doxorubicin, and gemcitabine,) were added in triplicate wells. For combination studies, scFV23/TNF and each of five chemotherapeutic agents were combined at their individual IC_{25} concentrations. To examine the effect of caspase inhibitor on the cytotoxicity of combination, L3.6pl cells were pre-treated with or without 200 μ M general caspase inhibitor (Z-VAD-FMK), caspase-8 inhibitor (Z-IETD-FMK), or caspase-3 inhibitor (Z-DEVD-FMK) (R&D) for 2 hr and then treated with their individual IC_{25} concentrations. After incubation for an additional 72 hr, remaining adherent cells were stained by adding 50 μ l of crystal violet solution (0.5% w/v in 20% MeOH/H₂O). Dye-stained cells were solubilized by addition of 100 μ l of Sorenson's buffer [100 mM sodium citrate (pH 4.2) in 50% ethanol], and absorbance was measured at 630 nm using an ELISA plate reader (Bio-Tek Instruments, Inc., Winooski, VT).

The synergistic, additive, or antagonistic effects of drug combinations were assessed according to the median effect principle as described by Chou and Talalay [28]: $fa/fu = (D/D_m)^m$

Where D is the dose of the drug, D_m is the IC_{50} , fa is the fraction affected by the dose, fu is the fraction unaffected, and m is a coefficient that determines the sigmoidicity of the curve.

Western Blot Analysis

To check the status of HER-2/neu, TNF receptor-1, and TNF receptor-2, four human pancreatic cancer cell lines (AsPc-1, Capan-1, Capn-2, and L3.6pl) were washed two times with phosphate buffered saline (PBS) and lysed on ice for 20 min in 0.3 ml of lysis buffer (10 mM Tris-HCl, pH 8, 60 mM KCl, 1 mM EDTA, 1 mM DTT, 0.2% NP-40). L3.6pl cell lines were seeded at 5×10^5 cells/60 mm petri-dish, allowed to grow overnight, and then treated with IC₂₅ concentrations of 5-FU, scFv23/TNF, or combination. After treatment, cell lysates were prepared as described above. Cell lysates (50 µg) were fractionated by 8-15% SDS-PAGE and electrophoretically transferred to PVDF membranes (Millipore Corporation, Bedford, MA) overnight at 4°C in transfer buffer [25 mM Tris-HCl (pH 8.3), 190 mM Glycine, 20% methanol]. The PVDF membranes were blocked for 1 hour in Tris-buffered saline (TBS) containing 5% non-fat milk and then probed with different primary antibodies for 1 hour. Goat anti-mouse/anti-rabbit or swain anti-goat antibodies conjugated with horseradish peroxidase (Bio-Rad Laboratories, Hercules, CA) were used to visualize immunoreactive proteins at a 1:4000 dilution using ECL detection reagent (Amersham Pharmacia Biotech Inc., Piscataway, NJ). Data are presented as the relative density of protein bands normalized to β-actin. The intensity of the bands was quantified using Histogram.

Detection of Apoptosis

The development of apoptotic cell death was detected by TUNEL assay. To assess apoptosis, L3.6pl cells were plated on glass cover slips, allowed to adhere overnight and then treated with IC₂₅ concentrations of 5-FU, scFv23/TNF, or combination for 48 hr. The cells were washed with PBS, permeabilized (0.1% Triton X-100, 0.1% sodium citrate), and then fixed in

4% paraformaldehyde. Fixed cells were stained with an *in situ* cell death detection kit (Roche).

Cells undergoing apoptosis were identified by fluorescence microscopy (Nikon, Japan).

Results

Status of HER-2/neu, TNF-R1, and TNF-R2 in Four Human Pancreatic Cancer Cell Lines

HER-2/neu has previously been found to be over-expressed in pancreatic tumor biopsy specimens and HER-2/neu expression has been proposed as a negative prognostic marker in pancreatic intraepithelial neoplasia [9]. We therefore determined HER-2/neu expression in four pancreatic cancer cell lines (AsPc-1, Capan-1, Capan-2, and L3.6pl). All four pancreatic cancer cell lines expressed HER-2/neu, TNF-R1, and TNF-R2. We compared the expression levels of HER-2/neu, TNF-R1, and TNF-R2 in each cell line with levels in AsPc-1 cells. Compared with AsPc-1 cells, Capan-1 and L3.6pl cells expressed higher levels of HER-2/neu and TNFR-1 (3.3 – 3.8 fold vs. 2.3-3.0 fold, respectively) whereas Capan-2 cells expressed similar levels of HER-2/neu and TNF-R1 (Figure 1).

Dose-Response Curves of Various Agents on Four Pancreatic Cancer Cell Lines

The ability of various agents to inhibit cell proliferation *in vitro* was markedly different among the four cell lines tested. All pancreatic cancer cell lines were highly resistant to the cytotoxic effects of TNF ($IC_{50} > 4 \mu M$). 5-fluorouracil, cisplatin, and etoposide showed IC_{50} values between 1 μM and 300 μM whereas doxorubicin, gemcitabine, and scFv23/TNF were comparatively more active with IC_{50} values ranging between 6 nM and 700 nM. Interestingly, L3.6pl cells expressing the highest levels of HER-2/neu, TNF-R1, and TNF-R2 were the most sensitive to the tested drugs, whereas Capan-2 cells expressing comparatively lower levels of HER-2/neu, TNF-R1, and TNF-R2 were the most resistant to the tested drugs. AsPc-1 cells expressing similar levels of HER-2/neu and TNF-R1 as Capan-2 showed the moderate resistant to the tested drugs (Figure 2 and Table 1).

Cytotoxic Effect of scFv23/TNF in Combination with Various Chemotherapeutic Agents

Studies combining scFv23/TNF and various chemotherapeutic agents demonstrated a synergistic cytotoxic effect of scFv23/TNF with 5-fluorouracil and an antagonistic effect of scFv23/TNF with doxorubicin in all pancreatic cancer cell lines. However, the addition of cisplatin or gemcitabine to scFv23/TNF resulted in antagonistic cytotoxic effects in 3/4 cell lines tested whereas the addition of etoposide to scFv23/TNF resulted in synergistic effect in 3/4 pancreatic cancer cell lines (Table 2). These results suggest that targeting HER-2/neu and TNF-R1 expressing tumor cells using the immunocytokine scFv23/TNF may be an effective therapy for pancreatic cancer especially when utilized in combination with specific chemotherapeutic agents such as 5-FU.

Inhibition of Akt Phosphorylation by Combination Treatment

HER-2/neu over-expression results in activation of different downstream pathways such as the Akt kinase pathway, which leads to cell proliferation and cell survival. To determine whether combination treatment affects this survival pathway, L3.6pl cells were treated with IC₂₅ doses of 5-fluorouracil, scFv23/TNF, or 5-FU + scFv23/TNF. The activation of Akt kinase was then assessed by Western blot analysis using antibodies to Akt and to phospho-Akt. As shown in Figure 3, treatment of L3.6pl cells with 5-FU, scFv23/TNF as single agents or combination had no impact on the total levels of Akt while the combination treatment of scFv23/TNF plus 5-FU inhibited phosphorylation of the Akt protein by 50%. These results suggest that 5-FU + scFv23/TNF-induced cytotoxicity may be mediated, at least in part, by an inhibitory effect on Akt phosphorylation events.

Effect of Combination Treatment on Bcl-2 Expression

Increased levels of the anti-apoptotic protein Bcl-2 contribute to cellular resistance of tumor cells to a variety of chemotherapeutic agents including cyclophosphamide, methotrexate, anthracycline, cytarabine, paclitaxel, and corticosteroids [29]. To determine whether the cytotoxic effects of combination treatment are mediated through changes in cellular levels of Bcl-2, L3.6pl cells were treated with IC₂₅ doses of 5-fluorouracil, scFv23/TNF, or 5-FU + scFv23/TNF. As shown in Figure 4, treatment of cells with 5-FU had no impact on cellular levels of Bcl-2 while scFv23/TNF or 5-FU + scFv23/TNF inhibited Bcl-2 expression levels 43% and 71%, respectively. These results suggest that 5-FU + scFv23/TNF-induced cytotoxicity may be mediated, at least in part, by inhibition of Bcl-2 expression.

Induction of Apoptosis and Caspases Cleavage by Combination Treatment

To determine whether the cytotoxic effect of combination treatment was associated with apoptosis, L3.6pl cells were assayed for apoptosis by TUNEL staining. L3.6pl cells were treated with IC₂₅ doses of 5-fluorouracil, scFv23, TNF, or 5-FU + scFv23/TNF. As shown in Figure 5, 5-FU + scFv23/TNF-treated cells demonstrated a marked induction of apoptotic cell death within 48 hrs after treatment. The caspase series of proteins is known to be a central mediator of the apoptotic effects of TNF and other cytokines. To determine whether caspase-8 and caspase-3 were activated in L3.6pl cells during 5-FU + scFv23/TNF-induced cell death, we investigated the cleavage of caspase-8, caspase-3, and its substrate poly (ADP)-ribose polymerase (PARP). Treatment with IC₂₅ dose of 5-FU had no effect on caspase-8, caspase-3, and PARP cleavage whereas exposure of the cells to the scFv23/TNF or scFv23/TNF plus 5-FU combination resulted

in cleavage of caspase-8 and caspase-3. In addition, combination treatment induced PARP cleavage at 48 hr (Figure 6). We only observed PARP cleavage in 5-FU+scFv23/TNF-treated L3.6pl cells (Figure 7).

To determine whether 5-FU + scFv23/TNF-induced apoptosis was dependent on activation of the caspase pathways, we examined the effect of caspase inhibitors on the cytotoxicity of 5-FU + scFv23/TNF against L3.6pl cells. As shown in Figure 8, pre-treatment with the caspase inhibitors followed by combination treatment (5-FU + scFv23/TNF) was able to inhibit the synergistic cytotoxic effects observed. This suggests that the synergistic cytotoxic effects of the combination may depend, at least in part, on a caspase-driven pathway.

Discussion

Human epidermal growth factor receptor-2 (HER-2/erbB-2) belongs to a family of four transmembrane receptors (HER-1, HER-3, and HER-4) and it plays a key role in the HER family signaling events, cooperating with other HER receptors via a complex signaling network to regulate cell growth, differentiation, and survival [30-32]. Over-expression of HER-2/neu has been observed in several cancers where it is associated with multiple drug resistance, higher metastatic potential, and decreased patient survival times [9, 33-37]. To evaluate the influence of HER-2/neu expression in pancreatic cancer as it relates to clinical response to therapeutic agents, a variety of groups have used several HER-2/neu targeting strategies including using HER-2/neu targeted ribozymes [38-40], humanized anti-HER-2/neu antibody (Herceptin), and combination chemotherapeutic treatment regimens with Herceptin [21, 41-43].

Our approach was to utilize HER-2/neu expression on the surface of tumor cells as a therapeutic target employing the HER-2/neu single chain antibody to deliver TNF directly to tumor cells. Previous studies in our laboratory demonstrated that the immunocytokine scFv23/TNF was highly cytotoxic even to tumor cells resistant to TNF itself [26, 27] and sensitized HER-2/neu-overexpressing SKBR-3 cells to TNF via up-regulation of TNFR-1 [27]. We examined in depth the mechanistic effects of the immunocytokine scFv23/TNF in combination with chemotherapeutic agents on a panel of four pancreatic cancer cell lines, which were characterized for various levels of oncogene expression and comparative response to chemotherapeutic agents.

The chemotherapeutic agents utilized in this study were selected to present a spectrum of different cellular targets and are representative of the major classes of agents with therapeutic value. The potential combinations of tumor-targeted delivery of TNF in combination with

chemotherapeutic agents have not been previously examined. Our studies combining scFv23/TNF and various chemotherapeutic agents clearly demonstrated a uniform synergistic effect of scFv23/TNF and 5-FU in all pancreatic tumor cell lines. L3.6pl cells expressing the highest levels of HER-2/neu, TNF-R1, and TNF-R2 were the most sensitive to the tested drugs. Pegram *et al* reported that 5-FU has an antagonistic effect *in vitro* in combination with anti-HER-2/neu monoclonal antibodies whereas cisplatin, etoposide, and doxorubicin, previously showed a synergistic or an additive effect in combination with Herceptin [43]. However, we found a uniform synergistic effect of scFv23/TNF in combination with 5-FU and an antagonistic effect of scFv23/TNF in combination with doxorubicin in against all four pancreatic cancer cell lines (Table 2).

Over-expression of HER-2/neu is known to activate the Akt pathway and to confer resistance to apoptosis induced by many therapeutic drugs [44]. Treatment of L3.6pl cells with combination 5-FU + scFv23/TNF resulted in significant reduction in Akt phosphorylation. Our result suggests that 5-FU + scFv23/TNF-induced cytotoxicity may be mediated, at least in part, by the inhibition of Akt survival signaling pathway.

Over-expression of Bcl-2 has also been shown to contribute to the cellular resistance of a variety of chemotherapeutic drugs, including cyclophosphamide, methotrexate, anthracycline, cytarabine, paclitaxel, and corticosteroids [29]. Sasaki *et al* reported that the level of Bcl-2 in cancer cells was an indicator of 5-FU efficacy [45]. We found that scFv23/TNF or 5-FU + scFv23/TNF inhibited 43% and 71%, respectively. However, treatment of cells with IC₂₅ dose of 5-FU had no impact on the levels of Bcl-2. Down-regulation of Bcl-2 by scFv23/TNF may be induced the sensitization of L3.6pl cells to be more sensitive to 5-FU. Therefore, scFv23/TNF in combination with 5-FU accelerates the inhibition of Bcl-2 expression.

We also found that another critical factor in the mediation of 5-FU + scFv23/TNF synergy is activation of the caspase cascade. Binding of TNF to TNFR-1 can induce the formation of signaling complexes, TNF-R1-TRADD-FADD-pro-caspase-8, resulting in the activation of caspase-8 [46]. The activation of caspase-8 is thought to result in proteolytic cascade activation of the other caspases [47]. The activation of caspase-3 contributes to paclitaxel-induced apoptosis in HER-2/neu-overexpressing SKOV3.ip1 [48] and immunotoxin-induced apoptosis in cancer cells [49]. We observed that treatment with scFv23/TNF alone or 5-FU + scFv23/TNF combination resulted in activation of caspase-8, caspase-3 and PARP cleavage.

Taken together, we observed that treatment of L3.6pl cells with scFv23/TNF in combination with 5-FU resulted in down-regulation of p-Akt and Bcl-2, and apoptosis through cleavage of caspase-8, caspase-3, and PARP. The immunocytokine scFv23/TNF targeting Her-2/neu demonstrated a synergistic cytotoxic effect with 5-FU in TNF-resistant pancreatic cancer cells. Delivery of the cytokine TNF to HER-2/neu expressing tumor cells using the immunocytokine scFv23/TNF may be an effective therapy for pancreatic cancer especially when utilized in combination with the chemotherapeutic agent 5-FU.

Table 1. IC₅₀ of various agents against four human pancreatic cancer cell lines.

Drug	IC ₅₀ (μ M)			
	AsPc-1	Capan-1	Capan-2	L3.6pl
5-Fluorouracil (5-FU)	7.5	6	300	1
Cisplatin (CIS)	14	4.5	50	3.6
Etoposide (ETO)	28	2	40	2
Doxorubicin (DOX)	0.32	0.06	0.5	0.03
Gemcitabine (GEM)	0.2	0.02	0.15	0.006
scFv23/TNF	0.5	0.7	0.4	0.15
TNF	> 4*	> 4*	> 4*	> 4*

* Highest concentration achieved.

The IC₅₀ values were determined after 72 hr of exposure to the drugs and were defined as the concentration causing 50% growth inhibition in treated cells compared to control cells.

Table 2. Analysis of cytotoxicity induced by scFv23/TNF in combination with other chemotherapeutic agents.

Treatment	Combination Index (CI)			
	AsPc-1	Capan-1	Capan-2	L3.6pl
5-FU + scFv23/TNF	0.632 ± 0.015	0.611 ± 0.027	0.548 ± 0.026	0.366 ± 0.016
CIS + scFv23/TNF	2.250 ± 0.095	0.566 ± 0.028	1.532 ± 0.118	4.667 ± 0.247
ETO + scFv23/TNF	0.498 ± 0.023	0.869 ± 0.017	0.664 ± 0.019	1.640 ± 0.067
DOX + scFv23/TNF	1.805 ± 0.061	1.203 ± 0.000	2.084 ± 0.140	3.578 ± 0.172
GEM + scFv23/TNF	2.375 ± 0.114	1.250 ± 0.054	0.703 ± 0.027	2.833 ± 0.252

To analyze the cellular interaction between the 2 agents, combination index (CI) values were calculated as proposed by Chou [28]: $CI = (D)_1 / (Dx)_1 + (D)_2 / (Dx)_2 + \alpha D_1 D_2 / (Dx)_1 (Dx)_2$. Where $(D)_1$ and $(D)_2$ in combination kill X% of cells, and $(Dx)_1$ and $(Dx)_2$ are the estimated dose of the drug alone capable of producing the same effect of the combined drugs. $\alpha=1$ or 0 depending on whether the drugs are assumed to be mutually nonexclusive or mutually exclusive, respectively, in their action. If CI near to 1 indicates additive effect, $CI>1$ indicates antagonism, $CI<1$ indicates synergism.

References

- [1] Haycox A, Lombard M, Neoptolemos J, and Walley T (1998). Review article: current treatment and optimal patient management in pancreatic cancer. *Aliment Pharmacol Ther* **12**, 949-964.
- [2] Ward S, Morris E, Bansback N, Calvert N, Crellin A, Forman D, Larvin M, and Radstone, D (2001). A rapid and systematic review of the clinical effectiveness and cost-effectiveness of gemcitabine for the treatment of pancreatic cancer. *Health Technol Assess* **5**, 1-70.
- [3] Kulke MH (2002). Metastatic pancreatic cancer. *Curr Treat Options Oncol* **3**, 449-457.
- [4] Permert J, Hafstrom L, Nygren P, and Glimelius B (2001). A systematic overview of chemotherapy effects in pancreatic cancer. *Acta Oncol* **40**, 361-370.
- [5] Matsuno S, Egawa S, and Arai K (2001). Trends in treatment for pancreatic cancer. *J Hepatobiliary Pancreat Surg* **8**, 544-548.
- [6] van Moorsel CJ, Peters G J, and Pinedo HM (1997). Gemcitabine: Future Prospects of Single-Agent and Combination Studies. *Oncologist* **2**, 127-134.
- [7] Carmichael J (1997). Clinical response benefit in patients with advanced pancreatic cancer. Role of gemcitabine. *Digestion* **58**, 503-507.
- [8] Michael M, and Moore M (1997). Clinical experience with gemcitabine in pancreatic carcinoma. *Oncology (Huntingt)* **11**, 1615-1622.
- [9] Tomaszewska R, Okon K, Nowak K, and Stachura J (1998). HER-2/Neu expression as a progression marker in pancreatic intraepithelial neoplasia. *Pol J Pathol* **49**, 83-92.

- [10] Sakorafas GH, Lazaris A, Tsiotou AG, Koullias G, Glinatsis MT, and Golematis BC (1995). Oncogenes in cancer of the pancreas. *Eur J Surg Oncol* **21**, 251-253.
- [11] Williams TM, Weiner DB, Greene MI, and Maguire HC Jr (1991). Expression of c-erbB-2 in human pancreatic adenocarcinomas. *Pathobiology* **59**, 46-52.
- [12] Lemoine NR, Hughes CM, Barton CM, Poulson R, Jeffrey RE, Kloppel G, Hall PA, and Gullick WJ (1992). The epidermal growth factor receptor in human pancreatic cancer. *J Pathol* **166**, 7-12.
- [13] Ozawa S, Ueda M, Ando N, Abe O, and Shimizu N (1988). Epidermal growth factor receptors in cancer tissues of esophagus, lung, pancreas, colorectum, breast and stomach. *Jpn J Cancer Res* **79**, 1201-1207.
- [14] Yokoyama M, Yamanaka Y, Friess H, Buchler M, and Korc M (1994). p53 expression in human pancreatic cancer correlates with enhanced biological aggressiveness. *Anticancer Res* **14**, 2477-2483.
- [15] Hahn SA, and Kern SE (1995). Molecular genetics of exocrine pancreatic neoplasms. *Surg Clin North Am* **75**, 857-869.
- [16] Dergham ST, Dugan MC, Joshi US, Chen YC, Du W, Smith DW, Arlauskas P, Crissman JD, Vaitkevicius VK, and Sarkar FH (1997). The clinical significance of p21 (WAF1/CIP-1) and p53 expression in pancreatic adenocarcinoma. *Cancer* **80**, 372-381.
- [17] Gjertsen MK, and Gaudernack G (1998). Mutated Ras peptides as vaccines in immunotherapy of cancer. *Vox Sang* **74**, 489-495.

- [18] Gunzburg WH, and Salmons B (2001). Novel clinical strategies for the treatment of pancreatic carcinoma. *Trends Mol Med* **7**, 30-37.
- [19] Jaffee EM, Hruban RH, Biedrzycki B, Laheru D, Schepers K, Sauter PR, Goemann M, Coleman J, Grochow L, Donehower RC, Lillemoe KD, O'Reilly S, Abrams RA, Pardoll DM, Cameron JL, Yeo CJ (2001). Novel allogeneic granulocyte-macrophage colony-stimulating factor-secreting tumor vaccine for pancreatic cancer: a phase I trial of safety and immune activation. *J Clin Oncol* **19**, 145-156.
- [20] Kaufman HL, Di VJ Jr, and Horig H (2002). Immunotherapy for pancreatic cancer: current concepts. *Hematol Oncol Clin North Am* **16**, 159-197.
- [21] Buchler P, Reber HA, Buchler MC, Roth MA, Buchler MW, Friess H, Isacoff WH, and Hines OJ (2001). Therapy for pancreatic cancer with a recombinant humanized anti-HER2 antibody (herceptin). *J Gastrointest Surg* **5**, 139-146.
- [22] Xiong HQ, and Abbruzzese JL (2002). Epidermal growth factor receptor-targeted therapy for pancreatic cancer. *Semin Oncol* **29**, 31-37.
- [23] Buchsbaum DJ, Bonner JA, Grizzle WE, Stackhouse MA, Carpenter M, Hicklin DJ, Bohlen P, and Raisch KP (2002). Treatment of pancreatic cancer xenografts with Erbitux (IMC-C225) anti-EGFR antibody, gemcitabine, and radiation. *Int J Radiat Oncol Biol Phys* **54**, 1180-1193.
- [24] Rosenblum MG, Cheung L, Mujoo K, and Murray JL (1995). An antimelanoma immunotoxin containing recombinant human tumor necrosis factor: tissue disposition,

- pharmacokinetic, and therapeutic studies in xenograft models. *Cancer Immunol Immunother* **40**, 322-328.
- [25] Rosenblum MG, Cheung L, Murray JL, and Bartholomew R (1991). Antibody-mediated delivery of tumor necrosis factor (TNF-alpha): improvement of cytotoxicity and reduction of cellular resistance. *Cancer Commun* **3**, 21-27.
- [26] Rosenblum MG, Horn SA, and Cheung LH (2000). A novel recombinant fusion toxin targeting HER-2/NEU-over-expressing cells and containing human tumor necrosis factor. *Int J Cancer* **88**, 267-273.
- [27] Lyu MA, and Rosenblum MG (2005). The immunocytokine scFv23/TNF sensitizes HER-2/neu-overexpressing SKBR-3 cells to tumor necrosis factor (TNF) via up-regulation of TNF receptor-1. *Mol Cancer Ther* **4**, 1205-1213.
- [28] Chou TC, and Talalay P (1984). Quantitative analysis of dose-effect relationships: the combined effects of multiple drugs or enzyme inhibitors. *Adv Enzyme Regul* **22**, 27-55.
- [29] Wuchter C, Karawajew L, Ruppert V, Buchner T, Schoch C, Haferlach T, Ratei R, Dorken B, and Ludwig WD (1999). Clinical significance of CD95, Bcl-2 and Bax expression and CD95 function in adult de novo acute myeloid leukemia in context of P-glycoprotein function, maturation stage, and cytogenetics. *Leukemia* **13**, 1943-1953.
- [30] Lohrisch C, and Piccart M (2001). An overview of HER2. *Semin Oncol* **28**, 3-11.
- [31] Yarden Y (2001). Biology of HER2 and its importance in breast cancer. *Oncology* **61**, 1-13.
- [32] Rubin I, and Yarden Y (2001). The basic biology of HER2. *Ann Oncol* **12**, S3-S8.

- [33] Hynes NE, and Stern DF (1994). The biology of erbB-2/neu/HER-2 and its role in cancer. *Biochim Biophys Acta* **1198**, 165-184.
- [34] Singleton TP, and Strickler JG (1992). Clinical and pathologic significance of the c-erbB-2 (HER-2/neu) oncogene. *Pathol Annu* **27**, 165-190.
- [35] Stancovski I, Sela M, and Yarden Y (1994). Molecular and clinical aspects of the Neu/ErbB-2 receptor tyrosine kinase. *Cancer Treat Res* **71**, 161-191.
- [36] Torre EA, Salimbeni V, and Fulco RA (1997). The erbB 2 oncogene and chemotherapy: a mini-review. *J Chemother* **9**, 51-55.
- [37] Safran H, Steinhoff M, Mangray S, Rathore R, King TC, Chai L, Berzein K, Moore T, Iannitti D, Reiss P, Pasquariello T, Akerman P, Quirk D, Mass R, Goldstein L, and Tantravahi U (2001). Overexpression of the HER-2/neu oncogene in pancreatic adenocarcinoma. *Am J Clin Oncol* **24**, 496-499.
- [38] Thybusch-Bernhardt A, Aigner A, Beckmann S, Czubayko F, and Juhl H (2001). Ribozyme targeting of HER-2 inhibits pancreatic cancer cell growth in vivo. *Eur J Cancer* **37**, 1688-1694.
- [39] Aigner A, Hsieh SS, Malerczyk C, and Czubayko F (2000). Reversal of HER-2 overexpression renders human ovarian cancer cells highly resistant to taxol. *Toxicology* **144**, 221-228.

- [40] Suzuki T, Anderegg B, Ohkawa T, Irie A, Engebraaten O, Halks-Miller M, Holm PS, Curiel DT, Kashani-Sabet M, and scanlon KJ (2000). Adenovirus-mediated ribozyme targeting of HER-2/neu inhibits in vivo growth of breast cancer cells. *Gene Ther* **7**, 241-248.
- [41] Waldmann TA, Levy R, and Collier BS (2000). Emerging Therapies: Spectrum of Applications of Monoclonal Antibody Therapy. *Hematology (Am Soc Hematol Educ Program)*, 394-408.
- [42] Butera J, Malachovsky M, Rathore R, and Safran H (1998). Novel approaches in development for the treatment of pancreatic cancer. *Front Biosci* **3**, E226-E229.
- [43] Pegram MD, Lopez A, Konecny G, and Slamon DJ (2000). Trastuzumab and chemotherapeutics: drug interactions and synergies. *Semin Oncol* **27**, 21-25.
- [44] Knuefermann C, Lu Y, Liu B, Jin W, Liang K, Wu L, Schmidt M, Mills GB, Mendelsohn J, and Fan Z (2003). HER2/PI-3K/Akt activation leads to a multidrug resistance in human breast adenocarcinoma cells. *Oncogene* **22**, 3205-3212.
- [45] Sasaki M, Kumazaki T, Tanimoto K, and Nishiyama M (2003). Bcl-2 in cancer and normal tissue cells as a predication marker of response to 5-fluorouracil. *Int J Oncol* **22**, 181-186.
- [46] Nagata S (1997). Apoptosis by death factor. *Cell* **88**, 355-365.
- [47] Medema JP, Scaffidi C, Kischkel FC, Shevchenko A, Mann M, Krammer PH, and Peter ME (1997). FLICE is activated by association with the CD95 death-inducing signaling complex (DISC). *EMBO J* **16**, 2794-2804.
- [48] Ueno NT, Bartholomeusz C, Herrmann JL, Estrov Z, Shao R, Andreeff M, Price J, Paul RW, Anklesaris P, Yu D, and Hung MC (2000). E1A-mediated paclitaxel sensitization in HER-

FIGURE LEGENDS

Figure 1. *Expression Pattern of HER-2/neu, TNF-R1, and TNF-R2 in Four Human Pancreatic Cell Lines. Four pancreatic cancer cell lines (AsPc-1, Capan-1, Capan-2, and L3.6pl) were seeded at 5×10^5 cells/ ϕ 60 mm petri-dish and incubated for 24 hr after which cell lysates were collected. Whole cell lysates (50 μ g) were analyzed by SDS-PAGE and immunoblotting with anti-HER-2/neu, TNF receptor-1, and TNF receptor-2 antibodies, followed by incubation with an anti-mouse or anti-rabbit horseradish peroxidase-labeled antibody and chemiluminescent detection. Actin was used as a loading control for protein loading. Data are presented as the relative density of protein bands normalized to β -actin. The intensity of the bands was quantified using Histogram.*

Figure 2. *Dose-Response Curves of various agents. AsPc-1, Capan-1, Capan-2, and L3.6pl. Cells were treated with different drugs for 72 hr and then assessed growth inhibition by crystal violet staining. Values are means \pm SD from at least three independent exposures.*

Figure 3. *Effects of combination treatment on the expression of phospho-Akt. L3.6pl cells were treated with IC_{25} of 5-FU, scFv23/TNF, or scFv23/TNF plus 5-FU combination for 48 hr. For combination studies, scFv23/TNF and 5-FU were combined at their individual IC_{25} concentrations. After treatment, whole cell lysates (50 μ g) were analyzed by SDS-PAGE and immunoblotting with anti-Akt and phospho-Akt antibodies, followed by incubation with an anti-rabbit horseradish peroxidase-labeled antibody and chemiluminescent detection. Actin was used as a loading control. Data are presented as the relative density of protein bands normalized to β -actin. The intensity of the bands was quantified using Histogram.*

Figure 4. *Effects of combination treatment on the expression of Bcl-2. L3.6pl cells were treated with IC₂₅ of 5-FU, scFv23/TNF, or 5-FU plus scFv23/TNF combination for 48 hr. For combination studies, scFv23/TNF and 5-FU were combined at their individual IC₂₅ concentrations. After treatment, whole cell lysates (50 µg) were analyzed by SDS-PAGE and immunoblotting with anti-Bcl-2 antibody, followed by incubation with an anti-rabbit horseradish peroxidase-labeled antibody and chemiluminescent detection. Actin was used as a loading control. Data are presented as the relative density of protein bands normalized to β-actin. The intensity of the bands was quantified using Histogram.*

Figure 5. *Effects of combination treatment on the apoptosis in L3.6pl cells. L3.6pl exposed to IC₂₅ of 5-FU, scFv23/TNF, or combination for 48 hr. After treatment, the cells were washed with PBS, permeabilized in permeabilization solution (0.1% Triton X-100, 0.1% sodium citrate), and then fixed in 4% paraformaldehyde. Fixed cells were stained with in situ cell death detection kit (Roche). Cells undergoing apoptosis were determined by fluorescence microscope (x 400).*

Figure 6. *Effects of combination treatment on the activation of caspase-8, caspase-3, and PARP cleavage. L3.6pl cells were treated with IC₂₅ of 5-FU, scFv23/TNF, or combination for 48 hr. For combination studies, scFv23/TNF and 5-FU were combined at their individual IC₂₅ concentrations. After treatment, whole cell lysates (50 µg) were analyzed by SDS-PAGE and immunoblotting with anti-caspase-8, caspase-3, and PARP antibodies, followed by incubation with an anti-mouse horseradish peroxidase-labeled antibody and chemiluminescent detection. Actin was used as a loading control.*

Figure 7. *Effects of combination treatment on PARP cleavage. L3.6pl cells were treated with IC_{25} of various chemotherapeutic agent, scFv23/TNF, or combination for 48 hr. For combination studies, scFv23/TNF and chemotherapeutic agent were combined at their individual IC_{25} concentrations. After treatment, cell lysates (50 μ g) were analyzed by SDS-PAGE and immunoblotting with anti-PARP antibody, followed by incubation with an anti-mouse horseradish peroxidase-labeled antibody and chemiluminescent detection. Actin was used as a loading control.*

Figure 8. *Influence of caspase inhibitors on the viability of 5-FU+ scFv23/TNF-treated L3.6pl cells. L3.6pl cells pre-treated with or without 200 μ M general caspase inhibitor (Z-VAD-FMK), caspase-8 inhibitor (Z-IETD-FMK), or caspase-3 inhibitor (Z-DEVD-FMK) (R&D) for 2 hr and then treated with their individual IC_{25} concentrations. After 72 hr of exposure, viability was determined using an XTT assay.*

2/neu-overexpressing ovarian cancer SKOV3.ip1 through apoptosis involving the caspase-3 pathway. *Clin Cancer Res* **6**, 250-259.

- [49] Keppler-Hafkemeyer A, Brinkmann U, and Pastan I (1998). Role of caspases in immunotoxin-induced apoptosis of cancer cells. *Biochemistry* **37**, 16934-16942.

Figure 1 Mi-Ae Lyu

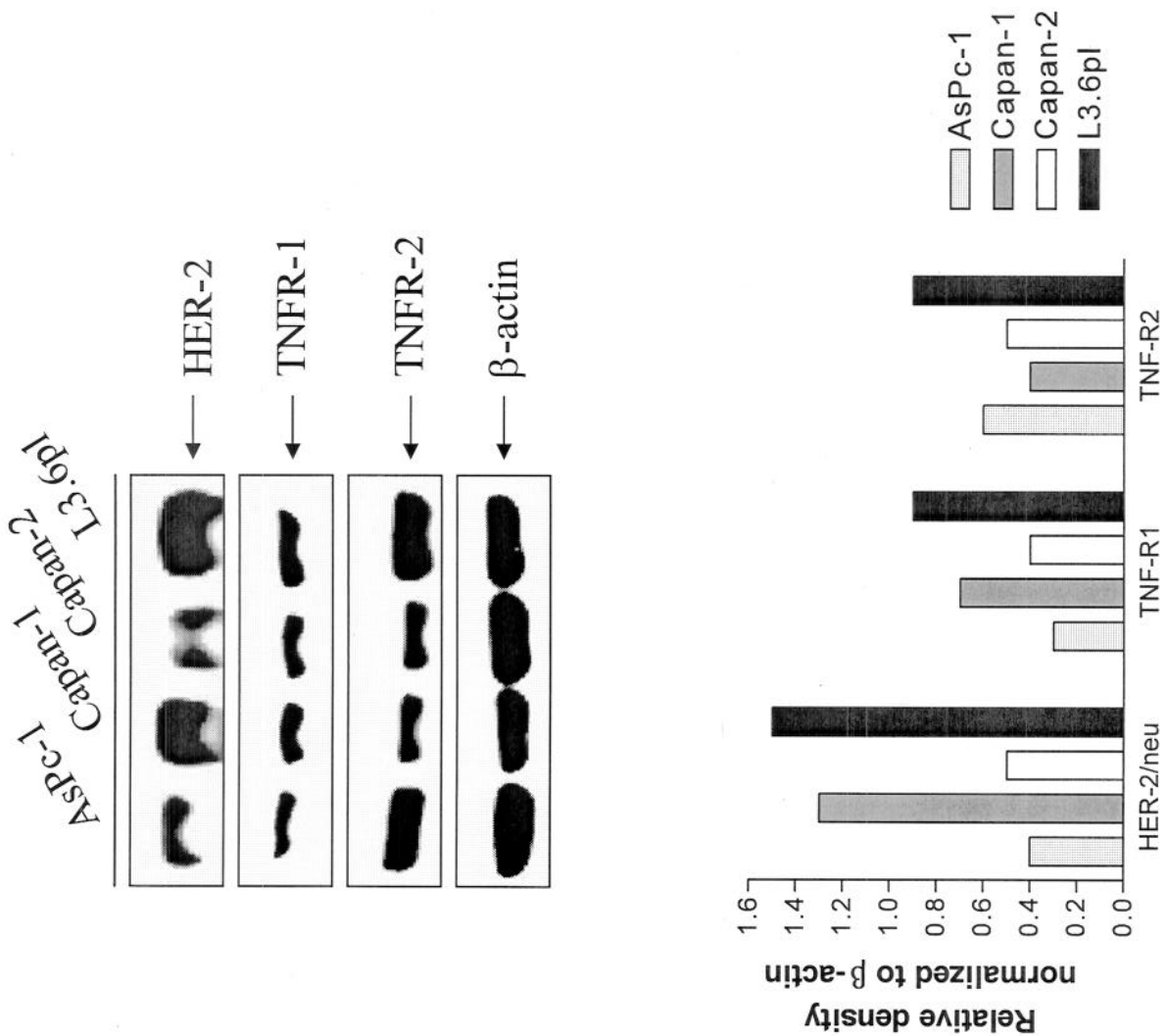


Figure 2 Mi-Ae Lyu

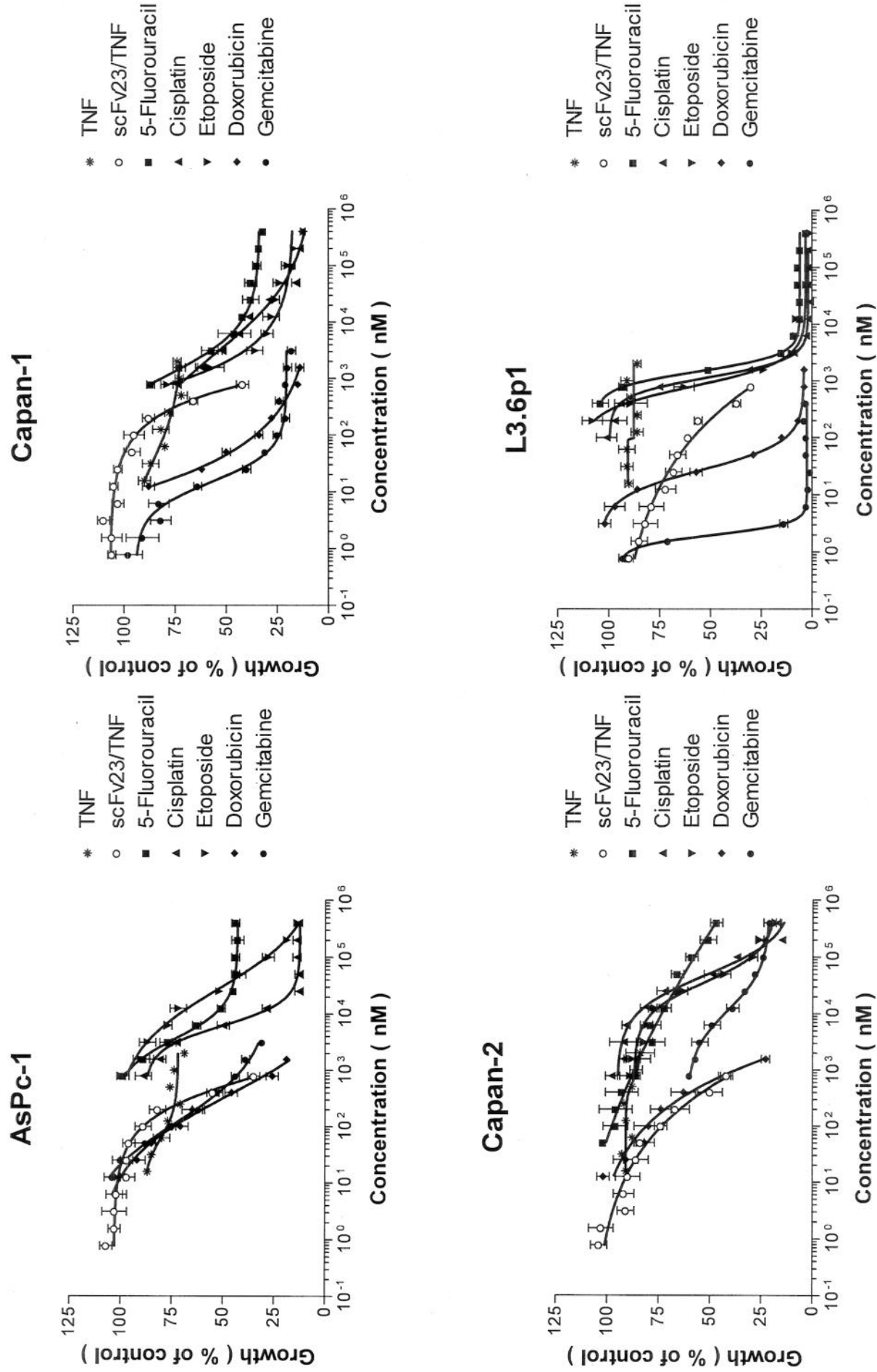


Figure 3 Mi-Ae Lyu

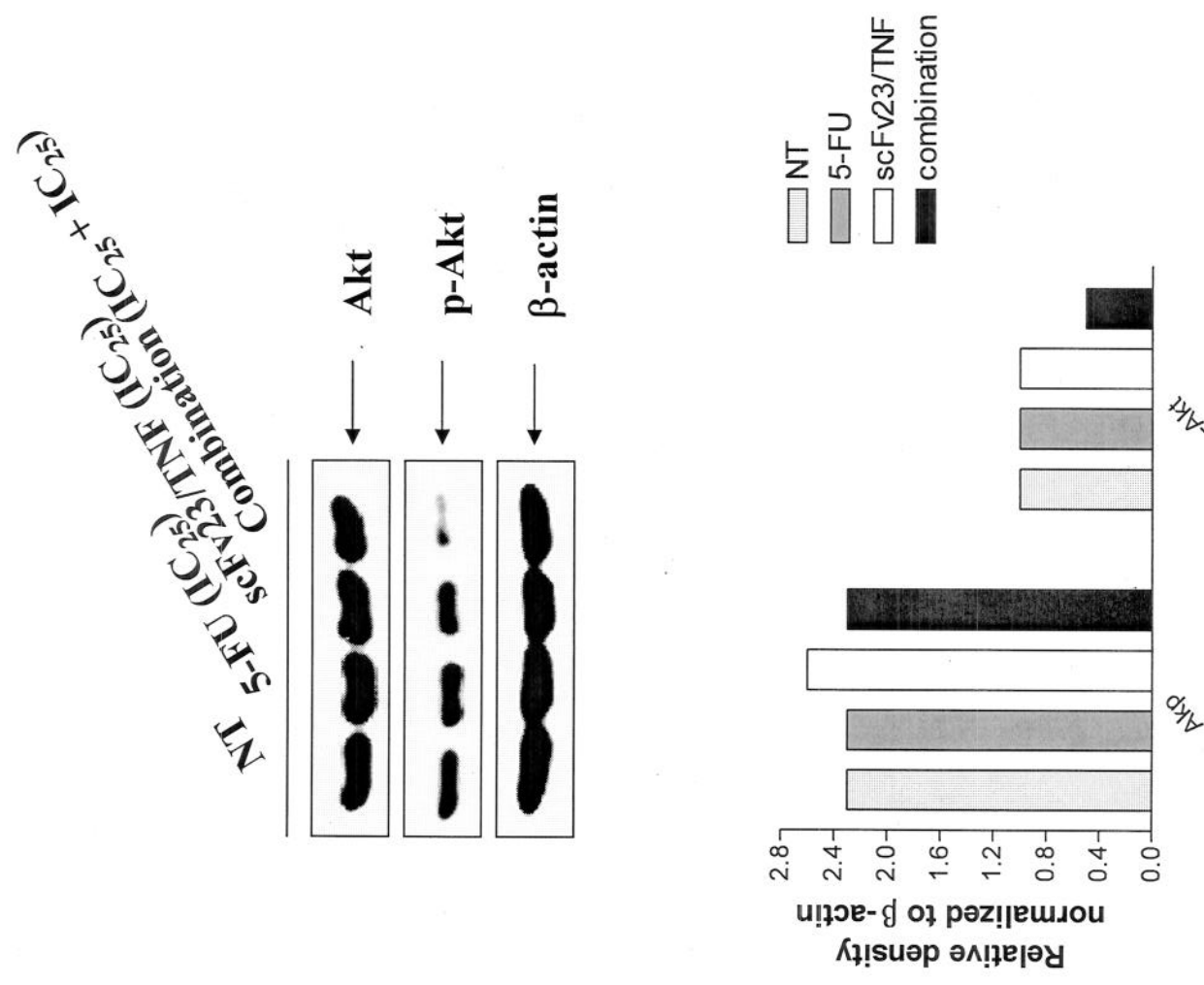


Figure 4 Mi-Ae Lyu

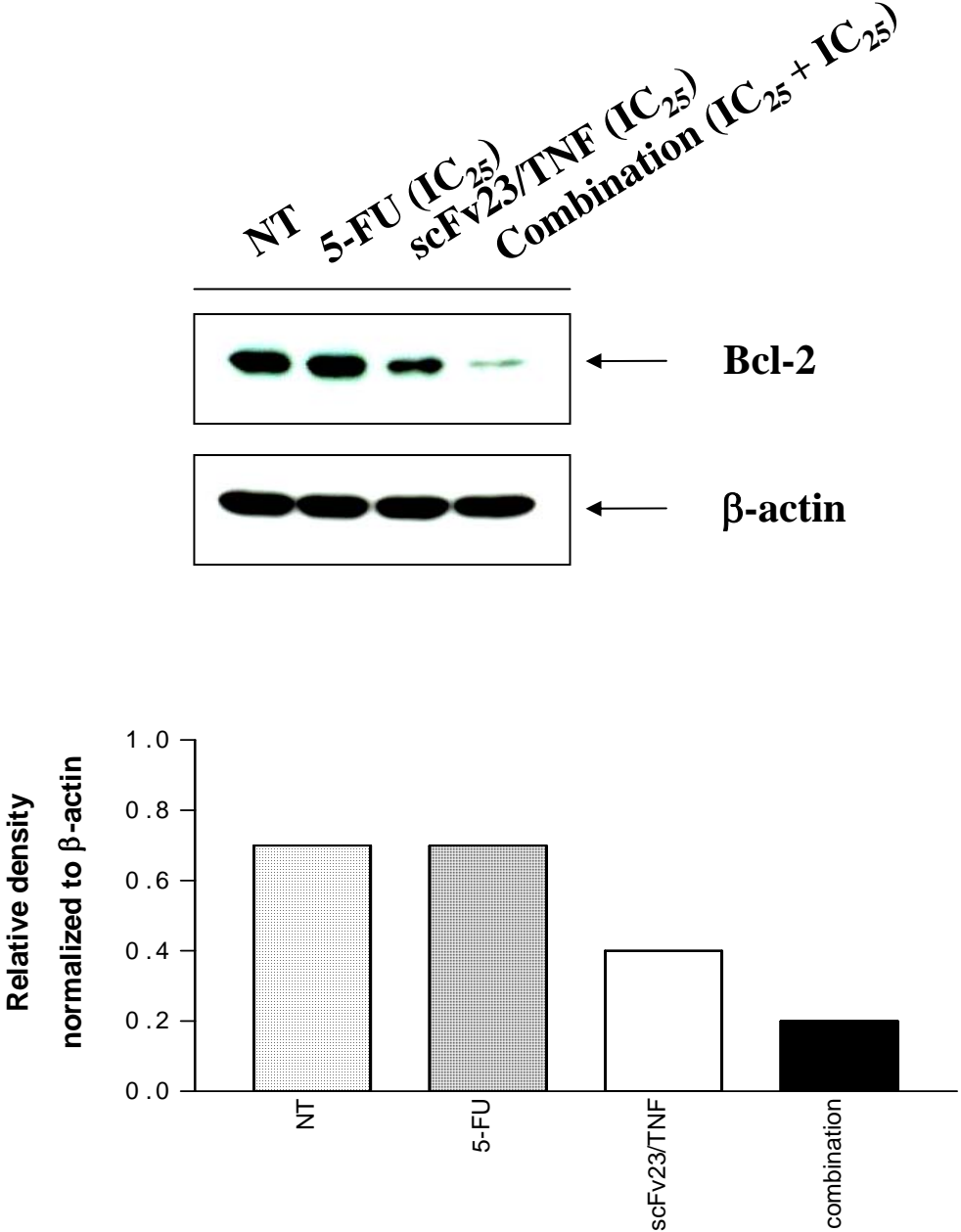
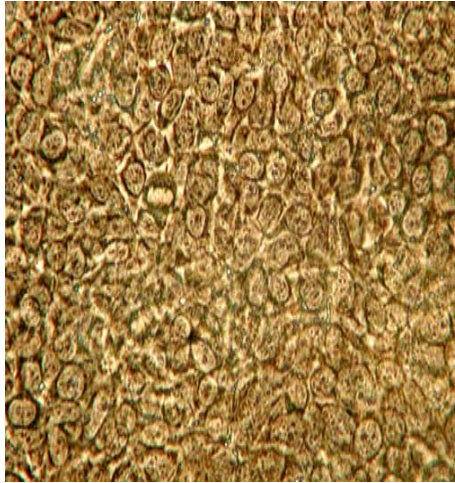
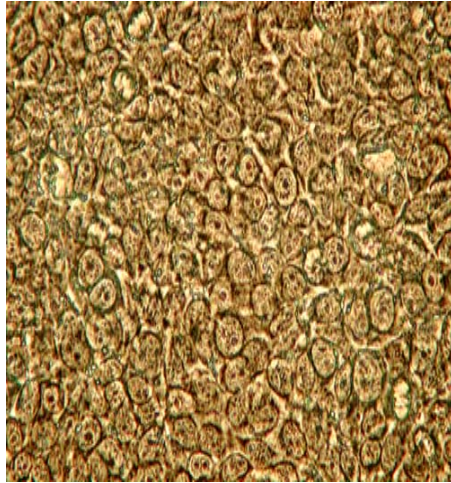


Figure 5 Mi-Ae Lyu

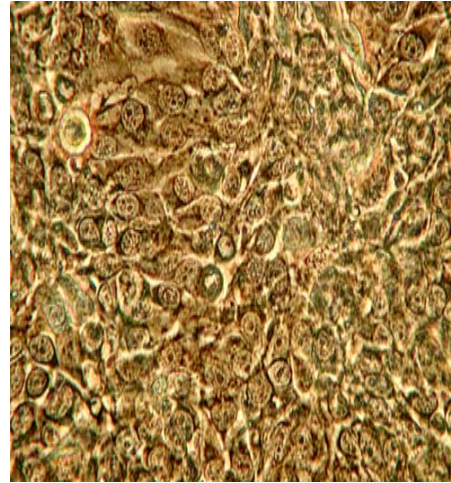
NT



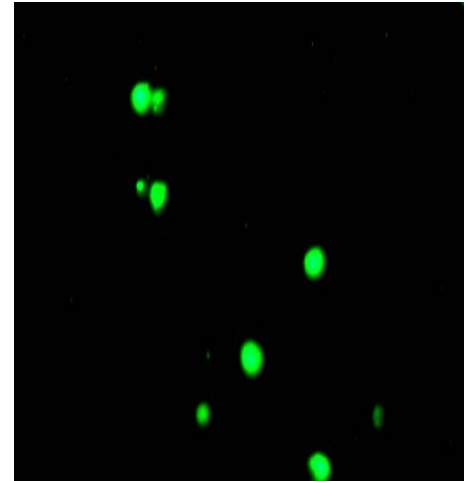
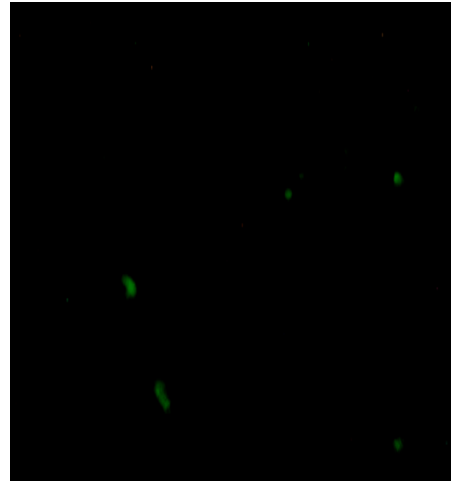
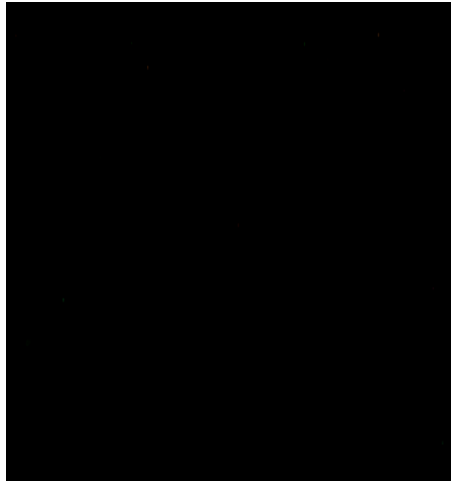
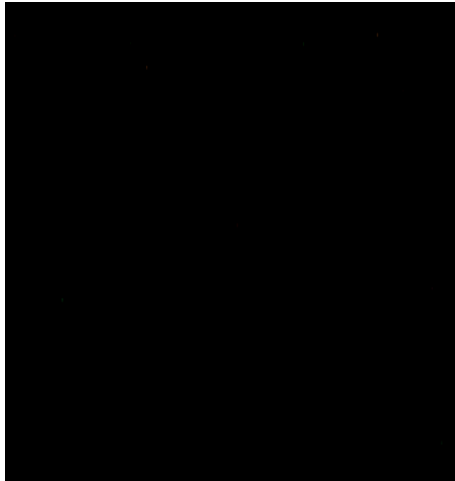
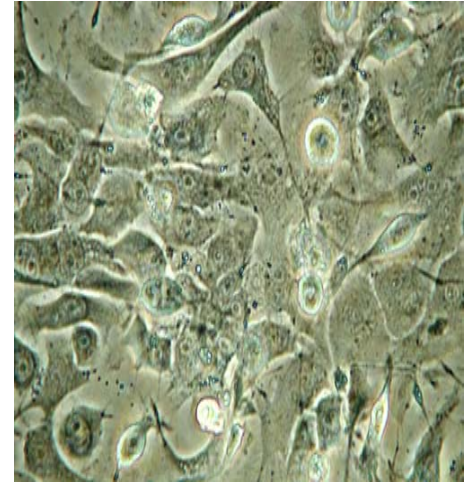
5-FU (IC₂₅)



scFv23/TNF (IC₂₅)



Combination (IC₂₅+IC₂₅)



(x 400)

Figure 6 Mi-Ae Lyu

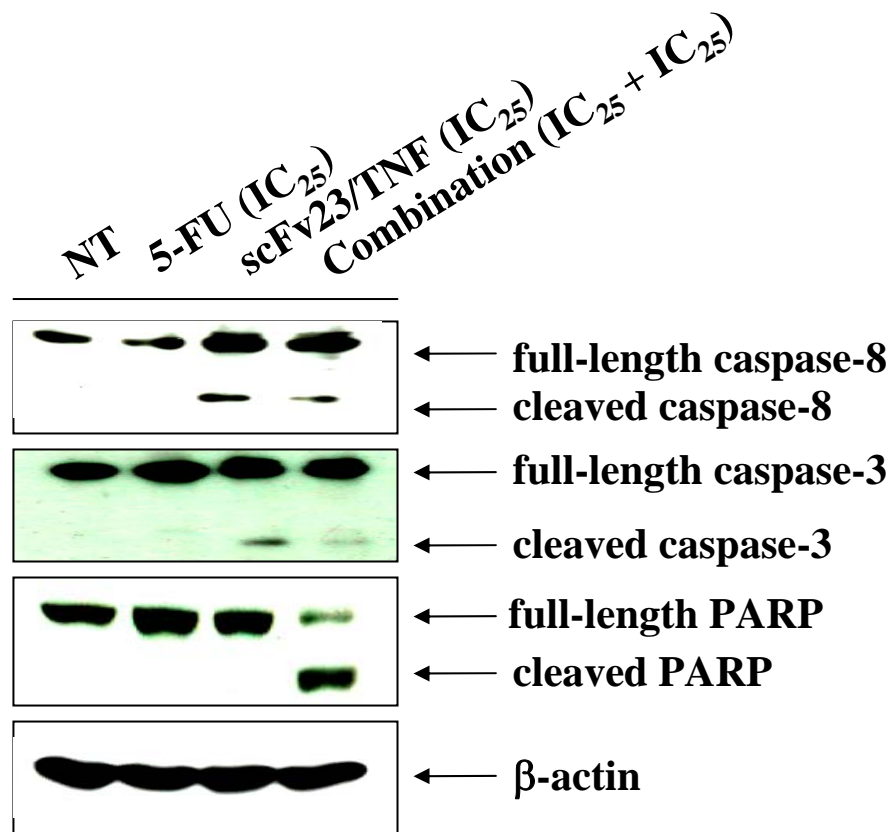


Figure 7 Mi-Ae Lyu

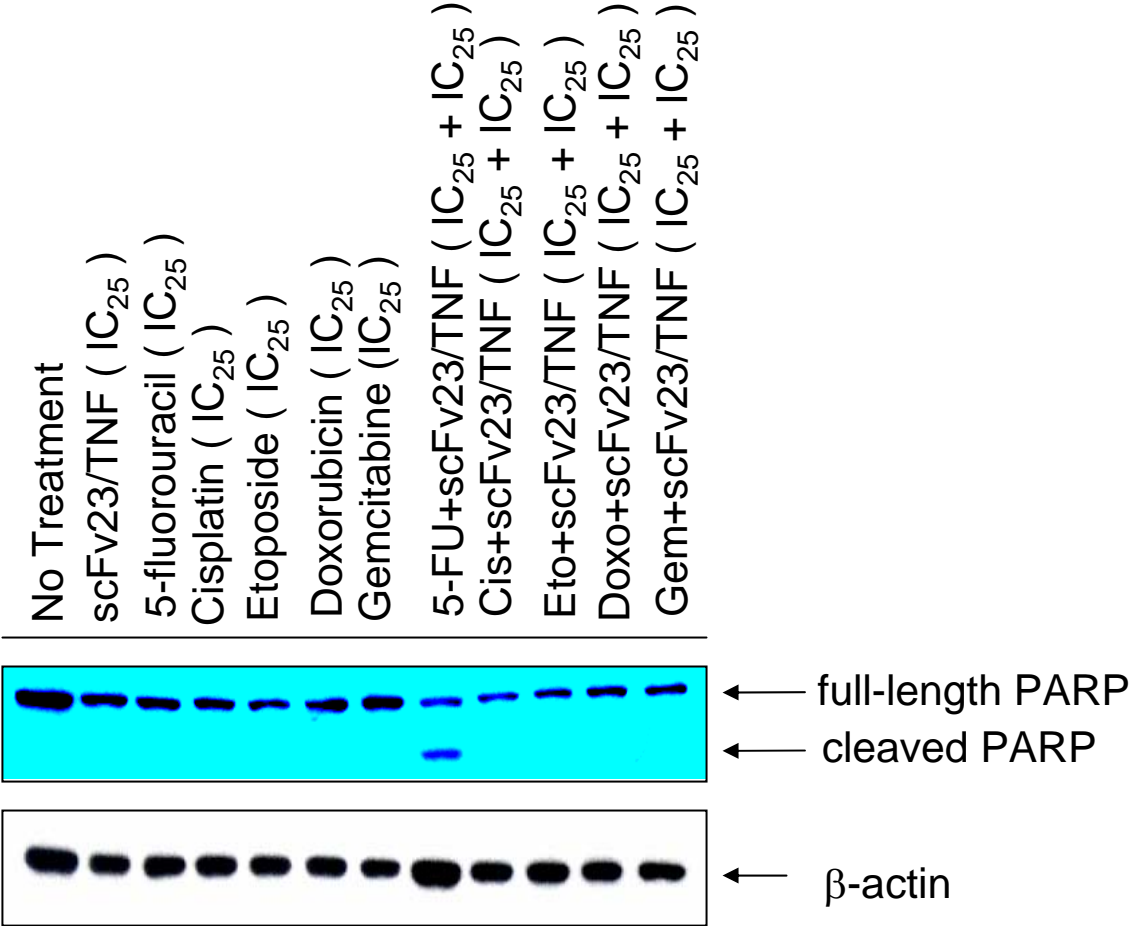
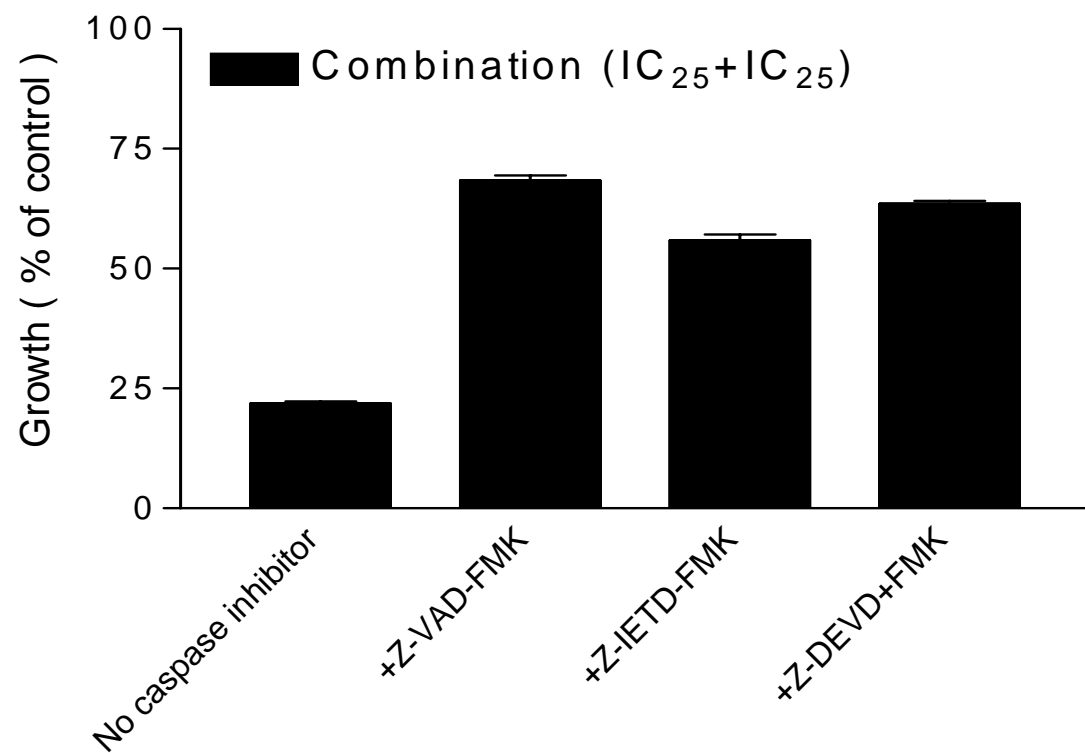


Figure 8 Mi-Ae Lyu



VEGF₁₂₁/rGel Fusion Toxin Targets the KDR Receptor to Inhibit Vascular Endothelial Growth *In Vitro* and *In Vivo*: Specific Effects Assessed Using Microarray Analysis*

**Khalid A. Mohamedali[‡], Candelaria Gomez-Manzano[§], Latha Ramdas[¶], Jing Xu[§],
Lawrence Cheung[‡], Wei Zhang[#], Philip Thorpe^{||} and Michael G. Rosenblum^{‡**}**

Running Title: Inhibition of Angiogenesis by VEGF₁₂₁/rGel

** To whom correspondence should be addressed: Department of Bioimmunotherapy, Unit 44, The University of Texas M. D. Anderson Cancer Center, 1515 Holcombe Blvd., Houston, Texas 77030. Tel: 713-792-3554; Fax: 713-794-4261 or 713-745-3916; E-mail: mrosenbl@mdanderson.org.

From the Departments of [‡]Bioimmunotherapy, [§]Neuro-Oncology, [¶]Experimental Radiation Oncology, and [#]Pathology, The University of Texas M. D. Anderson Cancer Center, Houston, Texas 77030, and ^{||}Department of Pharmacology, Simmons Comprehensive Cancer Center, The University of Texas Southwestern Medical Center, Dallas, Texas 75390

Key Words: Fusion toxin, VEGF, gelonin, vascular targeting, angiogenesis, microarray

* This research was conducted, in part, by the Clayton Foundation for Research and supported by DAMD grant 17-02-1-0457. Work done at the Cancer Genomics Core Lab was supported by the Tobacco Settlement Funds appropriated by the Texas State Legislature, by a generous donation from the Michael and Betty Kadoorie Foundation, by a grant from the Goodwin Fund, and by Cancer Center Core Grant P30 CA016672 28 from the National Cancer Institute.

SUMMARY

VEGF₁₂₁/rGel, a fusion protein composed of the growth factor VEGF₁₂₁ and the recombinant toxin gelonin targets the tumor neovasculature and exerts impressive cytotoxic effects on cells by inhibiting cellular protein synthesis. We assessed the effects of VEGF₁₂₁/rGel on angiogenesis in vitro and in vivo. 1 nM VEGF₁₂₁/rGel was sufficient to inhibit tube formation by over 50% of endothelial cells overexpressing VEGFR-2 on Matrigel-coated plates. In contrast, endothelial cells overexpressing VEGFR-1 were relatively insensitive to VEGF₁₂₁/rGel, requiring 100 nM to inhibit tube formation by over 50%. In vascularization studies using chicken chorioallantoic membranes, 1 nM VEGF₁₂₁/rGel completely inhibited bFGF-stimulated neovascular growth. Treatment with VEGF₁₂₁/rGel decreased the number of newly-sprouting vessels but did not affect mature vessels. Treatment with gelonin alone at equivalent concentrations had no effect. Examination by microarray analysis of VEGF₁₂₁/rGel-induced cytotoxicity against HUVECs revealed that 22 genes were upregulated by VEGF₁₂₁/rGel treatment, including genes involved in the control of cell adhesion, apoptosis, transcription regulation, chemotaxis, and inflammatory response. RT-PCR of selected genes, including E-selectin, cytokine A2, NF-κB inhibitor alpha and tumor necrosis factor alpha-induced protein 3, confirmed their upregulation. Our data suggest that VEGF₁₂₁/rGel induces the expression of a unique “fingerprint” profile of genes that mediate the cytotoxic effects of this construct on tumor vascular endothelial cells. The cytotoxic effects of VEGF₁₂₁/rGel appear to be necrotic rather than apoptotic since no TUNEL staining or alterations in the protein levels of the apoptotic markers Bax, Bcl-XL, or caspase-3 were observed. Together, these data represent the first analysis of genes governing intoxication of mammalian cells by a toxin-based targeted therapeutic agent. These data also confirm the selectivity of the fusion construct for KDR-

overexpressing endothelial cells and support the use of this molecule in understanding the role of VEGFR-2 expression in the development of toxic effects of VEGF-containing fusion toxin constructs.

INTRODUCTION

Angiogenesis has emerged as a critical process in numerous diseases and intervention in neovascularization may have therapeutic value in diabetic retinopathy (1-4), arthritis (5-8) and in tumor maturation and metastatic spread (9-12). Indeed, because tumor neovascularization provides an available target for therapeutic intervention, numerous groups have focused drug development strategies on the elements of this process. Inhibitors of various growth factor receptor tyrosine kinases (13-15), blocking antibodies that interfere with receptor signal transduction (16-19) and strategies that trap growth factor ligands (20-22) have all been used with varying degrees of success in preclinical and clinical studies.

Although tumor neovascularization is increasingly being revealed as highly complex as factors that can play a role in driving critical events continue to be identified, vascular endothelial growth factor-A (VEGF-A)¹ and its receptors, Flt-1 and KDR, are exceptionally important in many aspects of neovascularization (15;23-25). Therefore, numerous laboratories have developed recombinant growth factor fusion constructs of VEGF-A and various toxins (26-30) to target cells bearing receptors of VEGF-A. We described a novel fusion toxin composed of the 121-amino-acid splice variant of VEGF-A (designated VEGF₁₂₁) and containing the highly potent recombinant toxin gelonin (rGel) (31). Recent studies in our laboratory have demonstrated that this construct is highly cytotoxic at nanomolar concentrations to both log-phase and confluent endothelial cells that overexpress the KDR receptor and not specifically cytotoxic to cells that overexpress the Flt-1 receptor (31). In addition, tumor xenograft studies demonstrate impressive tumor growth-inhibitory effects of the fusion construct when administered systemically against established melanoma and prostate tumors. In ongoing studies in our

laboratory, we are examining the effects of VEGF₁₂₁/rGel on numerous other orthotopic and metastatic models.

Although toxin-based therapeutic agents have been studied for many years, the exact molecular mechanisms within the target cell that occur as part of the cytotoxic effect have never been clearly identified. Therefore, we sought to quantify the ability of VEGF₁₂₁/rGel to inhibit tube formation in vitro and basic fibroblast growth factor (bFGF)-mediated angiogenesis in vivo and intracellular effects of this agent on cells in culture using microarray technology to delineate molecular mechanisms that uniquely define the effects of this agent at the genetic level.

EXPERIMENTAL PROCEDURES

Materials-- Bacterial strains, pET bacterial expression plasmids and recombinant enterokinase were obtained from Novagen (Madison, WI). All other chemicals were obtained from Sigma Chemical Company (St. Louis, MO) or Fisher Scientific (Pittsburgh, PA). bFGF was purchased from R&D Systems (Minneapolis, MN). TALON metal affinity resin was obtained from Clontech Laboratories (Palo Alto, CA). Other chromatography resin and materials were from Pharmacia Biotech (Piscataway, NJ). Tissue culture reagents were from Invitrogen (Carlsbad, CA) or Mediatech Cellgro (Herndon, VA). Rabbit anti-gelonin antiserum was obtained from the Veterinary Medicine Core Facility at The University of Texas M. D. Anderson Cancer Center. Antibodies against the following proteins were purchased from Santa Cruz Biotechnology, Inc. (Santa Cruz, CA) (catalog numbers are given in parentheses): KDR (sc-504), phosphorylated KDR (p-KDR) (sc-16628-R), Bcl-2 (sc-7382), Bcl-XL (sc-7195), Bax (sc-493), cytochrome C (sc-8385), caspase-3 (sc-7148), caspase-6 (sc-1230), E-selectin (14011), actin (sc-1616), MKP-1 (sc-1199), and ERK2 (sc-1647).

Cell Culture-- Porcine aortic endothelial (PAE) cells transfected with the KDR receptor (PAE/KDR) or the Flt-1 receptor (PAE/Flt-1) were a generous gift from Dr. Johannes Waltenberger. The KDR and Flt-1 receptor sites in these cell lines were previously determined (27;32). Both cell lines have been used as in vitro models of the tumor neovasculature (33-35). Cells were maintained as a monolayer in F12 nutrient medium (HAM) supplemented with 100 units/ml penicillin, 100 units/ml streptomycin, and 10% fetal bovine serum (FBS). Human umbilical vein endothelial cells (HUVECs) were maintained in EBM medium (Cambrex, East Rutherford, NJ). Cells were harvested by treatment with Versene (0.02% EDTA/PBS).

Purification of VEGF₁₂₁/rGel-- Construction and purification of VEGF₁₂₁/rGel was essentially as described (31). VEGF₁₂₁/rGel was concentrated and stored in sterile PBS at –20°C.

Cytotoxicity of VEGF₁₂₁/rGel and rGel-- The quantification of the cytotoxicity of VEGF₁₂₁/rGel and rGel against log-phase PAE/KDR, PAE/Flt-1, and HUVECs was performed as follows. Log-phase cells (1 x 10⁴ HUVECs, 1 x 10³ PAE/KDR or PAE/Flt-1 cells) were plated in 96-well flat-bottom tissue culture plates and allowed to attach overnight. Purified VEGF₁₂₁/rGel and rGel were diluted in culture media and added to the wells in 5-fold serial dilutions. Cells were incubated for 72 h. The remaining adherent cells were stained with crystal violet (0.5% in 20% methanol) and solubilized with Sorenson's buffer (0.1 M sodium citrate, pH 4.2, in 50% ethanol). Absorbance was measured at 630 nm.

Effect of VEGF₁₂₁/rGel on Phosphorylation of KDR-- Whole cell extracts of HUVECs and PAE/KDR cells, either untreated or treated with VEGF₁₂₁/rGel for up to 48 h at their respective IC₅₀ doses, were prepared. Cells were lysed in 50 mM Tris (pH 8.0), 0.1 mM EDTA, 1 mM DTT, 12.5 mM MgCl₂, 0.1 M KCl, 20% glycerol, 1% Triton-X100, 2 µg/ml leupeptin, 1.5 µg/ml aprotinin, and 1 mM PMSF. Twenty micrograms of cell lysate was run on a sodium dodecyl sulfate polyacrylamide gel electrophoresis (SDS-PAGE) gel and the protein transferred to a PVDF/Imobilon membrane (Millipore, Billerica, MA). The membrane was blocked with 5% bovine serum albumin SA followed by incubation for 1 h with the following primary antibodies: anti-KDR, anti-p-KDR, and actin. Appropriate secondary antibodies were used at a 1:2000 dilution for 1 h and detected using an ECL detection kit (Amersham Biosciences, Buckinghamshire, England).

Effect of VEGF₁₂₁/rGel on E-Selectin Protein Levels-- Whole cell extracts of HUVECs and PAE/KDR cells treated for up to 48 h with VEGF₁₂₁/rGel at their respective IC₅₀ doses were analyzed for changes in levels of E-selectin. Whole cell extracts and western blots were prepared as detailed above.

Endothelial Cell Tube Formation Assay-- PAE/KDR and PAE/Flt-1 cells were grown to 80% confluence, detached using Versene, and plated at a concentration of 2×10^4 cells per well in a 96-well Matrigel-coated plate under reduced serum (2% FBS) conditions. Cells were treated with 100 nM, 10 nM, 1 nM, 0.1 nM, or 0.01 nM VEGF₁₂₁/rGel or rGel, in triplicate, for 24 h. Inhibition of tube formation was assessed by counting the number of tubes formed per well under bright field microscopy. The ability of VEGF₁₂₁/rGel to inhibit tube formation as a function of incubation time before plating on Matrigel was studied by incubating PAE/KDR cells at the IC₅₀ dose (1 nM) for different periods up to 24 h. Cells were detached and plated in 96-well Matrigel-coated plates under the conditions described above and the tubes in each well were counted.

Angiogenesis Assessment in Chicken Chorioallantoic Membranes (CAMs)-- Fertilized chicken eggs (SPAFAS; Charles River Laboratories, Wilmington, MA) were incubated at 37°C at 55% humidity for 9 days. An artificial air sac was created over a region containing small blood vessels in the CAM as described (36). A small “window” was cut in the shell after removal of 3 ml of albumen. Filter disks measuring 6 mm in diameter were coated with cortisone acetate in absolute ethanol (3 mg/ml). Each CAM was locally treated with filter disks saturated with a

solution containing bFGF (50 ng/disk) and VEGF₁₂₁/rGel (1 or 10 nM), rGel (1 or 10 nM), or buffer (PBS). The filter was placed on the CAM in a region with the lowest density of blood vessels and, as a reference, in the vicinity of a large vessel. Angiogenesis was documented photographically 3 days after treatment; images were captured using an Olympus stereomicroscope (SZ x12) and Spot Basic software (Diagnostic Instruments, Inc.). The relative vascular density was determined by measuring the area occupied by blood vessels (37). This analysis was performed on a Macintosh computer using the public domain NIH Image program (developed at the U.S. National Institutes of Health and available on the Internet at <http://rsb.info.nih.gov/nih-image/>). The numbers of blood vessel branch points were quantified by two researchers (C.G-M. and J.X) and compared with the numbers in the treatment controls (36).

RNA extraction-- HUVECs and PAE/KDR cells were treated with their respective IC₅₀ VEGF₁₂₁/rGel doses for various periods up to 48 h. Control cells were treated with PBS. Total RNA was extracted using the RNeasy mini-kit (Qiagen, Valencia, CA) and its integrity verified by electrophoresis on a denaturing formaldehyde-agarose gel and on a 2100 Bioanalyzer (Agilent, Foster City, CA).

Gene expression analysis-- HUVEC RNA was amplified using protocol previously described (38). The test and control samples (HUVECs treated with VEGF₁₂₁/rGel or saline, respectively, for 24 h) were labeled using Cy3- and Cy5-dCTP in the reverse transcription reaction. Duplicate experiments were conducted by dye swapping. The labeled samples were hybridized to a cDNA array of 2304 sequence-verified clones in duplicate printed by the Cancer Genomics Core

Laboratory of the Department of Pathology at M. D. Anderson Cancer Center. The array included 4800 genes involved in signal transduction, stress response, cell cycle control, hypoxia, and metastatic spread. Hybridization was performed overnight at 60°C in a humid incubator. After washing, the hybridized slides were scanned using a GeneTAC LS IV laser scanner (Genomic Solutions, Ann Arbor, MI) and the signal intensities were quantified with ArrayVision (Imaging Research Inc., St. Catharines, Ontario, Canada). The local background-subtracted spot intensities were used for further analysis, which was performed by the M. D. Anderson in-house program for microarray analysis (39). Differentially expressed genes were identified on the basis of a cutoff value of the T value. Generally, a cutoff value of $|3|$ is considered statistically significant.

The dye swapping experiments were designed to limit dye bias, which raises concern in microarray experiments. The two factors addressed by this design are the differences in dye incorporation and the gene-specific effects of the dye. Normalization of the data typically corrects for differences in incorporation of the dye that affects all the genes. Dye-specific effects can be insignificant compared with other sources of variation in the experiment (40). Hence, the dye swapping experiments were treated as duplicates. The signal-to-noise ratio of the images was evaluated to determine the quality of the array. Only those spots with a signal-to-noise ratio of ≥ 2 were evaluated (80%). Genes that showed values greater than $|2|$ in at least 3 of 4 arrays were identified, and the average fold change was determined.

RT-PCR Correlative Analysis-- Microarray data were verified by performing RT-PCR analysis on the genes that showed the highest level of induction, namely E-selectin (SELE), cytokine A2 (SCYA2, MCP-1), tumor necrosis factor alpha induced protein 3 (TNFAIP3) and NF- κ B

inhibitor alpha (NF- κ BI α). Primers were designed on the basis of the accession numbers from the microarray and confirmation of homology using BLAST (NCBI). Induction of E-selectin in PAE/KDR cells was also verified by RT-PCR. GAPDH primers were used as controls. The primers were as follows: SELE forward - 5'GGTTTGGTGAGGTGTGCTC; SELE reverse - 5' TGATCTTTCCCGGAACTGC; SCYA2 forward - 5' TCTGTGCCTGCTGCTCATAG; SCYA2 reverse - 5' TGGAATCCTGAACCCACTTC; TNFAIP3 forward - 5' ATGCACCGATAACACTGGA; TNFAIP3 reverse - 5' CGCCTTCCTCAGTACCAAGT; NF- κ BI α forward - 5' AACCTGCAGCAGACTCCACT; NF- κ BI α reverse - 5' GACACGTGTGGCCATTGTAG; porcine E-selectin (PORESEL) forward - 5' GCCAACGTGTAAAGCTGTGA; PORESEL reverse - 5' TCCTCACAGCTGAAGGCACA; GAPDH forward - 5' GTCTTCACCACCATGGAG; and GAPDH reverse - 5' CCACCCTGTTGCTGTAGC. Isolated RNA was subjected to first-strand cDNA synthesis as described by the manufacturer of the Superscript First Strand synthesis system (Invitrogen, Carlsbad, CA). RT-PCR was performed using a Minicycler PCR machine (MJ Research, Inc., San Francisco, CA).

Effect of VEGF₁₂₁/rGel on Apoptotic Markers-- Whole cell extracts of HUVEs and PAE/KDR cells treated for 24 h with VEGF₁₂₁/rGel at their respective IC₅₀ doses were analyzed for changes in levels of the apoptotic markers caspase-3, caspase-6, cytochrome C, Bcl-XL, Bcl-2, and Bax. Whole cell extracts and western blots were prepared as detailed above.

TUNEL Assay—Log-phase PAE/KDR and PAE/Flt-1 cells were diluted to 2000 cells/100 μ l. Aliquots (100 μ l) were added in 16-well chamber slides (Nalge Nunc International, Rochester,

NY) and incubated overnight at 37°C with 5% CO₂. Purified VEGF₁₂₁/rGel was diluted in culture medium and added at 72-, 48-, and 24-h time points at a final concentration of 1 nM, which is twice the IC₅₀ dose. The cells were then processed and analyzed for TUNEL as described by the manufacturer of the reagent. Positive control cells were incubated with 1 mg/ml DNase for 10 min at 37°C.

RESULTS

VEGF₁₂₁/rGel Is Specifically Cytotoxic to Endothelial Cells that Overexpress KDR-- The cytotoxic effect of VEGF₁₂₁/rGel and rGel *in vitro* was examined employing both HUVECs and PAE cells transfected with either the human Flt-1 receptor (PAE/Flt-1) or the human KDR receptor (PAE/KDR). Each cell type expressed the KDR receptor at varying levels (27;32;41). Treatment of log-phase cells with VEGF₁₂₁/rGel for 72 h showed the greatest cytotoxic effect against PAE/KDR cells, with an IC₅₀ of 1 nM (Fig. 1). In contrast, the IC₅₀ of VEGF₁₂₁/rGel on HUVECs and PAE/Flt-1 cells was approximately 300 nM. The cytotoxic effects of the untargeted rGel were similar in all three cell lines (IC₅₀ ~ 150 nM).

VEGF₁₂₁/rGel Treatment Activates the KDR Receptor-- We previously showed that the cytotoxicity of VEGF₁₂₁/rGel is mediated via VEGFR-2 (KDR) and not VEGFR-1 (Flt-1) (31). However, we hypothesized that the VEGF component of VEGF₁₂₁/rGel could also stimulate cell growth through interaction with the receptors for VEGF. In the present study, we investigated this hypothesis by evaluating endogenous levels of p-KDR in endothelial cells that had been treated with VEGF₁₂₁/rGel. PAE/KDR cells expressed levels of p-KDR that increased within 2 h after VEGF₁₂₁/rGel treatment. The levels of p-KDR peaked at 4 h and gradually decreased to endogenous levels by 24 h posttreatment (Fig. 2). Endogenous levels of total KDR were also increased by 4 h and were reduced to pretreatment levels by 24 h (Fig. 2A). In contrast, endogenous levels of total KDR in HUVECs were decreased slightly at 24 h after treatment with VEGF₁₂₁/rGel, whereas p-KDR levels after 24 h were markedly upregulated compared with the

levels of untreated cells (Fig. 2B). Thus, the cytotoxic effect of the rGel component of VEGF₁₂₁/rGel does not interfere with the stimulatory effect of the VEGF component.

Cytotoxic Effects of VEGF₁₂₁/rGel on Endothelial Cells Are Not Mediated via Apoptotic

Mechanisms-- To investigate the mechanisms of the cytotoxic effects of VEGF₁₂₁/rGel on endothelial cells, we performed a TUNEL assay on cells treated with the construct for 24, 48, and 72 h. As shown in Fig. 3, we found no TUNEL staining in PAE/KDR cells exposed to VEGF₁₂₁/rGel for periods of up to 72 h. In contrast, the nuclei of positive control cells showed intense staining. These findings clearly indicate that the mechanism of cytotoxicity of VEGF₁₂₁/rGel is necrotic rather than apoptotic. To confirm and validate these observations, we examined various key apoptotic signaling events using western blot analysis (Fig. 4). After HUVECs and PAE/KDR cells were treated with VEGF₁₂₁/rGel or saline for 24 h, their whole cell extracts were harvested and analyzed. Levels of the pro-apoptotic proteins cytochrome C and caspase-6, as well as the anti-apoptotic protein Bcl-2 were undetectable before or after treatment (data not shown). Levels of caspase-3 (full length pre-cursor), Bax (a pro-apoptotic protein), and Bcl-XL (an apoptosis inhibitor) were not affected by VEGF₁₂₁/rGel treatment. In addition, the p11 and p20 subunits of activated/cleaved caspase-3 were not detected after treatment with the fusion construct.

Microarray Analysis of HUVECs Treated with VEGF₁₂₁/rGel-- To further elucidate the biochemical mechanisms that govern the effects of VEGF₁₂₁/rGel on endothelial cells, we treated HUVECs with saline or the IC₅₀ dose of VEGF₁₂₁/rGel for 24 h. RNA was isolated, evaluated for integrity, and subjected to microarray analysis and a dye-swap comparison was performed for

reproducibility. Only those differentially expressed genes whose levels were elevated to at least 2 times the baseline value in repeated experiments were selected. On this basis, 22 genes (out of the 4800 in the microarray) were upregulated by VEGF₁₂₁/rGel at 24 h (Table I). In addition to upregulating select genes known to be induced by VEGF alone, treatment with VEGF₁₂₁/rGel upregulated genes involved in inflammation, chemotaxis and transcription regulation. The genes with the highest levels of expression from four gene classifications were validated by RT-PCR analysis. When normalized for GAPDH, all four of the other PCR products were increased after treatment with VEGF₁₂₁/rGel, thus validating the results observed in the original microarray (Fig. 5A). However, the induction of E-selectin protein levels did not match the induction of mRNA (Fig. 5B).

Because PAE/KDR cells have been used as *in vitro* models for endothelial cells in the tumor neovasculature, we investigated the effect of VEGF₁₂₁/rGel on gene induction and protein expression in these cells. PAE/KDR cells were treated with saline or the IC₅₀ dose of VEGF₁₂₁/rGel for up to 48 h. As shown in Fig. 6A, PCR analysis for E-selectin confirmed the increase in message within 2 h after treatment of cells with VEGF₁₂₁/rGel. In addition, western blot analysis demonstrated a slight increase in E-selectin protein expression, although the increase in cellular protein levels was slight compared with the observed increase in message (Fig. 6B). Western blots using anti-MKP-1 and anti-ERK2 antibodies also showed no change in protein expression (data not shown).

VEGF₁₂₁/rGel Inhibits Tube Formation in KDR-Expressing Endothelial Cells—We

investigated the anti-angiogenic effect of VEGF₁₂₁/rGel *in vitro* by examining the inhibition of tube formation in receptor-transfected PAE cells. PAE/KDR and PAE/Flt-1 cells were placed on

Matrigel-coated plates, to which either VEGF₁₂₁/rGel or rGel at various concentrations was added, and tube formation was assessed 24 h later. As shown in Fig. 7A, the addition of 1 nM VEGF₁₂₁/rGel significantly inhibited tube formation in KDR-transfected cells, whereas rGel alone had little effect at this dose level. Doses of rGel alone caused ~42% inhibition at only the highest concentration tested (100 nM). Endothelial cells expressing VEGFR-1 (PAE/Flt-1) were not as sensitive to VEGF₁₂₁/rGel as were the PAE/KDR cells, requiring 100 nM VEGF₁₂₁/rGel or rGel to inhibit tube formation by 50% (Fig. 7B). To determine whether pre-treatment of PAE/KDR cells with VEGF₁₂₁/rGel affects tube formation, cells were treated with the IC₅₀ dose of VEGF₁₂₁/rGel for 4, 16, and 24 h, washed with PBS, detached, added to Matrigel-coated plates in VEGF₁₂₁/rGel-free medium, and incubated for an additional 24 h. This prior incubation of cells with VEGF₁₂₁/rGel for 16 or 24 h virtually abolished tube formation (Fig. 8).

VEGF₁₂₁/rGel Inhibits Angiogenesis in the CAM of Chicken Embryos-- We investigated the antiangiogenic effects of VEGF₁₂₁/rGel *in vivo* using a chicken CAM model. Angiogenesis in the CAMs of 9-day-old chicken embryos were stimulated by treatment with filter disks containing either bFGF alone, bFGF plus VEGF₁₂₁/rGel (at 1 or 10 nM), rGel (at 1 or 10 nM), or buffer (PBS) alone (45). CAMs were treated for 72 h and the effect of each treatment was quantified by determining the relative vascularized area: the area taken up by blood vessels in treated CAMs, normalized to that in CAMs treated with PBS (equal to 100%). The vascularized area was about 35% higher in the CAMs treated with bFGF than in those treated with PBS, and the difference was significant ($P < 0.001$; *t*-test, double-sided; Figs. 9A and 10A). This observation was consistent with the finding of more than a 60% increase in the number of newly sprouted vessels in the bFGF-treated CAMs compared with the PBS-treated CAMs ($P < 0.001$; *t*-test,

double-sided; Fig. 10B). Incubation of CAMs with bFGF without or with 10 nM rGel resulted in angiogenic activity and the formation of an ordered neovasculature (Figs. 9A and 9B). In contrast, treatment with 1 or 10 nM VEGF₁₂₁/rGel resulted in considerable destruction of the neovasculature (Fig. 9C). Treatment with VEGF₁₂₁/rGel also completely inhibited bFGF-stimulated angiogenesis ($P < 0.001$; t -test, double sided; Fig. 10). Many of the treated CAMs also appeared to be devoid of vessel infiltration. Interestingly, the number of branching points in the VEGF₁₂₁/rGel-treated CAMs was similar to that in the PBS-treated CAMs ($P > 0.5$; t -test, double-sided; Fig. 10B), suggesting that VEGF₁₂₁/rGel mainly inhibits bFGF-mediated formation of newly sprouting branches from preexisting vessels. As expected, the disks treated with bFGF in combination with rGel (at 1 or 10 nM) consistently showed extensive vascularization that was comparable to that found in those treated with bFGF alone ($P > 0.5$; t -test, double-sided).

DISCUSSION

Our study clearly demonstrates that the VEGF₁₂₁/rGel fusion construct is specifically cytotoxic to KDR-overexpressing endothelial cells and that the cytotoxic effect of the treatment is due to necrosis rather than to apoptosis. Previous studies of gelonin-based immunotoxins targeting tumor cells showed that intoxicated cells did not appear to display apoptotic characteristics (42). The toxin gelonin appears to be distinct from toxins such as engineered diphtheria toxin (DT) (43;44) and pseudomonas exotoxin (PE) (45;46), both of which have been demonstrated to cause apoptotic damage to target cells. A closely related toxin, ricin-A chain (RTA), also causes apoptotic damage to target cells (47;48); however, Baluna et al (47) suggest that different portions of the RTA molecule are responsible for generating apoptotic and necrotic effects.

VEGF-A was shown to play a role in tube formation of endothelial cells *in vitro* (49;50) and in angiogenesis (51-53). In the present study, the effect of VEGF₁₂₁/rGel on tube formation of endothelial cells on Matrigel-coated plates was striking in that cells overexpressing the KDR receptor, but not cells overexpressing the Flt-1 receptor, were affected. This result is consistent with our findings that VEGF₁₂₁/rGel is cytotoxic only to KDR-expressing endothelial cells(31) and that VEGF₁₂₁/rGel is internalized only into endothelial cells that express KDR but not Flt-1 (manuscript submitted). The fact that the IC₅₀ dose for cytotoxicity is identical to the IC₅₀ dose for preventing tube formation in PAE/KDR cells suggests that VEGF₁₂₁/rGel action *in vitro* immediately disrupts angiogenic tube formation as a temporal prelude to its eventual cytotoxicity to rapidly dividing endothelial cells. Our preliminary results examining *in vivo* endothelialization of Matrigel plugs appear to support the observation that the VEGF₁₂₁/rGel construct can ablate neovascularization at several steps in this complex process.

CAM membrane assays are frequently used to assess the antiangiogenic potential of agents (54-57). The inhibition by VEGF₁₂₁/rGel of tube formation *in vitro* translates well to inhibition of both vascular endothelial growth and neovasculature *in vivo*. Treatment with VEGF₁₂₁/rGel at doses as low as 1 nM resulted in complete ablation of bFGF-induced neovasculature. Not surprisingly, the CAM assay also demonstrated that treatment with the construct did not affect mature vessels. This critical finding suggests that VEGF₁₂₁/rGel does not affect mature vessels in either normal tissues or tumors. Therefore, small, newly vascularizing tumors and metastases may be the lesions most responsive to therapy with this agent.

To better understand the cytotoxic effects of VEGF₁₂₁/rGel at the molecular level, we treated HUVECs with VEGF₁₂₁/rGel for 24 h, and harvested the RNA for microarray analysis. The results suggest that treatment of HUVECs with VEGF₁₂₁/rGel increases the RNA levels of several genes that are involved in inflammation, chemotaxis, intermediary metabolism, and apoptotic pathways (Table I). A previous report showed that only two of these genes, MKP-1 and CXCR4, were also upregulated after treatment with VEGF₁₆₅ for 24 h (58). Therefore, for most of the genes found to be upregulated in our present study, the upregulation appears to be attributable to the VEGF₁₂₁/rGel construct and not the VEGF component itself. To our knowledge, this microarray analysis was the first to be performed on cells treated with a plant-derived protein toxin such as gelonin.

Of all the molecules we studied, the highest level of mRNA induced was that of the cell adhesion molecule E-selectin. In previous studies, treatment with VEGF induced adhesion molecules (E-selectin, VCAM-1, and ICAM-1) in HUVECs (59-61) via an NFκB-mediated process. E-selectin has been shown to be upregulated after VEGF treatment (50) or in response to inflammation (60;62) and plays an important role in both tube formation and angiogenesis.

Previous studies have shown that E-selectin also plays a major role in the adhesion of epithelial cancer cells to the endothelium (63) and that the ability of cancer cell clones to bind E-selectin on endothelial cells is directly proportional to their metastatic potential (62;64). Moreover, drugs that inhibit the expression of E-selectin, such as cimetidine, block the adhesion of tumor cells to the endothelium and prevent metastasis (65). However, E-selectin does not necessarily have a role in the adhesion of all cancer cells (66;67), nor do all cancer cells require expression of the same endothelial adhesive molecule (68;69). Our present study shows that VEGF₁₂₁/rGel is a member of the class of molecules that can prevent E-selectin-mediated metastasis because protein levels barely doubled in both PAE/KDR and HUVECs after treatment with VEGF₁₂₁/rGel. We observed a similar pattern of induction of RNA but not protein levels with other genes as well. For example, although MKP-1 RNA levels were induced in HUVECs after treatment with VEGF₁₂₁/rGel, western blots of PAE/KDR and HUVEC whole cell extract did not show a corresponding increase in protein levels (data not shown). In addition, levels of ERK2, which was previously shown to be upregulated by MKP-1 in HUVECs after endothelial cell injury (59), did not show a change up to 48 h after VEGF₁₂₁/rGel treatment. Taken together, we conclude VEGF₁₂₁/rGel induces an increase in mRNA levels of genes that are important in cell adhesion, migration, and spread but generally does not induce a concomitant increase in protein expression. Since the rGel component of the fusion construct operates by inhibiting protein synthesis, VEGF₁₂₁/rGel could inhibit synthesis of critical proteins that are important for suppression of these specific genes. Our data also suggest that in addition to exerting a cytotoxic effect, VEGF₁₂₁/rGel may act through cellular mechanisms involved in inflammation and stress.

Previous studies have showed that several genes HUVECs are induced as a result of cellular inflammation. For example, Early growth response factor 1 (EGR1), SCYA2, E-selectin

and VCAM-1 are all up-regulated in HUVECs (60;70), and all of these genes are induced by treatment with VEGF₁₂₁/rGel. In addition, several members of the small inducible cytokine (SCYA) family of proteins are overexpressed after VEGF₁₂₁/rGel treatment. All of these SCYA proteins respond to inflammation stimuli and play a role in chemotaxis: SCYA2 plays a role in inflammation and wound healing (71-73); SCYA4 (MIP-1 β) is involved in directional migration of cells during normal and inflammatory processes (74;75); and SCYA7 (MCP-3) and SCYA11 (eotaxin) share 65% amino acid sequence identity and play major roles in the recruitment and activation of eosinophils in allergic disorders (71;73) while binding to different receptors and having different modes of action (76). Another molecule that plays a role in chemotaxis is CXCR4. Although treatment with VEGF₁₂₁/rGel increases the CXCR4 level to less than twice the level without treatment, array spot intensities and reproducibility data indicate that the increase is significant.

Transcription factors represent one of the larger classes of genes to be upregulated by treatment with VEGF₁₂₁/rGel. Interestingly, two of them, NF- κ B α (I κ B- α) and NF- κ B (p105 subunit), are from the NF- κ B family. Since NF- κ B and I κ B- α interact in an autoregulatory mechanism, the upregulation of I κ B- α is most likely due to NF- κ B's mediating activation of the I κ B- α gene, resulting in replenishment of the cytoplasmic pool of its own inhibitor (77-80). NF- κ B may play a role in the upregulation of several genes, including SCYA2, SCYA7, SCYA11, and JunB (81;82). Another transcription factor, Kruppel-like factor (KLF4), has not been shown to be expressed in endothelial cells. However, this molecule is an important nuclear factor in the up-regulation of histidine decarboxylase, an enzyme that catalyzes the conversion of histidine to histamine, a bioamine that plays an important role in allergic responses, inflammation, neurotransmission, and gastric acid secretion (83).

Among the molecules governing apoptosis, TNFAIP3, a putative DNA binding protein in the NF- κ B signal transduction pathway, functions by inhibiting NF- κ B activation and TNF-mediated apoptosis (84). BIRC3, another gene that is upregulated by treatment with VEGF₁₂₁/rGel, forms a heterodimer with a caspase-9 monomer *in vitro* and prevents the activation of caspase-9 in apoptosis (85). Surprisingly, we found in this study that several genes involved in the control of the apoptotic pathway were modulated in response to the fusion toxin even though the overall cytotoxic effect on target cells did not include an observable impact on the apoptotic pathway.

A critical finding of this study is the identification of several genes that are regulated in response to treatment with the VEGF₁₂₁/rGel fusion construct. Since many of these genes regulate cell adhesion, chemotaxis, and inflammatory responses, the construct may influence tumor development in addition to exerting direct cytotoxic effects on the tumor neovasculature. Therefore, important considerations for future study are the effects of VEGF₁₂₁/rGel cytotoxicity on tumor endothelial cells and the potential bystander effects of the construct on adjacent tumor cells. In our laboratory, current studies are under way in breast and prostate orthotopic and metastatic (i.e., lung and bone) tumor cells to further characterize the effects of this drug *in vitro* and *in vivo*.

FIGURE LEGENDS

Fig. 1. Cytotoxic effects of VEGF₁₂₁/rGel on endothelial cells. Log-phase HUVECs, PAE/KDR cells, and PAE/Flt-1 cells were plated in 96-well plates and incubated with serial dilutions of VEGF₁₂₁/rGel and rGel for 72 h as described in Experimental Procedures. The cytotoxicity experiment was performed in triplicate, and data points represent the means.

Fig. 2. Decreased KDR and increased p-KDR levels in PAE/KDR cells and HUVECs treated with VEGF₁₂₁/rGel at IC₅₀ doses for 24 h. To determine the effects of VEGF₁₂₁/rGel on the levels of KDR and activated KDR levels, samples were prepared as described in Experimental Procedures and probed with anti-KDR and anti-p-KDR antibodies. Actin levels were used as a loading control. A, total KDR and p-KDR levels in PAE/KDR cells show an increase within 2 h after the start of treatment and gradually level off by 48 h. B, at 24h after the start of treatment of HUVECs with VEGF₁₂₁/rGel, KDR levels are decreased slightly but p-KDR levels are increased. NT, not treated.

Fig. 3. TUNEL assay of endothelial cells treated with VEGF₁₂₁/rGel. After PAE/KDR cells were grown overnight, and 1 nM VEGF₁₂₁/rGel was added, the cells were further incubated for 24, 48, and 72 h. The cells were then analyzed by TUNEL. Positive control cells were incubated with 1 mg/ml DNase for 10 min at 37°C. The results show that cytotoxicity of VEGF₁₂₁/rGel in PAE/KDR cells does not result in apoptosis. NT, not treated.

Fig. 4. Lack of effect of VEGF₁₂₁/rGel on apoptotic markers in endothelial cells. To understand the mechanism of cytotoxicity of VEGF₁₂₁/rGel, protein levels of key markers of apoptosis were assessed 24 h after treatment. Protein levels of Bax, Bcl-XL and caspase-3 remained unchanged, suggesting that the mechanism of cell death induced by the construct is not apoptotic. Levels of cytochrome C, caspase-6, and Bcl-2 were undetectable (data not shown). NT, not treated.

Fig. 5. Analysis of HUVECs treated with VEGF₁₂₁/rGel. A, validation of the microarray analysis by PCR is shown. Upregulation of genes for E-selectin, TNFAIP3, NF-κB1α and SCYA2 were validated by RT-PCR. GAPDH levels were assessed as a control. B, protein levels of E-selectin in HUVECs treated with VEGF₁₂₁/rGel are shown. NT, not treated.

Fig. 6. Inhibition of translation of upregulated E-selectin RNA by VEGF₁₂₁/rGel. A, RNA from PAE/KDR cells that were untreated or treated with VEGF₁₂₁/rGel for the periods indicated were examined by PCR for upregulation of E-selectin, one of the genes identified by microarray analysis. GAPDH primers were used as a control for loading. RNA levels of E-selectin were all upregulated in PAE/KDR cells, as in HUVECs. B, protein levels of E-selectin are also upregulated.

Fig. 7. VEGF₁₂₁/rGel-mediated inhibition of tube formation in PAE/KDR cells. PAE/KDR and PAE/Flt-1 cells were added to Matrigel-coated plates, treated with VEGF₁₂₁/rGel and rGel at the concentrations indicated, and analyzed for tube formation after 24 h. A, A 1 nM dose of VEGF₁₂₁/rGel was sufficient to inhibit tube formation by 50%, whereas the same degree of

inhibition was seen with rGel only at 100 nM. B, up to 100 nM VEGF₁₂₁/rGel was needed to inhibit tube formation in PAE/Flt-1 cells, the same concentration as the untargeted gelonin toxin.

Fig. 8. Time-dependent inhibition of tube formation of PAE/KDR cells by VEGF₁₂₁/rGel.

PAE/KDR cells were treated with 1 nM VEGF₁₂₁/rGel for the periods indicated, detached, incubated on Matrigel-coated plates for 24 h, and assessed for tube formation. Incubation of PAE/KDR cells with VEGF₁₂₁/rGel for as little as 9 h was sufficient to abolish the ability of these cells to form tubes by 50%.

Fig. 9. VEGF₁₂₁/rGel-mediated inhibition of angiogenesis in chicken embryo CAMs.

Shown are vessels in representative CAMs treated with bFGF alone (50 ng), bFGF in combination with VEGF₁₂₁/rGel (1 nM), or bFGF in combination with rGel (10 nM) (x0.5 objective). Angiogenesis was induced on CAMs from 9-day-old chicken embryos by filter disks saturated with bFGF. Disks were simultaneously treated with VEGF₁₂₁/rGel or rGel. At 72 h, CAMs were harvested and examined using an Olympus stereomicroscope. Experiments were performed twice per treatment, with 6 to 10 embryos per condition in every experiment. A, the photograph shows the vasculature of a CAM after stimulation with bFGF alone. B, the photograph shows that rGel had no effect on angiogenic stimulation of bFGF at either 1 nM or 10 nM. C, the photograph shows that 1 nM VEGF₁₂₁/rGel in the presence of 50 ng of bFGF inhibited angiogenesis.

Fig. 10. VEGF₁₂₁/rGel-mediated reduction of the vascular area and number of vascular branches in the CAM assay. Quantitative evaluation of VEGF₁₂₁/rGel-mediated inhibition of

angiogenesis in the CAM model was determined, after the indicated treatments, by image analyses, and the results were normalized to CAMs treated with buffer (PBS; equal to 100%). A, VEGF₁₂₁/rGel at both 1 and 10 nM decreased the vascular area. As expected, rGel alone had no effect. Data represent the means \pm standard deviations from replicated experiments. *, $P < 0.001$; t -test, double-sided. B, VEGF₁₂₁/rGel decreased the number of newly sprouting vessels. VEGF₁₂₁/rGel at a concentration of 1 nM dramatically affected the formation of the neovasculature, completely inhibiting bFGF-mediated stimulation of the neovasculature. As expected, rGel did not affect the number of newly sprouting vessels. Data shown represent the means \pm standard deviations from replicated experiments. *, $P < 0.001$; t -test, double-sided.

Acknowledgments— We thank Kate Ó Súilleabháin (UT MD Anderson Cancer Center Department of Scientific Publications) for editing the manuscript.

¹The abbreviations used are: VEGF-A, vascular endothelial growth factor-A; VEGF₁₂₁, 121-amino-acid splice variant of VEGF-A; rGel, recombinant toxin gelonin; bFGF, basic fibroblast growth factor; p-KDR, phosphorylated KDR; PAE, porcine aortic endothelial; FBS, fetal bovine serum; HUVEC, human umbilical vein endothelial cell; PBS, phosphate-buffered saline; SDS-PAGE, sodium dodecyl sulfate-polyacrylamide gel electrophoresis; CAM, chorioallantoic membrane; SCYA2, cytokine A2; TNFAIP3, tumor necrosis factor alpha-induced protein 3; NF- κ BI α , NF- κ B inhibitor alpha.

REFERENCES

1. Folkman, J. (1993) *C. R. Acad. Sci. III* **316**, 909-918
2. Schultz, G. S. and Grant, M. B. (1991) *Eye* **5 (Pt 2)**, 170-180
3. Sebag, J. and McMeel, J. W. (1986) *Surv. Ophthalmol.* **30**, 377-384
4. Rand, L. I. (1981) *Am. J. Med.* **70**, 595-602
5. Koch, A. E. (1998) *Arthritis Rheum.* **41**, 951-962
6. Szekanecz, Z., Szegedi, G., and Koch, A. E. (1998) *J. Investig. Med.* **46**, 27-41
7. Oliver, S. J. and Braun, E. (1996) *J. Rheumatol. Suppl* **44**, 56-60
8. Brown, R. A. and Weiss, J. B. (1988) *Ann. Rheum. Dis.* **47**, 881-885
9. Verheul, H. M., Voest, E. E., and Schlingemann, R. O. (2004) *J. Pathol.* **202**, 5-13
10. Bogenrieder, T. and Herlyn, M. (2003) *Oncogene* **22**, 6524-6536
11. Aoun, E. and Taher, A. (2002) *J. Med. Liban.* **50**, 32-38
12. Folkman, J. (2002) *Semin. Oncol.* **29**, 15-18
13. Bergers, G., Song, S., Meyer-Morse, N., Bergsland, E., and Hanahan, D. (2003) *J. Clin. Invest* **111**, 1287-1295
14. Klags, W. D., Fry, D. W., and Kraker, A. J. (1997) *Curr. Opin. Oncol.* **9**, 562-568

15. Manley, P. W., Martiny-Baron, G., Schlaeppli, J. M., and Wood, J. M. (2002) *Expert. Opin. Investig. Drugs* **11**, 1715-1736
16. Rosen, L. S. (2002) *Hematol. Oncol. Clin. North Am.* **16**, 1173-1187
17. Ruegg, C., Dormond, O., and Foletti, A. (2002) *Endothelium* **9**, 151-160
18. Veronese, M. L. and O'Dwyer, P. J. (2004) *Eur. J. Cancer* **40**, 1292-1301
19. Zondor, S. D. and Medina, P. J. (2004) *Ann. Pharmacother.* **38**, 1258-1264
20. Kim, E. S., Serur, A., Huang, J., Manley, C. A., McCrudden, K. W., Frischer, J. S., Soffer, S. Z., Ring, L., New, T., Zabski, S., Rudge, J. S., Holash, J., Yancopoulos, G. D., Kandel, J. J., and Yamashiro, D. J. (2002) *Proc. Natl. Acad. Sci. U. S. A.* **99**, 11399-11404
21. Holash, J., Davis, S., Papadopoulos, N., Croll, S. D., Ho, L., Russell, M., Boland, P., Leidich, R., Hylton, D., Burova, E., Ioffe, E., Huang, T., Radziejewski, C., Bailey, K., Fandl, J. P., Daly, T., Wiegand, S. J., Yancopoulos, G. D., and Rudge, J. S. (2002) *Proc. Natl. Acad. Sci. U. S. A.* **99**, 11393-11398
22. Wulff, C., Wilson, H., Rudge, J. S., Wiegand, S. J., Lunn, S. F., and Fraser, H. M. (2001) *J. Clin. Endocrinol. Metab.* **86**, 3377-3386
23. Cavallaro, U. and Christofori, G. (2000) *J. Neurooncol.* **50**, 63-70
24. Shinkaruk, S., Bayle, M., Lain, G., and Deleris, G. (2003) *Curr. Med. Chem. Anti.-Canc. Agents* **3**, 95-117

25. Verheul, H. M. and Pinedo, H. M. (2000) *Clin. Breast Cancer* **1 Suppl 1**, S80-S84
26. Arora, N., Masood, R., Zheng, T., Cai, J., Smith, D. L., and Gill, P. S. (1999) *Cancer Res.* **59**, 183-188
27. Backer, M. V., Budker, V. G., and Backer, J. M. (2001) *J. Control Release* **74**, 349-355
28. Hotz, H. G., Gill, P. S., Masood, R., Hotz, B., Buhr, H. J., Foitzik, T., Hines, O. J., and Reber, H. A. (2002) *J. Gastrointest. Surg.* **6**, 159-166
29. Masood, R., Kundra, A., Zhu, S., Xia, G., Scalia, P., Smith, D. L., and Gill, P. S. (2003) *Int. J. Cancer* **104**, 603-610
30. Ramakrishnan, S., Wild, R., and Nojima, D. (2001) *Methods Mol. Biol.* **166**, 219-234
31. Veenendaal, L. M., Jin, H., Ran, S., Cheung, L., Navone, N., Marks, J. W., Waltenberger, J., Thorpe, P., and Rosenblum, M. G. (2002) *Proc. Natl. Acad. Sci. U. S. A.* **99**, 7866-7871
32. Waltenberger, J., Claesson-Welsh, L., Siegbahn, A., Shibuya, M., and Heldin, C. H. (1994) *J. Biol. Chem.* **269**, 26988-26995
33. Bussolati, B., Dunk, C., Grohman, M., Kontos, C. D., Mason, J., and Ahmed, A. (2001) *Am. J. Pathol.* **159**, 993-1008
34. Joki, T., Machluf, M., Atala, A., Zhu, J., Seyfried, N. T., Dunn, I. F., Abe, T., Carroll, R. S., and Black, P. M. (2001) *Nat. Biotechnol.* **19**, 35-39
35. Kroll, J. and Waltenberger, J. (1999) *Biochem. Biophys. Res. Commun.* **265**, 636-639

36. Brooks, P. C., Montgomery, A. M., and Cheresch, D. A. (1999) *Methods Mol. Biol.* **129**, 257-269
37. Jiang, B. H., Zheng, J. Z., Aoki, M., and Vogt, P. K. (2000) *Proc. Natl. Acad. Sci. U. S. A.* **97**, 1749-1753
38. Shmulevich, I., Hunt, K., El Naggar, A., Taylor, E., Ramdas, L., Laborde, P., Hess, K. R., Pollock, R., and Zhang, W. (2002) *Cancer* **94**, 2069-2075
39. Baggerly, K. A., Coombes, K. R., Hess, K. R., Stivers, D. N., Abruzzo, L. V., and Zhang, W. (2001) *J. Comput. Biol.* **8**, 639-659
40. Dobbin, K., Shih, J. H., and Simon, R. (2003) *J. Natl. Cancer Inst.* **95**, 1362-1369
41. Brogi, E., Schatteman, G., Wu, T., Kim, E. A., Varticovski, L., Keyt, B., and Isner, J. M. (1996) *J. Clin. Invest* **97**, 469-476
42. Rosenblum, M. G., Cheung, L. H., Liu, Y., and Marks, J. W., III (2003) *Cancer Res.* **63**, 3995-4002
43. Foss, F. M. (2000) *Clin. Lymphoma* **1**, 110-116
44. Hall, P. D., Kreitman, R. J., Willingham, M. C., and Frankel, A. E. (1998) *Toxicol. Appl. Pharmacol.* **150**, 91-97
45. Wang, L., Liu, B., Schmidt, M., Lu, Y., Wels, W., and Fan, Z. (2001) *Prostate* **47**, 21-28
46. Brinkmann, U. (2000) *In Vivo* **14**, 21-27

47. Baluna, R., Coleman, E., Jones, C., Ghetie, V., and Vitetta, E. S. (2000) *Exp. Cell Res.* **258**, 417-424
48. Burbage, C., Tagge, E. P., Harris, B., Hall, P., Fu, T., Willingham, M. C., and Frankel, A. E. (1997) *Leuk. Res.* **21**, 681-690
49. Ruggeri, B., Singh, J., Gingrich, D., Angeles, T., Albom, M., Yang, S., Chang, H., Robinson, C., Hunter, K., Dobrzanski, P., Jones-Bolin, S., Pritchard, S., Aimone, L., Klein-Szanto, A., Herbert, J. M., Bono, F., Schaeffer, P., Casellas, P., Bourie, B., Pili, R., Isaacs, J., Ator, M., Hudkins, R., Vaught, J., Mallamo, J., and Dionne, C. (2003) *Cancer Res.* **63**, 5978-5991
50. Aoki, M., Kanamori, M., Yudoh, K., Ohmori, K., Yasuda, T., and Kimura, T. (2001) *Tumour. Biol.* **22**, 239-246
51. Leopold, J. A., Walker, J., Scribner, A. W., Voetsch, B., Zhang, Y. Y., Loscalzo, A. J., Stanton, R. C., and Loscalzo, J. (2003) *J. Biol. Chem.* **278**, 32100-32106
52. Kim, K. Y., Kim, S. O., Lim, H., Yoo, S. E., and Hong, K. W. (2003) *Eur. J. Pharmacol.* **465**, 219-228
53. Itokawa, T., Nokihara, H., Nishioka, Y., Sone, S., Iwamoto, Y., Yamada, Y., Cherrington, J., McMahon, G., Shibuya, M., Kuwano, M., and Ono, M. (2002) *Mol. Cancer Ther.* **1**, 295-302
54. Favot, L., Keravis, T., Holl, V., Le Bec, A., and Lugnier, C. (2003) *Thromb. Haemost.* **90**, 334-343

55. Hembrough, T. A., Ruiz, J. F., Swerdlow, B. M., Swartz, G. M., Hammers, H. J., Zhang, L., Plum, S. M., Williams, M. S., Strickland, D. K., and Pribluda, V. S. (2004) *Blood* **103**, 3374-3380
56. Ribatti, D., Nico, B., Vacca, A., Roncali, L., and Presta, M. (1999) *Angiogenesis* **3**, 89-95
57. Wang, F. S., Wang, C. J., Chen, Y. J., Chang, P. R., Huang, Y. T., Sun, Y. C., Huang, H. C., Yang, Y. J., and Yang, K. D. (2004) *J. Biol. Chem.* **279**, 10331-10337
58. Yang, S., Toy, K., Ingle, G., Zlot, C., Williams, P. M., Fuh, G., Li, B., de Vos, A., and Gerritsen, M. E. (2002) *Arterioscler. Thromb. Vasc. Biol.* **22**, 1797-1803
59. Kim, F. and Corson, M. A. (2000) *Biochem. Biophys. Res. Commun.* **273**, 539-545
60. Kim, W., Moon, S. O., Lee, S., Sung, M. J., Kim, S. H., and Park, S. K. (2003) *Arterioscler. Thromb. Vasc. Biol.* **23**, 1377-1383
61. Kim, I., Moon, S. O., Kim, S. H., Kim, H. J., Koh, Y. S., and Koh, G. Y. (2001) *J. Biol. Chem.* **276**, 7614-7620
62. Nubel, T., Dippold, W., Kleinert, H., Kaina, B., and Fritz, G. (2004) *FASEB J.* **18**, 140-142
63. Takada, A., Ohmori, K., Yoneda, T., Tsuyuoka, K., Hasegawa, A., Kiso, M., and Kannagi, R. (1993) *Cancer Res.* **53**, 354-361
64. Sawada, R., Tsuboi, S., and Fukuda, M. (1994) *J. Biol. Chem.* **269**, 1425-1431

65. Kobayashi, K., Matsumoto, S., Morishima, T., Kawabe, T., and Okamoto, T. (2000) *Cancer Res.* **60**, 3978-3984
66. Laferriere, J., Houle, F., Taher, M. M., Valerie, K., and Huot, J. (2001) *J. Biol. Chem.* **276**, 33762-33772
67. Laferriere, J., Houle, F., and Huot, J. (2002) *Ann. N. Y. Acad. Sci.* **973**, 562-572
68. Khatib, A. M., Kontogiannia, M., Fallavollita, L., Jamison, B., Meterissian, S., and Brodt, P. (1999) *Cancer Res.* **59**, 1356-1361
69. Zetter, B. R. (1993) *Semin. Cancer Biol.* **4**, 219-229
70. Kadl, A., Huber, J., Gruber, F., Bochkov, V. N., Binder, B. R., and Leitinger, N. (2002) *Vascul. Pharmacol.* **38**, 219-227
71. Johnston, C. J., Williams, J. P., Okunieff, P., and Finkelstein, J. N. (2002) *Radiat. Res.* **157**, 256-265
72. Lu, B., Rutledge, B. J., Gu, L., Fiorillo, J., Lukacs, N. W., Kunkel, S. L., North, R., Gerard, C., and Rollins, B. J. (1998) *J. Exp. Med.* **187**, 601-608
73. Wagner, K., Dendorfer, U., Chilla, S., Schlondorff, D., and Luckow, B. (2001) *Genomics* **78**, 113-123
74. Guo, C. J., Lai, J. P., Luo, H. M., Douglas, S. D., and Ho, W. Z. (2002) *J. Neuroimmunol.* **131**, 160-167

75. Guo, C. J., Douglas, S. D., Lai, J. P., Pleasure, D. E., Li, Y., Williams, M., Bannerman, P., Song, L., and Ho, W. Z. (2003) *J. Neurochem.* **84**, 997-1005
76. Chung, I. Y., Kim, Y. H., Choi, M. K., Noh, Y. J., Park, C. S., Kwon, d. Y., Lee, D. Y., Lee, Y. S., Chang, H. S., and Kim, K. S. (2004) *Biochem. Biophys. Res. Commun.* **314**, 646-653
77. Brown, K., Park, S., Kanno, T., Franzoso, G., and Siebenlist, U. (1993) *Proc. Natl. Acad. Sci. U. S. A.* **90**, 2532-2536
78. Sun, S. C., Ganchi, P. A., Ballard, D. W., and Greene, W. C. (1993) *Science* **259**, 1912-1915
79. Scott, M. L., Fujita, T., Liou, H. C., Nolan, G. P., and Baltimore, D. (1993) *Genes Dev.* **7**, 1266-1276
80. de Martin, R., Vanhove, B., Cheng, Q., Hofer, E., Csizmadia, V., Winkler, H., and Bach, F. H. (1993) *EMBO J.* **12**, 2773-2779
81. Schwamborn, J., Lindecke, A., Elvers, M., Horejschi, V., Kerick, M., Rafigh, M., Pfeiffer, J., Prullage, M., Kaltschmidt, B., and Kaltschmidt, C. (2003) *BMC. Genomics* **4**, 46
82. Wuyts, W. A., Vanaudenaerde, B. M., Dupont, L. J., Demedts, M. G., and Verleden, G. M. (2003) *Respir. Med.* **97**, 811-817
83. Ai, W., Liu, Y., Langlois, M., and Wang, T. C. (2004) *J. Biol. Chem.* **279**, 8684-8693

84. Van Huffel, S., Delaei, F., Heyninck, K., De Valck, D., and Beyaert, R. (2001) *J. Biol. Chem.* **276**, 30216-30223
85. Shiozaki, E. N., Chai, J., Rigotti, D. J., Riedl, S. J., Li, P., Srinivasula, S. M., Alnemri, E. S., Fairman, R., and Shi, Y. (2003) *Mol. Cell* **11**, 519-527

Table I

HUVEC genes that increase following treatment with VEGF₁₂₁/rGel for 24 hours, compared to untreated cells

Gene classification	Accession number	Symbol	Gene	Mean fold change
Cell adhesion	H39560	SELE	E-selectin (endothelial adhesion molecule 1) ^a	94.6
	H07071	VCAM	Vascular cell adhesion molecule 1	4.9
	AA284668	PLAU	Plasminogen activator, urokinase	2.3
Apoptosis	AA476272	TNFAIP3	Tumor necrosis factor alpha-induced protein 3 ^a	13.5
	H48706	BIRC3	baculoviral IAP repeat-containing 3	3.3
Transcription regulation	T99236	JUNB	jun B proto-oncogene	4.9
	W55872	NF-κB1α	nuclear factor of kappa light polypeptide gene enhancer in B-cells inhibitor, alpha ^a	4.8
	AA451716	NF-κB1	nuclear factor of kappa light polypeptide gene enhancer in B-cells 1 (p105)	2.3
	H45711	KLF4	Kruppel-like factor 4	2.3
Chemotaxis	AA425102	SCYA2	small inducible cytokine A2 (MCP-1) ^a	20.2
	H62985	SCYA4	small inducible cytokine A4 (MIP-1β)	5.8
	AA040170	SCYA7	small inducible cytokine A7 (MCP-3)	5.5
	T62491	CXCR4	chemokine (C-X-C motif), receptor 4 (fusin)	1.85
Structural organization	NM004856	KNSL5	kinesin-like 5 (mitotic kinesin-like protein 1)	6.4
	AA479199	NID2	nidogen 2	3.1
	AA453105	H2AFL	H2A histone family, member L	2.5
Inflammatory response	W69211	SCYA11	small inducible cytokine A11 (Cys-Cys) (eotaxin)	8.4
	NM_001964	EGR1	early growth response 1	3.9
	NM_000963	PTGS2	prostaglandin-endoperoxide synthase 2 (COX-2)	3.3
	AA148736	SCD4	syndecan 4 (amphiglycan, ryudocan)	3.2
Signalling	W65461	DUSP5	dual specificity phosphatase 5 (MKP-1)	2.7
Metabolic	AA011215	SAT	spermidine/spermine N1-acetyltransferase	2.1

^a Confirmed by RT-PCR at 4 and 24 h posttreatment

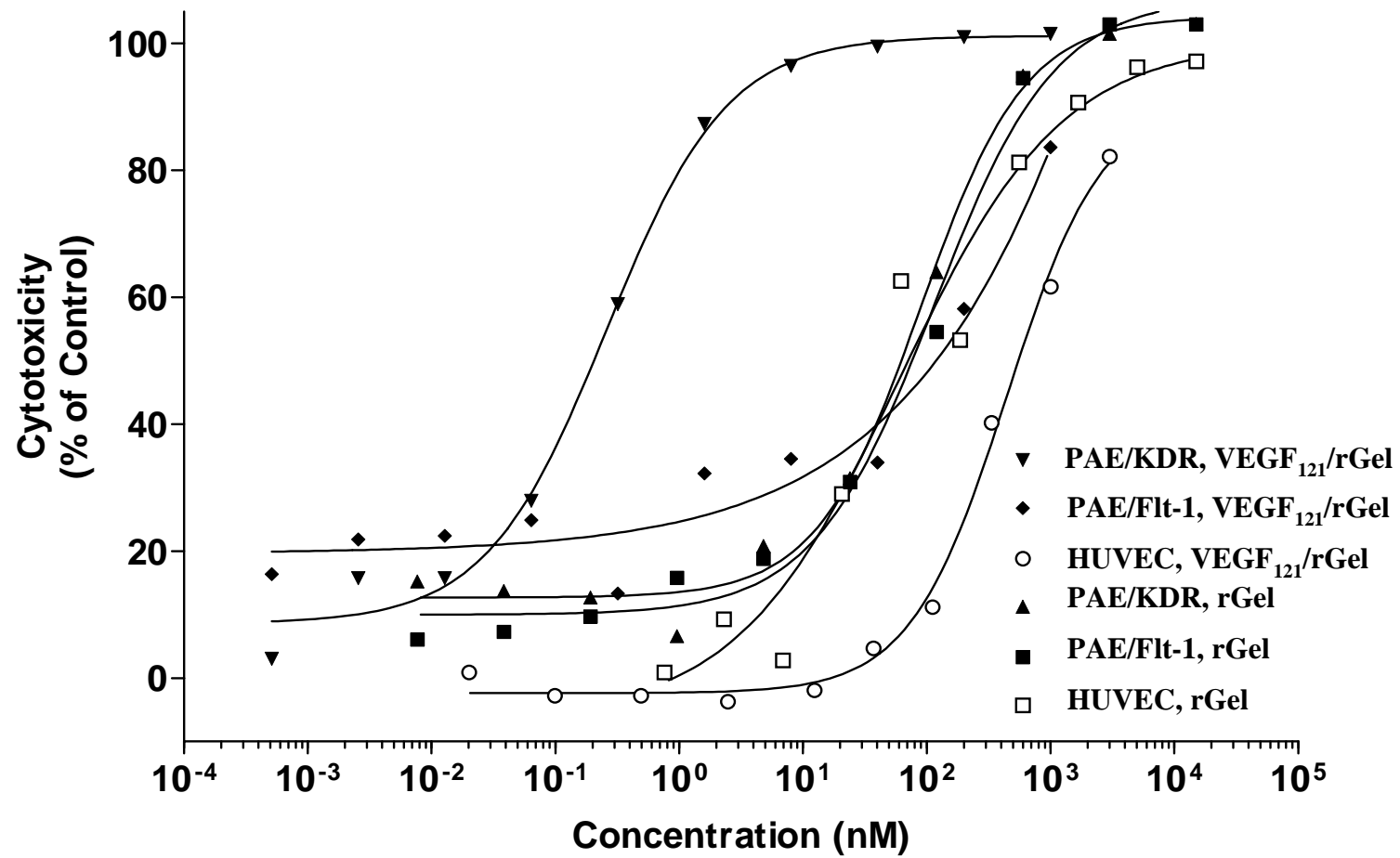


Figure 1

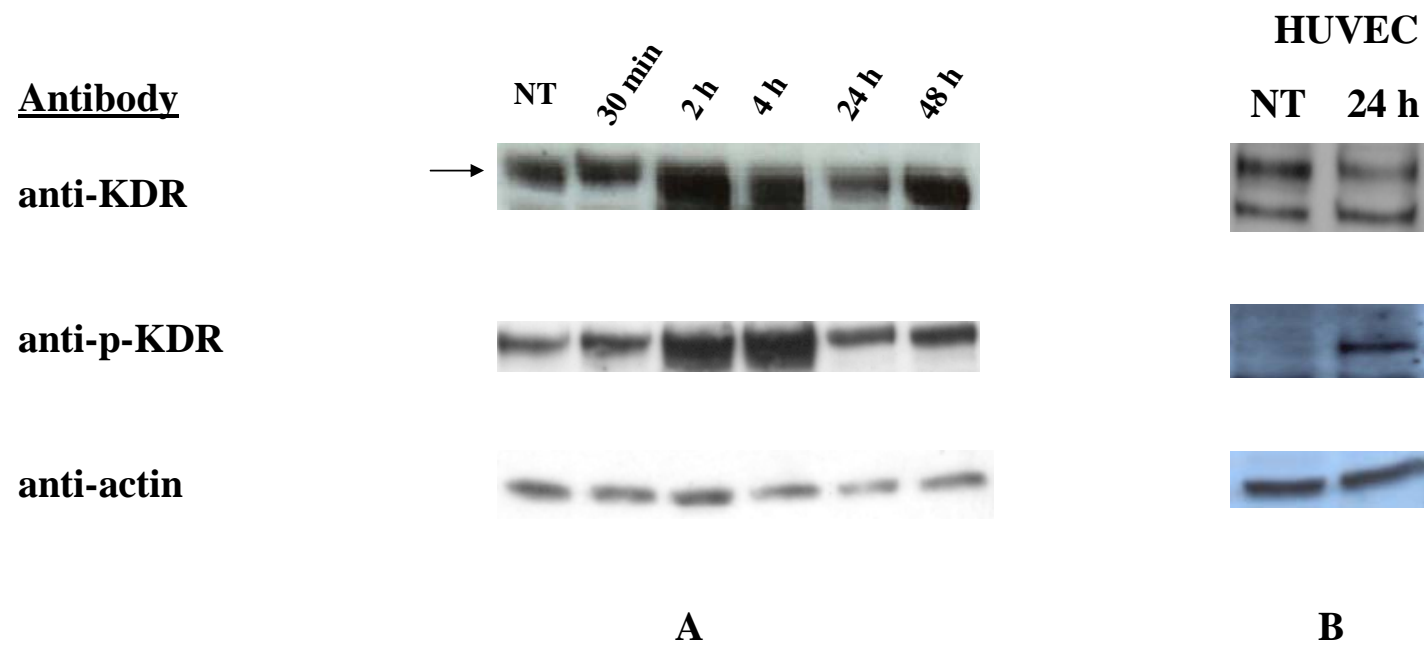
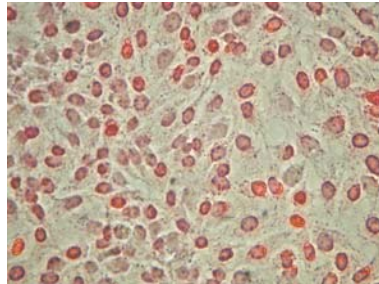
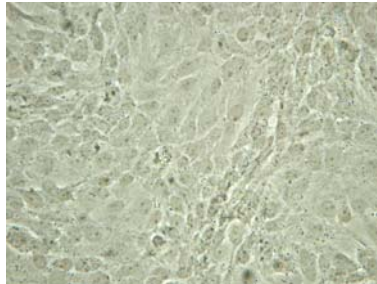


Figure 2

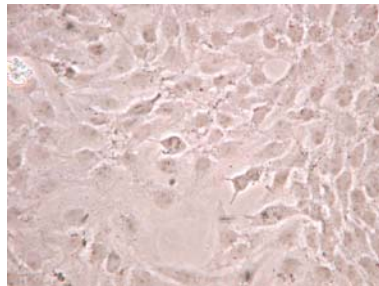
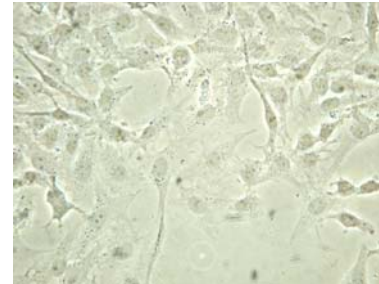
Positive Control



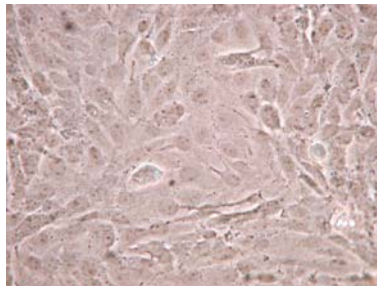
NT



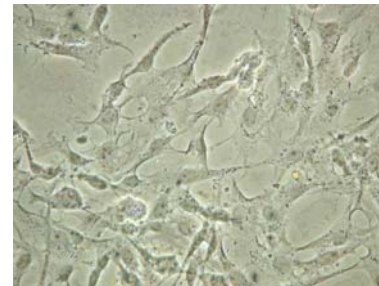
48 h



Negative Control



24 h



72 h

Figure 3

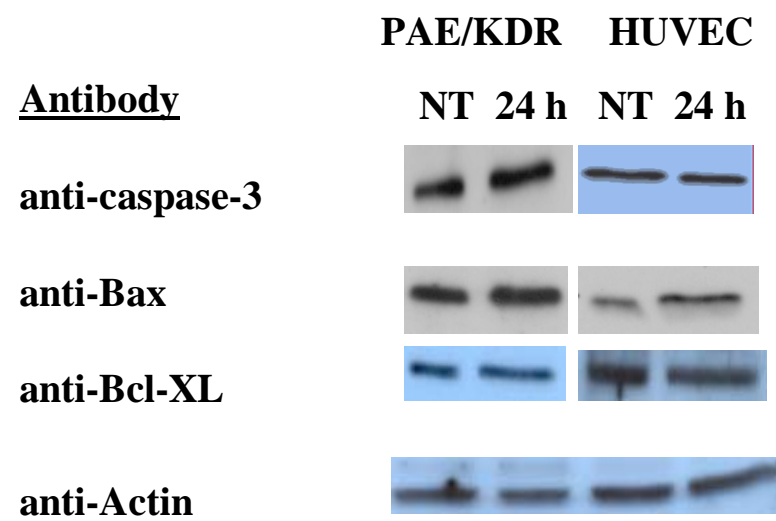
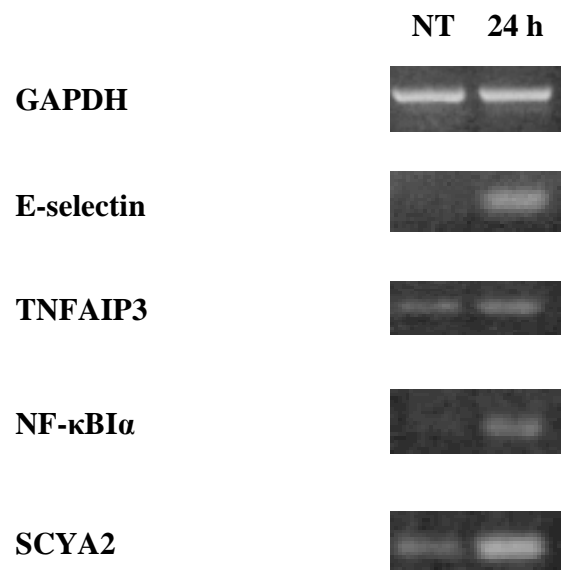


Figure 4



A



B

Figure 5

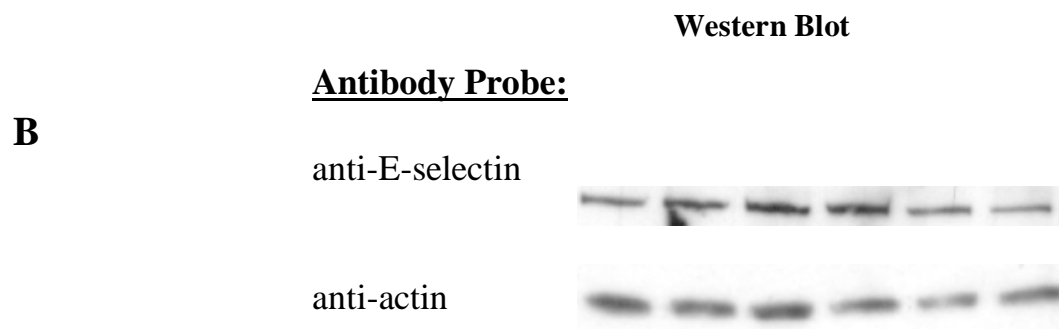
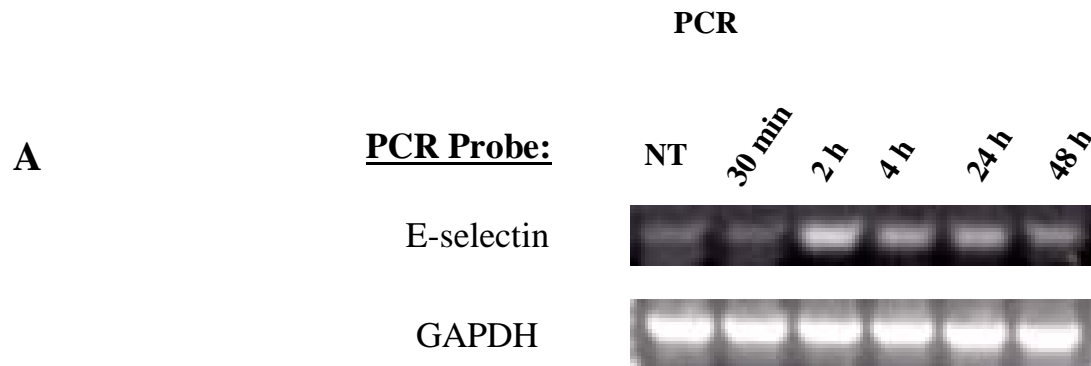


Figure 6

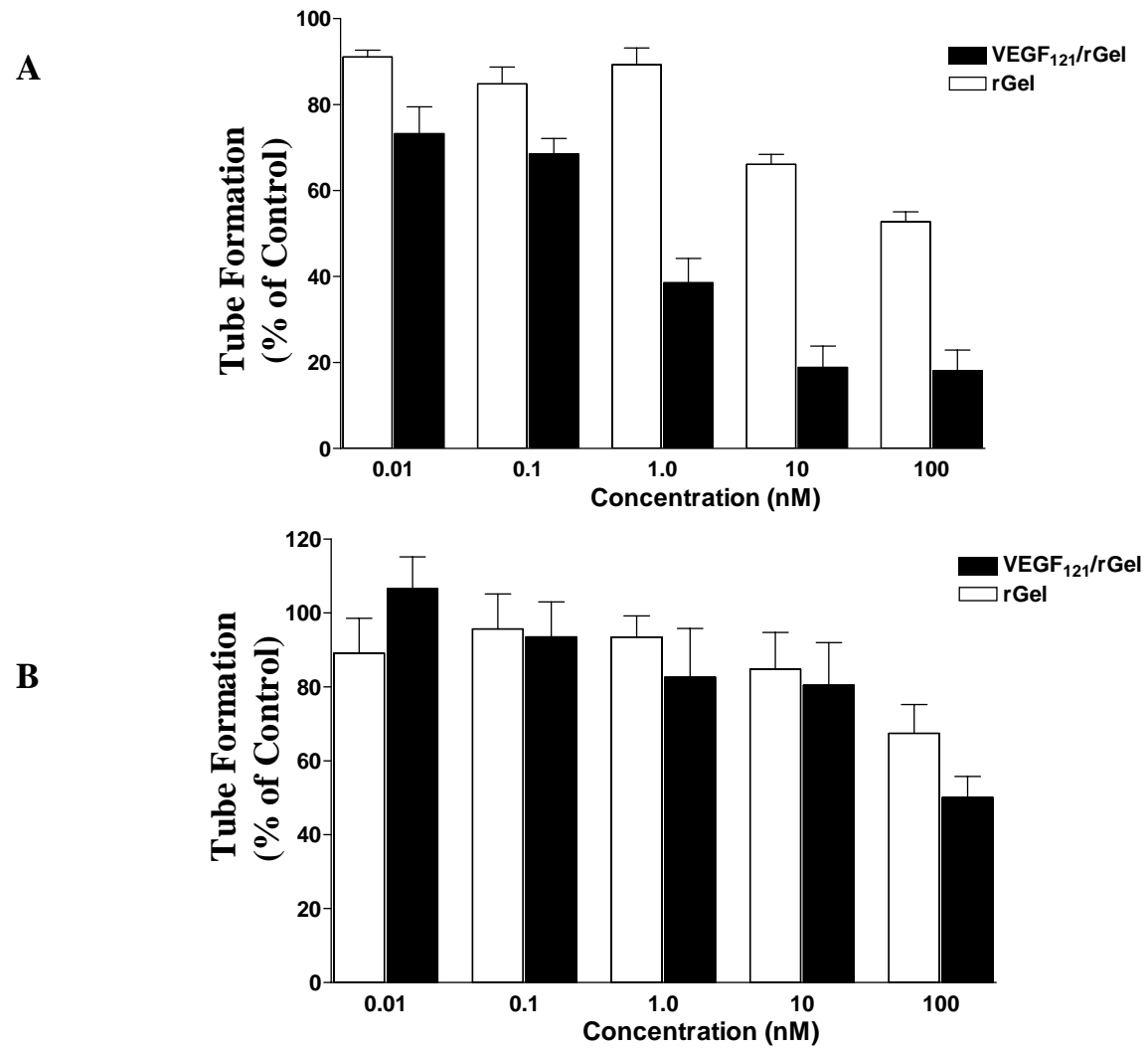


Figure 7

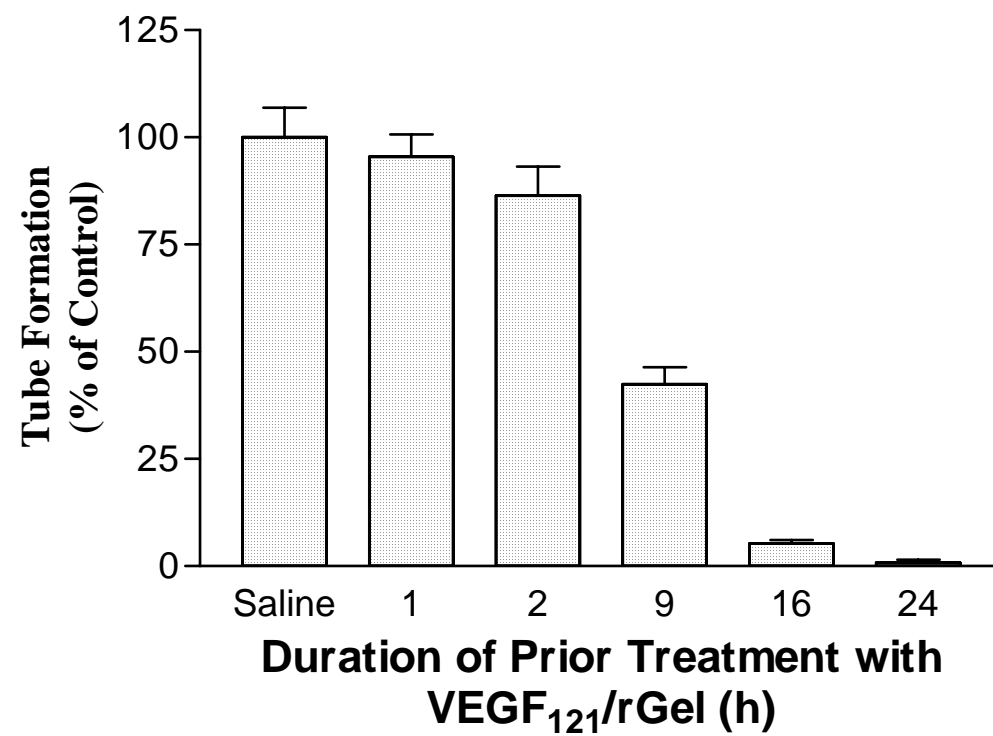
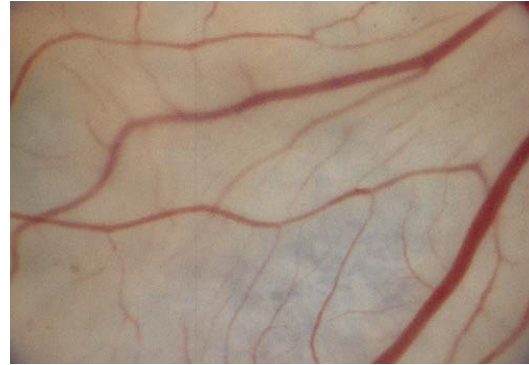


Figure 8

A



B



C

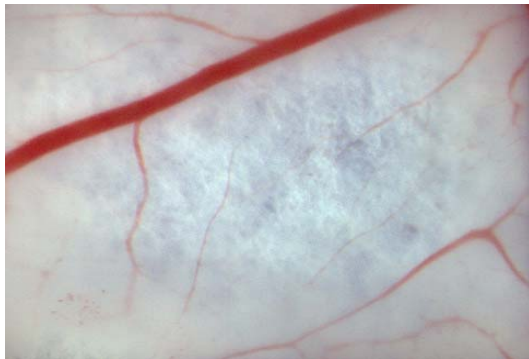


Figure 9

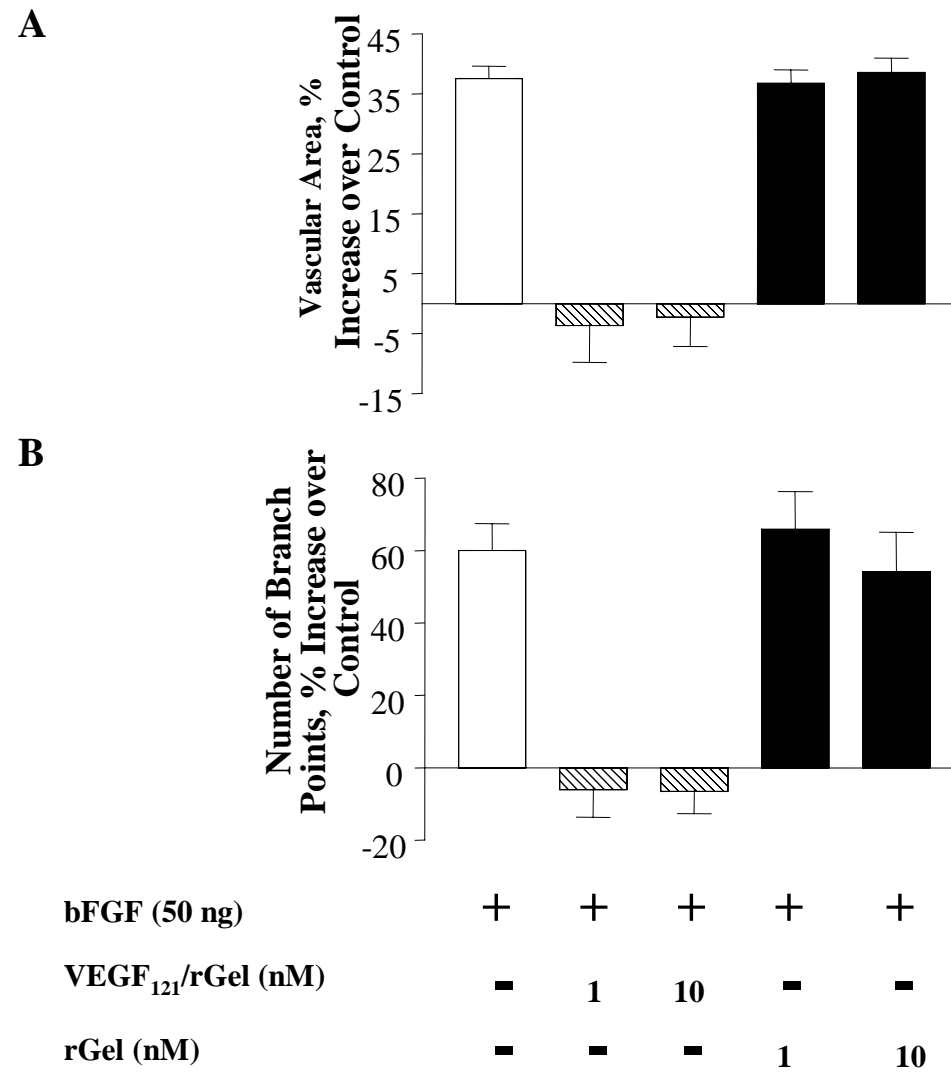


Figure 10

**MECHANISTIC AND INTERNALIZATION STUDIES OF VEGF₁₂₁/rGEL:
CYTOTOXICITY ON ENDOTHELIAL CELLS MEDIATED BY VEGFR2 BUT NOT BY
VEGFR1**

Khalid A. Mohamedali¹, Sophia Ran⁴, Lawrence Cheung¹, John W. Marks¹, Walter N.
Hittelman², Johannes Waltenberger⁵, Philip Thorpe³, Michael G. Rosenblum^{1*}

Running Title: VEGF₁₂₁/rGel cytotoxicity mediated by VEGFR2

*Author to whom correspondence and requests for reprints should be addressed.

Departments of ¹Bioimmunotherapy and ²Experimental Therapeutics, The University of Texas
M. D. Anderson Cancer Center, 1515 Holcombe Blvd., Unit 44, Houston, TX 77030, USA,

Tel: 713-792-3554, Fax: 713-794-4261 or 713-745-3916.

E-mail: mrosenbl@notes.mdacc.tmc.edu)

³Department of Pharmacology, Simmons Comprehensive Cancer Center, University of Texas
Southwestern Medical Center, Dallas, TX

⁴Department of Microbiology and Immunology, Southern Illinois University, School of
Medicine, Springfield, IL

⁵Department Internal Medicine II, Ulm University Medical Center, Ulm, Germany

Keywords: fusion toxin, vascular targeting, gelonin, VEGF, KDR

Journal Category: Cancer Cell Biology

Research conducted, in part, by the Clayton Foundation for Research.

Research supported by DAMD 17-02-1-0457 and NIH/NCI P30 CA16672.

ABSTRACT

We have previously reported that the chimeric fusion toxin VEGF₁₂₁/rGel targets the neovasculature of solid tumors. Although both receptors for VEGF₁₂₁, namely VEGFR1 (FLT-1) and VEGFR2 (KDR/Flk-1) are over-expressed on the endothelium of tumor vasculature, our *in vitro* studies have shown VEGF₁₂₁/rGel to be cytotoxic to log-phase and confluent cells over-expressing KDR (IC₅₀ = 0.5 nM) but not FLT-1 (IC₅₀ = 300 nM), compared to gelonin alone (IC₅₀ = 300 nM). The biological effect of VEGF₁₂₁/rGel on endothelial cells transfected with KDR or FLT-1 was analyzed by cell ELISA, western blotting, and immunofluorescence. The mechanism of cytotoxicity was investigated by TUNEL. VEGF₁₂₁/rGel binds to both PAE/KDR and PAE/FLT-1 cells. Incubation of PAE/KDR and PAE/FLT-1 cells with ¹²⁵I-VEGF₁₂₁/rGel demonstrated specific binding of the fusion toxin that was competed with unlabeled VEGF₁₂₁/rGel but not with unlabeled gelonin. Immunofluorescence of PAE/KDR and PAE/FLT-1 cells incubated with VEGF₁₂₁/rGel shows internalization of VEGF₁₂₁/rGel into PAE/KDR cells within one hour of treatment. In contrast, VEGF₁₂₁/rGel was not detected in PAE/FLT-1 cells up to 24 hours after treatment. The mechanism of VEGF₁₂₁/rGel-induced cytotoxicity was necrotic rather than apoptotic since treated cells were TUNEL-negative and we found no evidence of PARP cleavage. Thus, while VEGF₁₂₁/rGel binds to both FLT-1 and KDR, internalization of VEGF₁₂₁/rGel is mediated only by KDR and not by FLT-1 receptors. VEGF₁₂₁/rGel is an important molecule useful to probe the biology of KDR and FLT-1 receptors and may be effective as a therapeutic agent targeting tumor neovasculature.

INTRODUCTION

Angiogenesis is a hallmark of cancer. Vascular endothelial growth factor-A (VEGF-A) plays a key role as the primary stimulant of vascularization in solid tumors⁽¹⁻³⁾. VEGF-A enhances endothelial cell proliferation, migration, and survival⁽³⁻⁶⁾ and is essential for blood vessel formation⁽⁷⁾. Other roles of VEGF include wound healing⁽⁸⁾, vascular permeability and the regulation of blood flow⁽⁹⁻¹¹⁾. The VEGF-A family of isomers range from 121 to 206 amino acids in length with varying receptor and heparin binding affinities as a result of alternate splicing⁽¹²⁻¹⁵⁾.

VEGF is released by a variety of tumor cells and studies have demonstrated that the VEGF receptor KDR/Flk-1, over-expressed on the endothelium of tumor vasculature, is primarily responsible for mediating the tumor neovascularization properties of VEGF. KDR/Flk-1 is almost undetectable in the vascular endothelium of adjacent normal tissues. VEGF₁₂₁ exists in solution as a disulfide linked homodimer and binds to KDR and FLT-1 in a heparin-independent manner. It does not bind neuropilin-1 or neuropilin-2. VEGF₁₂₁ has been shown to contain the full biological activity of the larger variants.

We have previously defined a novel fusion construct of VEGF₁₂₁ and the highly cytotoxic plant toxin Gelonin (rGel). Gelonin is a 28.5 kDa single-chain toxin with a mechanism of action similar to that of ricin A-chain. The VEGF₁₂₁/rGel fusion toxin was shown to be highly cytotoxic to endothelial cells that over-express the KDR/Flk-1 receptor, but not to cells that over-express the FLT-1 receptor⁽¹⁶⁾, even though VEGF₁₂₁ binds to FLT-1 with affinity in the picomolar range⁽¹⁴⁾. In this report, we extend our initial findings and further characterize the biological effects of this fusion toxin on endothelial cells, determine the binding profile of VEGF₁₂₁/rGel to receptors expressed on the cell surface, as well as investigate the internalization VEGF₁₂₁/rGel

into endothelial cells.

MATERIAL AND METHODS

Materials

Bacterial strains, pET bacterial expression plasmids and recombinant enterokinase were obtained from Novagen (Madison, WI). All other chemicals were from Sigma Chemical Company (St. Louis, MO) or Fisher Scientific (Pittsburgh, PA). TALON metal affinity resin was obtained from Clontech laboratories (Palo Alto, CA). Other chromatography resin and materials were from Pharmacia Biotech (Piscataway, NJ). Endothelial cell growth supplement (ECGS) from bovine neural tissue was obtained from Sigma Chemical Company. Murine brain endothelioma (bEnd.3) cells were provided by Professor Werner Risau (Max Plank Institute, Munich, Germany). Tissue culture reagents were from Gibco BRL (Gaithersburg, MD) or Mediatech Cellgro (Herndon, VA). Rabbit anti-gelonin antisera was obtained from the Veterinary Medicine Core Facility at MDACC. Anti-flt-1 (sc-316), anti-flk-1 (sc-504), and anti-PARP (sc-8007) antibodies were purchased from Santa Cruz Biotechnology, Inc. (Santa Cruz, CA).

Cell culture

Porcine aortic endothelial cells transfected with the KDR receptor (PAE/KDR) or the FLT-1 receptor (PAE/FLT-1) were a generous gift from Dr. J. Waltenberger. KDR and FLT-1 receptor sites per cell have been previously determined.¹⁶⁻¹⁷ Cells were maintained as a monolayer in F12 Nutrient Media (HAM) supplemented with 100 units/ml penicillin, 100 units/ml streptomycin, and 10% fetal bovine serum and passaged twice weekly. Cells were harvested by treatment with Versene (0.02% EDTA).

Purification of VEGF₁₂₁/rGel

Construction and purification of VEGF₁₂₁/rGel was essentially as described, with minor modifications.¹⁵ E. coli cells were lysed with 100 ml 0.1mm glass beads (BioSpec Products, Inc) in a Bead Beater (BioSped Products, Inc) for eight cycles of 3 minutes each. The lysate was ultracentrifuged at 40,000 rpm for 90 minutes at 4°C. The supernatant was carefully collected and adjusted to 40 mM Tris-HCl (pH 8.0), 300 mM NaCl, and incubated at 4°C with metal affinity resin. The resin was washed with 40 mM Tris-HCl (pH 8.0), 0.5 M NaCl buffer containing 5 mM Imidazole and eluted with buffer containing 100 mM Imidazole. After pooling fractions containing VEGF₁₂₁/rGel, the sample was dialyzed against 20 mM Tris (pH 8.0), 200 mM NaCl and digested with recombinant Enterokinase at room temperature. Enterokinase was removed by agarose-linked soybean trypsin inhibitor. Other proteins of non-interest were removed by Q Sepharose Fast Flow resin and metal affinity resin as described previously.¹⁵ VEGF₁₂₁/rGel was concentrated and stored in sterile PBS at -20°C.

Rabbit reticulocyte lysate assay

The functional activity of rGel and VEGF₁₂₁/rGel were assayed using a cell-free protein translation inhibition assay kit from Amersham Biotech (Arlington Heights, IL) as described by the manufacturer.

ELISA analysis

The ability of the chimeric fusion protein to bind to Flk-1 was tested on microtiter plates coated with soluble mouse Flk-1. All steps of the ELISA procedure were performed at room temperature unless stated otherwise. Plates were treated with 2 µg/ml of NeutrAvidin (Pierce,

Rockford, IL) for 6 h. The extracellular domain of Flk-1 was expressed in Sf9 cells, purified to homogeneity,¹⁸ and biotinylated. Biotinylated receptor (1 µg/ml) was incubated with NeutrAvidin-coated wells for 2 h. VEGF₁₂₁ or VEGF₁₂₁/rGel was added to the wells at concentrations ranging from 0.002 to 2 nM in the presence of 2% BSA diluted in PBS or normal mouse serum. After 2 h of incubation, plates were washed and incubated with non-blocking mouse monoclonal anti-VEGF antibody, 2C3¹⁹ or rabbit polyclonal anti-gelonin IgG. For competition studies of VEGF₁₂₁/rGel and VEGF₁₂₁, binding of the VEGF₁₂₁/rGel fusion protein was detected using a rabbit anti-gelonin antibody. In competition experiments, a 10-fold molar excess of VEGF₁₂₁ was premixed with VEGF₁₂₁/rGel before it was added to the plate. Mouse and rabbit IgG were detected by HRP-labeled goat anti-mouse and anti-rabbit antibodies, respectively (Daco, Carpinteria, CA). Peroxidase activity was measured by adding O-phenylenediamine (0.5 mg/ml) and hydrogen peroxide (0.03% v/v) in citrate-phosphate buffer (pH 5.5). The reaction was stopped by addition of 100 µl of 0.18 M of H₂SO₄. The absorbance was read at 490 nM. Presence of KDR and FLT-1 on cells was tested as follows: 50,000 cells (PAE/KDR or PAE/FLT-1) were aliquoted per well and dried overnight at 37°C. Non-specific binding sites were blocked for 1 hour with 5% BSA. Wells were treated with anti-KDR or anti-FLT-1 antibodies, followed by incubation with HRP-conjugated secondary antibody (1:5000) for 1 hour.

Western blot analysis

Whole cell lysates of PAE/KDR and PAE/FLT-1 cells were obtained by lysing cells in Cell Lysis buffer (50 mM Tris, pH 8.0, 0.1 mM EDTA, 1 mM DTT, 12.5 mM MgCl₂, 0.1 M KCl, 20% glycerol) supplemented with protease inhibitors (leupeptin (0.5%), aprotinin (0.5%) and

PMSF (0.1%). Protein samples were separated by SDS-PAGE under reducing conditions and electrophoretically transferred to a PVDF memberane overnight at 4 °C in transfer buffer (25 mM Tris-HCl, pH 7.6, 190 mM glycine, 20% HPLC-grade methanol). The samples were analyzed for KDR with rabbit anti-flk-1 polyclonal antibody and FLT-1 using an anti-flt-1 polyclonal antibody. The membranes were then incubated with goat-anti-rabbit IgG horseradish peroxidase (HRP) developed using the Amersham ECL detection system and exposed to X-ray film.

Immunoprecipitation

Cells were lysed as described (see Western protocol). 500 µg MDA-MB-231 and L3.6pl cell lysates were mixed with 2 µg anti-flk-1 antibody in a final volume of 250 µl and incubated for two hours at 4°C. 100 µg PAE/KDR and PAE/FLT-1 cell lysates were immunoprecipitated as controls. The mixtures were then incubated overnight with 20 µl Protein A beads that had been blocked with 5% BSA. The beads were washed 4 times in lysis buffer and the samples, along with 30 µg PAE/KDR cell lysate, were run on a gel, transferred overnight onto a PVDF membrane and probed using an anti-flk-1 polyclonal antibody.

Binding of radiolabeled VEGF₁₂₁/rGel to PAE/KDR and PAE/FLT-1 cells

100 µg of VEGF₁₂₁/rGel was radiolabeled with 1mCi of NaI¹²⁵ using Chloramine T²⁰ for a specific activity of 602 Ci/mMol. Cells were grown overnight in 24-well plates. Non-specific binding sites were blocked for 30 minutes with PBS/0.2% gelatin followed by incubation for 4 hours with ¹²⁵I-VEGF₁₂₁/rGel in PBS/0.2% gelatin solution. For competition experiments, cold VEGF₁₂₁/rGel or gelonin were pre-mixed with ¹²⁵I-VEGF₁₂₁/rGel. Cells were washed four times with PBS/0.2% gelatin solution, detached and bound cpm was measured.

Cytotoxicity of VEGF₁₂₁/rGel and rGel

Cytotoxicity of VEGF₁₂₁/rGel and rGel against log phase PAE/KDR cells was performed as described.¹⁵ Cells were grown in 96 well flat-bottom tissue culture plates. Purified VEGF₁₂₁/rGel and rGel were diluted in culture media and added to the wells in 5-fold serial dilutions. Cells were incubated for 72 hours. The remaining adherent cells were stained with crystal violet (0.5% in 20% methanol) and solubilized with Sorenson's buffer (0.1 M sodium citrate, pH 4.2 in 50% ethanol). Absorbance was measured at 630 nm. To assess if the activity of VEGF₁₂₁/rGel was affected by the exposure time to endothelial cells, log-phase PAE/KDR cells were grown and treated with VEGF₁₂₁/rGel as above. Media containing the cytotoxic agent was removed at varying time-points and the cells were washed once with 200 µl culture media. Fresh culture media was added to the wells and the cells were then returned to the incubator. Seventy-two hours after the start of the experiment, the number of remaining adherent cells was assessed using crystal violet and Sorensen's buffer as described above.

Internalization of VEGF₁₂₁/rGel into PAE/KDR cells

PAE/KDR and PAE/FLT-1 cells were incubated with 4 µg/ml VEGF₁₂₁/rGel at the timepoints indicated. Glycine buffer (500 mM NaCl, 0.1 glycine, pH 2.5) was used to strip the cell surface of non-internalized VEGF₁₂₁/rGel. Cells were fixed with 3.7% formaldehyde and permeabilized with 0.2% Triton X-100. Non-specific binding sites were blocked with 5% BSA in PBS. Cells were then incubated with a rabbit anti-gelonin polyclonal antibody (1:200) followed by a TRITC-conjugated anti-rabbit secondary antibody (1:80). Nuclei were stained with propidium iodide (1µg/ml) in PBS. The slides were fixed with DABCO media, mounted and

visualized under fluorescence (Nikon Eclipse TS1000) and confocal (Zeiss LSM 510) microscopes.

TUNEL assay

Log phase PAE/KDR and PAE/FLT-1 cells were diluted to 2000 cells/100 μ l. Aliquots (100 μ l) were added in 16-well chamber slides (Nalge Nunc International) and incubated overnight at 37°C with 5% CO₂. Purified VEGF₁₂₁/rGel was diluted in culture media and added at 72, 48 and 24-hour time points at a final concentration of 1 nM (twice the IC₅₀). The cells were then processed and analyzed for TUNEL as described by the manufacturer of the reagent. Positive control cells were incubated with 1mg/ml DNase for 10 minutes at 37°C.

PARP cleavage

Effects of VEGF₁₂₁/rGel on PARP-mediated apoptosis were investigated by pre-incubating PAE/KDR cells with 100 mM Na₂VO₄ for 5 minutes at 37°C followed by stimulation with VEGF₁₂₁/rGel or VEGF₁₂₁ for 5 minutes, 30 minutes, 4 h, 24 h and 48 h. Cells were washed and lysed and the cell lysate was analyzed by Western using an anti-PARP antibody.

RESULTS

We have previously demonstrated the successful use of VEGF₁₂₁/rGel fusion construct for the targeted destruction of tumor vasculature *in vivo*.

Biological activity of the rGel component

The ability of VEGF₁₂₁/rGel and rGel to inhibit translation in a cell-free system was determined by using a rabbit reticulocyte translation assay (Fig. 2). The purified VEGF₁₂₁/rGel and rGel had IC₅₀ values of 47 and 234 pM, respectively, showing that fusion of rGel and VEGF₁₂₁ did not reduce the activity of the toxin component.

Binding of VEGF₁₂₁/rGel to soluble Flk-1 receptor

The fusion protein was tested for its ability to bind to the Flk-1 receptor by ELISA. The extra-cellular domain of recombinant Flk-1 was purified, biotinylated and incubated with wells coated with NeutrAvidin. The receptor was treated with VEGF₁₂₁ or VEGF₁₂₁/rGel, and binding of the ligand to the receptor was assessed by anti-VEGF and anti-gelonin antibodies. (Fig. 3) shows that VEGF₁₂₁/rGel and native human VEGF₁₂₁ bind equally well to Flk-1 at all concentrations, indicating that the VEGF component of the fusion protein is fully capable of binding to Flk-1. To confirm that the binding of VEGF₁₂₁/rGel to Flk-1 was specific, free VEGF₁₂₁ (10-fold molar excess) was used to compete with VEGF₁₂₁/rGel for binding to the receptor, followed by detection of VEGF₁₂₁/rGel binding by an anti-gelonin antibody. Binding of VEGF₁₂₁/rGel to the Flk-1 extra-cellular domain was dramatically reduced in the presence of VEGF₁₂₁ (Fig. 4) indicating that the VEGF₁₂₁ domain of the fusion toxin retained activity and that binding to the receptor was specific.

VEGF₁₂₁/rGel binds to both KDR and FLT-1

VEGF₁₂₁ has been shown to bind to the FLT-1 receptor with greater affinity than to KDR.¹⁴ Because cytotoxicity of VEGF₁₂₁/rGel to KDR-expressing cells was found to be nearly 600-fold

greater than for FLT-1 expressing cells, we investigated the relative binding of VEGF₁₂₁/rGel to PAE cells expressing each of the receptors. ELISA analysis was performed to confirm the expression of both receptors on the cell surface using receptor-specific antibodies (data not shown). Expression of VEGFR-1 (FLT-1) and VEGFR-2 (KDR) was confirmed by western blot (Fig. 5a). In order to confirm that VEGF₁₂₁/rGel bound to human VEGFR-1 and VEGFR-2 and that the presence of recombinant gelonin did not interfere with the binding properties of VEGF₁₂₁, we investigated the binding of radiolabeled VEGF₁₂₁/rGel to both KDR and FLT-1 receptors expressed on the surface of PAE cells. Our results (Fig. 5b) show that the binding of ¹²⁵I-VEGF₁₂₁/rGel to both cells was nearly identical. In order to confirm that the binding on the cell surface was receptor-specific, competition studies of ¹²⁵I-VEGF₁₂₁/rGel with unlabeled VEGF₁₂₁/rGel and rGel were performed. Binding of VEGF₁₂₁/rGel to both PAE/KDR and PAE/FLT-1 cells was competed by unlabeled VEGF₁₂₁/rGel but not by unlabeled gelonin indicating that binding of VEGF₁₂₁/rGel was mediated by VEGF₁₂₁ and, therefore, receptor-specific.

Internalization of VEGF₁₂₁/rGel into PAE/KDR and PAE/FLT-1 cells

We investigated the internalization of VEGF₁₂₁/rGel into PAE/KDR and PAE/FLT-1 cells using immunofluorescence staining. Cells were attached, treated with VEGF₁₂₁/rGel or rGelonin at various time points, and internalized VEGF₁₂₁/rGel or rGelonin was visualized by treating cells with polyclonal rabbit anti-gelonin primary antibody and FITC-conjugated secondary antibody. VEGF₁₂₁/rGel was detected in PAE/KDR cells within 1 hour of treatment with the immunofluorescence signal progressively increasing to 24 hours (Fig. 6). As expected, cell density also decreased over the 24 hour time period. No VEGF₁₂₁/rGel was detected in

PAE/FLT-1 cells up to 24 hours after treatment with the fusion toxin. Treatment of cells with the same concentration of rGelonin showed no internalization (data not shown), confirming that entry of VEGF₁₂₁/rGel into PAE cells was specifically via the KDR receptor.

Exposure duration of VEGF₁₂₁/rGel on endothelial cells

The IC₅₀ of VEGF₁₂₁/rGel incubated for 72 hours on log-phase PAE/KDR cells has been shown to be about 1 nM.¹⁵ However, VEGF₁₂₁/rGel internalizes into these cells within one hour of incubation. To study the cytotoxic effect of VEGF₁₂₁/rGel as a function of exposure time of this agent on endothelial cells, we incubated cells with VEGF₁₂₁/rGel from 1-72 hours and assessed its cytotoxicity on PAE/KDR cells at the end of the 72-hour period. While VEGF₁₂₁/rGel retained cytotoxicity even after a one-hour incubation, appreciable cytotoxicity was observed after 24 hours and maximal cytotoxic effect of VEGF₁₂₁/rGel on PAE/KDR cells was observed after 48 hours (Fig. 7). The cytotoxic effect of VEGF₁₂₁/rGel on PAE/FLT-1 cells was also affected as a function of exposure duration (data not shown).

TUNEL assay and PARP cleavage

In order to investigate the mechanism of cytotoxicity of VEGF₁₂₁/rGel to PAE/KDR cells, we performed a TUNEL assay for 24, 48 and 72 hours. No TUNEL staining was observed with PAE/KDR cells exposed to VEGF₁₂₁/rGel up to 72 hours (Fig. 8). In contrast nuclei of positive control cells showed intense staining, indicating that the mechanism of cytotoxicity of VEGF₁₂₁/rGel is not apoptotic. PARP cleavage was tested on PAE/KDR cells by treating cells with VEGF₁₂₁/rGel or VEGF₁₂₁ for periods ranging from 5 minutes to 48 hours. Western blot

analysis of these cells by an anti-PARP antibody shows that VEGF₁₂₁/rGel did not activate PARP-mediated apoptosis (Fig. 9).

DISCUSSION

Agents targeting the neovascularization process in tumors have significant potential for therapeutic impact. Molecules which interfere with the growth and development of vascular endothelial cells by targeting the VEGF/receptor complex have an additional advantage since these agents do not have to penetrate into the tumor parenchyma and the receptor targets are expressed on the luminal surface of tumor vascular endothelium.

Although this study demonstrates that the VEGF₁₂₁/rGel fusion can bind to both the KDR and FLT-1 receptors, we found that only endothelial cells which express KDR were able to internalize the construct thereby delivering the toxin component to the cytoplasmic compartment. This property of the fusion protein has targeting advantages that can be exploited. Zeng et al.³ suggest that it is the interaction of VEGF with the KDR receptor but not the FLT-1 receptor which is responsible for the growth proliferative signal on endothelial cells and other studies suggest that the KDR receptor is primarily responsible for mediating the vascular permeability effects of VEGF-A.²¹ Studies suggest that the FLT-1 receptor can modulate signaling of the KDR receptor³ and may impact monocyte response to VEGF,²² but its role in neovascularization has not been well defined.

The possible binding of VEGF-containing constructs to the neuropilin receptor could be a source of unwanted toxicity and mis-targeting of the complex, however, studies by Gluzman-Poltorak et al.²³ have demonstrated that the VEGF₁₂₁ fragment as opposed to other forms of VEGF-A does not appear to bind to this receptor.

Another important aspect of this study was the observation that the cytotoxic effects of the construct on vascular endothelial cells did not involve an apoptotic mechanism. This is in sharp contrast to studies of other toxins such as ricin A chain (RTA) and pseudomonas exotoxin (PE) which demonstrate generation of apoptotic effects which appear to be mediated, at least in part, by caspase activation.²⁴⁻²⁶ Recently, Keppler-Hafkemeyer, et al.²⁷ have suggested that PE toxins may generate cytotoxic effects through both caspase-dependant and protein synthesis inhibitory mechanisms. Despite the sequence homology of RTA and rGel²⁸ and the known similarities in their mechanism of action,²⁹⁻³⁰ it appears that these two toxins differ in their pro-apoptotic effects. One possible explanation for the observed differences in apoptotic effects between RTA and rGel toxin could be in the cell types examined. The cells targeted in the current study of rGel are non-transformed endothelial cells while those in the RTA study were tumor cells.

The exposure duration studies for the VEGF₁₂₁/rGel fusion toxin demonstrate that as little as 1 hr exposure to target cells is required to develop a cytotoxic effect 72 hrs later. However, continual exposure for up to 48 hrs was shown to improve the cytotoxic effect by almost 10-fold. Should pharmacokinetic studies demonstrate a relatively short plasma half-life for this agent, this may suggest that optimal therapeutic effect could be achieved by maintaining blood concentrations of drug at therapeutic concentrations for at least 48 hrs. This could be achieved by frequent interval dosing or continuous infusion but may be important in the development of pre-clinical and clinical dosing strategies.

In conclusion, our results show that the biological effects of VEGF₁₂₁/rGel on cells that over-express KDR, but not on cells that over-express FLT-1, are due to internalization of VEGF₁₂₁/rGel by KDR, but not by FLT-1. This is significant as KDR is the primary VEGF

receptor involved in the tumor neovascularization. VEGF₁₂₁/rGel can play a useful role in delineating the roles of FLT-1 and KDR.

REFERENCES

1. Reference List

1. Dvorak, H. F. (2000) *Semin.Perinatol.* **24**, 75-78
2. Senger, D. R., Van De, W. L., Brown, L. F., Nagy, J. A., Yeo, K. T., Yeo, T. K., Berse, B., Jackman, R. W., Dvorak, A. M., and Dvorak, H. F. (1993) *Cancer Metastasis Rev.* **12**, 303-324
3. Zeng, H., Dvorak, H. F., and Mukhopadhyay, D. (2001) *J.Biol.Chem.* **276**, 26969-26979
4. Bernatchez, P. N., Rollin, S., Soker, S., and Sirois, M. G. (2002) *J.Cell Biochem.* **85**, 629-639
5. Orre, M. and Rogers, P. A. (1999) *Int.J.Cancer* **84**, 101-108
6. Taraseviciene-Stewart, L., Kasahara, Y., Alger, L., Hirth, P., Mc, M. G., Waltenberger, J., Voelkel, N. F., and Tuder, R. M. (2001) *FASEB J.* **15**, 427-438
7. Tomanek, R. J., Holifield, J. S., Reiter, R. S., Sandra, A., and Lin, J. J. (2002) *Dev.Dyn.* **225**, 233-240
8. Van Setten, G. B. (1997) *Acta Ophthalmol.Scand.* **75**, 649-652
9. Hariawala, M. D., Horowitz, J. R., Esakof, D., Sheriff, D. D., Walter, D. H., Keyt, B., Isner, J. M., and Symes, J. F. (1996) *J.Surg.Res.* **63**, 77-82
10. Yang, H. T., Yan, Z., Abraham, J. A., and Terjung, R. L. (2001) *Am.J.Physiol Heart Circ.Physiol* **280**, H1097-H1104
11. Zhang, Z. G., Zhang, L., Jiang, Q., Zhang, R., Davies, K., Powers, C., Bruggen, N., and Chopp, M. (2000) *J.Clin.Invest* **106**, 829-838
12. Guo, P., Xu, L., Pan, S., Brekken, R. A., Yang, S. T., Whitaker, G. B., Nagane, M., Thorpe, P. E., Rosenbaum, J. S., Su Huang, H. J., Cavenee, W. K., and Cheng, S. Y. (2001) *Cancer Res.* **61**, 8569-8577
13. Keyt, B. A., Nguyen, H. V., Berleau, L. T., Duarte, C. M., Park, J., Chen, H., and Ferrara, N. (1996) *J.Biol.Chem.* **271**, 5638-5646
14. Keyt, B. A., Berleau, L. T., Nguyen, H. V., Chen, H., Heinsohn, H., Vandlen, R., and Ferrara, N. (1996) *J.Biol.Chem.* **271**, 7788-7795
15. Whitaker, G. B., Limberg, B. J., and Rosenbaum, J. S. (2001) *J.Biol.Chem.* **276**, 25520-25531
16. Veenendaal, L. M., Jin, H., Ran, S., Cheung, L., Navone, N., Marks, J. W., Waltenberger, J., Thorpe, P., and Rosenblum, M. G. (2002) *Proc.Natl.Acad.Sci.U.S.A* **99**, 7866-7871

FIGURE LEGENDS

Fig. 1. Design and construction of VEGF₁₂₁/rGel. Constructs of the targeting molecule

(VEGF₁₂₁) to the cytotoxic agent (gelonin) were expressed in two orientations, with either

VEGF₁₂₁ or gelonin at the N-terminus. A G4S tether was used to fuse VEGF₁₂₁ and gelonin and reduce steric hindrance.

Fig. 2. Rabbit reticulocyte assay to determine the ability of VEGF₁₂₁/rGel and rGel to inhibit translation in a cell-free system. The fusion of VEGF₁₂₁ and recombinant gelonin does not reduce the activity of the toxin component.

Fig. 3. ELISA demonstrating that VEGF₁₂₁/rGel binds to the receptor. VEGF₁₂₁/rGel, VEGF₁₂₁ and rGel were incubated with biotinylated mouse flk-1 receptor attached to NeutrAvidin-coated plates. Binding was assessed using anti-gelonin and anti-VEGF antibodies.

Fig. 4. Binding to the anchored flk-1 receptor is specific for VEGF₁₂₁/rGel. VEGF₁₂₁/rGel or VEGF₁₂₁ was incubated with flk-1 receptor as described in Materials and Methods. Binding of VEGF₁₂₁/rGel was competed with VEGF₁₂₁ and a rabbit anti-gelonin antibody was used for detection. VEGF₁₂₁ specifically reduced binding of VEGF₁₂₁/rGel to flk-1. VEGF₁₂₁ was not detected by the anti-gelonin antibody (data not shown).

Fig. 5. Expression of KDR and FLT-1. (A) Whole cell lysate (30 µg) of PAE/KDR and PAE/FLT-1 was run on an SDS-PAGE gel, transferred to a PVDF membrane and immunoblotted using the appropriate antibody. Expression of both receptors on their respective cell-lines was confirmed. (B) Receptor-specific binding of radiolabeled VEGF₁₂₁/rGel is demonstrated on cells expressing these receptors. Binding was reduced with unlabeled VEGF₁₂₁/rGel but not by unlabeled gelonin.

Fig. 6. Internalization of VEGF₁₂₁/rGel into PAE/KDR and PAE/FLT-1 cells. PAE/KDR cells were incubated with 4 µg/ml VEGF₁₂₁/rGel at the timepoints indicated. The cell surface was then stripped and internalized VEGF₁₂₁/rGel was visualized by incubating the cells with an anti-gelonin polyclonal antibody (1:200) followed by a FITC-conjugated secondary antibody (1:80).

Nuclei were stained with propidium iodide. VEGF₁₂₁/rGel enters PAE/KDR cells within one hour of treatment. However, PAE/FLT-1 cells did not internalize VEGF₁₂₁/rGel even after 24 hours of incubation with VEGF₁₂₁/rGel.

Fig. 7. Effect of exposure time of VEGF₁₂₁/rGel on PAE/KDR cells on cytotoxicity.

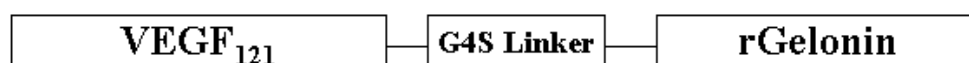
VEGF₁₂₁/rGel was incubated with PAE/KDR cells for varying lengths of time, as described in Materials and Methods. While VEGF₁₂₁/rGel retained cytotoxicity towards PAE/KDR cells even with a 1 h exposure time, cytotoxicity of this fusion toxin was markedly enhanced by an exposure time of 48 hours.

Fig. 8. Cytotoxicity of VEGF₁₂₁/rGel to PAE/KDR cells does not result in apoptosis. PAE/KDR cells were grown overnight. 1 nM VEGF₁₂₁/rGel (twice the IC₅₀) was added and incubated for 24, 48 and 72 hours. The cells were analyzed for TUNEL. Positive control cells were incubated with 1 mg/ml DNase for 10 minutes at 37°C.

Fig. 9. Treatment of PAE/KDR cells with VEGF₁₂₁/rGel does not result in PARP cleavage.

PAE/KDR cells were stimulated with VEGF₁₂₁/rGel or VEGF₁₂₁ for the times indicated. Cells were washed and lysed and the cell lysate was analyzed by Western using an anti-PARP antibody. No PARP cleavage was observed.

Orientation “A”



Orientation “B”



Figure 1

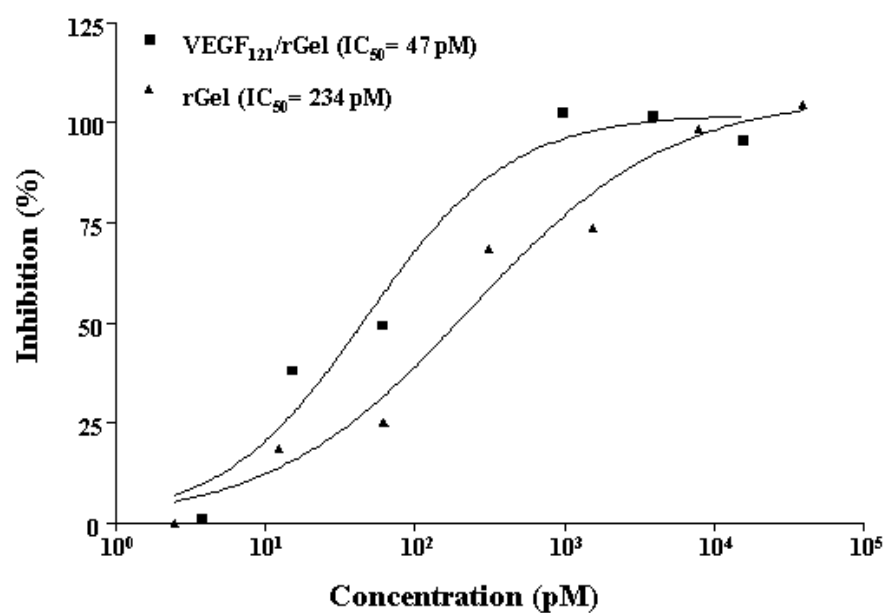


Figure 2

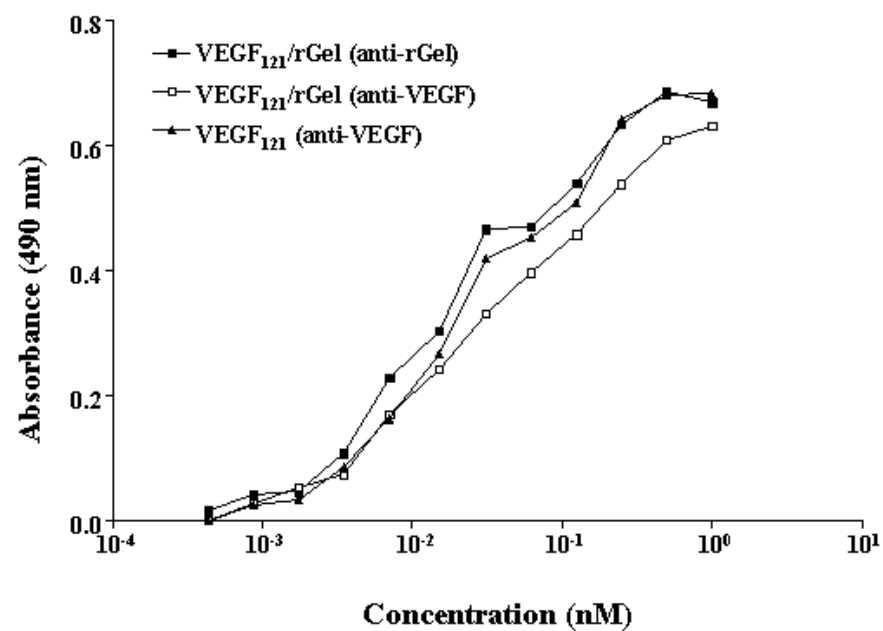


Figure 3

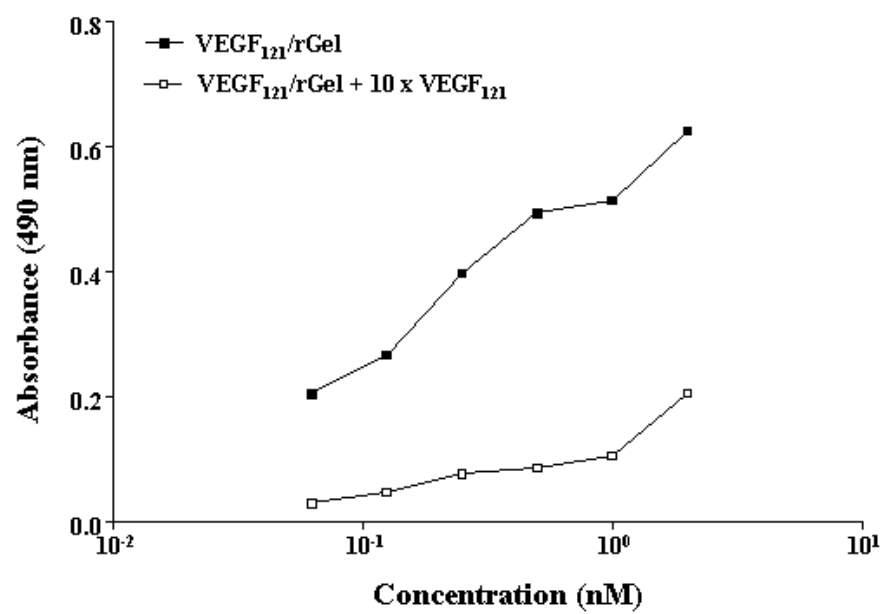


Figure 4

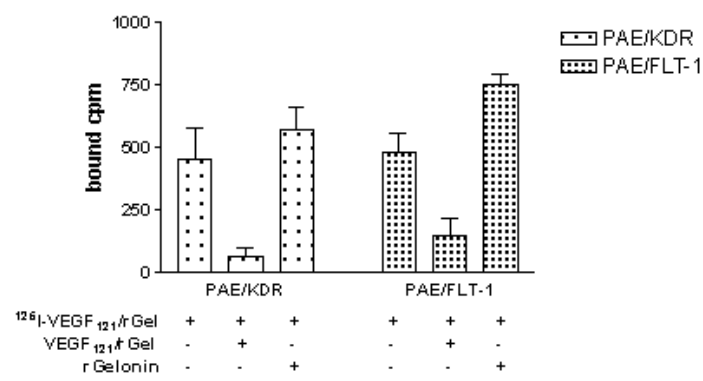
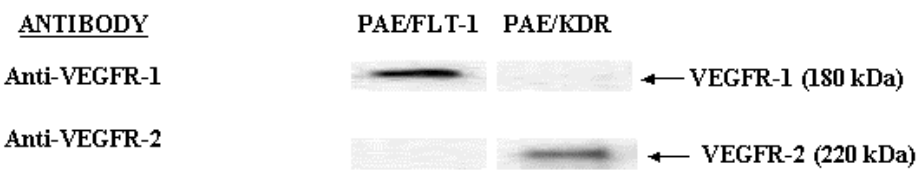


Figure 5a (top) and 5b (bottom)

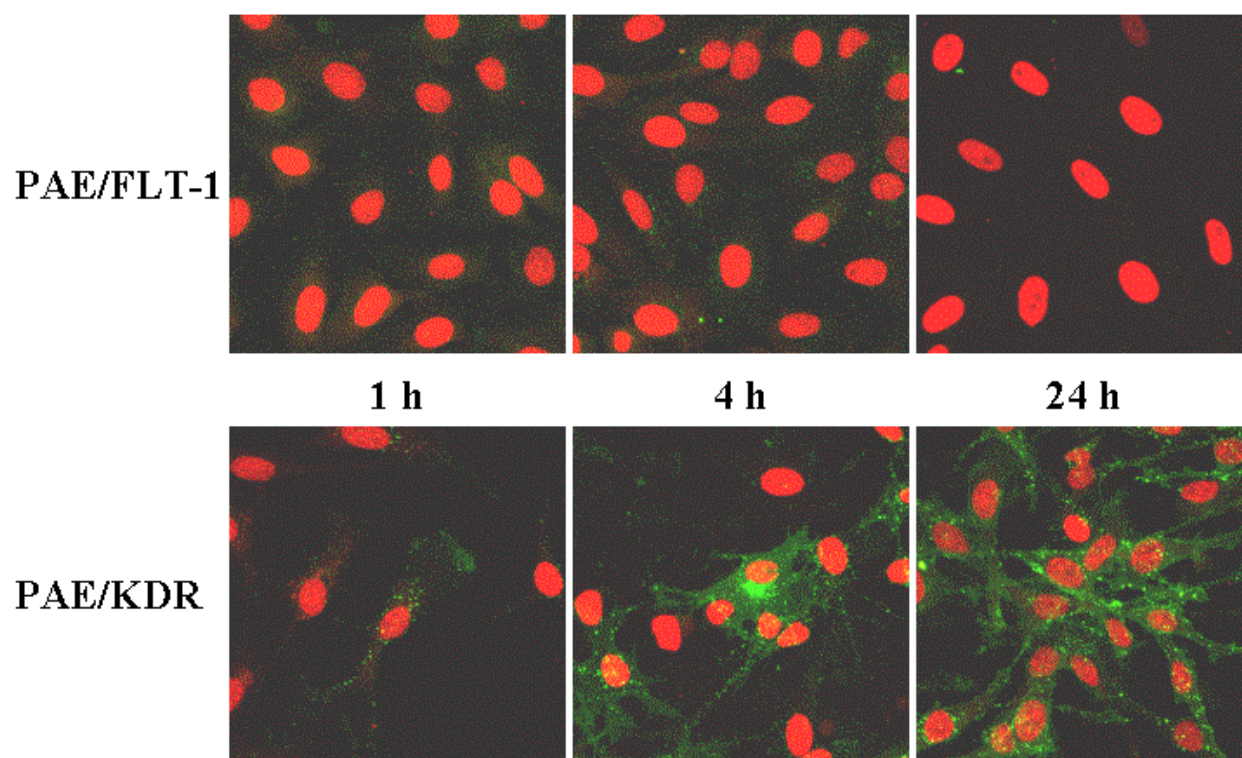


Figure 6

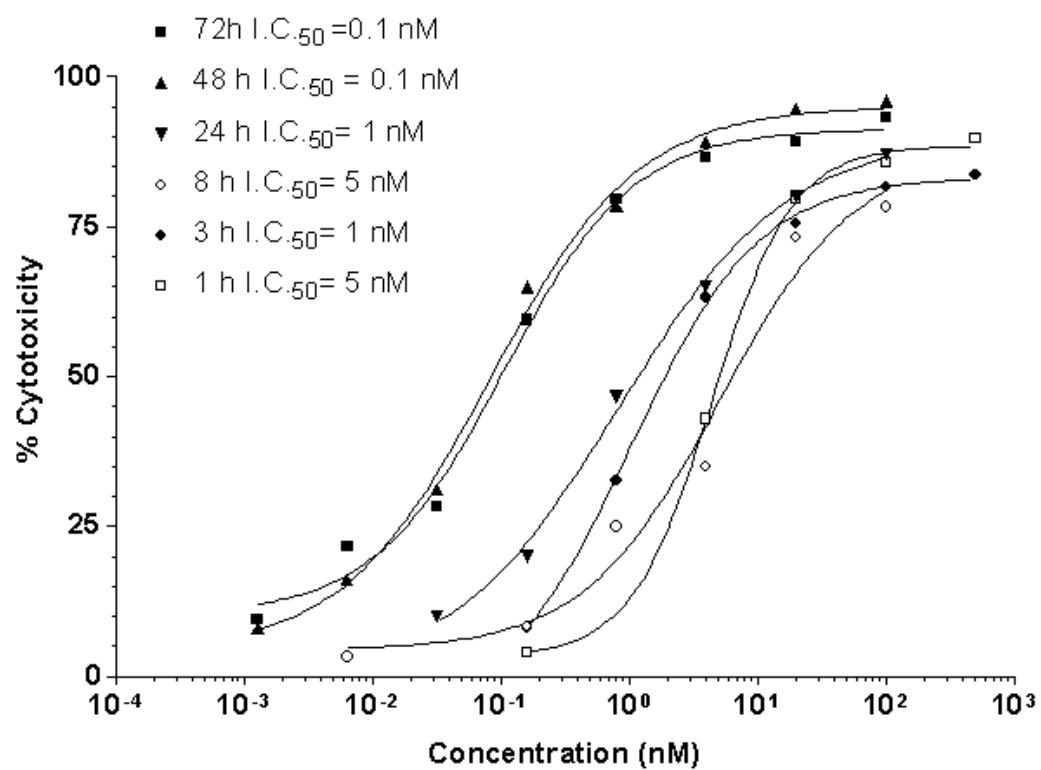


Figure 7

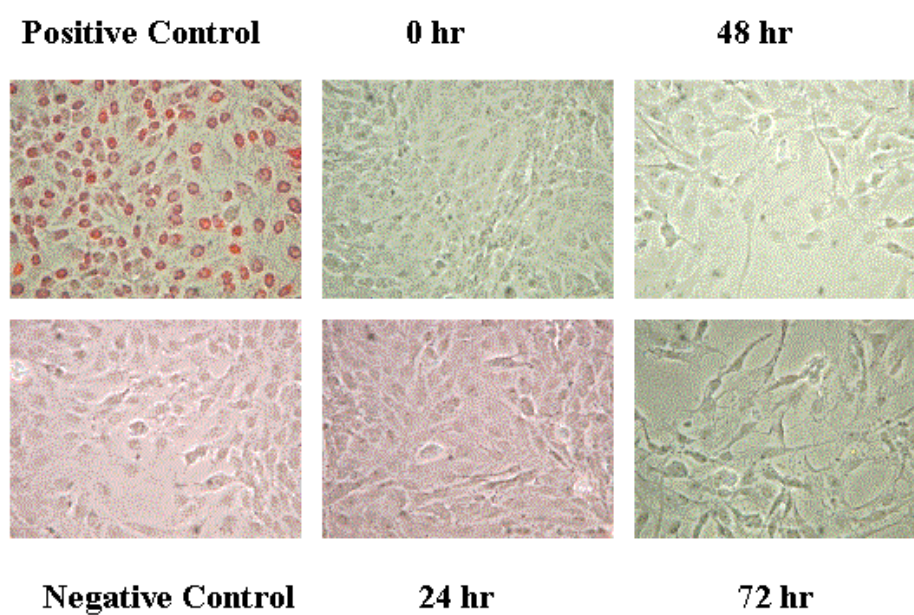
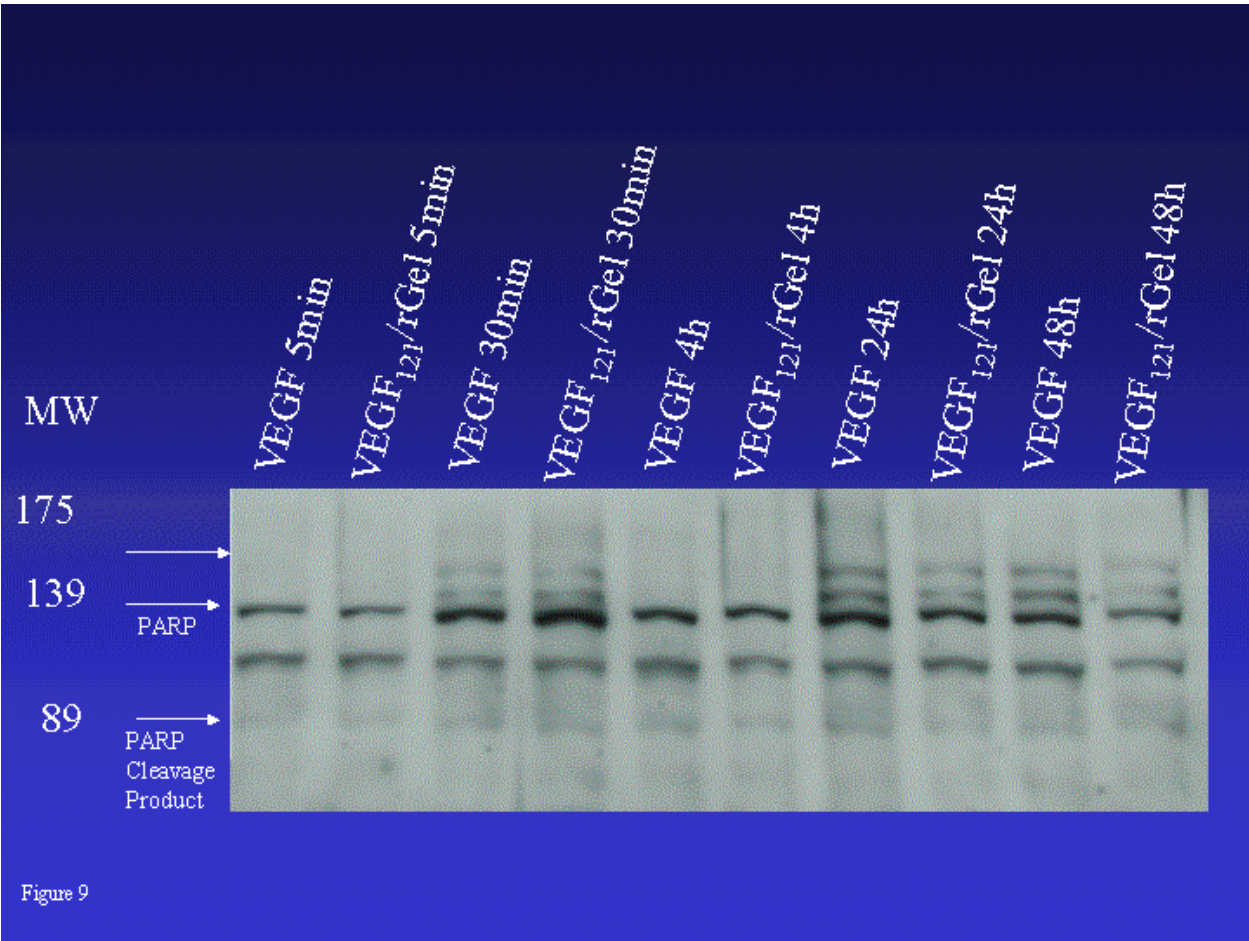


Figure 8



TRA-8/paclitaxel and TRA-8/adriamycin groups were not significantly different from each other, but they both were significantly larger than all other treatment groups. In addition, TRA-8, paclitaxel, and adriamycin alone were not significantly different from one another, but TRA-8 and paclitaxel were significantly larger than no treatment. Adriamycin was not significantly larger than no treatment. The percentage complete tumor regression was 0% in the untreated control group, 21.4% for TRA-8, 0% for adriamycin, 0% for paclitaxel, 66.7% for TRA-8 plus adriamycin, and 37.5% for the combined TRA-8 and paclitaxel group. TRA-8/adriamycin and TRA-8/paclitaxel had a significant increase in the proportion of regressions over TRA-8 ($p=0.023$), but they were not significantly different from each other ($p=0.296$). Thus, TRA-8 anti-DR5 antibody combined with chemotherapy significantly inhibited tumor growth and produced complete tumor regressions in mice bearing human breast cancer xenografts expressing DR5. Combined therapy with antibody against DR5 and chemotherapy represents a novel strategy to potentially enhance anti-cancer therapy for metastatic breast cancer. Supported in part by Sankyo Co., Ltd. and NCI 1 P50 CA89019-01 SPORE in Breast Cancer.

#4985 Comparison of the *in vivo* efficacy of anti-CD20 antibodies in human tumor xenograft models: Anti-B1 antibody (tositumomab) vs. rituximab (C2B8). C. Pan, F. Zhou, D. Grillo, Y. Wang, M. Quinn, D. Buckman, D. King, B. Hill, C. Bebbington, G. Yarranton, P. Cardarelli, D. Colcher, and L. Pickford. Corixa Corporation, South San Francisco, CA.

CD20 is expressed throughout the B cell lineage, from pre-B cells to resting and activated mature B cells, as well as, on a majority of B cell lymphomas and leukemias. Rituxan® (rituximab), a mouse/human chimeric IgG1 anti-CD20 antibody, has been approved for the treatment of relapsed, low-grade and follicular lymphoma. Bexxar® therapy, which contains the ¹³¹I-labeled form of a mouse IgG2a anti-CD20 antibody, i.e., the Anti-B1 Antibody (tositumomab), is currently under clinical investigation for the treatment of low-grade non-Hodgkin's lymphoma. Differing activities of the two MAbs (non-radiolabeled) were observed *in vitro* using a panel of B cell lines, including Ramos and Raji. Anti-B1 Antibody, but not rituximab, induced apoptosis in the absence of cross-linking antibodies. Complement dependent cytotoxicity (CDC) was highest with rituximab ($EC_{50} = 0.1 \mu\text{g/ml}$ using Ramos cells). Both MAbs showed similar potency in an antibody dependent cell mediated cytotoxicity (ADCC) assay ($EC_{50} = 0.03 \mu\text{g/ml}$ using Raji cells). Apoptosis, CDC and ADCC may also be important in the *in vivo* anti-tumor efficacy of both antibodies. B cell lymphoma xenograft models have been set up in athymic mice to compare anti-tumor efficacy *in vivo*. Both MAbs were compared at a well-tolerated range of doses from 0.04 to 4 mg/kg administered *i.v.* to mice implanted s.c. with Ramos cells. The two MAbs could be differentiated based on relative dose responses in tumor growth and survival, based on a tumor endpoint of >1.5 g tumor weight. At day 18 after dosing, which was the first day that any tumor reached the >1.5 g endpoint, Ramos tumors reached a mean weight of $1306 \pm 231 \text{ mg}$ ($100 \pm 18\%$; $N=10$, survival = 60%) in vehicle control treated animals. Anti-B1 Antibody at 0.04 mg/kg (Q7Dx2) significantly inhibited tumor growth by $52 \pm 24\%$ ($p<0.05$, unpaired *t* test), with 90% survival. In contrast, rituximab treatment at the same dose resulted in only minimal growth inhibition ($3 \pm 38\%$) with 60% survivors at day 18, equivalent to the vehicle control group. By day 30, the 0.04 mg/kg dose group of Anti-B1 Antibody had 70% and rituximab 50% remaining with tumors <1.5 g (control 10%). At a higher dose of 4 mg/kg both MAbs were completely effective in inhibiting tumor growth. Anti-tumor efficacy of two clinically efficacious MAbs with different constant regions will be discussed in the context of CDC, ADCC and apoptosis induction, based on these *in vitro* and *in vivo* results.

#4986 VEGF₁₂₁-gelonin fusion toxin specifically localizes to tumor blood vessels and induces robust vascular damage in human tumor xenograft models. Sophia Ran, Khalid Mohamedali, Lawrence Cheung, Philip E. Thorpe, and Michael G. Rosenblum. Southwestern Medical Center, UT at Dallas, TX, Dallas, TX, and M.D. Anderson Cancer Center, Houston, TX.

VEGF₁₂₁/rGel fusion protein is a vascular targeting agent composed of a non-heparin binding isoform of VEGF and the highly active plant toxin gelonin. Both receptors for VEGF (R1 and R2) are strongly up-regulated on tumor neovasculature compared to normal endothelium. The bacterially-produced, purified VEGF₁₂₁/rGel was selectively cytotoxic to both log-phase and confluent endothelial cells, displaying an IC_{50} of 0.5 nM compared to 150 nM for free gelonin under the same conditions. This study focused on biodistribution of VEGF₁₂₁/rGel and its effect on the tumor and normal vessels in tumor bearing mice. The fusion protein was examined in orthotopic MDA MB 231 breast carcinoma, PC-3 prostate carcinoma and L540 Hodgkin's lymphoma. Tumor-bearing mice were injected *i.v.* with 50 μg of the fusion protein and 30 min later, tumors and all organs were either snap-frozen or formalin-fixed. VEGF₁₂₁/rGel was detected on frozen sections using rabbit anti-rGel antibody. Gelonin-positive structures were identified as endothelial vessels using double labeling of anti-rGel and anti-CD31 antibodies. VEGF₁₂₁/rGel was detected on the majority of tumor vessels in all three models. Mean values of positive vessels per mm^2 were 85, 76 and 91 for 231, PC-3 and L540 tumors, respectively. These values represent 50-65% of total blood vessels detected by anti-CD31 antibody in the examined fields. The "hot spots" in these tumors contained up to 90% of vessels that were positive for the localized protein. MDA-MB 231 tumors pre-treated with anti-VEGF antibody 2C3 demonstrated a 2 to 3-fold reduced localization of VEGF₁₂₁-rGel. This confirms

the specificity of the detection method and suggests that anti-VEGF treatment suppresses the expression of VEGF receptors. VEGF₁₂₁/rGel was also detected in kidney glomeruli but not on the vasculature of other normal organs. This indicates that number of VEGF receptors on normal endothelium is significantly reduced compared to tumor vessels. H&E slides showed thrombi, hemorrhages and disintegration of vessels in VEGF₁₂₁/rGel treated tumors, but not normal organs. Necrotic regions were frequently observed surrounding damaged vasculature. There were no signs of vascular injury or morphologic abnormalities in rGel-treated mice. Therefore, VEGF₁₂₁ can specifically deliver rGel to tumor endothelium where it is internalized and exerts its cytotoxic effect. Furthermore, the number of VEGF₁₂₁ receptors and functional status of dividing endothelial cells may play a crucial role in differential cytotoxicity of this construct towards normal and tumor vessels. Research conducted, in part, by the Clayton Foundation for Research and Susan G. Komen Breast Cancer Foundation.

#4987 Y-90 labeled anti-Flk-1 antibody (anti-FIk-1-NP-Y90): A novel anti-angiogenesis therapy using nanoparticles. Lingyun Li, Charles A. Warchow, Zhimin Shen, Neal Dechene, John Pease, Shouheng Ning, Mark D. Bednarski, and Susan J. Knox. Stanford University, Stanford, CA, and Targesome, Inc., Palo Alto, CA.

Vascular endothelial growth factor (VEGF) has been shown to be actively involved in tumor-induced angiogenesis. VEGF receptor 2 (Flk-1) is expressed at much higher levels on neovascular endothelial cells in tumors relative to normal tissues. Radioimmunotherapy that targets Flk-1 is a novel anti-angiogenesis strategy for treating a wide variety of solid tumors. In this study, we investigated the potential therapeutic effect of a three-component radiopharmaceutical agent [which combines a targeting molecule (the anti-FIk-1 monoclonal antibody), a nanoparticle (NP), and yttrium-90 (Y90)] on the growth of well established murine tumors. The murine melanoma model K1735-M2 was used to assess the efficacy of the anti-FIk-1-NP-Y90 complex. Therapy was administered in a single dose by *i.v.* injection. In K1735-M2 tumors, treatment with anti-FIk-1-NP-Y90 (0.36 $\mu\text{g/g}$ anti-FIk-1, 5 $\mu\text{Ci/g}$ Y90) caused a significant tumor growth delay ($P<0.05$, Wilcoxon test) compared to untreated tumors, as well as tumors treated with anti-FIk-1, anti-FIk-1-NP, and conventional radioimmunotherapy with Y90-labeled anti-FIk-1. The time required for a given tumor to reach 4x the initial tumor size (Tumor Volume Quadrupling Time: TVQT) was delayed from 6 days in untreated tumors to 7, 9, 9, and 13 days in tumors treated with anti-FIk-1, anti-FIk-1-NP, Y90-labeled anti-FIk-1, and the anti-FIk-1-NP-Y90 complex, respectively. Biodistribution and histological studies (stainings for vessel density and apoptosis) are ongoing and will be correlated with therapeutic response. These encouraging results demonstrate the potential therapeutic efficacy of the anti-FIk-1-NP-Y90 complex as an anti-angiogenic agent for the treatment of solid tumors.

PREVENTION AND SURVIVORSHIP RESEARCH 9: Advances in Cancer Prevention

#4988 Measurement of chemopreventive efficacy of oral vitamin A with nuclear morphometry. M. S. Stratton, J. A. Warneke, R. F. Goldman, R. C. Miller, Y. Liu, J. G. Einspar, D. B. Thompson, P. H. Bartels, and D. S. Alberts. Arizona Cancer Center, Tucson, AZ.

Nonmelanoma skin cancer (NMSC) is the most common type of cancer in the U.S. Although mortality due to NMSCs is relatively low over 10% of squamous cell carcinomas are invasive and will metastasize. Therefore, development of chemopreventive agents that prevent skin cancer or reverse the process of actinic damage at an early stage is a high public health priority. However, a validated and objective technique by which efficacy of skin cancer preventive agents can be tested is not available. Our data demonstrate that chromatin pattern changes measured by nuclear morphometric analyses (karyometry) can be recorded with precision and reproducibility and be plotted on a monotonic curve. Therefore, the technique is not dependent on subjective measures. Furthermore, changes in nuclear chromatin reflect reversible events that respond within a short time. Previously, our Phase III trial of vitamin A in 2290 participants with actinic keratoses revealed a 32% reduction of risk of squamous cell carcinoma. We now show that chemopreventive effects of oral Vitamin A can be measured in the skin of individuals with visually and histologically normal, sun-exposed skin. Using morphometric analysis, two numeric measures of deviation from normal were assessed. The nuclear abnormality for each nucleus isolated from shave biopsies of sun-exposed skin were computed in comparison with "normal" nuclei isolated from unexposed skin. Next, several discriminant function scores were derived. Discriminant function I was derived to separate nuclei in unexposed skin from normal appearing sun-exposed skin. Our data revealed that the nuclei isolated from histologically normal, sun-exposed skin were drastically different from unexposed normal skin confirming that karyometry can detect subtle abnormalities that are not observed with routine histopathological studies. The top 15% of highly abnormal nuclei were used as a dividing line to select features which were the best indicators of actinic damage in order to derive discriminant function II. Discriminant function II scores were divided into 24 intervals and the relative

condensation was lowest for 3—3—3—3—3 (0.25 μ M) and highest for spermidine (24 μ M). The efficacy of these polyamines in condensing DNA was in the following order: 3—3—3—3—3 < 3—4—3—4—3 \approx 3—3—4—3—3 < 3—3—3—4—3 \approx 3—4—4—3—3 \approx 4—3—3—4—3 < 3—4—3—3—4. Dynamic light scattering measurements indicated the presence of compact particles with hydrodynamic radii (Rh) of 5–10 nm for 21—37 mer ODN in the presence of 250 μ M spermine. Spermine homologs with $n = 3–6$ on the other hand condensed DNA with Rh in the range of 40–50 nm. Rh increased with further increase in the number of methylene chain separating the secondary amino groups of the polyamine. (Rh = 60–70 nm for $n = 11$ and 12). Hexamines, including 3—4—3—4—3 increased the uptake of a 37—mer ODN in breast cancer cells by ~ 10 fold compared to untreated controls. In addition, majority of the ODN was transported into the cell nucleus, indicating that DNA compaction is a possible mechanism for DNA transfection. Our data indicate that higher valent polyamine analogs might be useful in designing non—viral delivery vehicles for gene therapy.

#434 Antigene locks cause deletion of extra-chromosomal bacterial targets. Antony R. Parker, Soo Chin Lee, Craig Morrell, Li Hua, and James R. Eshleman. *Johns Hopkins School of Medicine, Baltimore, MD.*

Viral episomal DNA can be associated with transformation and some malignancies. We wished to test whether we could genetically select these elements. Padlock probes were originally designed for in-situ hybridization to detect single base mutations. They are large oligonucleotides whose 5' and 3' arms wrap around target DNA in an end-to-end orientation and are ligated if a perfect match between arms and the target exists. Since both arms are typically 20 bases each they are expected to wrap around a DNA target approximately four times before being locked through ligation. In this way they are inextricably bound to the target cell's DNA (hence 'padlock') and are subsequently detected. We asked the question whether padlock probes could be redesigned as therapeutic 'antigene locks' to select against genetic elements. We made two modifications. First, we made both the arms and the backbone homologous to the double stranded DNA target, unlike padlock probes, which have only homologous arms. Second, we created mispairing between the terminal bases of both arms and the backbone so that self-ligation would be prevented. For rapid evaluation of these locks, before use in eukaryotes, we assessed their inhibitory properties towards the lacZ and proA genes in the bacterial extra-chromosomal F' episome. Electroporation of either antigenic lock into an E.coli host, containing the lacZ and proA genes on an F' extrachromosomal episome, which are normally blue on X-gal plates, produced white colonies. To examine loss of blue colony color further, we performed three experiments: (1) the F' factor also contains the proA gene on the episome. The white colonies did not grow in the absence of exogenous proline suggesting the proline synthesis gene was functionally eliminated. (2) We attempted to PCR five F' factor genes from the white colonies: lacZ, proA, traK, repB and sopB. None of the genes amplified. (3) We attempted to conjugate the presumptive female white colonies with another F' strain to test for the ability to convert to male. Conjugation was successful suggesting that the lock treated cells had been converted to females. From our results we conclude that (a) antigenic locks interact with genetic elements within the cell and cause their elimination and (b) prokaryotes can be used for rapid evaluation of these locks.

EXPERIMENTAL/MOLECULAR THERAPEUTICS 6: Targeted Therapy: Breast and Prostate Cancer

#435 *In vitro* and animal model studies of VEGF121/rGel fusion toxin effects on breast cancer cells. Khalid A. Mohamedali, Lawrence H. Cheung, Sophia Ran, Philip Thorpe, and Michael G. Rosenblum. *M.D. Anderson Cancer Center, Houston, TX, and U.T. Southwestern, Dallas, TX.*

The angiogenic factor VEGF₁₂₁ fused with the recombinant plant toxin gelonin (rGel) exhibits potent cytotoxicity towards tumor neovasculature and inhibits tumor growth by virtue of its selective targeting of tumor vessels. We have used *in vitro* and animal models to further understand the mode of action of VEGF/rGel on tumor cells *in vivo*. Preliminary studies have suggested that interruption of blood flow to tumors with agents targeting tumor vasculature generates intratumoral hypoxia and concomitant changes in the surrounding pH. Vascular endothelial cells over-expressing flk-1 (PAE/flk-1) were treated with an IC₅₀ dose of VEGF/rGel for 24, 48 and 72 hours. At the appropriate timepoints treated and control cells were harvested and the effect of VEGF/rGel on intracellular events was examined by extraction of mRNA and microarray analysis of proteins involved in signal transduction, stress response, cell cycle control, hypoxia and metastasis. To examine the effect of VEGF/rGel on tumor cells, MDA-MB-231 breast cancer tumor cells were co-cultured with PAE/flk-1 with the two cell lines separated by a thin membrane, allowing exchange of nutrients. The endothelial cells were treated with various doses of VEGF/rGel and the effect on MDA-MB-231 cells was examined visually after 72 hours. PAE/flk-1 cells in the upper chamber were treated with an IC₅₀ dose of VEGF/rGel over 72 hours after which both control and treated PAE/flk-1 and MDA-MB231 cells were harvested, RNA extracted and subjected to microarray analysis. We repeated the above experiment and incubated the cells under hypoxic conditions to examine genetic

changes associated with hypoxic stress. These results are under analysis and will be reported. Internalization of VEGF-rGel into PAE/flk-1 cells was also investigated 1 hr, 2 hr, 10 hr, 16 hr and 24 hrs after treating with VEGF-rGel. VEGF-rGel was detected by both anti-VEGF and anti-rGel antibodies using immunofluorescence, and suggests internalization within one hour of incubation. Finally, the plasma clearance and tissue distribution of VEGF-rGel in tumor-bearing mice was examined. Nude mice bearing orthotopic MDA-MB231 tumors were injected with 1 μ Ci of ¹²⁵I-labeled VEGF-rGel and tissue distribution and plasma clearance was assessed 24, 48 and 72 hrs post injection. Research conducted, in part, by the Clayton Foundation for Research. [su]

#436 Administration of a recombinant TGF- β type III receptor (soluble sRIII) inhibits angiogenesis and tumor growth in human breast cancer xenograft. Abhik Bandyopadhyay, Fernando Lopez-Casillas, and Luzhe Sun. *University of Texas Health Science Center, San Antonio, TX, and Instituto de Fisiologia Celular, Mexico City, Mexico.*

Previously, we have demonstrated that the expression of TGF- β type III receptor (sRIII) could suppress the malignant properties of human carcinoma cells by antagonizing tumor promoting activity of TGF-beta. (A. Bandyopadhyay et al., *Cancer Res.*, 59: 5041-5046, 1999). In the current study, we investigated the potential therapeutic utility of a recombinant sRIII. We administered sRIII in human breast cancer MDA-MB-231 xenograft-bearing athymic nude mice model via peritumoral (50 mcg per tumor, twice a week) or systemic (100 mcg per animal, every alternate day) injection. Both methods of administration significantly reduced the tumor growth and metastasis in the lung and axillary lymph nodes. The tumor inhibitory activity of sRIII was found to be associated with the inhibition of angiogenesis. Microvessel density of tumors by histological analysis and CD-31 immunostaining, and tumor blood volume indicated by hemoglobin content showed significant reduction of angiogenesis after systemic sRIII treatment. In an *in vitro* angiogenesis assay, human dermal microvascular endothelial cells (HD-MEC) showed significant reduction in its ability to form capillary tube like structure on Matrigel after treatment with sRIII in a dose dependent manner. These findings support the conclusion that sRIII treatment suppresses tumor growth and metastasis at least in part by inhibiting angiogenesis and could be a useful therapeutic agent to antagonize the tumor-promoting activity of TGF-beta.

#437 Combination dose titration studies of targeted therapy of EGFR and HER2 receptors with ZD1839 (IressaTM) and trastuzumab (HerceptinTM) in a HER2 over-expressing breast tumor xenograft model. Stephen Chia, Tetyana Denyssevykh, Karen Gelmon, David Huntsman, Dana Masin, and Marcel Bally. *British Columbia Cancer Agency, Vancouver, BC, Canada.*

Background: The type I growth factor receptor family, of which EGFR and HER2 belong to, hetero- and homodimerize to activated downstream targets. Overexpression of EGFR and HER2 are established poor prognostic factors in breast cancer. Trastuzumab, a monoclonal antibody against the HER2 receptor, alone or in combination with chemotherapy has demonstrated improved clinical outcome in advanced HER2 overexpressing breast cancer. The strategy of targeted combined blockade with ZD 1839, a tyrosine kinase inhibitor of EGFR, and trastuzumab is a rationale strategy, however pre-clinical studies to demonstrate enhanced efficacy and to determine the appropriate dose levels are required prior to large scale clinical trials. Methods: A HER2 transfected MCF7 breast cancer cell line to produce a HER2 overexpressing xenograft breast tumor model in Rag-2 mice was utilized. Multiple dose titration studies of trastuzumab from 0.03 to 30 mg/kg i.p. 2X week for 5 weeks were performed. In the same breast tumor model, studies with ZD 1839 at doses of 20 to 200 mg/kg p.o. 5X/week for 5 weeks were done. The dose titration data was used to define a fixed ratio of the two drugs that was subsequently administered to determine an optimal dose level for this combination. Residual tumors were harvested at completion of 5 weeks of therapy for immunohistochemistry (IHC) studies. Results: Trastuzumab at increasing doses allowed us to define the maximal therapeutic dose at 10 mg/kg. At this dose, the mean tumor volume determined on day 35 was less than 0.05 cm³ as compared to tumors from controls, which were in excess of 0.35 cm³. The maximum therapeutic dose of ZD 1839 was defined as 200 mg/kg, where the mean tumor volume was estimated to be less than 0.25 cm³ at day 35. A fixed ratio of 20:1 for ZD 1839 to trastuzumab was defined for the 2-drug combination studies. The combination of ZD 1839 at 100 mg/kg and trastuzumab at 5 mg/kg produced the greatest response in the combination dose titration studies with a mean tumor volume of 0.068 cm³ on day 35. IHC studies of EGFR, HER2, phosphorylated (P)-EGFR, P-HER2, MAPK and P-MAPK will be performed to assess changes in downstream signaling pathways. Conclusion: The combined targeted blockade of both EGFR and HER2 with ZD 1839 and trastuzumab appears to be an active combination in a pre-clinical model of HER2 overexpressing breast cancer. This evidence supports the consideration of this strategy for further investigations in pre-clinical and clinical studies.

#438 Decreased phosphorylation and proteasome-mediated degradation of p27Kip1 during growth inhibition by anti-HER2 monoclonal antibodies in HER2-overexpressing breast cancer cells. Xiao-Feng Le, Amanda McWatters, Lance R. Ramoth, Francois-Xavier Claret, Mong-Hong Lee, Gordon B. Mills, and Robert C. Bast, Jr. *The University of Texas M. D. Anderson Cancer Center, Houston, TX.*

CELLULAR, MOLECULAR, AND TUMOR BIOLOGY 1: Cells and Their Receptors

#1 Expression of Neuropilin-1 in primary and metastatic human breast cancer. Anna Belcheva, Jane Wey, Marya McCarty, Fan Fan, Oliver Stoeltzing, Wenbiao Liu, Aysegul Sahin, and Lee M. Ellis. *M.D. Anderson Cancer Center, Houston, TX.*

Neuropilin-1 (NRP-1) was first described as a receptor for Semaphorins and a mediator of axonal guidance. NRP-1 has been found to be a co-receptor for VEGF on endothelial cells. More recently, NRP-1 expression has been noted on specific epithelial malignant cell types such as prostate and pancreatic cancer. We sought to determine the prevalence and relative expression of NRP-1 in human breast cancer cell lines and specimens. Eight human breast cancer cell lines were screened for NRP-1 expression by immunoblotting. All eight expressed NRP-1 with the metastatic cell lines showing stronger expression. To determine the prevalence of NRP-1 in malignant and non-malignant human breast tissue, we examined NRP-1 protein expression in paraffin embedded tissue from 20 lymph-node negative and 20 lymph-node positive breast cancer specimens of patients who had not received neoadjuvant chemotherapy. Immunohistochemical analysis of these specimens confirmed expression of NRP-1 in normal breast duct myoepithelial cells as well as in malignant tissue, including ductal carcinoma in situ, and mucinous, lobular, and infiltrating ductal carcinomas. NRP-1 in the non-malignant breast ducts was expressed in only the myoepithelial cells, but not the ductal cells. In contrast, NRP-1 was expressed in epithelial cells in all of the malignant tissues. The epithelium of the T1N1 specimens showed more intense staining than the T1N0 specimens. These data suggest that NRP-1 has higher expression in invasive breast carcinomas than in normal breast ductal epithelium. Given its role as a co-receptor for VEGF, NRP-1 may be an important receptor involved in breast cancer angiogenesis.

#2 Dominant loss of responsiveness to chemotactic factors caused by a three amino acid deletion of angiomin. Tetyana Levchenko, Boris Troyanovsky, Karin Aase, Anders Bratt, and Lars Holmgren. *Karolinska Institutet, Stockholm, Sweden.*

Angiogenesis is a complex process leading to the formation of new capillaries from pre-existing vessels. The molecules involved in endothelial cells migration, survival and vessel stabilization during vasculogenesis and angiogenesis may provide a new targets for anti-angiogenesis therapy. In a recent publication (Troyanovsky et al., JCB, March, 19, 2001) we have reported the isolation of the angiostatin-binding protein- angiomin. Angiomin is a member of a new protein family characterized by conserved coiled-coil domains and c-terminal PDZ binding motifs (Bratt et al, Gene, 2002). A role in cell motility is suggested by the findings that over-expression of angiomin in endothelial cells results in a potentiated response to chemotactic factors. Furthermore, angiostatin inhibits migration and tube formation in angiomin-transfected cells whereas control cells were unaffected. In further studies, we have deleted three amino acids in the PDZ-binding motif. Mouse aortic endothelial cells (MAE), expressing mutated protein were inhibited in their response to chemotactic factors in migration assays and did not assemble into network of tube-like structures in matrigel or collagen matrix. Next we generated transgenic mice expressing angiomin and angiomin mutant under the control of the TIE-promoter that is active in endothelial cells. TIE-angiomin mice developed normally as embryos analyzed at p.c. 9.5 and 13.5 and the phenotype did not differ to that of wt littermates. In contrast, TIE-angiomin-mutant embryos displayed severe vascular deficiencies at embryonic day 9.5. The transgenic embryos suffered from severe bleeding in the brain as well as in intersomitic vessels. In conclusion, our data show that inactivation of the PDZ-binding motif not only abrogates the stimulatory activity of angiomin on tube formation and migration, it also transforms angiomin into a dominant-negative repressor. These results indicate that mutations in the angiomin gene and angiostatin treatment have similar effect on endothelial cells and suggest that the c-terminal PDZ-binding motif of angiomin is a target for anti-angiogenic therapy.

#3 Validation of clinically relevant invasive and non-invasive techniques for measuring tumor oxygen status using VEGF+/VEGF- human melanoma xenografts. Chandrakala Menon, Glenn M. Polin, Indira Prabakaran, Alex Hsi, Cecil Cheung, Joseph P. Culver, James F. Pingpank, Chandra S. Sehgal, Arjun G. Yodh, Donald G. Buerk, and Douglas L. Fraker. *University of Pennsylvania, Philadelphia, PA.*

Tumor oxygen status is a reliable prognostic marker that impacts malignant progression and outcome of tumor therapy. Although the Eppendorf pO₂ histogram is the gold standard for tumor pO₂ measurements, results are often confounded by stromal damage caused by the large probe. In the present study, VEGF-transfected hypervascular human melanoma xenografts and their non-transfected

counterparts were used to validate other clinically relevant invasive and non invasive techniques to measure tumor oxygen status including pO₂, relative blood flow (BF), blood volume (BV) and blood oxygen saturation (OS). NIH1286 human melanoma cells were transfected with a retroviral vector \pm a 720 bp fragment of human VEGF₁₂₁. High VEGF₁₂₁ producing clones were selected by ELISA. Six to eight week old athymic nude mice were subcutaneously injected in the right flank with 5x10⁶ NIH1286/V+ (VEGF-transfected) or NIH1286/V- (vector-alone) cells. When tumors were 10-14 mm in maximum dimension, serum was analyzed for VEGF by ELISA. Cryo-preserved tumor tissue sections were immunostained for PECAM and microvessel density (MVD) measurements were made. In a first set of experiments, tumor bearing mice were anesthetized and pO₂ measurements were made in the two tumor types using Eppendorf pO₂ histogram (EPH) (300 μ m diameter) or recessed microelectrode (RM) (10 μ m tip). In a second set of experiments, tumor BF and BV were measured by quantitative analysis of color Doppler and power Doppler images. In a third set of experiments, diffuse light spectroscopies (DLS) (1), were used to measure tumor BF and OS variation. Near-infrared light sources injected photons centrally into the tumors; light transmitted through the tumor was captured by a set of detectors distributed radially around the source. Relative BF was computed from the temporal decay of the diffuse light autocorrelation function, and relative OS was computed by comparing diffuse light signals at 830 nm (oxyHb peak) and 750 nm (deoxyHb peak). Results are summarized below: (Table) RM correctly established a significant difference in median pO₂ between hypervascular and control tumor types. DUS and DLS validated each other as methods for analyzing tumor BF. DUS BF (V+/V-) = 3.4; DLS BF (V+/V-) = 3.2. DUS BV/BF for V+ = 1.99; V- = 1.17 suggesting sluggish flow in the V+ tumor type. DLS OS was 1.7 times greater in V+ than in V- consistent with increased BV and BF. 1) Cheung C, Culver JP, Takahashi K, Greenberg JH, Yodh AG. *Phys Med Biol* 46, 2053-65, 2001.

Tumor Type	In vitro VEGF ELISA	Serum VEGF ELISA	MVD 0.05 mm ² /mm	Median pO ₂ by EPH	Median pO ₂ by RM	Relative mean BF by DUS	Relative mean BV by DUS	Relative mean BF by DLS	Relative OS by DLS
V+	15,500 pg/ml	4211 pg/ml	74±11	<2.5mm Hg (n=7)	14mm Hg (n=5)	3.4±1 (n=5)	5.8±2.3 (n=5)	5.61±1.8 (n=7)	0.7±0.11 (n=7)
V-	10 pg/ml	9 pg/ml	39±4	<2.5mm Hg (n=7)	4 mm Hg (n=5)	1.0±0 (n=4)	1.2±0.45 (n=4)	1.73±0.6 (n=6)	0.4±0.11 (n=6)

#4 VEGF₁₂₁ gelonin fusion protein inhibits breast cancer metastasis in nude mice. Sophia Ran, Khalid Mohamedali, Philip E. Thorpe, and Michael G. Rosenblum. *University of Texas at Dallas, Dallas, TX and M.D. Anderson Cancer Center, Houston, TX.*

VEGF₁₂₁/rGel fusion protein is a vascular targeting agent composed of a non-heparin binding isoform of VEGF and the highly active plant toxin gelonin. Both receptors for VEGF-A (R1 and R2) are strongly up regulated on tumor neovasculature compared to normal endothelium. We have previously shown that VEGF₁₂₁/rGel was selectively cytotoxic to sub-confluent endothelial cells, displaying an IC₅₀ of 0.5 nM compared to 150 nM for free gelonin under the same conditions. Treatment of mice bearing various types of solid tumors with VEGF₁₂₁/rGel (17 mg/kg) inhibited the growth of primary tumors by 65-75% (Veenendaal et al., *PNAS* 99:7866-71, 2002). The goal of this study was to evaluate the effect of VEGF₁₂₁/rGel on metastatic growth of MDA-MB-231 tumor cells in nude mice. The MDA-MB-231 cells (0.5x10⁶ per mouse) were injected i.v. and the treatment began 8 days after injection. Mice (6 per group) were treated 6 times either with VEGF₁₂₁/rGel (100 μ g/dose) or with an equivalent amount of free gelonin. Three weeks after termination of the treatment, mice were sacrificed and their metastatic lungs as well as all other organs were harvested for examination. The number of surface lung foci in the VEGF₁₂₁/rGel - treated mice was reduced by 58 % as compared to gelonin control animals (mean numbers 22.4 and 53.3 for VEGF₁₂₁/rGel and control, respectively; $p < 0.05$). Immunohistochemical analysis revealed that the mean area of lung colonies from VEGF₁₂₁/rGel-treated mice was 50% smaller than that of the control mice (210 \pm 37 μ m versus 415 \pm 10 μ m for VEGF₁₂₁/rGel and control, respectively; $p < 0.01$). In addition, the vascularity of metastatic foci from VEGF₁₂₁/rGel-treated mice was reduced compared to that of control colonies. The mean number of blood vessels per mm² in metastatic foci was 198 \pm 37 versus 388 \pm 21 for treated and control, respectively. Approximately 62 % of metastatic colonies from the VEGF₁₂₁/rGel-treated group had fewer than 10 vessels per colony as compared to 23 % in the control group. The VEGF receptor 2, a major receptor that mediates angiogenic effects of VEGF-A, was intensely detected on the metastatic vessels in the control but not on the vessels in the VEGF₁₂₁/rGel-treated group. The treatment was well tolerated. No significant morphological changes were visible in either VEGF₁₂₁/rGel-treated or gelonin control mice. These data strongly suggest that anti-tumor vascular effect of VEGF₁₂₁/rGel could be utilized not only for treating primary tumors but also for inhibiting metastatic spread. This research was funded in part by the Clayton Foundation for Research and DOD Breast Cancer Program.

Vascular Targeting with VEGF₁₂₁/rGel Inhibits Angiogenesis: Specific Effects Assessed Using Micro-Array Analysis

Khalid A. Mohamedali, Candelaria Gomez-Manzano, Latha Ramdas, Jing Xu, Lawrence Cheung, Troy Luster, Philip Thorpe and Michael G. Rosenblum. U.T. MD Anderson Cancer Center, Houston, TX and U.T. Southwestern, Dallas, TX.

VEGF₁₂₁/rGel, a fusion protein of VEGF₁₂₁ and the plant toxin gelonin (rGel) targets the tumor neovasculature and exerts impressive cytotoxic effects by inhibiting cellular protein synthesis. We have previously shown that in vivo administration of this molecule inhibits tumor growth in melanoma, bladder, breast and prostate models. Further studies characterizing this molecule demonstrated that VEGF₁₂₁/rGel inhibited tube formation of endothelial cells over-expressing VEGFR-2 (PAE/KDR) on matrigel-coated plates. A concentration of 1 nM reduced by over 50% the number of tubes formed. In contrast, 100 nM of unconjugated gelonin resulted in the same degree of reduction of tube formation. Endothelial cells expressing VEGFR-1 (PAE/FLT-1) were not as sensitive to VEGF₁₂₁/rGel as PAE/KDR cells, requiring 100 nM VEGF₁₂₁/rGel to inhibit tube formation by 50%. PAE/KDR cells pre-treated with 1 nM VEGF₁₂₁/rGel prior to plating on matrigel showed significant reduction in tube formation that was dependent upon the length of pre-treatment. We investigated the effects of VEGF₁₂₁/rGel on angiogenesis in the chicken chorio-allantoic membrane (CAM) assay. CAMs of 9-day chicken embryos were stimulated using bFGF, and simultaneously treated with VEGF₁₂₁/rGel at a dose of 1 or 10 nM. Three days later vascular density was analyzed. Treatment with VEGF₁₂₁/rGel significantly inhibited the bFGF-mediated angiogenesis by 30% ($P < 0.001$, t-test, double sided). VEGF₁₂₁/rGel treatment decreased newly-sprouting vessels. As expected, the control protein gelonin, at equivalent concentrations, had no effect. We examined the mechanism of VEGF₁₂₁/rGel-induced cytotoxicity against cells in culture. Treated cells were TUNEL-negative and we found no evidence of PARP or caspase-3 cleavage and we concluded that the effects of this fusion construct were necrotic rather than apoptotic. To further delineate the activity of this construct, HUVECs treated with an IC₅₀ dose of VEGF₁₂₁/rGel for 24 hours were harvested and the effect of VEGF₁₂₁/rGel on intracellular events was examined by extraction of mRNA and microarray analysis of genes involved in signal transduction, stress response, cell cycle control, hypoxia and metastasis. The results were validated by RT-PCR. Our data suggests that VEGF₁₂₁/rGel induces expression of genes known to be induced by VEGF alone, in addition to genes involved in inflammation, chemotaxis and transcription regulation. Research conducted, in part, by the Clayton Foundation for Research and supported by DAMD 17-02-1-0457.

Category: CB14-01 Angiogenesis inhibitors

Key words: VEGF, gelonin, angiogenesis, microarray

Control/ Tracking Number: 04-AB-5397-AACR

Targeting Skeletal Metastases in Prostate Cancer with a Novel VEGF121 Fusion Toxin

A. T. Poblenz*, K. Mohamedali*, M. G. Rosenblum*, B. G. Darnay*. Experimental Therapeutics, University of Texas M.D. Anderson Cancer Center, Houston, TX, USA.

Presentation Number: SA099

Osteolysis that accompanies bone metastasis is a major cause of morbidity, often resulting in severe bone pain and susceptibility to fractures, and results in a significant decline in the quality of life of cancer patients with bone disease. Bone destruction is primarily mediated by osteoclastic bone resorption and cancer cells that have metastasized to bone stimulate the formation and activation of osteoclasts adjacent to metastatic foci. The progression of osteolytic metastases itself is a result of complex interaction between tumor cells, osteoclasts, osteoblasts, and the many factors in the bone microenvironment. There are numerous cytokines involved in tumor growth, neovascularization and bone resorption. Vascular endothelial growth factor-A (VEGF-A) and its cognate receptors Flt-1 and Flk-1/KDR have been identified as central mediators of tumor neovascularization. We previously developed a novel fusion construct designated VEGF121/rGel, composed of VEGF121 and the plant toxin gelonin, which targets the tumor neovasculature and exerts impressive cytotoxic effects by inhibiting cellular protein synthesis in target cells. We have previously shown that in vivo administration of this molecule inhibits tumor growth in melanoma, bladder, breast, and prostate tumor xenograft models. Treatment of mice (iv) bearing PC-3 intrafemoral tumor xenografts with VEGF121/rGel was shown to dramatically suppresses PC-3 skeletal metastases. All control mice were sacrificed by day 67. In contrast, 50% of the VEGF121/rGel-treated mice survived past day 140 without any sign of osteolysis. VEGF and its receptors participate in the complex process involved in tumor-directed bone resorption; however, their roles have not been identified. We have investigated the direct effect of VEGF121/rGel on differentiation of RAW cells and mouse bone marrow-derived monocytes (BMM). VEGF121/rGel was shown to inhibit RANKL-mediated osteoclastogenesis. The observed effect was not mediated by either VEGF121 or gelonin alone, but is a characteristic unique to the combined fusion protein. While immunofluorescence studies clearly show VEGF121/rGel penetration into RAW cells, the receptor responsible for mediating the cellular entry of VEGF121/rGel is unknown. Preliminary data indicate that VEGF121/rGel most likely inhibits the growth of mouse BMM through an unknown mechanism in vitro. These studies demonstrate the best combined therapy for prostate cancer metastases in which one agent provides both a multi-modal attack targeting the blood supply feeding the tumors and the osteoclast precursors which are instrumental in developing lytic bone lesions.

The Vascular Targeting Agent VEGF₁₂₁/rGel Inhibits Bone Remodeling and Skeletal Metastases through a Unique Mechanism. *Khalid A. Mohamedali, Ann T. Poblentz, Chuck Sikes, Troy Luster, Nora Navone, Philip Thorpe, Bryant Darnay and Michael G. Rosenblum.* University of Texas M.D. Anderson Cancer Center, Houston, TX and University of Texas Southwestern Medical Center, Dallas, TX.

Cancer metastases to bone are associated with significant morbidity and mortality and Patients with advanced cancer experience frequent bone metastasis. The pathophysiological processes leading to the development of skeletal metastases remains poorly understood. We developed a novel fusion construct designated VEGF₁₂₁/rGel, composed of VEGF₁₂₁ and the plant toxin gelonin(rGel), which targets the tumor neovasculature and exerts impressive cytotoxic effects by inhibiting cellular protein synthesis in target cells. We tested the ability of VEGF₁₂₁/rGel treatment to inhibit the growth of prostate cancer cells in a bone metastases model. VEGF₁₂₁/rGel inhibited tumor growth and enhanced survival of mice by targeting the tumor vasculature as well as normalizing the number of mature osteoclast found in bone. Treatment of mice bearing PC-3 intrafemoral tumor xenografts with VEGF₁₂₁/rGel was shown to dramatically suppress PC-3 skeletal metastases. All control mice developed lytic lesions and were sacrificed by day 67. In contrast, 50% of the VEGF₁₂₁/rGel-treated mice survived past day 140 without any sign of skeletal tumor lesions. In vitro studies showed that VEGF/rGel but not rGel could dramatically suppress RANKL-induced osteoclast differentiation of RAW cells into TRAP⁺ multi-nucleated osteoclasts. The observed effect was not mediated by either VEGF₁₂₁ or gelonin alone but is a characteristic unique to the combined fusion protein. The IC₅₀ of VEGF₁₂₁/rGel on dividing RAW cells was 40 nM as compared with 900 nM for rGel itself, indicating the presence of a receptor for VEGF₁₂₁. Similar results were obtained for VEGF₁₂₁/rGel-treated bone marrow-derived monocytes. While immunofluorescence studies clearly show VEGF₁₂₁/rGel penetration into osteoclast precursor (RAW) cells, the receptor responsible for mediating the cellular entry of VEGF₁₂₁/rGel is unknown. RT-PCR analysis of RAW cells indicates the presence of only VEGFR-1 (Flt-1). In addition, Flt-1 levels are downregulated following stimulation of osteoclastogenesis by RANKL demonstrating that mature osteoclasts express comparatively low levels of Flt-1 and are insensitive to VEGF₁₂₁/rGel cytotoxic effects. These studies suggest an important role for VEGF and its receptors in tumor-mediated osteoclastogenesis and demonstrate that VEGF₁₂₁/rGel appears to suppress osteolytic lesions by acting directly on osteoclast precursor cells as well as on suppression of tumor vasculature. This suggests a previously unrecognized role for this unique agent in the treatment of skeletal metastases. Research conducted, in part, by the Clayton Foundation for Research.

Key words: VEGF₁₂₁/rGel vascular PC-3 osteoclast

Category: TB4 Angiogenesis, Microcirculation, and Cellular Microenvironment
Subclassification: Novel pro- and antiangiogenic factors

Short title: VEGF₁₂₁/rGel blocks bone remodeling

Abstract #: 4624

Identification of the Role of VEGF Receptors in Bone Remodeling by the Vascular Targeting Agent VEGF₁₂₁/rGel. *Khalid A. Mohamedali, Ann T. Poblentz, Sehoon Kim, Jun Yang, Nora Navone, Philip Thorpe, Bryant Darnay and Michael G. Rosenblum.* University of Texas M.D. Anderson Cancer Center, Houston, TX and University of Texas Southwestern Medical Center, Dallas, TX.

The progression of osteolytic or osteoblastic metastases requires the establishment of close functional interactions between tumor cells and bone cells, and tumor-secreted soluble factors such as GM-CSF, M-CSF, interleukins, TGF- β and VEGF all play prominent roles. We have previously shown that VEGF₁₂₁/rGel, a chimeric fusion toxin composed of VEGF₁₂₁ and the plant toxin gelonin (rGel), binds to both Flt-1/FLT-1 and Flk-1/KDR receptors and that cytotoxicity and cellular internalization of VEGF₁₂₁/rGel on vascular endothelial cells is mediated through Flk-1/KDR and not Flt-1/FLT-1. Inhibition by VEGF₁₂₁/rGel of osteolytic PC-3 prostate tumor proliferation in bone prompted us to examine the role of VEGF receptors in tumor-associated bone remodeling. Analysis by flow cytometry and RT-PCR showed that both bone marrow-derived monocytes (BMM cells) and RAW264.7 murine osteoclast cells display high levels of Flt-1 but low levels of Flk-1 receptors for VEGF. In contrast, both primary mouse osteoblasts and the preosteoblast cell line MC3T3 display moderate levels of Flt-1, Flk-1 and VEGF transcript. In vitro treatment of BMM or RAW264.7 cell lines revealed that VEGF₁₂₁/rGel was selectively cytotoxic to osteoclast precursor cells but not to mature osteoclasts. Maturation of osteoclast precursor cells by treatment with RANKL resulted in down-regulation of Flt-1 and resistance to the cytotoxic effects of VEGF₁₂₁/rGel. Internalization of VEGF₁₂₁/rGel into RAW264.7 and BMM cells was suppressed by pre-treatment with an Flt-1 neutralizing antibody or by PlGF, but not with an Flk-1 neutralizing antibody. Finally, VEGF₁₂₁/rGel activated pp44/42 (MEK1/2), a known down-stream target of VEGF receptor activation, in a similar manner as an equimolar amount of VEGF₁₂₁. The rGel itself did not induce any stimulation of MEK1/2, indicating that the effect of VEGF₁₂₁/rGel is mediated by a VEGF₁₂₁ receptor, rather than by a non-specific mechanism. In contrast, targeted cytotoxicity of VEGF₁₂₁/rGel was not observed towards MC3T3 cells. Studies are ongoing to examine the role of VEGF receptors in cross talk between osteoblasts and osteoclasts and the potential role for VEGF₁₂₁/rGel in tumor-associated bone formation in mature and immature osteoblasts. Our results suggest that VEGF₁₂₁/rGel is selectively cytotoxic to osteoclast precursor cells rather than to mature osteoclasts and that VEGF₁₂₁/rGel cytotoxicity is mediated by the Flt-1 receptor, which is downregulated as osteoclast precursor cells differentiate to mature osteoclasts. Studies conducted, in part, by the Clayton Foundation for Research.

Keywords: Vascular Endothelial Growth Factor, Gelonin, Osteoclast, Osteoblast, bone

Category: Biological Therapeutic Agents

Subclassification: Growth factor receptors and other surface antigens as targets for therapy.